University of Strathclyde

Department of Biomedical Engineering

DEVELOPMENT AND VALIDATION OF A GASTROENTEROLOGY PROBE CAPABLE OF MEASURING THE POSITION OF THE SQUAMO-COLUMNAR JUNCTION.

James Gerald Holland Whiting, BSc.

A thesis presented in the fulfilment of the requirements for the degree of Doctor of Engineering

2014

This thesis is the result of the author's original research. It has been composed by the author and has not been previously submitted for examination which has led to the award of a degree.

Signed: 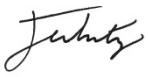

Date: 03/04/2014

Abstract

The squamocolumnar Junction is an important landmark in the upper gastro-oesophageal anatomy, acid reflux occurring above this causes heartburn and may lead to oesophageal cancer if prolonged. Currently no medical device takes into account the position of the squamo-columnar junction despite its importance. The aim of this doctoral work is to develop and validate a device which is capable of monitoring the position of the squamocolumnar junction with respect to simultaneous acid reflux and pressure measurements. Using Hall effect sensors on a custom flexible circuit board, and a magnet attached to the squamo-columnar junction, a device was produced which when inserted into the oesophagus, measured the relative position of the squamocolumnar junction to manometry and pH-metry catheters. The accuracy of the measurement was at most 5 millimetres, often better; a better resolution than either the high resolution manometer or custom pH device. The device was validated in-vivo, demonstrating a capability of measuring significant movement of the squamo-columnar junction during transient lower oesophageal sphincter relaxations.

The accuracy of the high resolution manometer was tested, which showed significant drift, capable of causing misdiagnosis. A correction algorithm was produced which corrected linear drift, removing time dependant drift leading to significantly more accurate pressure readings.

Catheter based upper gastro-oesophageal measurements have the potential to cause transient lower oesophageal sphincter relaxations by triggering mechanoreceptors in the pharynx; therefore a non-catheter based squamo-columnar junction locator was designed and tested. Using a larger magnet and significantly more sensitive Hall effect sensors and custom analogue circuitry, the squamo-columnar junction could be detected. The distance between the oesophagus and the skin is estimated to be between 8 and 9 centimetres for a healthy, non-obese male adult, the detection range for the non-catheter based squamo-columnar junction locator was 10.4 centimetres. The devices developed for this doctoral work has improved the field of gastroenterology research.

Acknowledgements

Firstly I would like to thank the Engineering and Physical Sciences Research Council for a Medical Devices Doctoral Training Centre Studentship that supported this work. I would also like to thank my supervisors, Professor Patricia Connolly and Professor Kenneth McColl for their advice, support and expertise in biomedical engineering and gastroenterology respectively.

I would also like to thank colleagues Yeong Yeh Lee, Elaine Robertson, Mohammad Derakshan, Angela Wirz and Nasser Djennati for their constant support and advice throughout the project. Thanks go to John Mclean, Alexander Weir and Douglas Smith who aided with both physical production of the devices and engineering expertise. Without the help of the following people, orchestrating meetings and research would have been made far more difficult: Carol McInnes, Dorothy Ronney and Janice Arnott.

A big thank you goes to all my friends and family who provided me with encouragement and comical relief for the duration of the project and beyond.

Symbol

A	Area
Aβ	Loop gain
B	Magnetic flux density
B_r	Residual flux density
C	Capacitance
d	Distance
e	Elementary charge
f	Frequency in degrees
F	Force
G	Gain
$G_{electronic}$	Electronic gain
$G_{magnetic}$	Magnetic field gain
H	Magnetising field
I	Current
k	Boltzmann constant
L	Length
l	Scalar vector
M_r	Magnetic remanence
M	Separation distance
m	magnetic moment
n	Charge carrier density

N_{VH}	Hall effect sensor output noise
N_{VH}^{th}	Thermal noise
N_{VH}^{LF}	Low frequency noise
p	Pressure
q_m	Magnetic pole magnitude
R	Resistance
r	Radius
S_A	Sensor sensitivity
S_{NEMI}	Noise equivalent magnetic induction spectral density
t	Thickness
T	Temperature in Kelvin
V_H	Hall effect sensor output voltage
V_n	Johnson noise
B	Bandwidth
ε	Permittivity of dielectric material
μ	Magnetic permeability
μ_0	Magnetic permeability of free space
μ_r	Relative permeability
ρ	Magnetic pole strength
ω	Frequency in radians

Abbreviations

AC	Alternating current
ADC	Analogue to digital converter
AMR	Anisotropic magnetoresistance
ASCII	American standard code for information interchange
BMI	Body mass index
BMS	Biomagnetic measurement system
BO	Barrett's oesophagus
BPF	Band pass filter
CT	Computed tomography
DC	Direct current
DIP	Dual in-line package
DNA	Deoxyribonucleic acid
DV	Digital Video
DVD	Digital versatile disc
EGJ	Esophageal gastric junction
EM	Electromagnetic
FC	Flux concentrator
FCB	Flexible circuit board
FDA	Food and drug administration
GI	Gastrointestinal
GMR	Giant magnetoresistance

GO	Gastro-oesophageal
GOJ	Gastro-oesophageal junction
GOPG	Gastro-oesophageal pressure gradient
GORD	Gastro-oesophageal reflux disease
HDD	Hard disk drive
HPZ	High pressure zone
HRM	High resolution manometry
IC	Integrated circuit
ICU	Intensive care unit
IDE	Integrated development environment
IQR	Inter-quartile range
LCD	Liquid crystal display
LES	Lower esophageal sphincter
LGA	Land grid array
LOS	Lower oesophageal sphincter
LPF	Low-pass filter
MHRA	Medicines and healthcare products regulatory agency
MII	Multichannel Intraluminal impedance
MM	Micro manometry
MMM	Magnetic marker monitoring
MR	Magnetoresistance
MRI	Magnetic resonance imaging

NEMI	Noise-equivalent magnetic induction
NG	Nasogastric
NHS	National health service
PACS	Picture archiving and communications system
PC	Personal computer
PCB	Printed circuit board
PCL	Polycaprolactone
PDIP	Plastic dual in-line package
PIP	Pressure inversion point
POL	Phreno-oesophageal ligament
PPI	Proton pump inhibitors
PSD	Phase sensitive detector
REC	Research ethics committee
RF	Radio frequency
RFID	Radio frequency identification
RMS	Root mean square
SCJ	Squamo-columnar junction
SCL	Serial clock line
SD	Secure digital
SDA	Serial data line
SMT	Surface mount technology
SNR	Signal to noise ratio

SQUID	Superconducting quantum interference device
TLOSR	Transient lower oesophageal sphincter relaxation
USB	Universal serial bus

Contents

List of tables

List of figures

Chapter 1

Introduction to the field

1.1 Introduction

Gastro-Oesophageal (GO) complaints such as acid reflux which may cause heart burn, is one of the most common incidents for General Practitioners in the world (Fletcher et al. 2004). The UK is one of the most prevalent countries in the world for this, providing an excellent opportunity to study its causes and effects on the local population. As yet, little is known about the mechanisms of acid reflux and its chronic causes, however currently strong risk factors are obesity, age, gender and the presence of a hiatus hernia. The relationship between obesity and increased abdominal pressure, an indicator for acid reflux, is very strong, however the method by which obesity increases acid reflux occurrence is unknown and highly debated. Some research groups believe the increased levels of hormones particularly sex hormone binding globulin and testosterone are the main causes of increased acid reflux (Menon et al. 2013), however others believe a mechanical effect due to obesity, or perhaps a combination, is the most likely and strongest argument.

Acid reflux is an indicator of an increased likelihood of further Upper Gastro-Intestinal (GI) complications, such as oesophagitis, Barrett's oesophagus (BO), Metaplasia and Adenocarcinoma.

There are many devices and techniques commercially available for measuring and investigating the Upper GI tract, however they all have a significant weakness, inherent to them, which means that to gain a full understanding of the digestive system, several techniques are often combined for a single study, however this can cause issues such as patient discomfort, synchronisation problems and requires strong reasoning for ethical approval. Often Endoscopy or MRI scans are performed for patients with severe symptoms in order to gain a detailed view of the patient,

however as these procedures are often undertaken on subjects with symptoms, there is a question about how similar these subjects are to the healthy population presenting with no symptoms. Several studies have shown that even symptom free volunteers may have frequent acid reflux events, calling in to question what is the anatomy of the healthy or symptom free population.

The primary aim of this research therefore, is to develop tools which can monitor the position of the Squamocolumnar junction for an extended period of time, whilst removing the limitations of current methods such as fluoroscopy. The Squamocolumnar junction is the transition between the stomach wall and oesophageal wall, manifested by an epithelial tissue type change between the squamous epithelium of the oesophagus and columnar epithelium of the stomach, visible upon endoscopy as the "Z-Line". The position measurement must be accurate to within 1cm as small movements of this anatomy may indicate important events within the digestive tract. The tools must be safe for use in patients and must also be compatible with the current set of Upper GI diagnostic and research technologies.

The technology researched and developed in this study may be used in conjunction with high resolution manometry, fluoroscopy, intraluminal impedance and pH-metry devices so much work adequately in their presence while not affecting the performance of the above tools.

The research should ideally achieve the design of a reusable system whereby some small parts may be single use, but the majority of technology should be reusable after sanitisation for efficiency. The research output will allow medical practitioners the opportunity to investigate the upper GI tract for longer and in significantly more detail and accuracy than ever before.

Within the digestive system (figure 1.1), there are several organs, each of which contribute specific functions to the processing of food material into useful nutrients, below is a detailed description of these organs and functions. All living organisms require nutrients for energy in order to maintain life, and humans are no exception. The digestive system is the set of organs dedicated to this task in humans, consisting predominantly of the mouth, oesophagus, stomach and intestines. The human

digestive system is responsible for several tasks: ingestion, mechanical processing, secretion, absorption and excretion. Ingestion is the process of entering of food into this system, via the mouth and is an active voluntary process. Mechanical processing is the physical breakdown of solid food stuffs into smaller pieces with larger surface area for digestion. The teeth and tongue are the main bodies by which food is mechanically broken down by mastication or chewing, while the tongue propels food around the mouth, for teeth to crush and indeed for mastication with saliva to allow smooth swallowing into the stomach. Digestion is the chemical break down of food by liquid and enzymes to split them into a size appropriate for absorption through the epithelium into the blood stream. Secretion is the act of releasing said liquids, acids enzymes and other chemicals into the digestive tract by specialised epithelia cells in the digestive tract wall or associated organs, often triggered by ingestion of food. Following thorough mixing of the secreted material, useful nutrients from the food mixture are then absorbed across the digestive wall, at different stages along the tract, until the remnants which are of little use are excreted from the body in a process called defecation.

1.2 Gastro-Oesophageal Anatomy

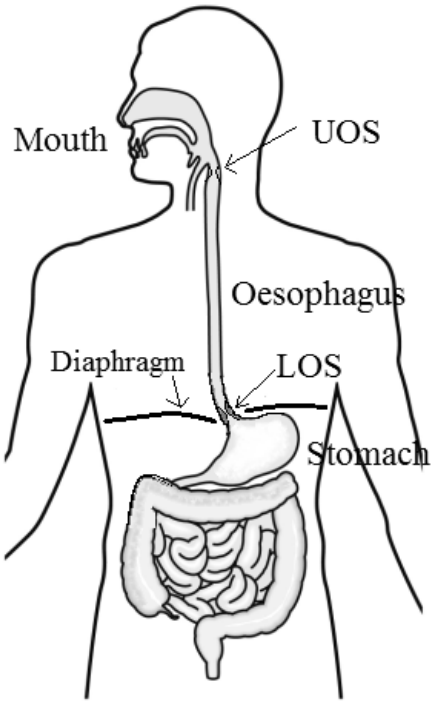

Figure 1.1 Human upper digestive tract anatomy. Adapted from Digestive Disease Group (www.digestivediseasegroup.com/procedures)

1.2.1 Oesophagus

The oesophagus is an enclosed tube through which food mixed with saliva, known as a bolus, is actively passed from the mouth into the stomach. The oesophagus has longitudinal and circular muscles, to facilitate the movement of the bolus into the stomach by waves of sequential muscle contractions. The wall of the oesophagus distends to pass the bolus as the contractile wave follows, and then retracts back to concentric mucosal folds, closing the lumen behind it. This food transport is a neuromuscular controlled action, called a swallow or primary peristalsis, but often a secondary peristaltic wave will follow to ensure all food content has been cleared, this process can pass food from the pharynx at the rear of the throat, to the stomach in approximately 9 seconds.

The oesophagus is joined at the proximal end to the back of the throat by the upper oesophageal sphincter and at the distal end to the stomach by the lower oesophageal sphincter, these physical barriers aim to stop the unwanted movement of oral or stomach content into the oesophagus, but relax to allow the passage of liquid or food. The length of the oesophagus varies with height and gender, but ranges from approximately 22 to 26 centimetres; however the length to the stomach from the incisors may be up to double this length. The oesophagus passes through from the thorax into the abdomen through the diaphragm at a gap called the diaphragmatic hiatus, through which the pressure increases. The mucosa of the oesophagus is predominantly stratified squamous epithelium, with little to no secretory cells or glands.

1.2.2 Stomach

The stomach performs the role of mechanical and chemical break down of ingested material, as well as the production of several chemical factors which allow progression and processing of food, further down the digestive tract.

The stomach is a muscular hollow section of the digestive system, where food is stored and processed, and as such its shape is variable and dependant on the presence and volume of food and liquid.

The stomach, although one unit, can be divided into four different regions, the cardia, fundus, body and pylorus. The cardia is the section immediately adjoined to the oesophagus, however the term is ambiguous and may refer to the general area around the distal stomach or to the more specific epithelium. It is generally accepted to refer to the superior two to three centimetres of the stomach with the histology of the cardia, predominantly columnar epithelium. The cardia often contains mucus secreting glands. The angle of His is the acute angle between the cardia and the oesophagus, which is created by the stomach muscle fibres, creating the fundus.

The fundus is the portion of the stomach which is next to the cardia, but often resides above the position of the Gastro-Oesophageal Junction (GOJ), this is where gastric

gas often resides after a meal. The columnar fundus epithelium often contains parietal or oxyntic acid secreting cells as well as peptic secreting glands and gastric pits. The body of the stomach has a similar epithelial and glandular profile to the fundus, located inferior to the cardia and fundus, the body makes up a large proportion of the stomach by surface area.

The pylorus is the inferior portion of the stomach, itself made up of the pyloric antrum and the pyloric canal, the latter of which empties into the duodenum.

As the parietal or oxyntic cells secrete hydrochloric acid into the stomach to aid digestion of food and kill most of the ingested micro-organisms, the stomach lining itself is very thick and resistant to acid damage. The lining also very proliferative, replacing the lining more quickly that the oesophagus, as stomach acid may be as strong as pH 1 postprandially. Due to the specialised nature of the thick lining of the stomach, very little absorption occurs here, most of which occurs in the intestinal tract.

1.2.3 Gastroesophageal Junction and Lower Oesophageal Sphincter

The Gastro-oesophageal junction is the transition between the oesophagus and the stomach, and its exact definition varies between research groups and the methods used to detect it (Seefeld et al. 1977; Holloway et al. 1995; Kahrilas et al. 1999; Al-Motabagani 2002; Logan et al. 2002; Fletcher et al. 2004; Gordon et al. 2004; Sifrim 2004; Pandolfino, Shi, et al. 2005; Conklin et al. 2009; Pandolfino, Ghosh, et al. 2006; Kuo et al. 2012; Roy et al. 2012). Some medical practitioners define the GOJ as the arbitrary change from the elongated tube of the oesophagus, to the sac like opening of the stomach, but this is a rather vague marker due to the lack of definable criteria. The definition is in no way helped by the extremely complex anatomy around this area and the tendency of the anatomy to move relative to one another. The two layer muscle wall of the oesophagus changes into the stomach with the addition of a third oblique layer of muscle, however this transition is gentle and does not allow high precision measurement, even with highly invasive methods. The

Lower Oesophageal Sphincter (LOS) is a prominent anatomy in this area, and as such, often LOS and GOJ are used interchangeably. The intrinsic LOS is a ring of musculature at the distal end of the oesophagus, however it is only reliably defined by the presence of an increased pressure between the oesophagus and stomach, and is almost anatomically unidentifiable, as the length of the oesophagus contains musculature for aforementioned swallowing and peristalsis. Pressure arises from radial sphincteric muscles which close to stop gastric contents flowing into the oesophagus where damage is then caused. Its visibility upon manometric or pressure recordings from inside the lumen show it is almost always contracted and a high pressure zone is visible before the beginning of the stomach (Chandrasoma & DeMeester 2006). The high pressure zone (HPZ) is not only the presence of the muscular LOS, but the augmentation of the diaphragm. Definition of the top of the diaphragm is most reliable when using manometric techniques, something which will be discussed in significant detail later, which shows a distal pressure significantly higher than oesophageal pressure. LOS pressure ranges from 10 to 35 Millimetres of mercury (mmHg) (Gordon et al. 2004) in healthy subjects, and can be higher but is often lower in patients with anatomical abnormalities. The distal end of the LOS which closes the GOJ at the stomach side, is much more difficult to define, as the gastric pressure is higher than the oesophagus and often fluctuates with the intake of a meal, change in posture or while straining. The accepted standard of definition of the lower end of the LOS is a step down of 2mmHg from the LOS into the stomach (Mattox et al. 1992), however this is a very unreliable method of definition for many reasons.

The technology itself is unreliable to this level of accuracy, High Resolution Manometry (HRM) –explained later has an inherent error that each sensor's accuracy varies by as much as +/-2 mmHg, so if two adjacent measurements are inaccurate by +/- 1 mmHg, the position of the lower end of the LOS may be misrepresented. Another error of this measurement using HRM is the distance between sensors, which are placed 1 centimetre apart due to spacing limitations within the probe, so the step down of 2mmHg could be anywhere in between the sensors and the associated software interpolates between two sensors, introducing another level of inaccuracy. The HRM device now produced by Given Imaging (USA) has been

shown by rigorous testing to suffer from a level of drift, which will be covered in detail in chapter 2, which when HRM is used for a long period of time, is highly significant and may cause large errors. The combination of the extensive areas for error to be introduced means that when measuring the length of the LOS which typically ranges from 31 to 53 mm a significant error can greatly over or under estimate the length of this important anatomy (Bonavina et al. 1986).

The main role of the LOS is to stop stomach contents retrograding into the oesophagus; the mix of digested food, acid and enzymes is known as chyme and can be strongly acidic, pH 1, so reflux of this material can cause damage, inflammation and can, after prolonged chronic exposure, lead to metaplasia or even cancers, so it is the role of the LOS to provide an anti-reflux barrier.

As briefly mentioned, the diaphragm increases the HPZ beyond the level that the LOS provides, augmenting the reliability of the anti-reflux barrier. The diaphragm is attached to the costal wall and separates the thoracic cavity from the abdominal cavity. The left and right Crus of the diaphragm are tendons which extend inferiorly from the diaphragm and attach to the lumbar vertebrae, the crura are attached to muscles which wrap around the oesophagus at the GOJ, forming a hiatus through which the oesophagus passes. Due to the changing pressures of the abdomen with movement of the chest wall for ventilation, the diaphragm often moves up and down in accordance with the rate of respiration, meaning the diaphragm is a dynamic addition to the anti- reflux barrier and is not sufficiently constant to enable precise location of the GOJ. The Phreno-Oesophageal Ligament (POL) is a set of ligaments which extend from the diaphragmatic hiatus and attach to the oesophagus at approximately the LOS height. The significance of the POL is still under investigation and they are often overlooked but recent studies tend to suggest they play an important role in hiatus hernia prevention (Al-Motabagani 2002; Gordon et al. 2004) by anchoring the oesophagus to the diaphragm rather than allowing it to shorten and move superiorly. A recent publication (Pandolfino, Ghosh, et al. 2006; Pandolfino, Zhang, et al. 2006) suggests the laxity of the POL is a dominant factor in allowing the stomach to move superiorly through the diaphragmatic hiatus, exposing a proportion of the stomach to thoracic pressure, known as a hiatus hernia, and

removing the augmentation of the crura to the anti-reflux barrier. As mentioned, the diaphragm acts as the divider between the thorax and the abdomen, as such, there exists a pressure difference at the GOJ, called the Gastro-Oesophageal Pressure Gradient (GOPG). The magnitude of the GOPG changes with respiration, and more importantly obesity, which could provide a basis for the argument of mechanical differences causing increased reflux episodes in the more obese. The angle of His is believed to create further augmentation of the anti-reflux barrier by creating what is termed a Flap Valve, when the stomach becomes more full, this acute angle acts to compress the LOS further. This has been shown in cadaveric studies but is much more difficult to prove in healthy volunteers, and the endoscopic validation techniques are predominantly observational. It has been shown via endoscopy that the flap valve is less visible in subjects suffering hiatus hernia. As the intrinsic LOS is augmented by a combination of the diaphragmatic crura and GOPG, often the term LOS is used when anti-reflux barrier would be more accurate, as this refers to the whole system rather than a specific anatomy.

1.2.4 Squamocolumnar junction

The Squamocolumnar junction (SCJ) is the change in the epithelial lining of the oesophagus to the stomach, the endoscopically visible manifestation known as the Z-Line, perceptible due to the difference in colour of the two epithelia.

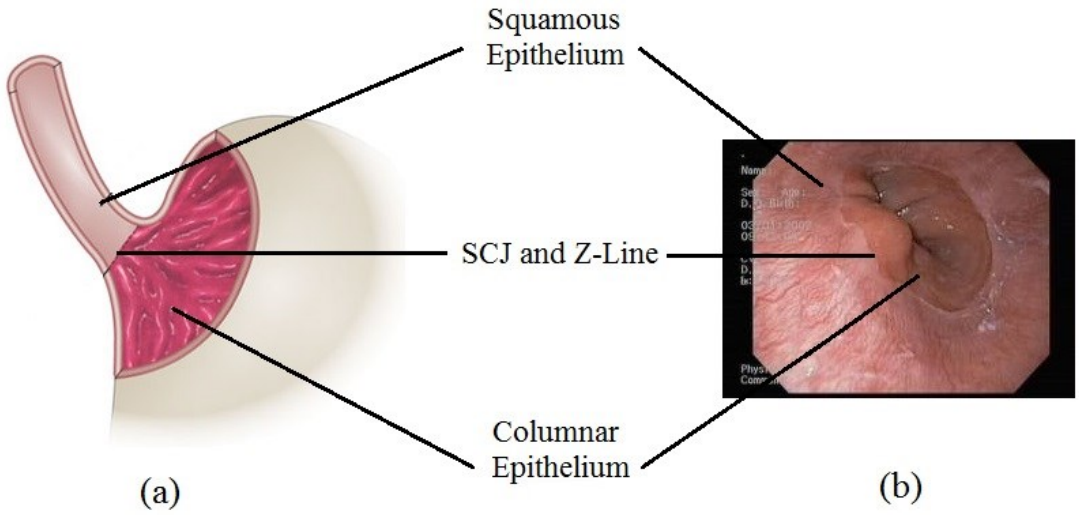

Figure 1.2 The Squamo-columnar Junction in (a) traditional anatomic illustration and (b) intra-oesophageal endoscopic view. Adapted from (Odze 2009).

The squamocolumnar junction is the tissue type change between the distal squamous epithelium of the oesophagus and the columnar lining of the proximal stomach. The SCJ is a very important anatomical landmark in upper GI research and investigation, as the more acid resistant columnar epithelium of the cardia abruptly changes into squamous cells, which are very sensitive to acid and other gastric content exposure.

Due to the close proximity of the squamocolumnar junction to the GOJ, many investigators assume that manometric measurements of the GOJ actually approximates the SCJ, however as the GOJ is a dynamic and variable anatomy, including influences from the motile diaphragm, this approximation is rather inaccurate, and any positional measurement claimed using this technique is likely to have errors of up to 5 centimetres.

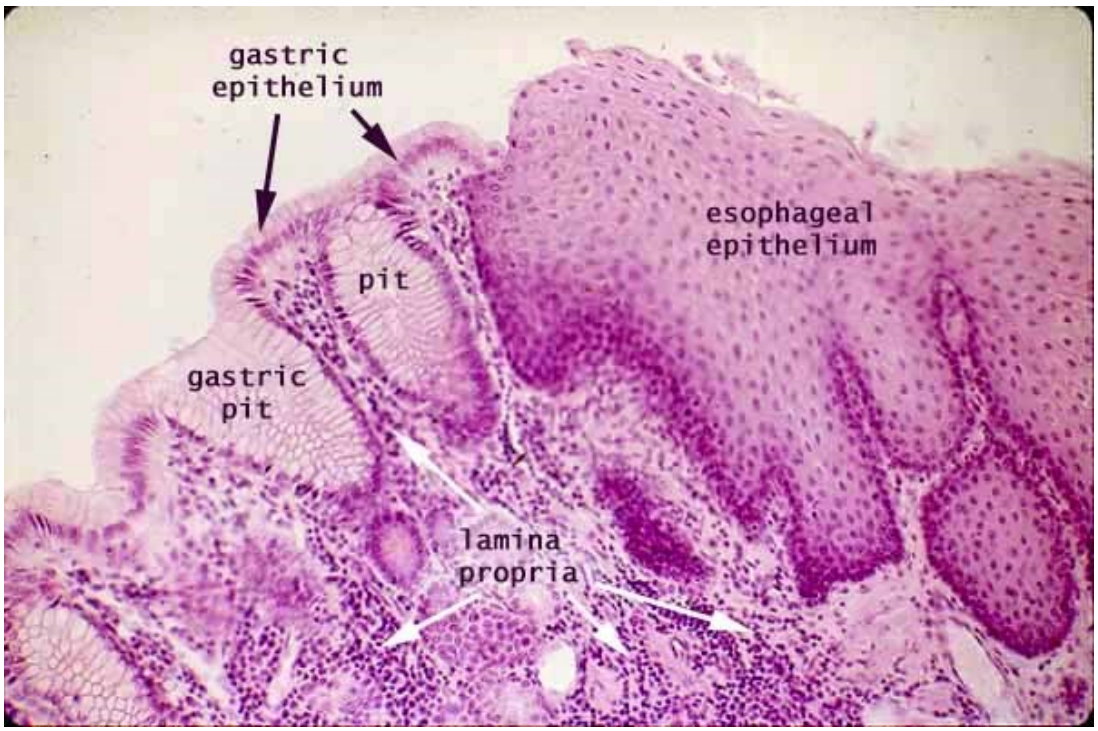

Figure 1.3 Histology of the Squamo-Columnar Junction. Showing stratified squamous epithelium of the oesophagus, simple columnar epithelium of the stomach and gastric pits. The arrow signifies the very distinct and abrupt tissue type change at the SCJ. SIU School of Medicine
(http://www.siumed.edu/~dking2/erg/images/GI086b.jpg)

Unlike the SCJ, the measurement of the position of the GOJ is much less accurate, depending entirely on the definition used, however as the Z-Line is endoscopically visible as shown in Figure 1.2(b), so called because of its irregular, occasionally crinkled appearance, and the SCJ much more significant with regards to acid reflux, it is vital to develop a method of accurately measuring the SCJ without the invasiveness of endoscopy, which can be employed for a long period of time, before and after a meal, allowing researchers to detect SCJ movement and its position relative to acid.

1.3 Problems and disease

1.3.1 Swallows and transient relaxations of the SCJ process outline

Swallowing is the process where a bolus of food stuff is moved from the mouth to the stomach, through the oesophagus. The process of swallowing or deglutition is an automatic, subconscious process, however it can be initiated voluntarily. Swallowing is often also performed to clear saliva build up in the mouth, or as an action to clear parts of a bolus which has not fully progressed down the oesophagus. It is estimated that swallowing is performed 2400 times per day, and the process can be divided into three distinct phases: buccal; pharyngeal and oesophageal.

The buccal phase is formation of a bolus, by the forcing together of food, liquid and saliva against the hard palate at the roof of the mouth by the tongue. The tongue then moves the bolus towards the rear of the mouth, where it passes into the pharynx, sealing off the nasopharynx with the soft palate. As the bolus passes into the pharynx, proprioceptive receptors at the base of the tongue, on the pharyngeal wall and the uvula, triggers the automatic swallowing reflex.

As the bolus presses against the posterior pharyngeal wall, the pharyngeal phase of swallowing begins. The medulla oblongata controls the swallowing process via the glossopharyngeal and trigeminal, initiating contraction of the pharynx muscles, simultaneously moving the larynx superiorly, moving the epiglottis in place to cover the glottis at the top of the trachea while the uvula and soft palate block reverse movement of the bolus, forcing the bolus to move towards and into the oesophagus.

As the bolus passes into the oesophagus, peristaltic contraction begins, forcing the bolus toward the stomach (figure 1.4), triggering the opening of the Lower Oesophageal Sphincter as it reaches the distal oesophagus.

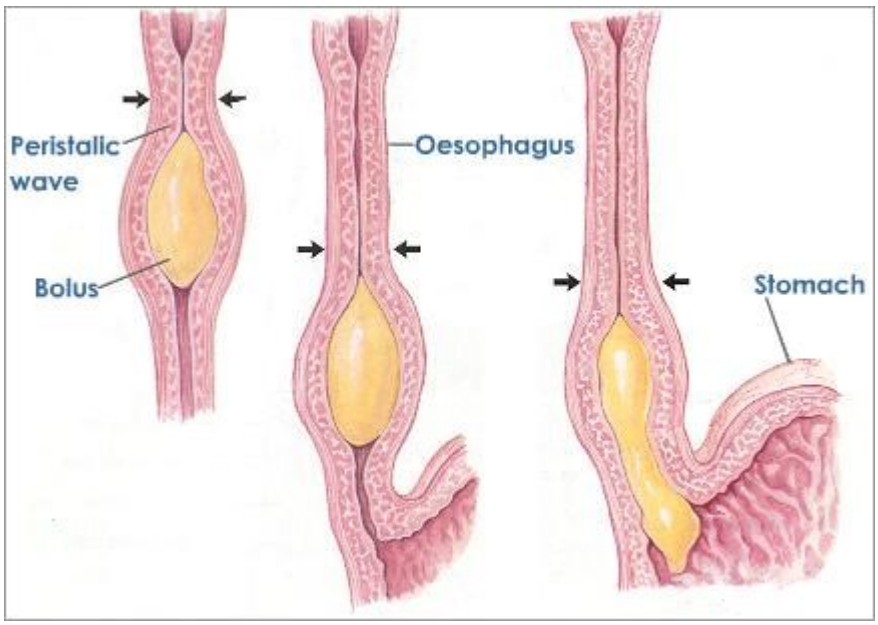

Figure 1.4 Peristalsis along the oesophagus triggering the relaxation of circular LOS muscles. Acquired from Tutor Vista (http://www.tutorvista.com/content/biology/biology-iv/animal-nutrition/pharynx.php)

Peristalsis is the symmetrical radial contraction of circular smooth muscle rings which propagate along the oesophagus behind the bolus, squeezing the food through into the stomach. Peristaltic waves are controlled and coordinated by afferent and efferent fibers in the glossopharyngeal and vagus nerves, the speed of which is controlled by stimulation of stretch and sensory receptors in the oesophageal wall by the bolus. Primary peristalsis is the initial strong contraction of the oesophagus to pass the bolus, but poorly lubricated or dry swallows may not propagate fully, or break up, leaving fragments of food in the oesophagus, which stimulate said oesophageal receptors, prompting secondary peristaltic waves. The length of the oesophagus decreases during normal swallows, due to the contraction of the longitudinal muscles.

1.3.2 Transient Lower Oesophageal Sphincter Relaxation

The release of trapped gastric air that is swallowed, is released in the form of a belch, which must be released otherwise the associated increase in gastric pressure is likely to cause over venting and subsequent acid reflux. This release of gastric gas decreases gastric pressure and distension, restoring the GOJ anatomy such as the flap valve, which can be distorted due to the presence of large amounts of air. In order to release this gas, the LOS must relax for a short period of time; a process known as a Transient Lower Oesophageal Sphincter Relaxation (TLOSR). It is suggested that TLOSRs are initiated by gastric distension via a stretch receptor in the stomach, however there is little anatomical evidence for this hypothesis as yet. It is also hypothesised that abdominal shortening sphincter relaxation occurs after shortening of the abdominal section of the LOS, typically precipitated by gastric distension. It has been purported that there is a close relationship between the extent of gastric distension required to overcome the sphincter and the anatomy of the GOJ (Holloway et al. 1985; Kahrilas et al. 1986), which has since been demonstrated by means of artificially induced gastric distension in reflux patients with hiatal hernia, increasing frequency of TLOSRs (Kahrilas et al. 2000). The majority of TLOSR research has been performed investigating symptomatic subjects with abnormal anatomy or high occurrence of heartburn or reflux associated pain. This bias away from healthy subjects questions the extent of knowledge of the normal sphincter.

The classification by which TLOSRs were detected and classified were very poor until, in 1995, Holloway et al (Holloway et al. 1995) developed a set of criteria to reliably identify the occurrence of TLOSRs. This study investivated 23 healthy and 9 subjects with Gastro-Oesophageal Reflux Disease (GORD) in order to measure several parameters of swallow and non-swallow induced TLOSRs. It was noted that previous studies showed non-swallow induced TLOSRs to be the main cause of reflux in healthy subjects and GORD patients alike, however the mechanism by which this manifested was poorly understood. Holloway et al used a multichannel perfusion manometer and a pH electrode placed 5 centimetres proximal to the SCJ to measure a range of TLOSR factors. Each subject was fasted overnight, and any that

were on pharmaceutical GI treatment, had this suspended for 48 hours prior to the study. The subjects had a 10 minute acclimatisation period after intubation before asked to perform 5 dry and 5 wet swallows, followed by gastric distension simulation with 200 millilitres fluid and for the following 30 minutes recorded gastric-normalised LOS pressure and pH. The time to swallow onset was larger for dry swallows than wet swallows, while duration of LOS relaxation was longer for wet swallows than dry, while nadir pressure was slightly but significantly higher in dry swallows, with time onset to completion and relaxation rate having no statistical significance. It was noted that resting LOS pressure was lower in patients suffering GORD than those of healthy subjects. The duration of relaxation for non-swallow associated TLOSRs was approximately 17 seconds, while dry and wet swallows lasted approximately 5 seconds, with the clear and large difference, providing a strong manometric detail to detect for TLOSRs. From other study parameters, classification may also include the absence of a swallow 4 seconds prior to the start of relaxation, a LOS relaxation rate of greater than 1mmHg/s, a nadir pressure of less than 2mmHg as well as the above duration of greater than 10 seconds. It was noted that full TLOSRs showed equalisation of gastric and oesophageal pressure, demonstrating LOS opening and allowing, although not always demonstrating, flow or reflux.

In 2001, Sifrim et al reviewed the literature regarding TLOSRs (Sifrim & Holloway 2001) to find that there were still conflicting reports with respect to frequency, the effect of posture and disease state of the subject, suggesting the strongest hypotheses for TLOSRs and their mechanisms. Four studies (Dodds et al. 1982; Holloway et al. 1997; Holloway et al. 1991; Penagini et al. 1998) found that patients suffering GORD had significantly higher number of TLOSR events compared to healthy asymptomatic subjects, however seven papers (Schoeman et al. 1995; Penagini et al. 1996; Penagini et al. 1998; Lidums et al. 2000; Holloway & Zhang 2000; Trudgill & Riley 2001) found no statistical difference between the same. A general consensus however was found, showing the number of TLOSRs with subsequent reflux episodes was up to double in GORD patients over healthy subjects. The body position with highest occurrence of acid associated TLOSRs was reported to be the recumbent, right lateral posture, however other studies have shown little to no

significant difference between positions. The review then suggested it was evident that all of the population, both healthy and GI disease sufferers, showed evidence of frequent TLOSRs however the determining difference was the number of harmful acid reflux associated episodes. The papers often use the measure of a pH sensor based 5cm proximal to the SCJ, which is the traditional method of detecting reflux, as more distal placement may lead to artefactual acid measurements with the diaphragm movements (Anggiansah et al. 1993), so concerned investigators and clinicians use the standard of 5cm proximal placement (Mattox & Richter 1990; Pandolfino et al. 2003). This is likely to hugely underestimate the number of reflux episodes as a rather large proportion of acid reflux occurs in very close proximity to the SCJ, which has been termed short segment reflux, The authors note the reasons for higher incidence of acid associated TLOSR are unclear, but go on to suggest mechanisms such as dysfunctional anti-reflux barriers, such as the intrinsic sphincter or crural diaphragm augmentation. Another mechanism which has since been widely adopted is the concept of increased acid volume in the stomach, which has now evolved into the idea of an acid pocket(Fletcher et al. 2004; Clarke et al. 2008; Holloway & Sifrim 2008), or more accurately an acid film (Pandolfino et al. 2007; Clarke et al. 2009); the result of post-prandial acid secretion by parietal cells in the stomach wall. With a large amount of such cells in the cardia, the amount of acid secreted below the SCJ can be quite large, which may suggest that the more acid secreting cells near the SCJ, the more acid reflux associated events will occur. Another factor suggested by Sifrim et al (Sifrim & Holloway 2001) is the gastric emptying time, those with slower gastric emptying were more likely to have TLOSR events with acid reflux as the acid was present at the SCJ for longer. Factors such as the difference in acid and food mixing were also suggested which strengthens the acid pocket hypothesis, with consumed food and drink causing a buffering effect if well mixed with acid. The paper finishes with suggested treatments against acid reflux caused damage, aiming to modify the anatomy in an attempt to increase the effectiveness of the GOJ, such as a fundoplication, however this surgical procedure is very invasive. The pharmaceutical alternative is the use of Proton Pump Inhibitors (PPI) which inhibit the secretion of acid into the stomach, so when reflux occurs, it is less corrosive to the SCJ and oesophagus (Chandrasoma & DeMeester 2006) . There

is no treatment as yet that simply decreases the number of TLOSR events, although this would be an ideal solution.

During full TLOSRs sphincter tone is lost and therefore understanding of the GOJ during this time is very poor as manometry can longer detect LOS position. It was because of this, that Pandolfino et al (Pandolfino, Zhang, et al. 2006) performed a study researching the movement of the SCJ and oesophageal shortening during TLOSRs. The study was designed to counteract this by the additional recording of simultaneous fluoroscopy, using manometry to identify the onset of a TLOSR, subsequently starting the fluoroscopic recording, which is of limited duration due to the dose of X-ray radiation associated with its use. 6 subjects without Hiatal Hernias had two radiopaque markers attached via endoscopy, one to their SCJ, and the other 10 centimetres proximal to this. The volunteers also had a pH catheter placed 5 centimetres above the LOS to detect acid reflux associated TLOSRs. High resolution manometry was used for 2 hours after a high fat meal, and the manometer was used to detect the onset of swallow and non-swallow induced TLOSRs, shortly after which, the fluoroscopy was started to record the movement of the clips due to oesophageal shortening. The authors summarised the events, stating that the key evens leading to full TLOSRs were the start of LOS relaxation; Crural diaphragm inhibition, oesophageal shortening and a large and positive GOPG. The duration of full TLOSRs with flow were approximately 20 seconds long, significantly longer than those without flow, lasting 17 seconds, both of which were significantly longer than swallow associated TLOSRs of approximately 7 seconds, with Crural inhibition following the same pattern. During the SCJ movement, two stages can clearly be identified, the initial proximal movement of the SCJ, and the return to original resting position, these are not detailed as velocities despite the data being recorded. Although SCJ and the proximal clip movements were observed, the start was detected via manometry, and fluoroscopy was started shortly after, the technique is likely to underestimate the duration and movement due to missing the onset of movement. For 93 manometrically detectable TLOSR events, only 62 had good fluoroscopy recordings. The fluoroscopic videos had to be post-processed one frame at a time by trained investigators, which would have taken a lot of time, not to mention the inaccuracies of fluoroscopy with ghosting and angle error. A successful

fluoroscopic recording rate of nearly two thirds is poor, when this is factored with the laborious post processing and inaccuracies of this technique, the method, although a very useful pilot study, is not efficient enough to provide an investigator with a reliable long term solution for researching TLOSRs, therefore a technique must be developed to accurately detect and measure such movements for long periods of time.

In 2000, Holloway described the antireflux barrier and mechanisms of acid reflux in a review paper collating all the latest hypotheses into a very conclusive article(Holloway 2000). Three key mechanisms for acid reflux emerged: LOS dysfunction; defective basal LOS pressure and the presence of a hiatus hernia. LOS dysfunction appears to be the main cause of reflux, as the LOS is the predominant contributor to the anti-reflux barrier, the loss of this therefore, is the underlying cause of reflux; LOS pressure must be lacking to allow reflux to occur. The majority of cases of loss of LOS pressure is acute, intermittent relaxations rather than chronic sustained lack of tone or pressure, and in healthy subjects, acid reflux as almost always associated with TLOSRs. The same can be said for GORD patients, with approximately 80% of reflux episodes associated with TLOSRs, with the remainder caused by swallow induces relaxation, longer term absent LOS pressure and strain. In a large review of the literature, Holloway summarised that in asymptomatic subjects, 40-60% of TLOSRs resulted in acid reflux, however in GORD sufferers, 60-70% of TLOSRs were associated with reflux. Although the incidence of acid associated TLOSRs is higher with GORD patients, this cannot without further investigation be defined as either a cause or effect, as it is unknown if GORD patients are inherently more likely to suffer the acid associated events before developing the disease, or if this is indeed a cause, having developed the disease. It is also reported that the likelihood of reflux during a TLOSR is increased postprandially, however the factors responsible are unknown. The rate of TLOSRs is independent of to the resting LOS pressure, however there are a number of events which appear to be swallow-induced however these last as long as a non-swallow induced TLOSR and often contain incomplete peristalsis, are believed to be coincidental, so are termed type 2 TLOSRs.

The rate of TLOSRs appears to be influenced by several factors. Gastric distension, particularly of the cardia, be that from a meal or simulated by a balloon or air, causes an increase in event frequency. Meals increase the frequency of TLOSRs however the content of the meal is insignificant, rather it appears that volume is the main factor. TLOSRs incidence can also be decreased in the supine posture, or sleeping and general anaesthesia; however the latter two could be contributed to by the supine posture effect. The paper details the neural control of TLOSRs which are mediated thorough vagal afferent pathways, and are thought to be triggered by meals in the stomach due to distension, and by pharyngeal stimulation, which accounts for the initialisation of swallow-induced TLOSRs. A number of pharmaceutical agents have been identified which act to reduce TLOSR frequency, such as: Cholecystokinin-A antagonists, Anti-cholinergic agents, Morphine, Somatostatin, nitric oxide synthase inhibitors, 5-hydroxythryptamine antagonists and gamma amino butyric acid agonists, however the sites of action for these drugs have yet to be identified.

This author highlighted the conflicting argument that some papers suggest that GORD sufferers have a higher rate of TLOSRs than do healthy subjects, however there is a proportion of papers which show the opposite, so this has yet to be decided, as each study was performed differently, using different methods and most importantly posture, which may account for the divide.

While the resting LOS pressure is lower in GORD sufferers, the wide range of basal pressures in both healthy and GORD subjects overlaps to a large extent, with GORD sufferers being in the lower area, however predominantly only those with severe oesophagitis have below normal range resting pressures. Despite this, during normal activities, only a fairly low basal pressure is required to provide an adequate anti-reflux barrier, however the lower resting pressures may be more easily overcome, accounting for the larger proportion of strain induced reflux episodes in GORD sufferers. Long duration studies of ambulatory and stationary subjects has shown that in practice very few reflux episodes occur via this mechanism, however in those with severe oesophagitis it may account for up to 23% of reflux incidences. The physical mechanism for a lower or defective basal pressure is unknown, however the diagnosis of oesophagitis and or the presence of a hiatus hernia accounts for a

reasonable decrease in the LOS pressure, as during herniation, the diaphragm is no longer aligned with the LOS, so any pressure augmentation is lost, which in healthy subjects, is increased during straining.

Patients with severe oesophagitis may have a missing LOS for up to 15 minutes which accounts for the higher incidence of absent LOS related reflux, as this is a prolonged relaxation than TLOSR. The pathogenic association between hiatus hernia and oesophagitis is a disputed one, however it is now accepted that a hiatal hernia is not causal, despite 54-95% of reflux oesophagitis sufferers having an endoscopic, radiological or MRI hiatus hernia diagnosis. Analysis has shown that the presence of a hiatus hernia predicts a greater frequency of TLOSRs than does basal LOS pressure; also hiatus hernia indicates more severe oesophagitis, Barrett's oesophagus and higher incidence of acid reflux. A hiatus hernia is classified as the movement of the LOS from inside the diaphragmatic hiatus, which causes a portion of the stomach to move cranially into the thorax, stretching of the phreno-oesophageal ligament (POL), loss of diaphragmatic pressure augmentation and often retention of stomach content in the hiatal section of the stomach. The oesophageal shortening during TLOSRs could lead to stretching of the POL, which may contribute to the development and progression of a hiatus hernia. Obesity has also been shown to be a very strong indicator of hiatus hernia presence. The loss of the flap valve at the GOJ is also suggested as a contributor to reflux; Hill et al (Hill et al. 1996) observed and categorised different grades of flap valve during cadaveric and endoscopic studies, with a grade I being normal and complete, ranging to grade IV which is non-existent, that the higher the grade of flap valve, the worse the barrier was at stopping reflux; it is suggested that loss of the flap valve is usually linked to the development of a hiatus hernia.

1.3.3 Acid Reflux

As mentioned in previous chapters, the stomach contains acid secreting parietal or oxcyntic cells, as well as gastric chief cells which secrete pepsinogen. Both cell types

are located within gastric glands, buried inside the stomach wall; together these two cell types secrete approximately 1.5 litres of gastric juice per day (Martini & Nath 2009) . The parietal cells, found at the proximal portion of the gastric gland, secrete hydrochloric acid (HCl) however they are very resistant to this acid as they do not produce this acid in the cytoplasm, as it would erode secretory vesicles and other cell contents. The acid secretion is performed by secreting hydrogen ions and chlorine ions independently by different mechanisms, hydrogen ions released into the gastric gland and the chlorine ions diffuse across the cell membrane through open chlorine channels, together forming hydrochloric acid in the gastric gland, which is secreted into the stomach, which can make the stomach strongly acidic (pH 1.5-2).

Chief cells are also present in the gastric pits, towards the base, and secrete an inactive proenzyme called pepsinogen. This is converted by luminal acid, into pepsin, an active proteolytic enzyme, which is a protein digesting enzyme which is optimum at pH 1.5-2. Pyloric glands in the stomach are responsible for secreting mucus and controlling acid secretion in the stomach. The glands in the antrum contain G cells, which secrete gastrin, which is directly responsible for stimulating chief and parietal cells to produce their products mentioned above, in addition to exciting stomach wall lining contractions for the mixing and digestion of gastric contents. Pyloric glands also contain D cells, which release somatostatin, the hormone responsible for inhibiting gastrin production, which acts as a feedback control system to ensure proper regulation of stomach contents. The inhibition of gastrin production by somatostatin can be countermanded by neural or hormonal stimuli, to allow for example, the preparation of the stomach for digestion by smell or sight of food, or during the digestion process.

The mucus secreted by the pyloric glands aid in covering the stomach wall, aiding in acid resistance, when combined with the high level of gastric lining proliferation, provides a high level of tolerance to gastric acid. The Oesophageal squamous epithelium however, is much less proliferative and does not produce a mucus layer for protection against acid, it is therefore much more susceptible to damage to stomach contents when refluxed into the oesophagus.

Although there is no precise definition of dyspepsia, it is detailed in medical teaching as an upper abdominal pain, thought to originate from the upper gastrointestinal tract, an occurrence which may arise with or without other symptoms. It has been suggested that the pain is the result of reflux, ulcer or motility based problems, however it could be a combination of these factors; unfortunately these symptoms are very poor indicators of underlying disease. It has been suggested that heartburn or acid reflux associated incidents are the predominant cause of dyspepsia however much of the evidence suggests this is inconclusive, as less than a fifth of reflux sufferers report dyspeptic symptoms. Several UK surveys have suggested that up to 40% of adults have had one or more dyspeptic episode in the last year, half of these surveyed adults reporting the pain to be moderate to severe (Logan et al. 2002). With those moderate to severe pain sufferers, over half were taking drugs for their symptoms, just under half of these being prescribed. A shocking statistic was that within the moderate-to-severe pain group, only 22% had consulted their general practitioner within the last year for this pain; approximately 9% of overall dyspepsia sufferers.

The prevalence of dyspeptic patients is high, however the majority of whom do not have any significant upper GI abnormalities upon investigation; 20% have reflux oesophagitis upon endoscopy, 15-20% have peptic ulcer disease including duodenitis, and a declining 2% present with gastric or oesophageal cancer, although theses are often associated with other indicators. With the number of dyspepsia patients so high, the work for the NHS for dyspepsia and its related treatment is time and cost demanding, with approximately 4% of the population on prescription drugs for these symptoms, which accounted for 10% of drug expenditure in primary care for England and Wales in 1999 (Logan et al. 2002) . Examination of patients presenting with dyspepsia is also costly, with the number of upper GI endoscopies approximately 450,000 in 1996 for England and Wales, nearly one procedure for every one hundred people. The cost per diagnostic endoscopy for the NHS in 2012/13 was £831 (S.D. £208); dyspepsia and abdominal pain is one of the most common reasons for hospital referral (Logan et al. 2002).

Traditional methods of detecting acid reflux is performed by attaching or positioning a pH sensor 5 centimetres above the LOS, however there is much variance in this placement as different studies may use the upper border of the LOS or the peak LOS pressure usually located in the centre, as the starting point for the 5 centimetre measurement. It is well known that the site of mucosal changes associated with reflux oesophagitis and intestinal metaplasia is much more distal than this, often within a centimetre above the SCJ, as the majority of acid is refluxed within a short distance above the upper border of the LOS; Therefore using the 5 centimetre pH measurement is likely to significantly underestimate acid reflux incidence.

A paper in 1976 by Nebel et al (Nebel et al. 1976) detailed the precipitating factors and indicators by way of a questionnaire completed by 446 hospitalised patients and 558 non-hospitalised subjects, aiming to gain a much better understanding of reflux and heartburn; only 121 of the patients were hospitalised at the GI clinic. Of the non-hospitalised volunteers, which comprised of a majority of hospital employees, 7% reported daily occurrence of heartburn type symptoms, compared to statistically significant higher 14% of the hospitalised patients; interestingly 15% of the patients admitted for GI reasons, which is very similar to those admitted to the hospital for any other reason, which included surgery inpatients and pregnancy for which 25% of pregnant women experienced daily reflux; 52% of obsetreic patients reported having at least monthly reflux, higher than other patients which were all about 40% and similar to the controls at 36%.

The study showed no statistical difference between gender, after excluding obstetric patients; the data also suggested age has no impact on heartburn symptoms. For the subjects who had daily reflux, 20 reported that they believed food to be the cause of their reflux, compared to 6 subjects with monthly reflux. The most common foods that the above subjects considered to be causing their symptoms were alcohol, fried or spicy foods; reflux episodes caused or contributed to by these food stuffs were over 80%. It is also noteworthy that 70-80% of daily reflux sufferers documented their belief that the following food items were causative of their symptoms: tomatoes; peppers; oranges; fruit juice and fatty foods. The authors suggested that while reflux may occur within subjects who suffer an incompetent sphincter, those

with borderline sphincter competency may require some specific food related LOS pressure lowering before reflux can occur. The authors also hypothesised that the highest reflux attributed food stuffs: spicy food; fried food and alcohol, may be so, because they directly irritate the stomach mucosa, initiating a reaction; said reaction which has been shown in previous papers which documented the lowering of the LOS pressure by fatty foods and alcohol.

A paper in 2000 published by Ho (Ho & Kang 2000), uses acid perfusion and pH monitoring demonstrated the extent of heartburn or dysphagic symptoms with oesophageal acid exposure in 15 age-matched, mixed gender (eight men) healthy, young volunteers. Oesophageal perfusion manometry was performed following an overnight fast, and 5 manometric parameters were recorded: basal LOS pressure; LOS relaxation; distal oesophageal contractile amplitude; distal oesophageal contractile duration and oesophageal peristaltic performance. An oesophageal acid perfusion test was performed immediately after the manometry test with the manometer still in place and subjects in the seated position. The most distal manometry perfusion hole was placed 5 centimetres above the upper border of the LOS, with an initial perfusion of saline followed by a perfusion of 0.1N HCl for the following 20 minutes or until chest pain. A positive test was classified by two or more chest pain events during perfusion, whereas a negative test was an asymptomatic response. A cathode based pH electrode was then placed at the traditional 5 centimetre position above the LOS, and extended ambulatory pH monitoring was observed for one day, with an event marker to be pushed when they changed posture; a reflux episode was classified as is traditional, by a fall of pH to below 4.

The median LOS pressure was 12 mmHg, distal oesophageal sphincter pressure 91mmHg and the distal oesophageal contractile duration 3.9 seconds. None of the 15 subjects reported pain during saline perfusion however three volunteers reported chest discomfort, within 6 minutes of the start of acid perfusion. For a median of 21 hours of ambulatory pH monitoring, 7.3 of those were in the supine position, presumably during sleep. A total of 366 acid reflux incidents were recorded with 84% of them occurring during the upright position; the longest reflux duration and

the percentage time that the oesophagus experienced pH less than 4, were also statistically greater in the upright, rather than the supine position, however no subjects experienced any symptoms during this period. This study is well performed and clearly shows that so called healthy volunteers still have a large number of traditional reflux episodes, an average over one per hour per subject, and yet do not have symptoms associated with any episodes, that the symptom dependence may be related with the sensitivity of the oesophagus to acid exposure, with similar previous studies suggesting that the oesophageal mucosa could become sensitised by acid. It has also been speculated that the pain response of the oesophagus is related to the hydrogen ion permeability of the squamous epithelium; a theory which has been demonstrated as a low potential difference in patients with reflux oesophagitis, which shows a difference in mucosal make up, but as yet no further evidence is purported.

A paper by Colas-Atger et al two years later reported a 24 hour oesophageal pH monitoring study, only this time with 244 subjects were recruited, with 111 patients presenting with signs of abnormal acid exposure (Colas-Atger et al. 2002). The study's aim was to use conventional pH-metry to establish a symptom association probability, concordance index and symptom sensitivity index. The study again used the traditional 5cm above LOS placement of a nasal catheter based pH probe, which remained in place for 24 hours, with the patients being fed standardised meals. Also all PPI treatment was stopped 8 days before the trial, H2RA and antacid drugs were stopped 48 hours before the trial. Patients used an event marker to log when they had heartburn type pain; with oesophageal reflux defined as traditional pH less than 4 defined by the catheter. Within the oesophagitis-free patients, 36% of subjects had no symptoms; with those with oesophagitis, only 47% of subjects had marked their symptoms correctly so could be subsequently analysed. In the abnormal acid exposure group, 43% of subjects were asymptomatic during the study, with 42% marking their symptoms correctly. Of those patients which were processable, the only statistical significance between groups was based on the length of time symptoms had been occurring, with the chronic oesophagitis patients suffering heartburn the longest; there was no statistical difference between age, frequency of symptoms or type of symptoms between normal and oesophagitis patients. Since the frequency and type of symptom were not statistically different between groups, it

suggests that either the length of time over which symptoms had occurred was the predominant factor for oesophagitis or that some people has a higher susceptibility to oesophagitis given the same exposure. One piece of information that was omitted but would have been very useful, is the strength of the acid during reflux, as the paper only includes the classic definition of pH less than 4; if the exact pH or average pH during reflux was included, this could be analysed to see if the strength of the acid correlates with GORD or oesophagitis.

Neither of these two studies commented on the potential anomaly source of catheter and sensor movement, although their use of the 5 centimetre distance should minimised the likelihood of the probe slipping into the stomach and incorrectly reporting reflux episodes.

In 2004 very thorough study was published in Gut by Fletcher et al (Fletcher et al. 2004), detailing an investigation into exactly this problem, whereby 11 dyspeptic negative subjects were successfully catheterised with a two pH electrode probe, anchored to the oesophageal wall in such a manner so that one sensor was placed 5 millimetres above the SCJ, and the other sensor 55 millimetres away from the SCJ, providing for the first time, a detailed investigation into what was, from then, termed short-segment reflux, versus traditional reflux. The very interesting outcome of the study was the proportion of time the sensors were exposed to acid stronger than pH 4; the 55 millimetre sensor was in an acidic environment a median of 1.8% of the time, however the closer 5 millimetre sensor was 11.7% of the time. This trend was also seen in the supine and upright seated position, pre and post-prandialy. This study showed conclusively that gastric acid exposure is much more likely at the SCJ, accounting for the higher incidence of metaplasia in the most distal segment of the oesophagus; it also showed that traditional 5 centimetre acid measurement greatly underestimated the amount of acid reflux into the oesophagus, so much so, that it was a completely unreliable method of detecting said reflux.

1.3.4 Gastro Oesophageal Reflux Disease

A paper by Boyle et al, (Boyle 2006) published in 2006, highlights the clinical variability and hence difficulties in classifying reflux episodes and hence diagnosing GORD. The paper starts by reminding the readers that reflux in the form of vomiting in infants less than 6 months old occurs daily in about 60% of the population, if defined by using the common drop in oesophageal pH below 4. If these infants were adults they would most likely be diagnosed with GORD, based on the increased frequency of reflux or extended acid exposure in the oesophagus; the only missing symptom being mucosal damage.

The author highlights the theory that TLOSRs are caused by three main mechanisms and are believed to be the reason for reflux: a vagovagal reflex caused by distension of the stomach; a sub-threshold swallow which doesn't trigger full peristalsis or a vagovagal reflex caused by cardiopulmonary receptors. The author highlihts the pathophysiology of GORD, detailing increased exposure to stomach contents; the strength and volume of these materials along with duration of exposure episodes all exacerbate heartburn and damage to the oesophageal wall, which over time leads to GORD. Another note is the inherent phenotype of the subject, an issues raised before, which claims that each individual has a different sensitivity to gastric contents, both acid and other materials, which may account for the fact that some individuals with the same amount of TLOSRs or reflux episodes have GORD while others who are less sensitive, do not. The clinical efficacy of GORD diagnosis in adults is generally by a trial of acid reducing drugs like Proton Pump Inhibitors (PPI) or Histamine-2 Receptor Antagonists (H2RA), where the diagnosis is assumed correct if the patient sees substantial reduction or elimination of reflux or dysphagic symptoms. However other tests for GORD are a Barium contrast upper GI test or tests, intra-oesophageal pH or impedance testing, or endoscopic biopsy. PH monitoring is the considered gold standard, as it enables detection of oesophageal acid for an extended period of time during normal physiological conditions, however with the aforementioned flaws with failure to detect short segment reflux, this technique, unless augmented with other devices, may be severely limited. New

wireless capsules with pH sensors may be used, however the author fails to suggest that they must be placed nearer the SCJ than the traditional 5 centimetres, as although pH monitoring has a high specificity with erosive oesophagitis patients, it must be used more accurately to enhance detection as without the adition of an endoscopy, the accuracy drops to 50%. The paper mentions a relatively new technology called intraluminal impedance, which is used to detect flow of acid, the technique will be described in detail in the following section. The new method has the ability to detect non-acid flow, which has the potential to evaluate the effectiveness of a drug by comparing the extent of acid reflux versus non-acid reflux before and after treatments. The author acknowledges the problem caused by lack of known normal values for acid reflux or even non-acid reflux with which to compare GORD patients with. When treatments such as those affecting gastric emptying, the author suggests fluoroscopy is far superior than any test, in assessing GI motility, however fails to mention high resolution manometry, an established, easy to use and interpret technology which also can investigate GI motility. The author summarises, saying that flouroscpy often provides better understanding than does pH-metry, it cannot be used for extended periods of time or during normal activities. The author draws the conclusion that although pH and fluoroscopy can detect reflux, this may not be directly linked to GORD; further testing such as endoscopic biopsies should be used in addition.

In 2008, Vela wrote a review highlighting the role of non-acid reflux and the pathophysiology of GORD and heartburn (Vela 2008). The paper begins by reviewing the current literature which states that the role of acid in reflux can cause GORD, a belief held by many Gastroenterologists, and for very good reason, as a multitude of studies have fairly conclusively shown this using pH-metry and other investigative methods. Vela then raises the issue that although sufferers of heartburn or dyspepsia often get placed on a common PPI treatment, their symptoms may continue despite there being less acid in the stomach to reflux. The paper introduces the concept of multichannel intraluminal impedance measurement, a catheter probe which can measure liquid or gas flow, and when combined with pH catheters, can give a better understanding about the number of acid and non-acid reflux.

Since the detection of *Helicobacter Pylori* in the GI tract over 30 years ago, the understanding of the relationship between *H. Pylori* infection and GORD has become more complicated and controversial (Ghoshal & Chourasia 2010) . Individuals with H. Pylori infection have a 10 to 20 percent increase in developing stomach ulcers and 1 to 2 percent increase in gastric cancer risk in their lifetime (Kusters et al. 2006), however it is reported to decrease oesophagitis and hence oesophageal cancer by reducing acid excretion (Koike et al. 2001). In an attempt to clear up the controversy, Ghoshal et al reviewed the literature in order to draw some conclusions from years of conflicting research (Ghoshal & Chourasia 2010). The paper begins by reminding the reader that GORD symptoms are often associated with a reduction of quality of life for the patient, especially those who endoscopically visible musocal damage when suffering from erosive oesophagitis, Barrett's oesophagus or other similar disease. In a lot of GORD patients there is no endoscopically visible sign of mucosal damage, where the proportion of this type of diagnosis is high worldwide. As the prevalence of GORD is high worldwide, it is rather common to find *H. Pylori* infection in these patients, however a lot of studies purport that *H. Pylori* may have an inhibitory effect on the development of GORD, or at least may reduce the severity of GORD.

Prevalence of *H. Pylori* infection is lower in developed countries such as North America and Western Europe, in addition, GORD and other upper GI diseases are higher in this population (Ghoshal & Chourasia 2010). Conversely, *H. Pylori* infection is higher in developing countries such as Africa, South America and Asia, with the severity of GORD being lower in these communities. There is also a globally decreasing trend for peptic ulcer disease and distal gastric carcinoma, along with a fall in *H. Pylori* infections, due to increasing hygiene and antibiotic treatment, but a rise in GORD and its complications. From this epidemiological perspective, the author suggests that there is a possible negative correlation between *H. Pylori* infection and the severity and frequency of GORD. Epidemiology based relationship has been well studied in the Asian medical community as different studies from china and Korea have shown that there is an inverse relationship between high *H. Pylori* infection and low incidence of reflux oesophagitis and GORD, with sufferers

often experiencing mild grades of the disease. In Japan, GORD patients are on the increase, however this is correlated with the decrease in *H. Pylori* infection.

There is further evidence based on *H. Pylori* eradication studies, where patients with peptic ulcers are cured of the infection by a course of antibiotics, as this is known to heal the ulcers and decrease recurrence (Ghoshal & Chourasia 2010). Many of these eradication studies have reported an increase in severity of GORD and BO after removal of infection, even in those without peptic ulcers. The increased rate of GORD development and or severity after eradication may be a result of the increased acidity of gastric contents and therefore refluxate, however development of GORD post eradication may indicate underlying motility complications. Two strong studies have shown the opposite, that there is a positive effect on reduction of GORD symptoms after eradication (Peek 2004; McColl 2010) .

One meta-analysis showed although the frequency of GORD was not higher after *H. Pylori* removal among dyspeptic patients, there was two fold increased danger of developing it in those with peptic ulcers versus untreated control subjects (Yaghoobi et al. 2010). In Asian studies, the antibiotic treatment of *H. Pylori* showed the opposite, that removal of the infection improved GORD, possibly due to the normalisation of gastric acidity, or if the ulcers themselves indirectly exacerbate GORD symptoms (Ishiki et al. 2004; Fujiwara & Arakawa 2009); whatever the reason, it is recommended in Japan that *H. Pylori* should be eradicated in GORD sufferers due to the high risk of associated gastric cancer. Gastric acid secretion is known to be changed under the influence of *H. Pylori* infection, which may do so in two ways. Light inflammation in the antrum is associated with the destruction of somatostatin secreting D cells, this removes the feedback loop for gastric acid secretion which increases parietal cell density and hyperchlorhydria which may increase GORD severity. Pangastritis also leads to destruction of the parietal cells of the gastric corpus which causes gastric atrophy with sequent hypo- or aclorhydria; which would reduce acid secretion, decreasing the strength of gastric contents, alleviating GORD symptoms.

Patients with more severe, higher grade GORD are less likely to be subject of a *H. Pylori* infection, as shown by several studies (Clark 2003; Rubenstein et al. 2014),

with some evidence for strain dependant erosive oesophagitis, rather than merely a *H. Pylori* infection itself. Both environmental and dietary factors affect GORD severity, but also physiological factors such as lower LOS basal pressure, delayed gastric emptying, hiatus hernia and other motility disorders are well known in GORD pathogenesis.

There may be genetic factors that influence GORD development and severity, but as yet, there is very little material on this concept; *H. Pylori* resistance or clearance may be related to the patient's genetics as well as bacterial strains. The role of genetics is an up and coming area of research, as a recent study demonstrated a greater concordance for GORD in monozygotic twins compared to dizygotic twins, which leads to the suggestion towards genetic over environmental, even *in utero* development (Cameron et al. 2002), however the author fails to acknowledge the role twin-to-twin transfusion or additional risk factors associated with monozygotic foetuses, such as a higher risk of premature birth associated disease due to a underdeveloped immune system and higher levels of post-natal intervention. Restricted studies have shown some alleles and genotypes are potential risk factors for BO and Oesophageal Adinocarcinoma (Queiroz et al. 2004; Mohammed et al. 2003; de Vries et al. 2009).

The presence of *H. Pylori* triggers the recruitment of leukocytes and over-expression and release of pro-inflammatory cytokines as an inflammatory response at the gastric mucosa, this may be due to materials released or excreted by the bacteria, which may result in the up regulation of inflammatory factors (Tsai & Hsu 2010). These materials may inhibit acid release by disrupting the membrane-cytoskeletal interaction of the parietal cells, reducing acidity of the gastric content and therefore refluxate. Lipopolysaccharides released by bacteria reduce acid secretion via the prostaglandin system and inhibition of H+/K+ -ATPase functional changes or cytoskeletal rearrangements in their subgroups rather than transcriptional down-regulation. *H. Pylori* neutrophil activating proteins can induce neutrophils which create reactive oxygen radicals which may cause damage to the gastric mucosa. As such, some studies have shown (Ando et al. 2006; Chourasia & Ghoshal 2008) genes affecting inflammatory factors, acid secretion pathways and DNA repair pathways

may cause increased reflux incidence. Genetic factors may therefore, account for why some GORD patients having similar number of reflux episodes as non-GORD patients, have more mucosal damage and or dysphagic symptoms, as their oesophageal wall is more sensitive to acid exposure. The author highlights that this material is scarce and in its infancy, so there are other genetic factors which may be associated with the aforementioned or as yet unassimilated pathways.

Occasionally an infection intestinal helminthes, a polyphyletic group of eukaryotic parasites, induces an immune response which may inadvertently clear the body of *H. Pylori* infection; these cytokine polymorphisms have been purported to affect gastritis severity in a range of literature. In developing countries, *H. Pylori* and concurrent helminthes prevalence is high because of low hygiene and living conditions; if an individual in such a country contracts helminthes first they will develop an immune response which limits *H. Pylori* infection, however if the patient has a concomitant infection of both *H. Pylori* and helminthes, the likelihood of which is higher, they might show an intermediate cytokine response, allowing persistent *H. Pylori* infection (Ghoshal & Chourasia 2010). Cytokine profile may be important therefore, to determine the level of gastric wall inflammation and GORD. Goshal concludes that the majority of evidence based studies support the epidemiology evidence that *H. Pylori* offers a protective role against GORD, through genetic factors predominantly via inflammation pathways and DNA repair pathways to a lesser extent. The author makes the interesting point that if potential susceptibility candidate genes can be identified and used for the reliable detection of GORD, they may be employed in a screening mechanism for such genetic markers, decreasing the rate of GORD associated complications.

1.3.5 Oesophageal sensitivity/non-acid heartburn/inconsistent symptoms

A paper by Wallace et al (Wallace & Granger 1996), outlines the different protective pathways of the gastric mucosa, a paper which seems to be overlooked by the above literature, despite making a worthwhile contribution to the Upper GI field (Wallace & Granger 1996). The paper details the role of acid in the stomach which is used to

kill ingested bacteria, with the significant exception of *H Pylori*, the acid is very capable of doing so, as there is an inversely proportional relationship between bacteria levels in the stomach and gastric acid secretion; antigen ingestion also strongly correlates with extended gastric emptying time, allowing longer exposure of the antigen to acid. The main exception to the above is *H Pylori*, which is not only capable of surviving, but as previously mentioned, alters the level of gastric acid by releasing various secretions. The stomach wall is therefore often exposed to very strong gastric acid, so the lining has several adaptations over normal epithelia; the mucus-bicarbonate barrier not only traps bacteria, immunocytes and antigens, it also provides a protective barrier for the gastric mucosa against the high levels of acid which damage less protected epithelium like the squamous oesophagus. The mucus also traps bicarbonates released by the gastric epithelium, which neutralises acid near the stomach wall; this has been supported by the evidence that although luminal pH may be 2, the pH of the epithelium remains near neutral. The gastric pits containing acid secreting parietal cells often have the highest levels of acid, whilst having no gastric mucosal secreting cells in close proximity, suggesting there may be other protective mechanisms for the stomach wall, which is augmented by the mucus-bicarbonate barrier. It is believed that surface active phospholipids act to repel gastric acid as the lining is strongly hydrophobic. The epithelium itself is adapted to the high levels of acid, by very proliferative replacement of the lining every two to four days, with the outer cell layer being extruded into the lumen. It is reported that mucosa replacement occurs from several deep lying stem cells rather than the wall lining itself, so to avoid replication of potentially genetically damaged cell linings, an idea which is supported by tests on the mucosa and submucosa, the latter being damaged much quicker and with a less acidic pH than that exposed to the mucosa. A high level of submucosal blood flow is suggested as another protective method which removes and dilutes antigens and toxins in the epithelium, supported by the increase in blood flow to any areas exposed to gastric irritants or acid. It is therefore believed that the stomach, by process of mucual secretion, quick repair and proliferation, combined with the high vascularity and acute inflammatory response of the lining, provides a good barrier and resistance to high levels of gastric acid.

1.4 Upper GI measurements

1.4.1 Manometric measurement

As mentioned in previous sections, the pressure along the oesophagus, in the stomach and at the LOS are vitally important, and are factors which can correlate strongly with disease and pain, for example TLOSRs allowing acid to retrograde into the oesophagus. Manometry refers to the measurement of pressure usually reported in the units of millimetres of mercury, (mmHg), which in Upper GI research and diagnostics, is done using one of a few techniques, in order to evaluate gastroesophageal pressure and hence motility. Both water perfusion and solid-state techniques are catheter based devices, with a probe being inserted either orally or nasogastriclly, until which point it passes through the upper oesophageal sphincter, through the oesophagus and into the stomach. Initially balloon based devices (Figure 1.5) were inserted at the end of a tube, and the pressure on the balloon at the top of the probe was measured by a displacement of air or fluid along the tube, equating to pressure.

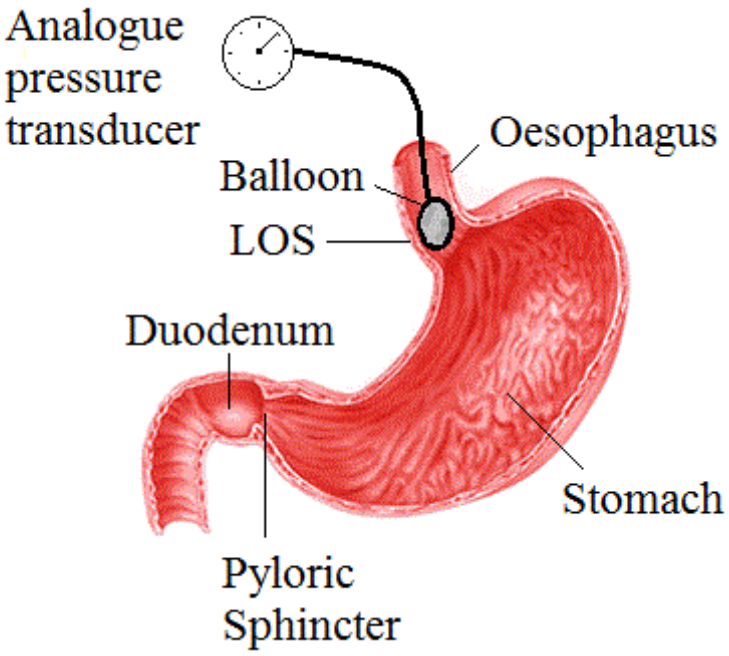

Figure 1.5 Balloon manometer. Pressure from the oesophagus on an in situ inflated balloon measuring LOS pressure. Adapted from Generic look medical encyclopedia (medicalterms.info/anatomy/stomach)

This bought about many concepts which were until previously unknown, as there was no method of investigation of the pressures inside a living subject; ideas of LOS and peristalsis could be investigated, as occasionally several balloons were used concurrently. Following the balloon technique, a perfusion method was developed, whereby a constant flow pneumohydraulic pump is attached to a tube with a narrow bore and hole at the tip; the pressure in the oesophagus or stomach affects the rate at which water can flow through compression of the narrow bore, which can be measured with an external transducer, measuring pressure (Arndorfer et al. 1977). This advancement provided an accurate method of detecting the pressure along the oesophagus, and quickly after their invention, they were widely adopted, with such adaptations as multiluminal catheters, each having their own bore and transducer (Thorpe 1981), as demonstrated in figure 1.6. These transducers can accurately and continuously measure the pressure along each channel, so much so, that the world of Upper GI motility was radically changed, and there were plenty of advances in the

understanding of this area (Wernly et al. 1980) (Lieberman 1988) (Silny et al. 1993) (Kahrilas et al. 1999).

As early as 1957, Botha et al were detailing manometric assessment of the GOJ, using pull through perfusion techniques. In 1975 Dodds et al. devised a method to overcome the disadvantages of conventional station pull-through manometry (Dodds et al. 1975); a rapid pull through technique during suspended respiration, which the author reported to remove artefact caused by respirator LOS and diaphragmatic movement, which more precisely measured the LOS, reporting an average LOS pressure of 24.3mmHg from 12 healthy volunteers, concluding that this technique was more reproducible than station pull through manometry.

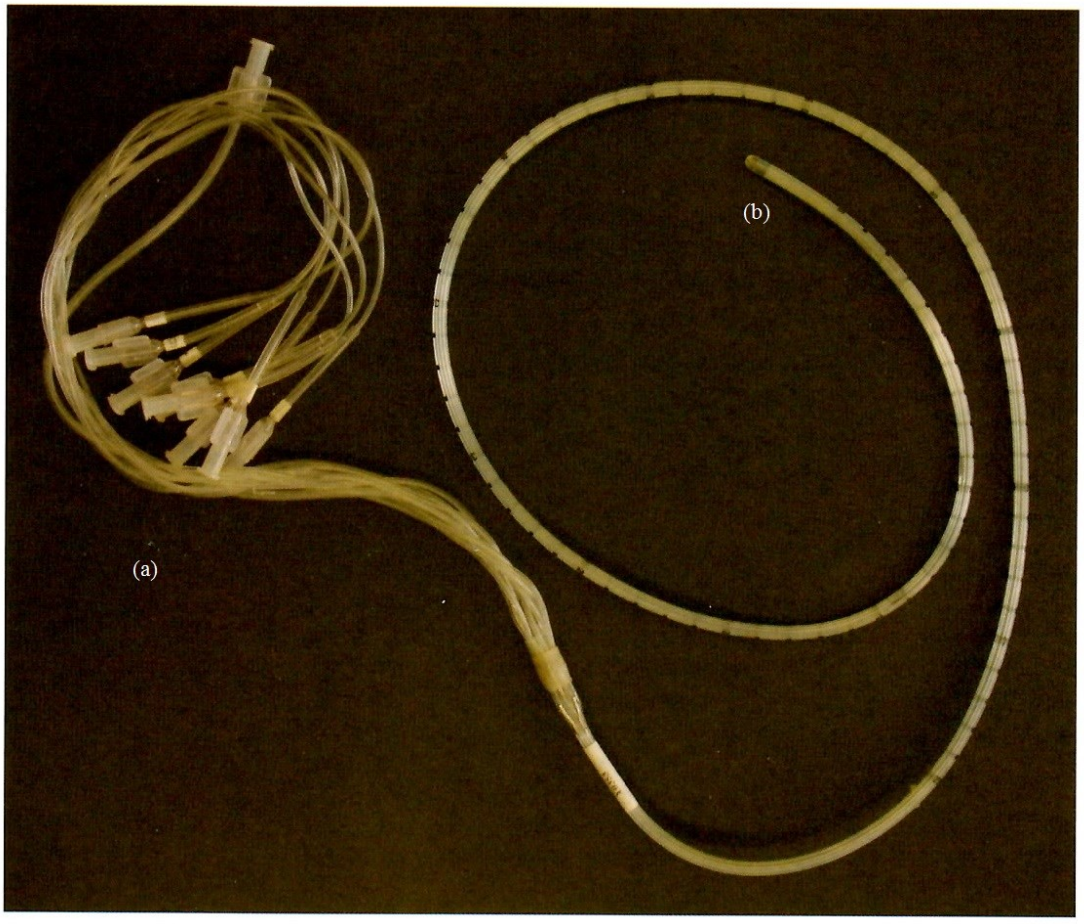

Figure 1.6 Water perfusion manometer, employing 9-channel polyvinyl tubes with side-holes at centimetre intervals. Connectors (a) attach to low compliance water pumps and volume-displacement transducers while the catheter (b) is inserted into

the subject, allowing water perfusion; changes in pressure limit the volume of water that can be released, which is converted to pressure recordings by the transducer. (Conklin et al. 2009).

One year later Dent reported a new technique for continuous sphincter measurement (Dent 1976), consisting of a validated 5 centimetre perfused side hole sensor sleeve, which allowed the detection of the maximal LOS pressure, free of artefacts associated with single sensor arrangements. Arndorfer and Dodds subsequently offered an improved infusion system consisting of a hydraulic capillary infusion system (Arndorfer et al. 1977), having low compliance; this 0.6 millilitre per minute enhanced result accuracy and minimised high-infusion rate associated over-watering of the oesophagus and stomach. A paper in 1980 by Goodall et al. published in Gut, reviewed the accuracy and repeatability of stationary pull through against rapid pull through, concluding that due to the high inter- and intra-volunteer on the same or different days meant that rapid pull though manometry was highly unreliable at this time; there was also no correlation between LOS length measured by this against stationary pull through techniques. The paper summarised that difference between this and the 1975 paper by Dodds et al, was merely lower infusion rates used for this study; in order to avoid flooding the oesophagus with perfused liquid. The author also noted that single hole perfusion may suffer artefact due to the asymmetry known to occur in the LOS as previously reported by Kaye and Showalter in 1971 (Kaye & Showalter 1971), possibly accounting for the large intra-patient variability. Multichannel manometers can provide detailed insight into the workings of the upper GI tract, the output from several sensors is portrayed on a pressure-time graph, in height order, so to best represent the pressure profile of the oesophagus and stomach, shown in figure 1.7.

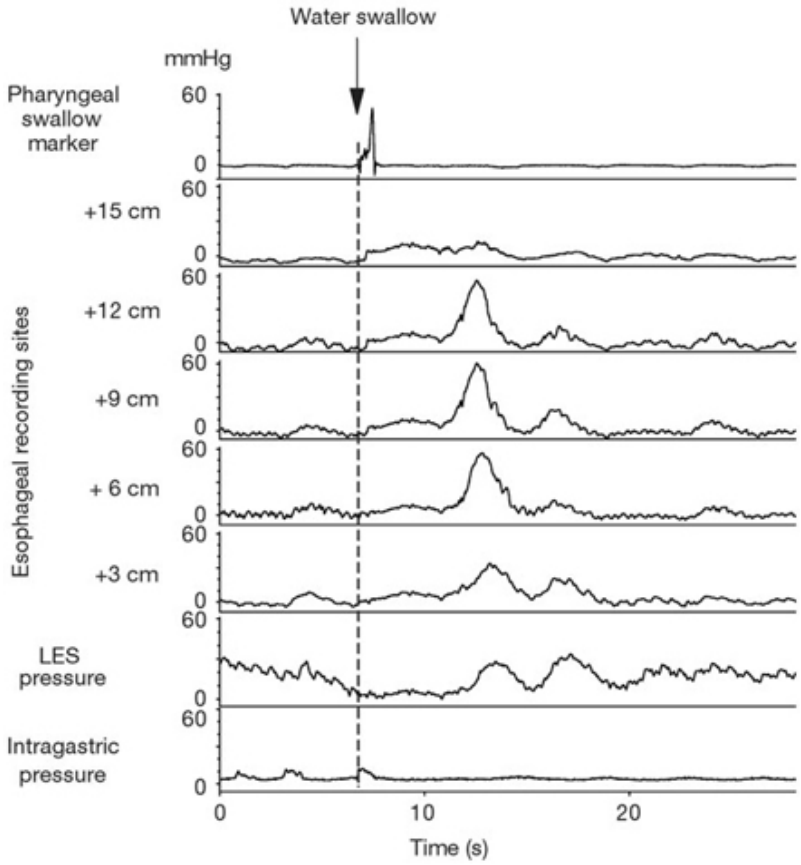

Figure 1.7 Pressure output from 8 channel perfusion manometer. One sensor has been positioned to detect intragastric pressure, another straddles the LOS, while the remaining sensors are placed at 3 centimetre intervals above this. (Conklin et al. 2009).

Today, a lot of medical centres and hospitals use perfusion manometry for motility testing as if it reliable and easy to use, however there are limitations; the limit of size of the overall catheter limits the number of lumens available within the probe, limiting the amount of information detected, even with areas of more dense holes which are placed at important landmarks such as the LOS. To counteract this limitation, pull through manometry was developed, which used a single or multichannel perfusion manometer, being pulled out of the oesophagus after full insertion, to detect the pressure along the full length of the oesophagus, however there were limitations of this technique too, as the tube had to be reinserted for each pull through manoeuvre and the pressure profile was subject to changing mid-pull through, in the event of a swallow or TLOSR.

The initial release of Micro-Manometry devices in 1996 (Holloway 2006) allowed a greater resolution of water perfusion devices, up to 1 centimetre apart, although often only this higher resolution in a small section of the catheter (Figure 1.5).

One such paper by Bredenoord et al in 2003 (Bredenoord et al. 2003), reinvestigated the Pressure Inversion Point, which is defined previously by pull through manometry as the polarity of pressure changes due to respiration; this transition is usually associated with the transition between the thorax and abdomen, and often attributed to the position of the diaphragmatic hiatus. The validity of this concept was tested using stationary perfusion micro-manometry. The study was performed on 6 healthy volunteers and 6 GORD patients without hiatus hernia. The paper rather controversially suggested the pressure inversion point (PIP) was caused by the high pressure zone sliding along the sensors rather than the abdominal-thoracic transition.

Bredenoord also published a paper in 2005 comparing the sleeve sensor against the perfusion micro-manometer (A. Bredenoord et al. 2005). This paper highlighted that sleeve sensors were at the time, the gold standard for detecting TLOSRs, as the sleeve system measured only the highest pressure along the length of the catheter, it was almost artefact free; this paper providing the first insight into detection of TLOSRs with this micro-manometer (MM). 12 subjects with GORD were subjected to a 90 minute postprandial manometric investigation, which combined impedance, pH and micro-manometer catheters, underneath a sleeve sensor. 145 TLOSRs were detected in total, with 117 micro-manometrically detected events and 108 sleeve sensor detected events, demonstrating no statistical difference. Based on these findings, the author concluded that MM was no less accurate at detecting TLOSRs than using the gold standard sleeve sensor.

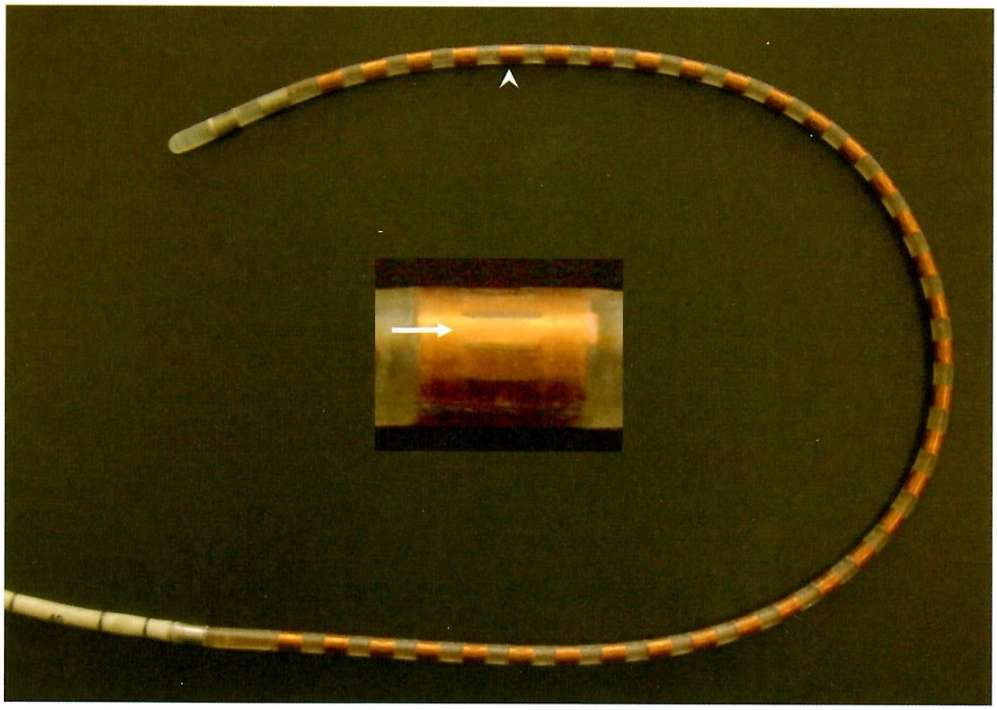

Figure 1.8 Solid State High-Resolution Manometry catheter. Showing a close up of a capacitive radial sensor; the sensors are placed 1 centimetre apart with a total sensing length of 36 centimetres. Adapted from (Conklin et al. 2009).

The advances of technology have paved the way for a new generation of manometers, these devices use solid state pressure transducers placed inside the lumen of a flexible catheter, which can be inserted nasally or orally and used in the same manner as perfusion devices; these offer a significant advancement of many more sensors inside the body. Each sensor averages the pressure from 12 radially placed circumferential transducers; these sensors are placed 1 centimetre apart in the catheter lumen, and 36 of them line the oesophagus and stomach, allowing for the first time, full detailed information on peristalsis and other motility interests (figure 1.8). The sensors along with associated software on a desktop computer, records the data from each sensor and calculates the pressure profile along the upper GI tract several times a second. The information is then plotted on a colour contour plot, where red areas are displayed for high pressures and blue for low pressure; this colour versus time plot allows for very easy interpretation of very complicated anatomies with little training (figure 1.9).

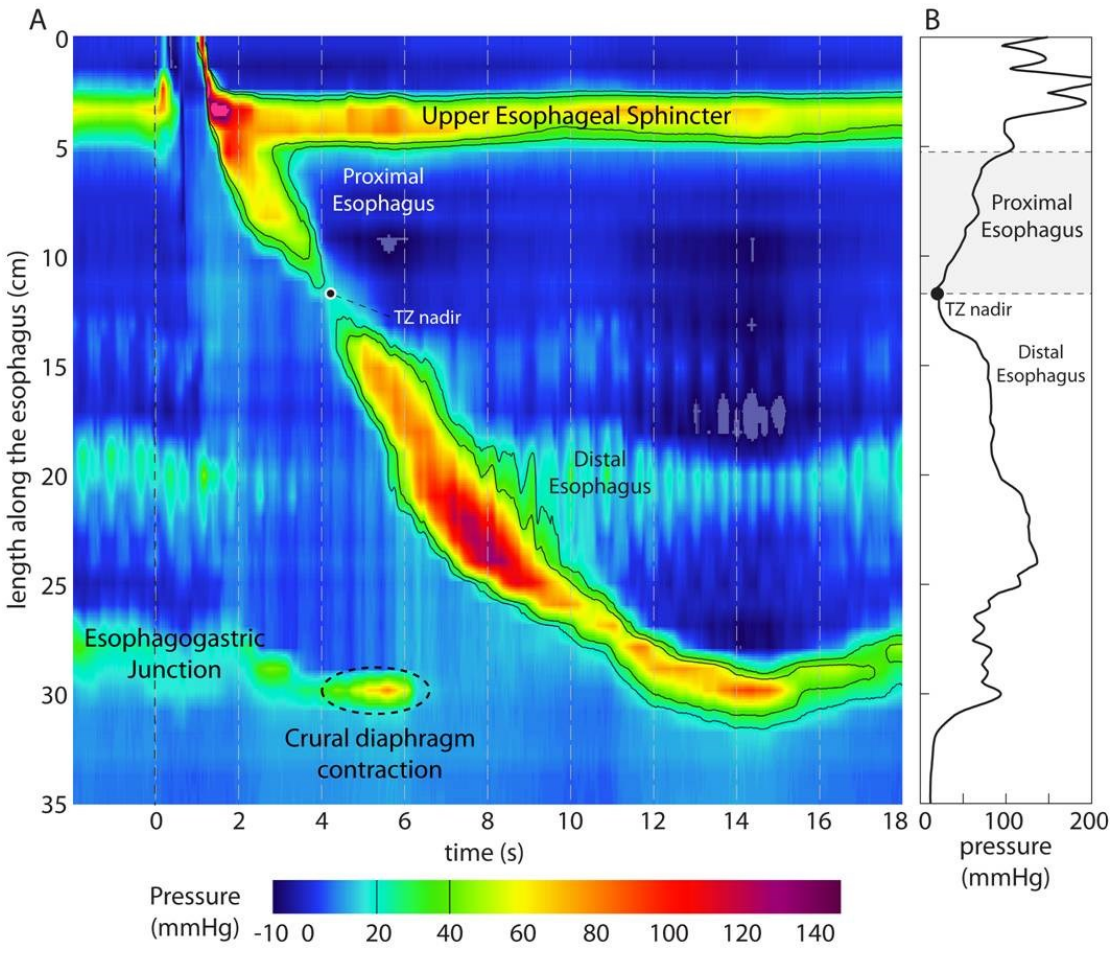

Figure 1.9 An example colour contour plot of the output of a high resolution manometer during a swallow, A, the pressure along the oesophagus at a specific time is also shown, B, which allows approximation of LOS measurement and other anatomical features.(Pandolfino, Ghosh, et al. 2006)

Due to the high density of sensors, the devices are know as High Resolution Manometers (HRM) and are available from a few different manufacturers; although available since their release, they have been relatively expensive, more delicate and harder to sterilise compared to water perfusion manometry. Despite this, the first recorded paper using HRM was published in early 2000 (Janiak et al. 2000), closely followed by another by the same author (Janiak et al. 2001); the mid-2000s soon saw a significant rise the number of papers published about studies using HRM, and soon perfusion manometry was out of fashion for researchers.

Initially papers were produced which retested previously researched concepts, repeating perfusion based studies with HRM, partly as a makeshift validation of the new technology, partly to inject new life into certain research topics but mostly to take advantage of the increased resolution and to demonstrate advance in data presentation, a significant improvement over the chart based output from perfusion manometry, the simple line graphs from which were difficult to interpret and understand; this advantage is clearly shown in figure 1.9.

One such paper by Bredenoord et al in 2003 (Bredenoord et al. 2003), reinvestigated the Pressure Inversion Point, which is defined previously by pull through manometry as the polarity of pressure changes due to respiration; this transition is usually associated with the transition between the thorax and abdomen, and often attributed to the position of the diaphragmatic hiatus. The validity of this concept was tested using stationary perfusion micro-manometry. The study was performed on 6 healthy volunteers and 6 GORD patients without hiatus hernia. The paper rather controversially suggested the PIP was caused by the high pressure zone sliding along the sensors rather than the abdominal-thoracic transition.

Bredenoord also reviews the literature of HRM and MM (Bredenoord 2007), although in this paper he uses the term HRM for both solid state and perfusion, although for this thesis, the terms above are used to avoid any confusion. Bredenoord makes the initial observation that both water perfusion and solid state manometry are reliable within limits, he makes the observation that while water perfusion devices are relatively robust and cheap, pressure artefacts can occur with capillary bubbles or obstructions; solid state HRM is capable of detecting rapidly changing motor activity of the pharynx and oesophageal sphincters as the sensors used are quicker to respond to changes in pressure. The problem of measuring LOS relaxation with a traditional single perfusion based sensor is overcome with the addition of a sleeve sensor, or with 1 centimetre spaced solid-state sensors or perfusion holes. The author highlights the importance of this higher resolution at 1 centimetre placement, however he subsequently acknowledges the improvement of speed and ease of use with solid-state HRM, removing the need for pull through techniques or specific placement around high density perfusion sidehole spacing; the only disadvantage that is noted

by the author is the relative cost of the solid state HRM system over water perfusion systems. A clinical benefit of solid state HRM, is the ability to identify a hiatial hernia, as the LOS and diaphragm can be detected separately observed. This high resolution ability has been used to demonstrate several useful phenomena, the positive correlation between this spatial separation and: increasing waist circumference and/or increased reflux episodes. Another advantage of solid state HRM is that it allows simultaneous measurement of the upper and lower oesophageal sphincter, which is advantageous in peristalsis studies. While the amount of research performed using HRM is on the increase, its use is still not clinically essential in diagnosing hiatus hernia, motility disorders or GORD diagnosis, making it more of a research tool than a diagnostic device. Some studies have shown that, when using HRM versus traditional manometry, HRM is capable of better prediction of ineffective bolus swallows, when using the gold standard barium fluoroscopy as a control, which shows the clinical potential for motility studies. The author concludes with stating that although HRM is not used widely, it offers better accuracy and much more simple operation however it may be cost that is still limiting its clinical use. One thing which is very clear is the research performed using HRM has significantly advanced the understanding of the upper GI tract pressures and its diseases, which is directly important and useful to clinicians in the area.

Bonavina et al suggested in 1986 that LOS length was important for maintaining the GOJ anti-reflux barrier (Bonavina et al. 1986), something known today to be very true. Bonavina described the sphincter, usually between 3 and 4 centimetres, but that a sphincter of less than 2 centimetres was much less capable at stopping reflux. A paper by Pandolfino in 2006 attempted a similar study (Pandolfino, Ghosh, et al. 2006), updating the detail of the GOJ and TLOSRs in 75 healthy asymptomatic volunteers using solid state HRM; however one small but important omission was made in the study protocol. Manometric calibration was performed, presumably according to the manufacturer's instructions, with a thermal compensation applied after the study was competed; it would be more appropriate and accurate to calibrate the temperature at 37 degrees Celsius than to apply a correction afterwards. The author misinterprets the accuracy of the device according to the manufacturer's definitions, stating that it is accurate to within 1mmHg; this is incorrect as the

manufacturer states that the accuracy is +/- 1mmHg, (Sierra Scientific n.d.) which is in fact within 2mmHg. The manufacturer also states that there is a small degree of drift or unmeasured pressure change per minute of use, which is not mentioned at all by the author, however while the author does mention that the drift is linear, states that it is thermally dependant and that the compensation function of the software, completely corrects the errors within the system, a statement which is questionable at best. Another source of error is the software, both Manoscan, the associated software (Given imaging, USA) and Mathworks Matlab (USA), which interpolates and smoothes the data for smarter, prettier presentation, however both smoothing and interpolation add sources of error.

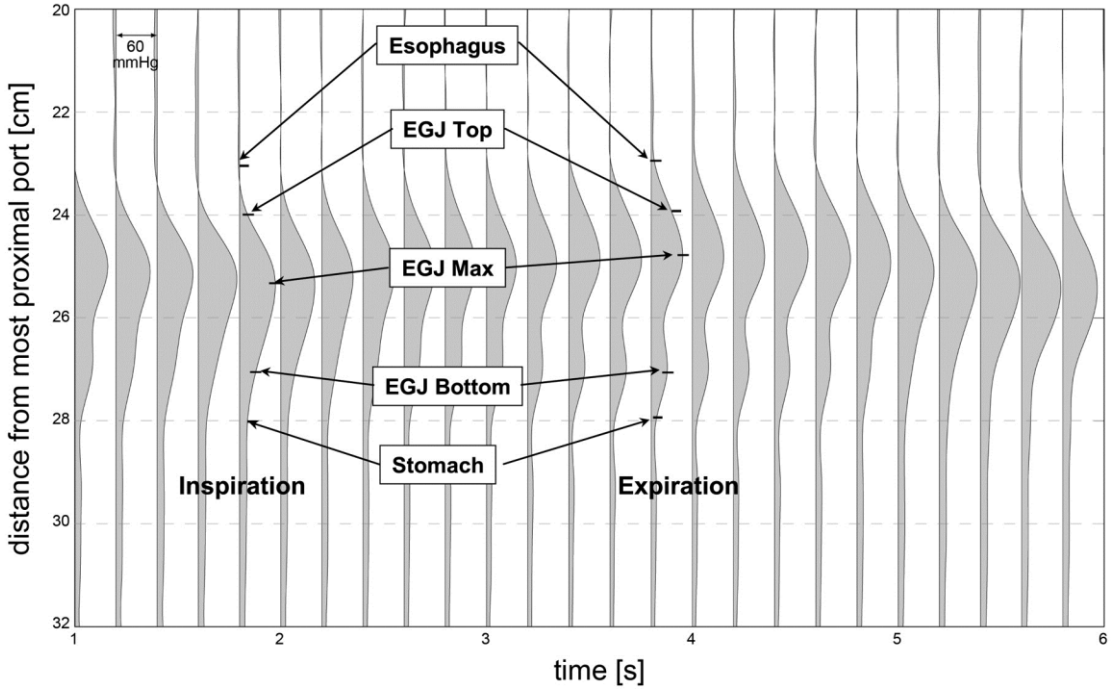

Figure 1.10 Image demonstrating the definition of the >2mmHg step up point used to define the LOS. While the EGJ or GOJ bottom and top are of lower pressure than EGJ(GOJ) max, they still are of greater pressure than the oesophagus or stomach respectively. (Pandolfino, Ghosh, et al. 2006)

The author continues, detailing the anatomy which has been detected by the HRM; with the proximal and distal border of the GOJ defined as a change greater than or equal to 2 mmHg per centimetre step up relative to intraoesophageal and intragastric pressure respectively, which with the actual error of the system, could be out by a

centimetre or more on either side, causing the significant over- or underestimation of the LOS length; this is shown neatly in figure 1.10, with EGJ Top and EGJ Bottom defining the LOS position. Unfortunately, this has become the standard for defining the proximal and distal borders; with a system inaccurate at these levels, there is inevitably going to be large errors, leading to further error when using the measurements to correlate to other motility or disease factors. The errors used to calculate statistical significance are too small due to the misinterpretation of the system's error, therefore the overall study and many others like it, have questionable results purely due to HRM, even if the studies themselves are very well planned and executed. The author concludes in summary, that the solid state manometer provides a seamless precise method of measuring the upper GI tract; while it is true that HRM offers a very compact and easy to use system, it is not without limitations, such as those mentioned above, introducing several sources of error.

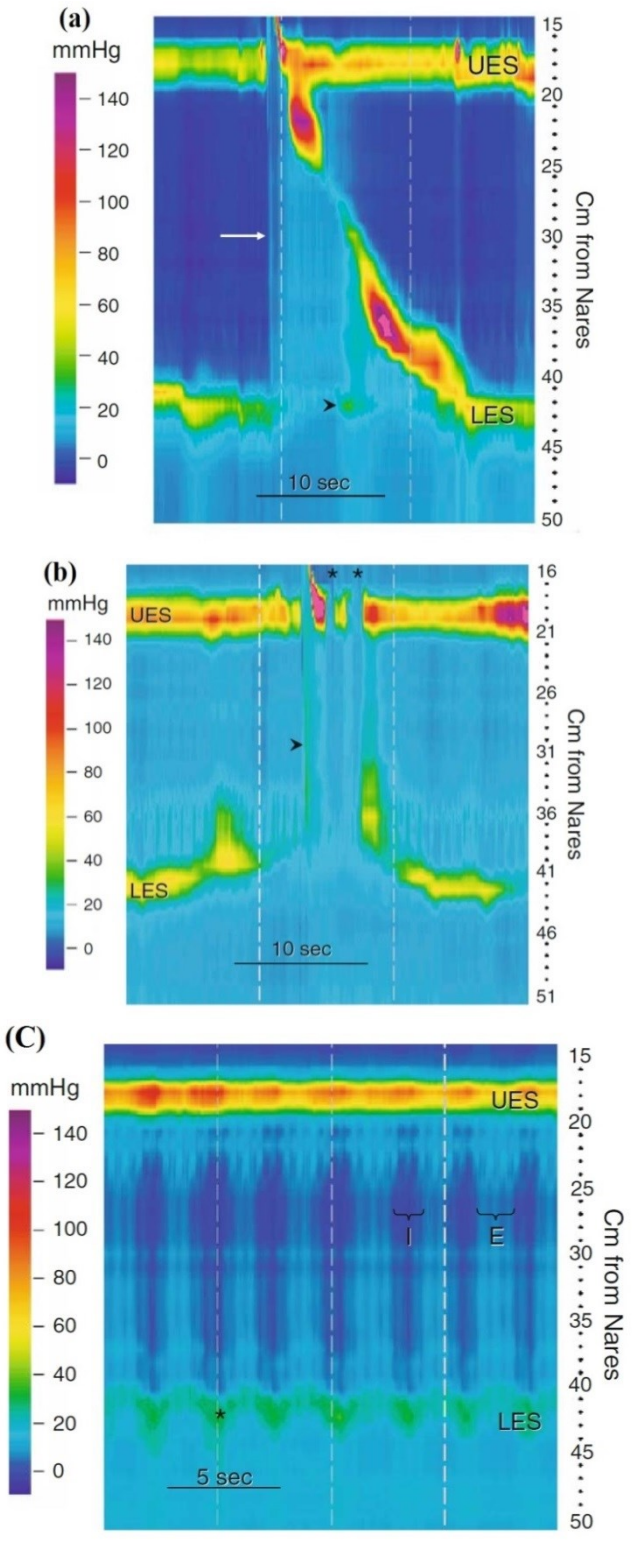

Figure 1.11 Manoscan high resolution manometry Images. (a) normal swallow; (b) swallow associated TLOSR; (c) sphincter tone at rest, demonstrating I, inspiration and E, expiration and the associated changes in LES/LOS pressure accordingly.(Conklin et al. 2009)

By way of example in figure 1.11, the comparison is shown between resting sphincter tone, a healthy swallow and a TLOSR, using a Manoscan High resolution Solid state Manometer, with 36 sensors, being displayed on the Manoview analysis software. The software interpolates the pressure along the oesophagus between each sensor, providing a smoother view using the colour plot; with the pressures of important anatomies potentially being inaccurately reported up to 1 centimetres, meaning detailed measurements of anatomies is inexact by as much as 2 centimetres (figure 1.12). In figure 1.12, the error of ±1 centimetre causes the underestimation of the LOS step up and step down point by 3 centimetres; the measured inaccurate measurement predicts the sphincter length to be 3 centimetres long (step up points at sensors 4-5 and step down at sensors 7 to 8) whereas the actual pressure indicates the sphincter length is 8 centimetres (step up point between sensors 1-2, step down point between sensors 9-10). The interpolation of several data points can cause error in anatomical estimation, as the actual pressure between two points is unknown, the interpolation used in the Manoscan software to produce attractive colour contour plots assumes a smooth transition between two pressure points which can again cause sphincter length inaccuracies as shown in figure 1.13. Interpolation could add to error in sphincter length calculation by over or underestimating the position of pressure in between sensors; as the pressure between sensors is unknown, detailing it as smoothed colour contour plots is introducing a source of error.

In addition to this, in a paper by Thorpe in 1981, the author raises his concerns not only about the fragility of the equipment, but the susceptibility of the sensors to thermal drift (Thorpe 1981); a problem which in the Manoscan system at least, was not resolved, as figure 1.14 shows; the removal of the manometer after an hour long study, leaving distinct and variable pressures when the probe was held in mid-air immediately after extubation. The device is often used for as little as 20 to 30 minutes for clinical investigation, and little drift appears after this time, however some research studies have used the manometer in a subject for as long as 3 hours; the pressures visible are in some cases higher than the LOS pressure itself, calling into question any recorded pressure measurement using this device for longer than 30 minutes, some of which are now clinical definitions, therefore it is vitally important

to understand the extent and nature of this drift, as well as devising a method to correct it.

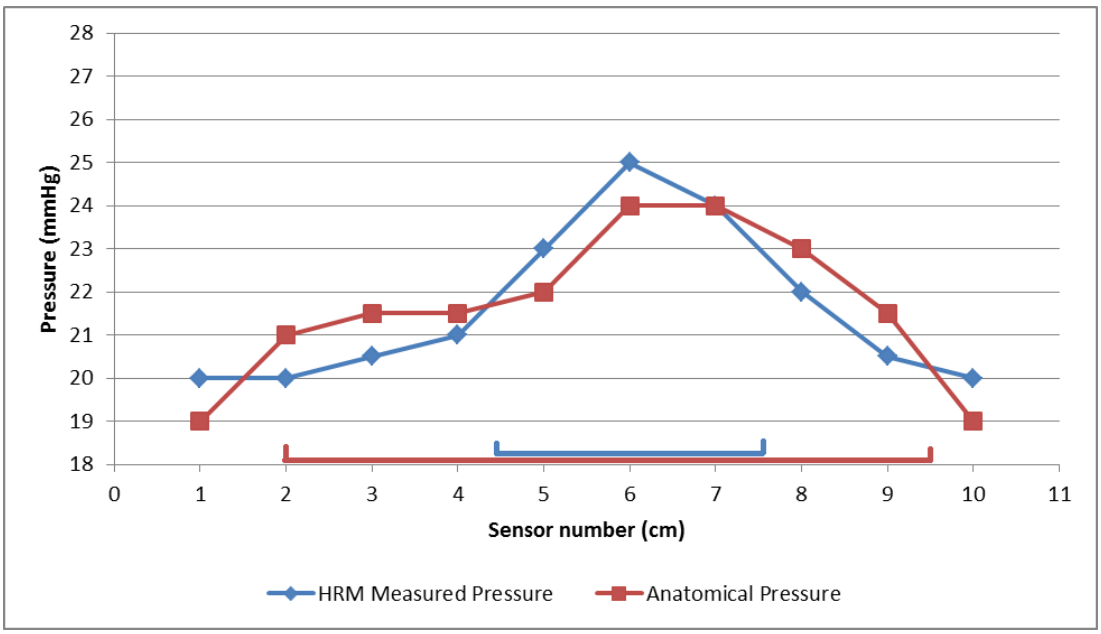

Figure 1.12 Introduction of error caused by sensor error. The would-be calculated sphincter lengths from simulated data are shown at the bottom of the graph to illustrate the effect of sensor error could have on the accuracy of the sphincter length measurement.

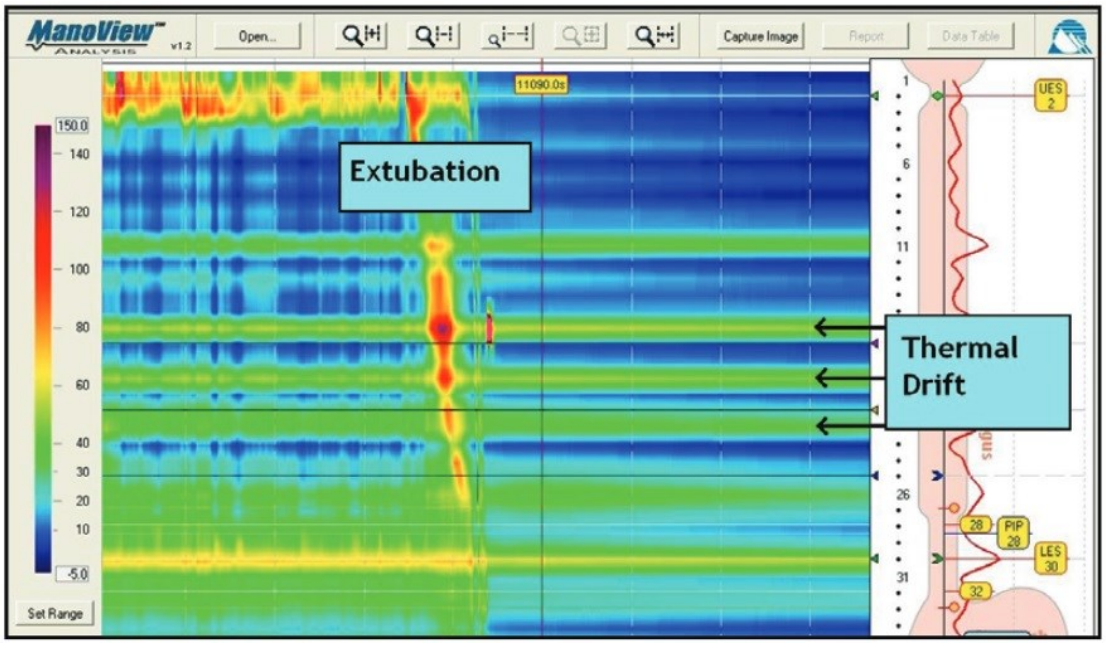

Figure 1.13 An example of the Manoscan HRM thermal drift. Green and yellow indicates high pressure, however after extubation there should be no pressure recorded, demonstrating individual sensor's drift.

Another problem for clinical definitions, is the inherent accuracy of the manometer, which is stated in the user guide to be +/- 2mmHg, and in the research world, the consensus for the pressure step up from the stomach to the LOS or oesophagus is 2mmHg, which is within the range of error for two adjacent sensors, meaning that any step up point used could be more inaccurate that 1cm, a substantial error when considering the length of the sphincter may be as little as 2 centimetres.

Problems in definitions with accurate perfusion being applied to less accurate HRM which is outside the sensors accuracy + drift means really cannot use the same markers (2mmHg step up for example).

1.4.2 Acid measurement

The role of acid in the stomach was discovered in the 1820s by William Beaumont, a surgeon in the United States Army, who became known as the father of modern gastric physiology for his research in the field. A shooting accident left Alexis St.

Martin with a hole in his stomach; Beaumont treated Martin for his wounds, leaving him with a fistula into his stomach, which allowed Beaumont to take gastric secretion and chyme samples at regular intervals, leading to the discovery of gastric acid, and its importance in digestion, which had previously been thought of as a mechanical breakdown. These findings were published in 1853 entitled *Experiments and Observations on the Gastric Juice, and the Physiology of Digestion.*

By the 1870s, the study of gastric acidity had developed, and the use of a test meal was developed to measure acidity and other gastric contents. The test meal, a high carbohydrate food, was given to subjects, and every 15 minutes, 10 millimetres of gastric fluid was removed (Lawrie & Forrest 1965). The pH of the removed contents was then titrated to determine its acidity, plotting a chart of acidity against time allows for the identity of the acidity curve, which highlights normal, hypo- or hyper-secretion. The paper Lawrie and Forrest conclude that the tests are neither precise, quantative or reproducible; it is also evident that the test is not a continuous measurement, and that movement of the tube may account for the poor reproducibility; it was also hypothesised that stronger food stimuli may provide better secretion results.

1.4.3 pH and sensors

pH is a scale of how acidic or alkaline a solution is; the scale itself is unitless and is directly calculated from the hydrogen ion concentration in a solution. The scale ranges from 0 (strongly acidic) to 13 (strongly basic or alkaline); the scale is logarithmic, with pH 7 being that of neutral water. pH measurement is usually performed using electronics which have a transducer which is sensitive to hydrogen ions. Typically a pH sensor consists of a pH sensing element, a temperature sensor, and analysis electronics which displays the value. The sensing element essentially is the combination of a reference or negative electrode, and a positive recording electrode; a voltage or potential difference arises between the recording and reference electrodes due to the presence of the hydrogen irons, which can be measured and displayed to the user. Calibration and temperature compensation are required as the output of the electronics is proportional to the hydrogen ion

concentration and temperature, the former requiring calibration between the voltage output and known pH solutions so that the pH meter is accurate throughout the sensing range. Analogue pH sensors and pH sensitive litmus paper are also ways of measuring pH however in the Gastroenterology world, only glass and antimony sensors being widely used (Tutuian & Castell 2006); figure 1.14, shows an antimony pH catheter and an antimony wireless pH sensor.

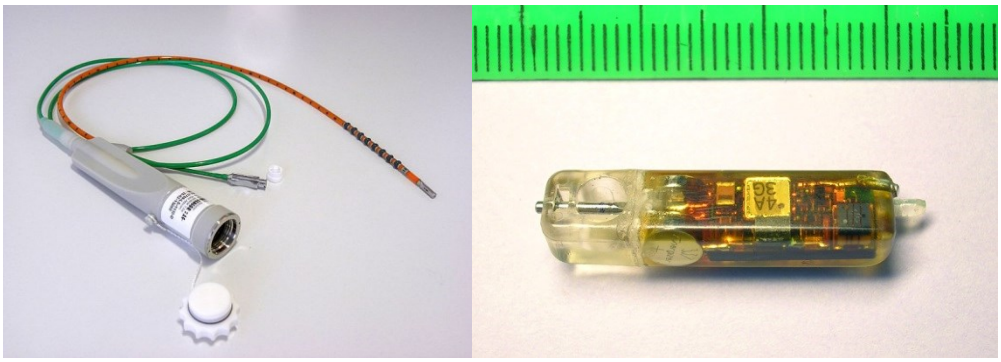

Figure 1.14 pH sensors used in Upper GI clinicians and researchers. Top Left - A commonly used multi-channel antimony pH sensor (Unisensor AG, Switzerland). Top Right – A wireless Bravo Capsule, pH sensor (Given Imaging, Israel).

In 1980, DeMeester et al, published a large paper concerning 24 hour Oesophageal pH monitoring, describing in detail the technique used and describing the results from a 393 subject study. Of the 393 patients, 199 had typical reflux symptoms, with others having a variety of dyspeptic symptoms, including thoracic or abdominal disease and some whom have undergone an antireflux procedure which failed to improve symptoms. Each patient's symptom severity was graded from 0 to 3 for reflux symptoms, performed 24 hours before the test; the patients also reviewed their own symptoms severity. 308 patients had an upper endoscopy at this time, determining and subsequently grading oesophagitis if present.

According to the paper, a 24 hour oesophageal pH study at the time of publication, uses a calibrated number 39043 Beckman pH electrode, at the end of a catheter, inserted thorough the subject's anesthetised nose and placed so the electrode is 5 centimetres above the distal LOS. This procedure is performed after a standard

oesophageal motility study, and the location of the LOS is determined for pH electrode placement, however the paper does not go into any detail about how this position is marked or known after the motility study is completed, highlighting a potential flaw in the positioning. A reference electrode is placed and secured onto the patient's forearm, with liberal amounts of electrocardiographic paste to ensure good conductivity for grounding. The equipment is plugged into a digital display meter and strip chart recorder via isolation. Coffee consumption and smoking are prohibited during the study as they are known to increase reflux episodes; a normal diet is prescribed with food and drink required to have a pH between 5 and 6; after completion, the pH sensor is advanced into the stomach to detect gastric pH levels. The technique enables 72 hour monitoring without equipment failure, patient intolerance, although not mentioned, ethical approval may not be granted for this length of time for a research study. Patients are asked to remain upright while awake, record any dyspeptic events or coughing during monitoring, and also note start and end time of eating. Acid reflux is classified as a drop in oesophageal pH to less than 4; the percentage time of oesophageal acid exposure is then calculated, and due to the patients recording posture etc, can be correlated with different events and postures. The ability of the oesophagus to clear acid can also be evaluated, by measuring the number of incidents of oesophageal acid exposure lasting longer than 5 minutes for a given duration. Measurements of oesophageal alkaline exposure can also be calculated, with the same method as acid, but using a cut off of pH greater than 7.

The 24 hour pH score is then calculated via a look-up table, values of which were determined by a rather small group of 15 asymptomatic volunteers, and if the pH factors such as duration of exposure to acid and number of reflux events, are outside two standard deviations of the normal group, then a positive acid test is given; this is performed in a similar manner, for alkaline pH score, which means that some patients may have positive acid and alkaline tests. The test sensitivity is 90.3%, so false positives should be expected in a small number of patients in a study of this size.

73% of the 199 typical reflux patients had a positive 24 hour pH recording, 64% of the 199 had endoscopic oesophagitis. The percentage of patients with other disorders

was fairly high, ranging from 46 to 68% of the groups; the number of patients with both oesophagitis and a positive test was slightly less, ranging from 24% to 73%. There were a very small number, 19, of patients with oesophagitis but a negative pH test. The author concludes that this method is a reliable and valuable method for determining the presence of acid reflux, which arose from a research tool into a clinical diagnostic tool. The author adds that the test is well tolerated, adding that without a pH test, a clinical would incorrectly diagnose reflux 45% of the time based on symptoms alone, highlighting the value of this test. The author states that the current method for reflux diagnosis is endoscopy, however is it rather insensitive for reflux detection due to the lack of pH detection equipment and large inconsistency between endoscopists, relying instead upon the detection of anatomical features or biopsies which suggest reflux, such as hiatus hernia presence, the angle of His and or oesophagitis. The author finally suggests that in 50% of 24 hour pH tests acid positive subjects, an antireflux procedure will relieve them of their symptoms.

The one cause of concern with this test is the lack of detail regarding the acid reflux events; the author makes no note of what pH is, other than it is less than 4. It is a safe assumption to assume that exposure of pH 1 on the oesophagus will be more damaging than a similar duration of exposure of pH 4, however this is not accounted for in the test. It would be interesting to determine if a short duration of pH 1 exposure would be more damaging than a long exposure of pH 4; due to the logarithmic nature of hydrogen ions along the pH scale, one might predict that a stronger acid, with substantially more hydrogen ions, would do more damage over a shorter period of time. It is also not noted what problems a positive alkaline test would show, as a near neutral pH of 8, may not have any damaging effects on the oesophagus or stomach.

Litmus Paper has also been used to measure pH of liquid for decades; it has also been used for the measurement of intragastric pH, predominantly in the Intensive Care Unit (ICU), where maintenance of gastric pH of greater than 3.5 is recommended in those with upper GI bleeds or ulcers (Rastegarpanah & Mojtahedzadeh 2007); the Medicine and Healthcare products Regulatory Agency

(MHRA, UK) recommend the confirmation of Naso-Gastric tube placement in the stomach with pH paper.

Litmus paper has been tested against pH sensor testing the obvious advantages of pH sensors being they can remain in place, allowing continuous monitoring, without the handling of gastric juice; the increase in sensor complexity allowed for the simple reading of pH via digital output, removing the sources of error from misinterpretation of pH paper reading. Due to the need for two tubes, one for feeding one for placement confirmation when using a pH sensor, litmus paper recording remains in the ICU, due to the increased risk of oesophageal or gastric bleeding associated with increased stress and intubation trauma when using two tubes.

A paper by Neill and Ahern published in 1993 compared the agreement between multiple-band litmus paper using aspirated versus a meter-read probe located in the tip of an NG tube (Neill et al. 1993). The paper shows a good correlation between the two methods' recorded pH, while the nurses greatly favoured the meter-read probe, citing reasons such as speed, safety and accuracy; this preference also grew with time.

A very similar study by Levine et al the following year, tested the efficacy of a H_2 antagonist receptor on gastric pH (Levine et al. 1994). A graphite-antimony pH probe was employed to continuously measure the gastric pH after initiation of the drug, with pH sensitive litmus paper used to measure gastric pH at 1, 2, 4 and 8 hour intervals. The correlation between the two pH measurements was very strong, concluding that both techniques were accurate at measuring gastric pH, stating that the aspiration-litmus test was the preferable method, due to the need for double intubation of pH probe and NG tube; presumably Neill et al's combined NG and pH catheter was not available or known about by the authors for this trial.

Some years later, expanding on their collaborative work with Neill et al, on the combined pH and NG tube in 1993, Rastegarpanah et al published further details of a Naso-Gastric tube which contains a pH sensor at the distal end, shown in figure 1.15 (Rastegarpanah & Mojtahedzadeh 2007). This allowed the advantage of needing only one NG tube that both feeds the patient and confirms the correct positioning of the

tip, while continuously monitoring gastric pH if so desired. The device trial of 20 patients showed a good correlation between litmus pH recording and the silver-silver chloride sensor pH recording, showing that the device was capable of measuring at least as accurately and was technically simple; providing a good alternative to litmus paper, while reducing the stress of double intubation.

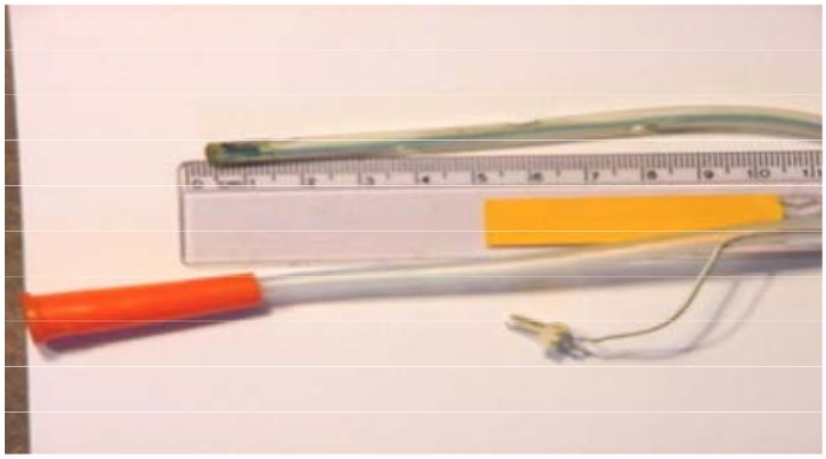

Figure 1.15 Nasogastric tube with integrated pH sensor. (expanded view for demonstration) (Rastegarpanah & Mojtahedzadeh 2007)

Several papers list the use of a single glass pH electrode inside a catheter which is placed inside the oesophagus and placed between 4 and 6 centimetres above the SCJ, which allows for the traditional acid reflux detection (DeMeester et al. 1980; Colas-Atger et al. 2002; A. Bredenoord et al. 2005; Scheffer et al. 2010), however more recently single antimony sensor catheters have been used for the same purpose (Murphy et al. 1989; Castell et al. 1992; Ho & Kang 2000). A review paper by Pohl in 2009 outlines the differences between glass and antimony pH sensors (Pohl & Tutuian 2009), suggesting that a sensor made from glass offers a faster *in vitro* response to a change in pH than does antimony; glass also offers less drift and better linearity to a range of pH. *In vivo* use of the sensors however shows little difference and due to the smaller size, antimony sensors are often favoured for their slimmer profile allowing better intubation and patient tolerance. Antimony sensors are also cheaper which allows for the production of low-cost single use or disposable

catheters, or more recently multiple electrode catheters. Dual sensor antimony catheters have been used to both investigate short segment reflux (Fletcher et al. 2004), or employing the most distal sensor to measure gastric pH and the second, more proximal sensor to detect acid reflux (Pandolfino et al. 2007; Clarke et al. 2008). Glass sensors are larger and therefore the number of glass pH sensors is limited, however due to the small size of antimony sensors, more than two sensors may be used, in fact as many as 15 antimony sensors have been used, placed 1 centimetre apart, to measure high-resolution pH along the oesophagus, through the GOJ and into the stomach (Clarke et al. 2008; Clarke et al. 2009). This technology, as mentioned in a previous section, has allowed much more detailed understanding of the acid pocket or acid film understanding, as well as showing new phenomena involving acid within the GOJ.

While microsensors exist which have a sub 150 micrometre size, they are not used in the upper gastroenterology field, with no evidence in academic or manufacturer's literature. There has been a reduction in size of pH sensors used in gastroenterology as they became widely adopted, with commonly used multi-channel antimony sensors used in catheters with a 1 millimetre diameter; these are easily intubated and are often included in other upper GI investigative tools such as manometers and impedance probes (Zephr system, Sandhill Scientific, USA).

Figure 1.16 Wireless Bravo capsule system. Showing the internal capsule which is clipped to the oesophagus wall and the belt-worn receiver which acts as a data logger. (www.givenimaging.com)

A recent advancement in pH-metry, is the invention of the Bravo Capsule (Given Imaging, Israel, formerly manufactured by Medtronic) shown in figure 1.16, a wireless pill shaped device which is attached and sits wholly in the oesophagus wall and continuously records pH, transmitting the data to a receiver outside the body, without having uncomfortable catheters, which impede the subjects' daily routine. This technology was first reported in 2003 by Pandolfino et al (Pandolfino et al. 2003); a 6 millimetre by 5.5 millimetre by 25 millimetre wireless radiotelemetry capsule, containing a pH sensor, reference electrode, transmitter, battery and suction well; all encased in epoxy. This device is placed onto the oesophageal musoca, via a custom delivery system passed down the nose, then a small suction well in the capsule, connected to the custom delivery system, sucks a small piece of the mucosa into the well, which is then pinned to the device. The pH sensor is an antimony pH electrode located at the distal tip of the capsule; the recordings using this sensor are transmitted to an external receiver using radiofrequency telemetry at 433 megahertz using digital transmission. The pH sensor records the pH every 6 seconds, after being calibrated before insertion using pH 7 and pH 1.68 liquid, with the transmission to the receiver also being checked; the range of the transmission was 3 to 5 feet while inside the body. Due to the wireless nature of the device, the study reported by

Pandolfino in this paper, included 44 healthy subjects without reflux symptoms, and 41 GORD patients; the aim of which, was to test the validity of the pH recording in vivo, although it did not simultaneously measure this against any gold standard, so the study was not for validation, rather for attachment efficacy, safety and tolerability. The study lasted 48 hours, with the subjects required to log activity, diet; the consumption of high fat meals and alcohol prohibited. Two volunteers required a replacement device after the capsule failed to detach from the delivery system, with another two requesting removal of the capsule after the study completion rather than waiting for detachment, due to discomfort; of the 85 subjects 73% required sedation for device placement. Of the patients able to tolerate subsequent detachment, only one device remained for 15 days after the trial ended, upon which, the capsule was endoscopically removed. Most subjects reported mild foreign body sensation, especially when consuming food, with 4 subjects suffering moderate chest pain due to the device. Satisfaction and tolerability were assessed by questionnaire, with a subset of 14 healthy volunteers and 15 GORD patients undergoing a further ambulatory study; within these subjects, the capsule had better procedure satisfaction and less throat discomfort than conventional pH catheter studies, although it did have more oesophageal discomfort, particularly within the healthy control group, while daily routines and diet were both inhibited in 37% in the catheter subgroup, the Bravo capsule inhibited none of the patients in the subgroup. The author reports that in nearly 95% of the Bravo trials, the pH tracings were interpretable, with technical malfunctions and the receiver being outside the range of the transmitter could be attributed to such uninterpretable results; the devices have since received antenna and capsule board improvements to reduce data loss. The study reported that GORD patients had significantly more oesophageal acid exposure time, however since the sensor was not directly tested against a known or gold standard technology, the validity of these results is questionable. The author concludes that successful 24 hour recordings were observed in 96% of subjects, and 48 hour recordings were 89% successful; with simple device deployment lasting less than 10 minutes. The only concern of this trial was the increase in pain or discomfort caused by the capsule, although the author suggests that this is less than for conventional pH studies. The advantages of this technology for simple clinical ambulatory pH studies seem many

and significant, however due to the lack of high spatial resolution recording, traditional catheter based technology with multiple pH sensors seems optimal for upper GI research.

Two years later, Pandolfino published a paper based on the above work, offering little extra to the field (Pandolfino 2005), however this time the author noted that oesophageal placement is confirmed with a chest radiograph. The paper did highlight several nuances of using the device, for the benefit of clinical investigators; transmission error was demonstrated as a signal of pH 0, so that they may be interpreted as artefact. The author demonstrates oesophageal detachment, followed by a low acid period of several hours, after which it passes into a neutral to alkaline pH environment, such as the small intestine. The author also details the endoscopic removal process for capsules which remain attached for longer than 15 days post study, again for clinicians' benefit. The author concludes that the uptake of the Bravo capsule will be determined by several considerations such as cost and diagnostic accuracy, the latter of which will be strengthened by validation experiments against traditional gold standard catheter pH-metry.

A paper published in *Gut* that same year by Holloway, offers a commentary on the use and advantages of wireless oesophageal pH-metry (Holloway 2005); Holloway writes that the two main advantages of Capsule pH recording are the much lower impact of 24 or 48 hour recording on the patients' activities such as eating, and the more significant improvement of prolonged monitoring, increasing the chances of reflux and reflux associated symptom detection. The author acknowledges that 48 hour catheter pH detection has been performed, comparison between them, resulting in validation has, been lacking at time of publication. In the same issue of *Gut*, a paper by Bruley des Varannes et al recorded simultaneous catheter and capsule pH-metry for 24 hours (Bruley des Varannes et al. 2005), demonstrating that the capsule detects 30% fewer pH less than 5 acid events than catheter methods, showing it to significantly underestimate the severity of diseases in clinical investigations; with Bruley des Varannes suggesting that reliability needs to be improved for widely adopted uptake. The other Bravo capsule validation paper in that issue of *Gut* was by Pandolfino et al (Pandolfino, Zhang, et al. 2005), which reported a similar validation

study comparing the Bravo capsule with a dual antimony catheter, but conversely reported that the Bravo capsule recorded almost three times as many reflux episodes of pH less than 4.25; most of which were fairly short in duration. Pandolfino reported the difference between the two methods was due to calibration error of the catheter system, which measured 0.77 pH error of the calibration liquid, with the capsule having a much lower error; this is of some concern as slim line catheters are in fairly common usage both clinically and in research groups. Holloway notes these papers in the same issue, and highlights the differences in the validation studies, which are potential causes for concern, although the two papers used different definitions of reflux events, both in acidity and duration. The papers showing a large discrepancy between reflux events using two technologies is a warning of caution, for both technologies; is catheter pH detection accurate, or is Capsule pH-metry more prone to error, as the differences in validation studies were not consistent. Holloway summarises his commentary by highlighting the potential advantages, mentioned before, however the significant difference in the two technologies, at least for clinical investigation, is cost; in Australia, a single use Bravo capsule costs $400, whereas a multiple use pH catheter costs $200. The uptake therefore will be dependant on further validation studies and research into symptom association, with an inevitable trade off of cost against the capsule's advantages.

In 2007, Maerten et al produce a review paper which analyses capsule pH monitoring, but with the focus on evaluating the capsule's ability to detect GORD (Maerten et al. 2007). As well as reviewing the above literature, the paper also mentions that from 5 papers, 10.5 to 65% of Bravo capsule subjects reported chest pain associated with the capsule; the paper highlights that wireless pH recording, such as that with the Bravo capsule, may not be as useful as combined pH and Multiple Intraluminal Impedance devices, which show more strongly, the association between reflux episodes and chest pain; a thought which was first shared in a paper by Lutsi and Hirano in the previous year (Lutsi & Hirano 2006). The authors suggested that the previous catheter based probes were a tarnished gold standard. The capsule too, has several disadvantages; such as difficult transnasal passage during attachment and the cost implications involved, especially if a second capsule is needed due to premature dislodging or poor attachment firing, as well as post-study

radiography and potential endoscopy needed for removal if remained attached after 15 days.

In 2008, Pandolfino produced yet another Bravo capsule paper (Kwiatek & Pandolfino 2008) reviewing the literature, highlighting the accuracy of sensor placement, which was, with endoscopic placement, within 1 centimetre, and when using the manometric upper LOS border definitions, 3.74 centimetres. An issue with catheter pH monitoring is sensor migration, which can happen over time with swallowing and oesophageal shortening, however this is not an issue with the mucosal clipped capsule. The author claims that catheter based studies are limited to 24 hours, although DeMeester et al stated studies could last 72 hours without equipment failure (DeMeester et al. 1980), Pandolfino doesn't mention this, but the only remaining potential limit must be ethics approval. Bravo capsules are used for 48 hours however potential 96 hour studies have been demonstrated, with 80-89% of the study resulting in successful recording. The author concludes with the same points as in his 2003 and 2005 papers, as well as those mentioned by Maerten et al, adding almost nothing to either clinical or research fields. A conflict of interest is highlighted by Pandolfino, yet the paper which may be why the important paper by DeMeester was conveniently omitted.

A paper by Sofi et al, reported on the placement accuracy using two different techniques, simultaneous endoscopic Bravo placement, and blind Bravo placement after initial endoscopy with subsequent placement verification endoscopy (Sofi et al. 2011). Both techniques demonstrated similar procedure duration, placement, and neither showed detachment, in a retrospective study of 58 patients; concluding that either method is safe and quick, although simultaneous endoscopic placement removed the need for a second endoscope placement procedure.

1.4.4 Impedance measurement

Although pH probes can measure acid reflux, and high resolution manometers, pressure including gas venting, for a long time, there was little knowledge about the

extent of neutral reflux events. Impedance measurements of the upper GI tract were used as early as 1983 with Sutton et al using an external, radiation-free epigastric impedance technique to measure the effect of different pharmaceutical agents on gastric emptying times (McClelland & Sutton 1985).

Impedance sensors work on the principal that the magnitude and phase of an alternating current changes when the conductive load changes; the load of air, water and acid all have different effects on the impedence at different frequencies. Since the load is not a conducting wire, the medium between a pair of conductors, across which the alternating current is applied acts as the load; in the oesophagus this is a combination of air, saliva, gastric contents and oesophageal wall. A catheter with multiple pairs of conductors along its length can calculate the impedance along the entire oesophagus and into the stomach. Figure 1.17 shows an example output of an impedance catheter measuring the movement of a bolus during swallowing; the timing of the impedance change can be seen, demonstrating that the bolus is moving down the oesophagus; the same time delay can demonstrate acid reflux.

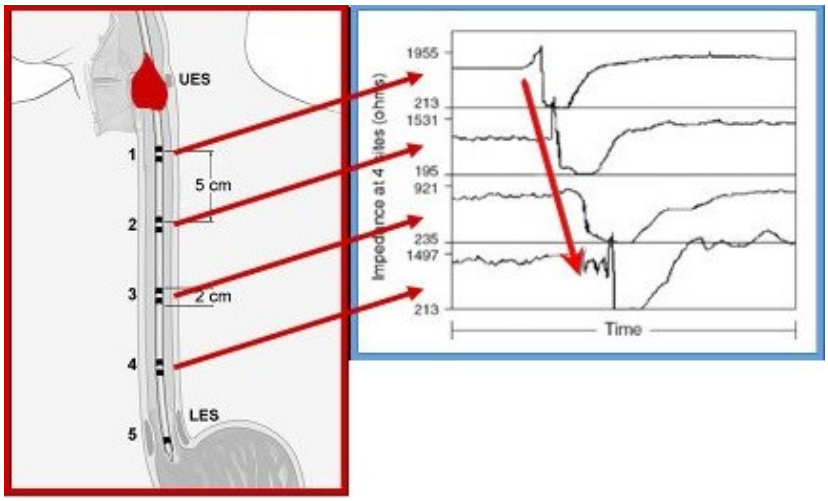

Figure 1.17 Impedance catheters. Output of an impedance probe showing bolus movement. Acquired from Medscape (www.medscape.org/viewarticle/567561).

However, it wasn't until 1991 that the first paper detailing intraluminal impedance of the oesophagus and stomach was published by Silny (Silny 1991). The novel device featuring multiple electric impedance electrodes, allows measurement of the

resistance to an alternating current between two electrodes, known as impedance. These electrodes are placed 2 centimetres apart for a working measurement length of 16 centimetres, are measured at 1 kilohertz, and have a stated sensitivity of 1 millivolt per ohm; for the subjects' safety the measurement current is less than 6 microamps. This paper demonstrates the ability of the device to measure gastric motility, with the capability of determining the contents of the stomach, differentiating between 0.9% saline, saliva, bile fluid, stomach contents, epidermis and water; with output being displayed on printed graph plot for used interpretation. A large amount of the items tested were not done so in vivo; a paper in 1993 by Silny et al details the in vivo verification of this device (Silny et al. 1993), improved with a working length of 32 centimetres, allowing greater range of impedance measurement. 49 asymptomatic subjects were tested with this device, which was combined with manometry for event validation. The bolus can be measured with both techniques, therefore following synchronisation, the two devices can be directly compared. Air swallows are also used to check the sensors, following which, the device is validated against fluoroscopy, where both the air bolus and sensors can be seen in the output video; this is used to validate the sensor output against the bolus presence. Silny concludes that the now verified device allows for safe and continuous measurement of gastric motility, where bolus velocity can be measured and a crude approximation of volume may also be made. The measurements allow the differentiation of gastric and oesophageal contents, as well as bolus or reflux content and state of matter; the device can clearly distinguish between a bolus of food matter and the air gap in front of it as it is swallowed during peristalsis. Measurements of gastric emptying and small bowel migration may also be made with this device, however one large flaw in the device, is when using it to investigate reflux across the GOJ, the device is unable to differentiate between acid and neutral or alkaline refluxate; the technology also has a poorer spatial resolution than HRM and some multi-channel pH catheters of 2 centimetres.

A paper published in 2002 by Shay et al, investigated the accuracy of the impedance technology (Shay et al. 2002), with the technology termed Multichannel Intraluminal Impedance (MII), a refined, commercially available form of the device that Silny had previously presented, with digital output and the important addition of a single pH

electrode for reflux detection. The paper compared MII with pH-metry and manometry for the detection of reflux episodes and evaluation of post reflux oesophageal acid clearing. The study was performed on 10 symptomatic patients and 10 asymptomatic control patients, with simultaneous HRM and MII usage. The number of reflux episodes in the symptomatic cohort was up to 30 times that of the asymptomatic subjects. A total of 119 acid reflux episodes were detected by manometry and pH, of which, 85% were also detected by MII; 289 non-acid reflux events were detected with pH and manometry, 99% of which were detected by MII. Of the reflux episodes detected by MII, 2% were gaseous refluxes, the rest were liquid, the acidity of which was determined by the MII's inbuilt pH sensor, rather than the impedance sensors themselves. The refluxate clearance time was the same when comparing MII and HRM, however pH reported a slower refluxate clearance time, which may be explained by the slow response properties of an antimony pH sensor.

The wide adoption of MII was demonstrated by a huge increase in the number of publications on the subject from 2005 onwards; Pandolfino published a paper which employed a combined MII and perfusion manometer in 8 healthy volunteers to measure the LOS in an effort to determine the adaptability of MII technology to this anatomical measurement (Pandolfino, Shi, et al. 2005). The study showed that the swallow induced LOS opening occurred top to bottom, and that the leading edge of the bolus was liquid in 83% of cases, rather than air as suggested by Shaw. The paper also showed that TLOSRs had the reverse sphincter opening properties, bottom to top, and that the leading edge was liquid in 76% of cases. The author concludes that MII can be used to differentiate between TLOSRs and swallow induced LOS relaxation, which may be or importance when using the technology for research or clinical purposes.

Bredenoord tested MII in 20 healthy volunteers for 90 minutes postprandially, with a view to assessing the technologies' reproducibility at detecting reflux (A. J. Bredenoord et al. 2005). The paper reported statistically significant concordances for gas and mixed reflux with concordance for liquid reflux showing a strong, near-

significant trend; suggesting that postprandial reflux episodes are as reproducible as those detected by pH-metry.

Hirano mentions MII in his review of modern upper GI investigation tools (Hirano 2006); highlighting the usefulness of MII when combined with other tools such as pH or manometry, at measuring the composition of reflux and investigating motility. The paper highlights the trend in research to uncover the clinical importance of non-acid reflux, which interestingly reports that patients on PPIs for acid reflux still suffer from heartburn even though the refluxate is non-acidic, asking the question if there is more to heartburn than just the acidity of refluxate. The paper also highlights Bilitec, a technology for spectrophotometrically detecting bile in refluxate, which may cause heartburn or GORD in conjunction with acid reflux.

Latter papers by Bredenoord were published but add little more than other papers, reviewing previous literature and are very similar to each other (Bredenoord et al. 2007; Bredenoord 2008); suggesting that MII is the new gold standard for reflux measurement, despite MII needing a combined pH sensor in order to actually detect acid. The placement and limitation of a small number of pH sensors is unable to cope with accurate detection of short segment reflux. The paper suggests that MII is becoming more widespread, and indeed it is, with the number of papers being published covering MII ever increasing, however the clinical relevance is somewhat less strong, with the tool yet to provide significant advantages over more well known technology such as manometry or pH-metry.

1.4.5 Radiographic measurement

X-ray images have been common in hospitals since the early twentieth century, but it wasn't until the late 1950s that video radioscopy was used to great effect, combining image intensifiers and video cameras allowed radiographers to view the video output from sequential X-ray images. Since then, fluoroscopy has been widely used in the medical field, and importantly in the upper GI tract, with the use of a barium meal;

the barium which is consumed allowed visualisation of oesophageal swallow, gastric emptying and intestinal transit.

In 1966, Griffith et al proposed the measurement of gastric emptying time using labelled Chromium-51 (Griffith et al. 1966), a radioactive isotope of chromium having a half-life of 27.7 days, which the subjects swallow, and can be visualised using radiograph during transition through the GI tract, or radiation levels may be measured by upon passage from the body .

Hinton et al later reported a novel technique for measuring passage of food through the gut (Hinton et al. 1969), which employs radiopaque polythene pellets containing 20% barium sulphate, these pellets were manufactured in three different sizes to enable the investigation of transit time on differently sized food stuffs. The subjects' stools were collected and underwent radiography to detect the number of pellets in each stool; the paper detailed all the practicalities of manufacture, collection and detection of these markers, allowing for the first time, a simple and quantative method for measuring digestive emptying times. If the procedure was performed as above, then the patient would not be subject to any radiation exposure, due to the nature of the pellets being radiopaque rather than radioactive with Griffith's suggestion.

Validation of this technique was performed against the Griffith method, showing almost exactly the same number of pellets passed out at varying times after ingestion.

The study showed in 25 male subjects, that after ingesting pellets at breakfast time, all subjects had passed their first pellet in under 66 hours, approximately 3 days, and all except one subject passed 80% of the pellets in 114 hours or five days.

This study did use radiography on the subject for visualisation of the transit through the gut, however this is not necessary for the clinical application of this test. The pellet size and shape had little effect on the time of passage in this cohort.

Later on, Feldman et al showed the wide acceptance of this technique but with the inclusion of multiple radiographs (Feldman et al. 1984), this time for investigating gut transit and gastric emptying times in patients with diabetes mellitus. 10

radiopaque markers were ingested with a small meal and hourly radiographs were performed for 6 hours, until all markers were emptied from the stomach; with most emptying after 4 hours, this was slower than normal gastric emptying time. The author concluded that sequential hourly radiographs were a reliable method of measuring gastric motor function than the alternative, radionuclide scintigraphy.

In 1999, Kahrilas et al developed a fluoroscopic technique which allowed the visualisation of the GOJ during hiatus hernia (Kahrilas et al. 1999). This paper detailed the novel method of attaching radiopaque markers to the oesophagus and SCJ allowing visualisation of the oesophageal wall and stomach during a hiatal hernia.

Until this method, the standard means of detecting a hiatus hernia was via endoscopy, and the main technique of visualising the anatomy was single radiography; these techniques showed that 50-94% of patients with GORD also had hiatus hernia, much higher than any control subjects. The author acknowledges that the consensus is that a hiatus hernia removes the contribution of the diaphragm on the LOS, thus decreasing its function as an antireflux barrier. The study was therefore conceived to evaluate the effect of a hiatus hernia on the GOJ using manometry to detect pressure along the GI tract while the stomach was herniated in the thorax; the concept of study itself is not terribly exciting, however the technique used to visualise movement of the junction during hernia with concurrent manometry allowed for continuous visualisation of the axial and radial characteristics of the hiatus hernia. the study was performed on 7 healthy volunteers and 7 hiatal hernia patients, who were fasted overnight, before having two 11 millimetre clips attached to their gastric mucosa via endoscopy; one clip was attached to the SCJ, while the other clip was attached to the stomach at the greater curvature. In herniated patients, the gastric clip marked the lower section of the diaphragmatic hiatus, whereas in healthy subjects, the gastric clip was correlated with the flap valve. Following the clip attachment, the subjects were allowed at least an hour of accommodation of the clip as well as allowing for endoscopic sedation to diminish; at which point, the manometric and fluoroscopic studies were initiated. Firstly the subjects were imaged fluoroscopically in the supine position to confirm the presence of a hiatus hernia if

diagnosed as such, then both groups swallowed two liquid barium solutions to determine end expiratory diaphragmatic position, which were recorded via fluoroscopy. The pull through perfusion manometer was then employed during suspended respiration to detect pressure along the oesophagus, stomach and importantly at the hiatus hernia, which was synchronised with the fluoroscopy using a video timer, accurate to 100^{th} of a second. Upon completion, the fluoroscopic data had to be manually assessed and measured using the vertebrae as a reference, however the author fails to mention how frequent the measurements were made throughout the 30 seconds of fluoroscopic video. The study showed that in those with a hiatus hernia, even during end expiration, the hiatal canal contributed to the pressure of the GOJ as demonstrated by the double peaked pressure profile recorded with manometry; separation of the intrinsic LOS and diaphragm was responsible for this, with an overall pressure decrease versus normal patients, a result of the misalignment of the anatomy. When the hernial clip showed reduction of herniation, a more normal LOS pressure was recorded; this occurred during abdominal compression or deep breathing. This may suggest that although present a lot of the time, a hiatus hernia is not a constant phenomenon, rather it is transient and of unknown duration and frequency. The author suggests that stretching or loosening of the phrenoesophageal ligaments, which maintain diaphragmatic position, allows more movement of the stomach through the diaphragmatic hiatus; a potential cause of this is due to the abdominal-thoracic pressure gradient.

This technique has undoubtedly inspired similar studies, and has established fluoroscopy as the gold standard for visualising the upper GI track and measurement of SCJ position with the use of radioscopically visible clips.

Validation studies of new technologies have been performed using fluoroscopy to visualise the position of upper GI tools, confirming their position relative to the SCJ thereby confirming their measurement. Multichannel Intraluminal impedance is once such example, where Srinivasan used fluoroscopy to confirm the position of impedance electrodes, which were partially visible in radiographic video (Srinivasan et al. 2001), to confirm acid reflux detection in the oesophagus.

Similar studies have been performed to validate the position of attachment of the Bravo capsule, 5 centimetres above the SCJ and with respect to traditional pH catheters with used simultaneously (Pandolfino, Zhang, et al. 2005; Bruley des Varannes et al. 2005).

Flouroscopy has been used to visualse swallows with a barium contrast meal (Boyle 2006), now a widely adopted technique to assess upper GI motility (Lodhia et al. 2007). It has also been employed to validate MII (Nguyen et al. 1997), HRM (Roman et al. 2009), and pH catheter positioning (Clarke et al. 2008).

In 2006, Pandolfino joined Kahrilas to investigate TLOSRs in detail using Kahrilas' fluoroscopic clip visualisation technique with simultaneous manometry (Pandolfino, Zhang, et al. 2006), in order to view the movement and pressure profile involved in TLOSRs; testing the hypothesis that oesophageal shortening is a requirement for GOJ opening. The study involved six volunteers with no evidence of hiatus hernia or treatment for upper GI disorders. The technique was almost identical to Kahrilas' earlier work and involved clipping subjects fasted for at least 6 hours before endoscopic clip attachment; 11mm clips were placed on the Squamocolumnar Junction which is endoscopically visible as the Z-line, and the second clip placed approximately 10 centimetres proximal to this. A calibrated HRM device was used for concurrent pressure recording. The cohort was required to take 10 water swallows and a 1000 calorie meal, after which point they were placed inside a fluoroscopy machine, and an investigator would watch the manometry tracing; when the investigator suspected there was an onset of a TLOSR the fluoroscopic recording of the remaining TLOSR was started until completion. The subjects were limited to a maximum of 5 minutes of fluoroscopy exposure for their safety; the fluoroscopy and manometry were synchronised for each recording using an unspecified event marker. Post study analysis, manometric transients were defined using the Holloway criteria (Holloway et al. 1995) with agreement of at least 2 of 3 researchers, with manometric flow defined as a change in pressure gradient changes across the GOJ, however despite previously publishing a paper, this implication may not be accurate for every event as air flow may account for this apparent change in gradient, due to an equilibrium effect. The paper did show a very interesting pattern of events;

shortening of the oesophagus was defined as a proximal migration followed by a return to original position several seconds later. The maximum proximal movement recorded by this technique was 9 centimetres.

Although demonstrating interesting events during a TLOSR, the technique failed to record the first two or three seconds of the TLOSR as there was some delay between identification of the event and the start of fluoroscopic recording, the event too, had to begin before it could be identified, adding to the delay in recording.

The technique highlighted 93 TLOSR events for all patients for a postprandial period of 2 hours, 78 of which had apparent manometric flow across the GOJ; those with flow had significantly longer GOJ relaxation but a similar nadir pressure. There was no statistical difference of crural inhibition between flow or flow-less TLOSRs.

Out of the 93 TLOSR events, only two thirds had sufficient fluoroscopic recording to accurately assess SCJ movement hence oesophageal shortening; of those it was observed that oesophageal shortening was most obvious in the distal clip, with the SCJ clip moving a median of 3 centimetres proximally before returning, interestingly the largest observed movement was 9 centimetres. The proximal clip moved a median of 1.2 centimetres; the median distance between the two clips at maximal proximal movement was 6.75 centimetres. The visualisation of the movement allowed a rather interesting measurement of speed of movement, with the shortening pattern being as such: SCJ migration was initially slow (0.36 centimetres per second), followed by a faster movement (0.46 centimetres per second) after full GOJ relaxation. Manometric flow was observed after the point of maximal proximal movement; after maximal movement the SCJ returned to its more distal position. Due to missing the first 3 seconds of recording, the full extent of movement is slightly inaccurate, due to missing the initial movement, which at a rate of 0.36 centimetres per second, could underestimate the distal movement by as much as a centimetre.

The median pressure gradient, which is actually a difference across the sphincter, of 0.2 seconds before TLOSR onset was between 7 and 8 mmHg, and those with a positive pressure gradient of median 7.1 mmHg during TLOSRs onset were

associated with manometric flow, whereas those without flow had a median pressure gradient of -1.6 mmHg, suggesting reflux during a TLOSR is caused by the presence of a larger positive pressure gradient, which would force gastric contents into the oesophagus in order to equalise the pressure.

The author concludes that GOJ opening happens because of three main elements: LES relaxation, crural diaphragm inhibition and distal longitudinal muscle contraction, the latter of which causes oesophageal shortening; it is worth noting that even with these three events, GOJ opening did not always happen. The author acknowledges Phrenoesophageal ligament laxity and attachment may play a role in determining the extent of proximal SCJ movement.

The paper shows for the first time, significant oesophageal shortening at the SCJ occurs, which highlights a potential flaw in pH recording with traditional catheters; shortening of the oesophagus may be mistaken for acid reflux events, as if the oesophagus moves more than 5 centimetres proximally during a TLOSR, the pH sensor will actually be inside the stomach, showing acid that a user may misinterpret as a reflux event; overestimating the frequency of acid reflux events potentially leading to a misdiagnosis.

This is a very interesting paper, stating that oesophageal shortening starts before oesophageal opening, however due to missing the first 3 seconds of TLOSR event and the fact that only two thirds of transients are assessable, this technique is an interesting insight into TLOSRs, however a more reliable, continuous method of SCJ position recording should be developed to provide significant further detail to the area, which has both research and clinical benefit.

1.4.6 Intraluminal Ultrasound measurement

Ultrasonic imaging is a safe method of visualising structures and organs of the body, and is widely used, requiring trained personnel to operate and interpret the graphical output. The technology was developed in the late 1980s into a catheter based device, was used to screen for rectal cancer, however the technology has been applied as a

method of investigating the upper GI tract by Miller et al (Miller, J. B. Liu, et al. 1992; Miller, J.-B. Liu, et al. 1992). Implying an inverse relationship between oesophageal wall cross sectional area and longitudinal length, while assuming perfect incompressibility of the oesophageal musculature, the user can estimate longitudinal oesophageal shortening, albeit rather inaccurately due to hardware limitations and inaccurate assumptions. Studies have shown its in vivo use (Nicosia et al. 2001; Mittal et al. 2005; Babaei et al. 2008), however it is only really useful when used with manometry, as both circular and longitudinal muscle must be measured for an accurate representation of oesophageal shortening. This tool is useful for investigating patients with certain diseases, helping to identify underlying muscle thickness or neurological causes, however due to its lack of solid validation, missing automatic analysis and operator dependence, its use is limited (Kuo et al. 2012).

1.4.7 Magnetic measurement

The concept of measuring gastric transit time with Scintigraphy has been mentioned in previous sections, where radioisotopes are ingested and their radiation detected to measure gastric emptying times; this exposes patients to gamma radiation which limits its use. To overcome such limitations Di Luzio et al suggested an alternative technique whereby a relatively small magnet is swallowed, and its position inside a subject is detected using a very sensitive magnometer based superconducting quantum interference device (Luzio et al. 1989). As the magnet moves inside the patient, relative to the SQUID sensors, its transit through the GI tract can be monitored allowing motility testing and gastric emptying time calculation.

In 1994, Weitschies et al proposed a system strongly based on Di Luzio's concept (Weitschies et al. 1994), whereby measurement was made of a 16.1 by 5.7 millimetre capsule containing approximately 27% magnetite, which was magnetised to a magnetic dipole moment of 100nA m^2. This measurement was made using a commercially available 7 channel DC-SQUID detector, in a magnetically shielded room, where magnetic fields are reduced by a factor of 10^4. Calibrating the magnet in vitro showed the device to be accurate to 2 millimetres in every direction; the device

was then tested in vivo on one volunteer, showing detection and localisation of the magnet within a 20 cm^3 space, providing the magnet was stationary for 5 seconds. The author suggested that with a 10 or 20 channel SQUID system, more accurate, prolonged recordings could be made, prompting an increasing interest in the area.

Three years later Weitschies published a follow up paper, this time using a custom 37-channel SQUID magnometer (Weitschies et al. 1997). The paper provided a very detailed method for magnetic capsule production of equal size and strength to the author's previous work. The custom made 37-channel SQUID system measured the magnet over a width of 21 centimetres, collecting data in a bandwidth between DC to 64 Hertz, at a sampling frequency of 250 Hertz; the paper also included a least squares fit algorithm which used a dipole mathematical model which was applied to the data, in order to detect the magnet.

The author details the in vivo test of one male volunteer, showing that during the initial swallow, the position measurement deviated by up to 25%, apparently due to unfavourable position of the magnet to the sensors, presumably the speed at which the capsule was moving during swallow also contributed to this error; once the capsule's movement was less, positional accuracy of 2 to 10% could be obtained; an error attributed to the additional noise of the magnetic field associated with the body and heart. The author concluded by summarising that the error was as little as 2mm in the best scenario, and the technology allowed the localisation of a magnetic capsule in a three-dimensional space, enabling GI motility studies to be performed; this was similar to scintigraphy but without the problem of radiation exposure. The author finishes by stating that with up to 50-channel liquid nitrogen-cooled ceramic SQUID sensors, uptake of this radiation free alternative may be increased.

In 2000, Hu et al suggested a method of magnetic pill tracking which had the further advantage of capsules designed to disintegrate when exposed to a specific pressure such as that present in the colon (Hu et al. 2000). Hu details the use of a commercially available Biomagnetic Measurement System (BMS), which consists of a 129-channel DC SQUID sensor device and coils; the BMS's typical use is for measuring the ionic currents generated by the nervous and musculoskeletal system. The report detailed the process whereby drugs could be encapsulated and

magnetically labelled with ferric oxide, which was then magnetised in a 0.5 Tesla MRI machine; this case the drug used for the trial was caffeine. Calibration was performed using a capsule at a variety of attitudes, with the data set for rotation being used to determine the in vitro orientation. The trial was performed on two healthy, male volunteers who were not taking any prescribed drugs with alcohol and caffeine consumption not allowed for 24 hours prior to the study. The procedure involved the trial being performed in a magnetically shielded room, with the patients swallowing a magnetically marked capsule, consuming a meal 4 hours later; the BMS was positioned over the subject and recorded the magnetic field in the abdomen. The magnetic capsule was detected in the body of the volunteers, and was shown to move along the GI tract at a within normal rate of transit; caffeine levels were also recorded in the patient's saliva in order to assess capsule breakdown and absorption. the working range at which the capsule could be detected was 20 centimetres or less, due to the weak magnetisation of the ferric oxide within the capsule however the author noted that the use of permanent magnets or electromagnets did not increase this range; the estimated accuracy when testing the device in vivo, was within about 3 centimetres.

In the same year, Andrä et al released a report on a similar method of detecting a magnetic marker within the GI tract using a movable magnetoresistive sensor (Andrä et al. 2000), with the advantage of being less cumbersome than SQUID sensors. The method not only allows for a much smaller detecting device, but the use of magnetic pulsing devices which may be used to orientate or disperse the capsule for in vitro locomotion and drug delivery respectively. The technology is employed by means of several orientation coils which enable the orientation of the magnetic field to the z-axis. This technology was tested not in a subject, but in a GI phantom, which had the advantage of measuring the position of the magnet along a very well known path, any deviation of the measurement from this path is considered error. The size of the capsule was 20 millimetres long and 7 millimetres diameter, inside which a freely rotatable permanent NeFeB magnet was placed with 3.5 millimetre diameter and 0.02 A m^2 magnetic moment; the mean error demonstrated of 10 millimetres, sufficient to differentiate between loops of the intestine. This technique demonstrates an advantage over a SQUID based system, as the latter has to be liquid cooled and is

significantly more expensive, neither does it have to be perfumed in a magnetically shielded room. The orientation of the magnet by the external coils requires at least 80 A m^2 which is significantly larger than external fields, which means no accidental rotation will occur from stray fields; the author notes that safety concerns regarding damage due to the force of movement of the capsule when orientating the magnet must be assessed for patient trials; magnetoresistive sensors also are less sensitive to the body's electromagnetic field interference than SQUID sensors.

The following year, Schlageter et al published a paper detailing the use of a permanent magnet and Hall effect matrix to calculate said magnet's position (Schlageter et al. 2001). This method involved a 6 millimetre diameter by 7 millimetre length rod shaped rare-earth permanent magnet with a magnetic moment of 0.2 A m^2, detected by a 4 by 4 grid of Hall effect sensors with built in flux concentrators. The distance between said sensors was 3 centimetres in both directions, and employing a Levenberg-Marquardt optimisation algorithm, provided an accuracy of a few millimetres up to 14 centimetres away, however at the larger end of this range, and in non-ideal orientation, the positional error may be up to 4 times as great. The author concluded that with double the number of sensors in the same area, the spatial accuracy would be greatly increased.

In 2005 another paper by Weitschies et al, detailed their improvements to the magnetic marker monitoring system (Weitschies et al. 2005). The system used a 83 channel SQUID sensor system claiming an accuracy of 1 millimetre at 15 centimetres away from the device. The system was employed on 100 capsules, to not only investigate transit, but in addition, could monitor the magnetic strength of the capsule, and by doing so, monitor the break up of the capsule in the stomach and the small intestine; this gives the user a potential advantage in being allowed to tailor their capsules' break up time, providing proof that their drug is either slow acting or fast acting.

The following year, two papers were published in a similar vein to Andrä's group; athough Wen-Hui et al produced a device whereby a small powered wireless 3-axis magnetoresistive sensor was placed inside the patient with three magnetic coils on the outside of the body to provide the sensor with fields to record. The recorded data

was then transmitted to a computer outside the body, which could interpret the signals into localisation data, accurate to between 4.17 and 22.14 millimetres when the distance between the sensor and the coils is at about 6 centimetres.

The other important paper in the area that year was written by Stathopoulos et al (Stathopoulos et al. 2005), which was also authored by Schlageter, and documented the in vivo use of the device published earlier (Schlageter et al. 2001). The study was performed on 5 male and 5 female asymptomatic volunteers who were fasted during the study; CT or X-ray scans were taken to confirm the magnet's position. The paper then details the times of passage through various digestive organs; concluding that device was reliably accurate, could be used with very little training and was easy to interpret. There were also noted contraindications for certain GI diseases, as well as recommending that no MRI studies were performed on the patient while the magnet was still inside the body.

A paper by Paixão in 2007 details another device for pill tracking, using magnetoresistive sensors with an excitation and detection coil (Paixão et al. 2007). One coil was supplied with a 10 kilohertz alternating current and the change in magnetic field between two coils, changed when ferrite powder was passed in between the coils; the field distortion of ferrite was measured by the magnetoresistive sensors orientated at 3 axes within the detection coil. As the powder is not in the form of a single magnet, its position cannot be calculated, however the amount of ferrite in between the coils can be measured, measuring the amount of ferrite in, say, the stomach. This is a similar technology however its application is less significant as it does not allow localisation or tracking of a given magnet.

Weitschies et al published another paper using their Magnetic Marker Monitoring (MMM) technique, which focuses strongly on the material properties to allow for different break down times (Weitschies et al. 2010). Comparing it to the Stathopoulos paper, suggesting that although the competing technology was simpler, it lacked the sensitivity that MMM had, instead opting to increase the size of the magnet, which compensated for the lack of sensitivity. Weitschies states that with this more sensitive equipment, he was capable of measuring milligrams of magnetite

in marked capsules; this means that they are able to provide greater detail of capsule breakdown, proving more helpful for pharmaceutical applications.

Goodman et al published a paper in collaboration with Weitschies, using a commercially available magnetoresistive based magnetic pill locator, investigating disintegration of magnetic capsules in the GI tract for pharmaceutical applications (Goodman et al. 2010). The paper tested 3 different types of marked pill, designed for immediate disintegration, intestinal disintegration and non-disintegration; the disintegration was as desired for both in vitro and in vivo testing, validated against scinitigraphy. One advantage of scintigraphy however was noted; once the magnet had dispersed, the scintigraphy equipment could still detect the scattering of the radiolabel, however once the magnetic capsule had disintegrated, it lost all magnetic moment, and could not be investigated further.

Worsøe published a paper the following year, using Schlageter's commercially available system, using a 16 millimetre by 5 millimetre magnetic pill, combined with a pillcam; an wireless endoscopic video camera technology (Worsøe et al. 2011). The pillcam which measures 11 millimetres by 26 millimetres was used which broadcasts two images per second and operates for 8 hours; the overall size of the pillcam and magnet after gluing and sealing was not mentioned. The test was performed in 8 healthy volunteers, demonstrating that the camera could be located and its orientation known, which provided information as to where the camera was aimed. This paper was very interesting, and if the technology could be developed such that the camera's position could manipulated via an external force, potentially an external magnetic field, then the pillcam could be operated much like a traditional endoscope, only without the need for large bore intubation.

1.5 Objectives of this study.

As has been demonstrated, the position of the Squamo Columnar Junction at the distal end of the oesophagus is a vital part of the anatomy in the human body's anti-reflux system; when it is exposed to acid, damage and pain may occur depending on

the severity and length of exposure. Precise understanding and measurement of the SCJ is critical to the understanding of tissue changes in the region, particularly precancerous tissue detection and research. The Lower Oesophageal Sphincter position often marks a position near to the SCJ, but in patients with various diseases aforementioned here, this can be at best a very crude approximation of position, or in the healthy population is only accurate to several millimetres; an precision which is not sufficient when trying to measure a gastric cardia section, which may only be a millimetre long. Furthermore during a Transient Lower Oesophageal Sphincter Relaxation, all knowledge of the LOS and the SCJ is lost during which, any measurements made which are said to report reflux cannot be trusted.

Being such a common complaint across the world, heartburn is a very widespread yet surprisingly poorly understood phenomenon; as described in this chapter, reflux events do not correlate reliably with dyspeptic-type pain. It is important therefore, to understand this symptom, and investigate the anatomy within the area, enabling research into more severe or end-stage diseases like Gastro-oesophageal Reflux Disease, hiatus hernia or Barrett's oesophagus; only then will we be able to form adequate and appropriate treatments. The pressure profile and pH step up point are both used for reflux detection and as mentioned above, could be inaccurate if oesophageal shortening or TLOSRs occur rather than reflux itself, therefore it is important to know the position of the SCJ relative to these markers, in order to confirm if acid reflux actually occurs; this is of very high clinical relevance as overestimation of reflux events could lead to misdiagnosis and subsequent prescription of superfluous and potentially dangerous drug or surgical treatment.

Crucial to this is the development of a tool for research and clinical use, which allows the precise and continuous measurement of the position of the SCJ, ideally with respect to other anatomical landmarks; this task forms the basis of this thesis and the following topics will be investigated as part of this work.

- Development and *in vivo* validation of a reliable method of measuring the SCJ which must not expose the patient to radiation or harm, be inherently accurate in its position measurement and be compatible with the current technologies used in this research area.
- Validation of the other devices used in conjunction with this technology must also be performed, ensuring that the concurrent measurements of the Upper GI tract are also precise and reliable for long periods of recording.

Chapter 2

Development of a catheter based Squamocolumnar Junction locator

2.1 Magnetic measurements

2.1.1 Magnetism and Dipoles

Magnetism is the property of a material to react to a magnetic field, caused by the fundamental spin of a particle known as a magnetic moment; these spins arise from the particles electrons' orbital angular motion around the nucleus, and the electrons' intrinsic magnetic moment which constitutes a magnetic dipole moment. Also the nuclear magnetic moments of the nuclei can be a source of magnetism, but are orders of magnitude smaller than the electron magnetic moments, so are only significant in the use of Nuclear Magnetic Resonance and Magnetic Resonance Imaging (MRI) applications. Magnetism may also be induced when current flows through a semiconductor which creates an electro-magnetic field. The spontaneous alignment of the magnetic moments determines what type of magnetism the material exhibits when exposed to a magnetic field; Ferromagnetism, ferrimagnetism and diamagnetism to name but a few.

Ferromagnetism is the most well-known by the general populous, and is manifested in a material by its attraction to a magnetic field, due to the alignment of the magnetic moments of individual atoms. These magnetic moments, when aligned, increase the overall magnetic moment of the material; creating an attraction to a magnetic field. Permanent magnets are those ferromagnetic materials which become magnetised by an external magnetic field and remain magnetised after the external field is removed; materials such as Iron, Cobalt, Nickel and their alloys exhibit this. A practical characteristic of ferromagnetic materials is the hysteresis loop, which is the irreversible nonlinear magnetisation $\boldsymbol{M}$, to an imposed magnetic field $\boldsymbol{H}$ both of

which are measured in Ampere per Metre (A m^{-1}). The ability of the material to hold the magnetisation determines the shape of the hysteresis loop; with Hard Magnets, a lot of the magnetisation is retained, producing a permanent magnet, with Soft Magnets there is a very weak retention of magnetisation and are only magnetised for a short period after removal of the H field. As seen in figure 2.1, several key points can be determined from the hysteresis loop, such as the saturated state when $M = M_s$, the remnant state in zero field where $M = M_r$, where M_r is known as Remanence, and the state at $H = H_c$, where H_c is the coercivity, the coercive field where M changes sign. The Curie temperature is that at which any magnetisation becomes zero, by disordering the magnetic moments, however these temperatures for permanent magnets are substantially high.

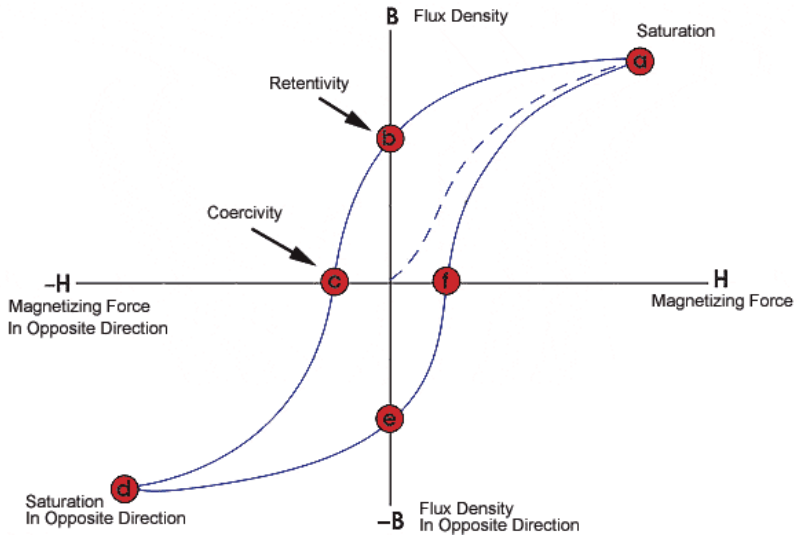

Figure 2.1 Magnetic Hysteresis. Aquired from NDT resource center (www.ndt-ed.org/EducationResources/CommunityCollege/MagParticle/Physics/HysteresisLoop.htm).

As mentioned above, there are other types of magnetism which exhibit a change when exposed to a magnetic field; antiferromagnetism is, as the name suggests, the opposite of ferromagnetism where the magnetic dipoles align in a regular pattern to a magnetic field with two opposite neighbouring parallel magnetic moment lattices.

This phenomenon generally occurs below a certain temperature, which differs between materials, above this temperature, known as the Néel Temperature, above which the same material typically exhibits paramagnetic properties. With no applied magnetic field, these materials show a vanishing total magnetisation while in the presence of a magnetic field, ferromagnetic behaviour is observed in the antiferromagnetic materials due to sublattice differences. Examples of antiferromagnetic materials include chromium and hematite, while synthetic materials consisting of several thin ferromagnetic layers separated by a non-magnetic layer are used in the giant magnetoresistive (GMR) sensors. GMR is a quantum mechanical effect of magnetoresistance occuring in thin-film structures of alternating non-magnetic and ferromagnetic conductive layers. The effect is seen as a change in the electrical resistance of the multilayer structure; magnometers often use this technology in sensor form to measure small magnetic fields.

Diamagnetism is evident in all materials to some extent, and is manifested by opposition to an applied magnetic field. Despite this occurring in all materials, other magnetisms are often significantly larger in magnitude, cancelling out this effect for practical purposes; it is only measurable in purely diamagnetic materials such as mercury, bismuth and silver. Superconductors are examples of perfect diamagnets as they repel all fields due to the Meissner effect

Paramagnetism is a type of magnetism in which the material is slightly attracted by an externally applied magnetic field and have a relative magnetic permeability greater than 1; however the magnetic moment produced by a magnetic field is often weak, requiring very accurate and sensitive magnetic detection equipment. Paramagnetic materials have unpaired orbiting electrons whose spins can be aligned by an external magnetic force, effectively reinforcing it; they differ from ferromagnetic materials in that they do not retain any magnetisation when an external magnetic field is applied then removed due to randomisation of the spin orientations caused by thermal motion.

Ferrimagnets have sublattices which have opposing direction to the neighbouring sublattices; these resultant opposing magnetic moments are not equal in magnitude therefore some net magnetisation remains. Magnetite and Yttrium Iron garnet are

examples of ferrimagnets, which, like ferromagnets, retain their magnetisation in the absence of an external field; magnetite was initially thought to be a ferromagnet due to the similarities until the discovery of ferrimagnetism.

2.1.2 Magnetic Field

The Magnetic Flux Density B, is identical to H in a vacuum, however differs through a material, but both are often used interchangeably, with the unit of B being Tesla, with a simple equation to convert between the two units.

$$B = \mu_0 H \tag{2.1}$$

Where u_0 is the magnetic constant, the magnetic permeability of free space.

The permeability of a material to a magnetic field is almost identical to equation (2.1) where μ replaces μ_0 and is a material's absolute magnetic permeability. Relative permeability is often used as a simple unitless indication of a materials permeability and is expressed by equation 2.2 (below)

$$\mu_{r=} \frac{\mu}{\mu_0} \tag{2.2}$$

The permeability of a material may be significantly large, and the higher the value, the more the material is magnetised by a given field. it is possible for a soft magnetic material to become saturated by a large enough external field, at which point it has the same permeability as free space; hard magnetic materials become magnetised proportionally to the magnetising field.

2.1.3 Hall effect

The Hall Effect is a physical principle which states that when a magnetic field is applied to a semiconductor or conductor, through which a current is passed, a voltage

perpendicular to the magnetic field will be generated (Ramsden 2006) , as shown in figure 2.2. This phenomenon was discovered by Edwin Hall in 1879, 18 years before the discovery of the electron. The principle occurs due to the movement of charge carriers in a conducting wire, whereby an external magnetic field alters the direction of these charge carriers such that it generates a potential difference across the wire, which can be conditioned and amplified as with any transducer (Figure 2.2).

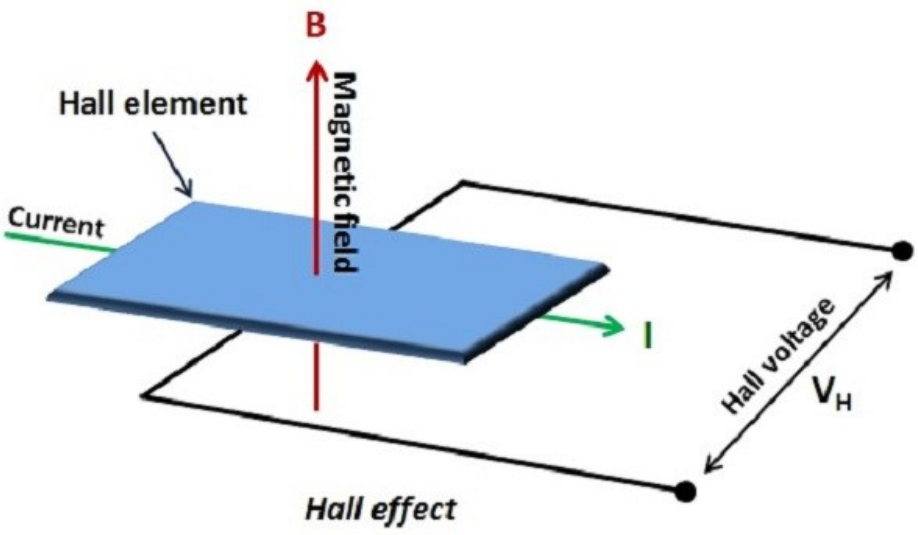

Figure 2.2 The principal of a Hall effect sensor. (http://dangerousprototypes.com/wp-content/media/2012/01/HallEffect.jpg)

The magnitude of the potential difference is a product of the current flowing through the conductor I and the magnitude of the magnetic field present upon the conductor, B.

$$V_H = -\frac{IB}{net} \tag{2.3}$$

Where V_H (equation 2.3) is the Hall voltage produced, *t* is the thickness of the conductor, *e* is the elementary charge, and *n* is the charge carrier density of the carrier electrons.

As with any transducer, there are sources of error, however a better, more sensitive transducer successfully minimises these; the Hall effect sensor is no exception. The most important characteristic of a linear output sensor, its sensitivity; which is simply

the magnitude of the output with a known input, in this case, the output of potential difference when the sensor measures a given unit of magnetic field, which has the units Volts per unit of magnetic field of bias current (Ramsden 2006). If the bias current of the sensor is constant, then the voltage output is directly proportional to the magnetic field it is measuring, determining its sensitivity; the units for sensitivity are often quotes as millivolts per gauss, mV/G and range from 1uV/G to 100uV/G in commercial transducers. Temperature affects the sensitivity of the transducer, however a small change in room temperature is unlikely to have much effect, with common commercial sensors having a temperature coefficient of sensitivity of approximately 1%/^{o}C.

Ohmic offset is another source of error in commercial sensors, and is the result of inhomogeneities in the Hall effect element, which manifests itself in the presence of a output voltage after transducer biasing, despite no magnetic field being present. Another contributor to ohmic offset is the strain placed on the Hall effect material during packaging and mounting, as the elements are also highly peizo-resistive, so any mechanical stress is likely to account for a degree of variation between sensors. Finally, misalignment of contact across the element at which the Hall voltage is produced is likely to increase this ohmic offset. Ohmic offset will also have a temperature effect, known as the Temperature Coefficient of Ohmic Offset, which will vary from device to device, and be largely unpredictable as a result of the peizo-resistive effects differing between package due to the different mechanical effect, and in order to best compensate for this, each sensor must be characterised within the expected set of circumstances and compensated depending on the output in these conditions; it is time consuming and costly so is only performed for instances where high precision is more valuable. An illustration of errors is shown in figure 2.3.

A third temperature coefficient is that of resistance, the input and output resistance should ideally be identical; any difference between the two will introduce a source of error, with the difference between the two subject to changing due to a change in operating temperature.

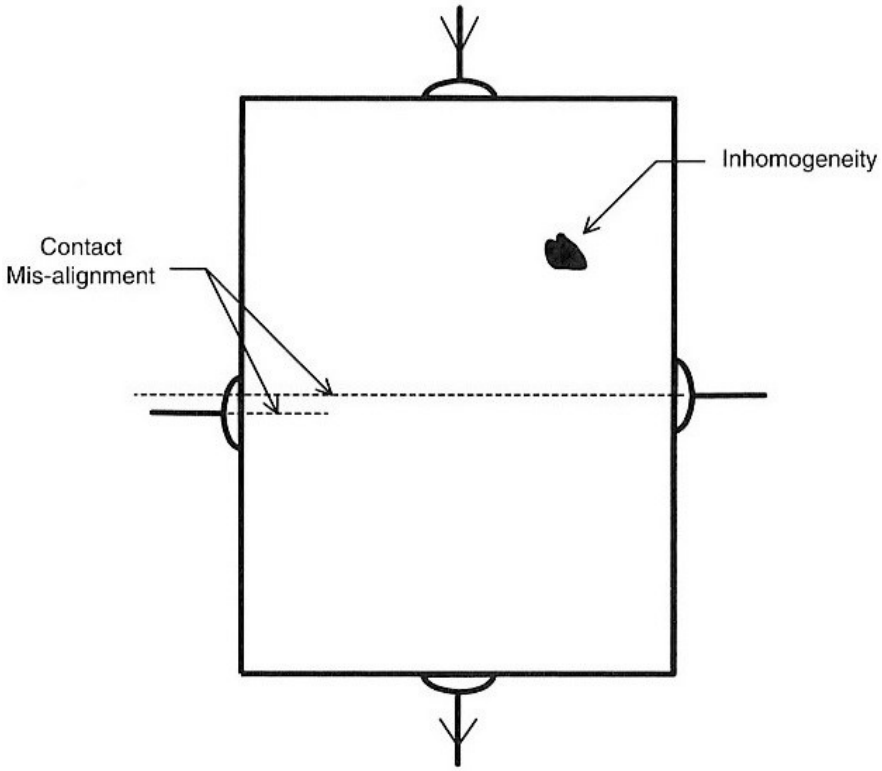

Figure 2.3 Potential causes of error in Hall effect sensors such as Ohmic offset error caused by contact misalignment and inhomogeneity. (Ramsden 2006)

The linearity of Hall effect transducers in limited by the passive nature of the devices, meaning the output is limited to a proportion of the input voltage; resulting in positive and negative saturation given a large enough external field. It is vitally important therefore, to choose a sensor with a high enough sensitivity and linearity over the range of expected field of use; a field may temporarily or permanently saturate the sensor if it is too large.

Possibly the most significant source of error in any transducer is noise, with some degree of noise totally unavoidable, however ideally tolerably low; Johnson Noise is thermally induced noise caused by the movement of electrons or other charge carriers through a conductive material. It is a function of the operating temperature and the resistance of the transducer itself, illustrated by the following formula (2.4).

$$V_n = \sqrt{4kTRB_w} \tag{2.4}$$

Where k is the boltzmann constant (1.38×10^{-23} K^{-1})

T is absolute temperature in Kelvin

R is the resistance in Ohms

B_w is the bandwidth in hertz

The bandwidth is a large factor of noise, the wider the bandwidth of the signal range, the greater the observed noise will be.

Flicker noise will often be a larger source of noise than Johnson noise, described by $1/f$ noise, where the quantity of noise per unit bandwidth is approximately inversely proportional to the frequency; due to the low frequency or near DC frequency applications of the Hall effect sensors, this noise can be significant. Thankfully this noise is determined by fabrication techniques and designs, it can be minimised in certain configuration types. Bulk transducers are essentially a small slice of semiconductor placed inside the IC package which is cheap and simple to produce and allows for easy interchangeability of semiconductor material, however it requires a relatively large current in order to obtain a sensitive output. Thin film transducers are constructed by placing very thin layers of semiconductor on a supporting, insulated structure, allowing for very small transducers with less bias current required for the same sensitivity; due to photolithographic techniques, mass production allows for cheaper unit cost compared to bulk transducers. The geometry of either type of transducer may be customised to reduce ohmic offset and contact misalignment.

The semiconductor material of the Hall effect device will also determine its sensitivity, with thin film Indium Arsenide being at the low end of the sensitivity scale (8μV/G at 10mA), bulk Indium Arsenide marginally higher (15μV/G at 150mA), silicon having a medium sensitivity (60μV/G at 3mA), and Gallium Arsenide having a very high sensitivity (100μV/G at 6mA). This is somewhat due to the semiconductor having a relatively low intrinsic charge carrier concentration, a value which also varies significantly with temperature. Materials are often doped to allow the choice of charge carriers, be that electrons or holes; the latter isn't available in metals, only semiconductors, this also decreases the influence of temperature on

the number of charge carriers, providing relatively stable concentration over a range of temperatures.

2.1.4 Sensor types

Due to many factors to be discussed, Hall effect sensors are probably the most commonly used to measure magnetic fields, with such applications as vehicles, personal computers, industry controls and many other electronic devices. Since the 1970s, sensors were produced on integrated circuits (ICs) with on board pre and post processing, meaning they could much more easily incorporated into complex devices due to their signal processing and internal amplifiers (Ramsden 2006). The ability to produce these reliable solid state specific ICs in small packages meant that they could also be mass produced, which saw a decrease in price per unit, allowing much higher uptake, with many mechanical-electrical contacts being replaced by the longer lasting and more reliable Hall effect devices, in such widespread applications as consumer keyboards. The increase in manufacturing precision has seen the decrease in size of Hall effect sensors, with the Hall effect element, on board signal processing and amplifiers being produced in a chip a few millimetres in size. As these packages have no moving parts, their reliability is very high, and the packaging ensures the internal circuitry stays free from moisture and other external factors, with most devices operating in a large range of temperatures with little adverse effect. Hall effect sensors are by no means the most sensitive or accurate of magnetic field measurement, they do offer an expected output which over a known range, is linear and is relatively hysteresis free, and can differentiate between north and south poles of the magnetic field which they are subjected to. Another significant factor in their uptake and therefore ongoing improvement and development, is cost; the sensors are very cheap to produce and reliable and fairly linear the uptake into industry has been significant, meaning these sensors are very widely available in a range of different configurations (Ramsden 2006).

Sensor interfacing is also important when using a transducer, as this could be the difference between a sensitive, linear reliable sensor, and one that is poor and unusable; the bias circuit and output conditioning can be used to improve an already

sensitive sensor and gaining better performance. Voltage or current biasing may be used, the former requiring compensation for a large temperature coefficient of sensitivity and simple circuit design, however is best suited for low current devices, the latter having an inherently low temperature coefficient of sensitivity without correction. The constant current bias method also means that given a low enough current, the sensor will not undergo internal heating and therefore will be relatively drift free (Ramsden 2006).

Post processing or amplification of the output of the sensor must be properly handled too, as this may lead to sources of error and noise; this may be performed inside the IC or with supporting circuitry. With a correctly biased sensor, a small differential potential difference is produced under the presence of a magnetic field, this must therefore be fed into an appropriate differential amplifier, which removes the common-mode signal, leaving only the ground referenced differential signal. These amplifiers have several parameters which determine their performance, such as differential gain, gain stability, common-mode rejection ration and input offset voltage and bias current, it is therefore important to choose an accurate amplifier which adds minimal noise while amplifying the signal to practical levels; other features such as filtering, temperature compensation or offset adjustment may also be desirable (Ramsden 2006).

Given certain requirements, a Hall effect sensor can be employed as a switch or latch, with the use of a combination of threshold detectors, comparators and logic gates, whereby if a given voltage threshold is reached, the output jumps from ground to high, which is useful in certain applications such as keyboards and other proximity sensors; latches and North-South switches can be produced using slightly different configurations (Ramsden 2006)

2.1.5 Magnetoresistive principal and sensors.

Magnetoresistance is the ability of a material to change its resistance in the presence of a magnetic field; initially having small resistance drops of 5% or less when discovered by Lord Kelvin in 1856. The small changes in resistance were latterly called ordinary magnetoresistance due to the magnitude of change, when larger magnitude changes were found in different materials (Feng & Jin 2005). Anisotropic magnetoresistance (AMR) is the phenomenon which shows an increase in resistance when the magnetic field is in the same direction as the current flowing through the material, and shows a negative change when the current flow is at 90 degrees to the current flow; the effect is the product of the magnetisation and orbit-spin interaction and is material dependant. The sensor typically consists of 4 nickel-iron AMR thin film sensors in a Wheatstone bridge arrangement, to reduce noise and temperature dependence. As a result of the relatively high sensitivity and directionality of this property, sensors have been developed which measure the Earth's magnetic field, current flow through wires, vehicle and large metal object detection, as well as angle or position measurement (Reig et al. 2009).

2.1.6 Catheter based SCJ measurement

Magnetic sensing technology has been used in the body for decades; the summary in the introductory chapter shows the vast history of magnetic based technology and probably the most well known magnetic sensing technology used today, MRI, is employed to non-invasively image the human body and its organs, using a high magnetic field to influence the magnetic spin of elements in the body and measuring the relative change in order to image the body. Magnetic measurement of the digestive tract is a less well known area, but one which is focused on motility and gastric emptying times; detecting magnetically coated food particles. It has been suggested by Professor Kenneth McColl of Glasgow University, that measuring the position of the squamocolumnar junction while simultaneously measuring pressure

and pH of the upper gastrointestinal tract would be extremely advantageous, and this thesis documents the trials, tribulations and successes of this project.

As stated, it would be ideal to continuously monitor the location of the Squamocolumnar Junction inside the human body. However there are several constraints which are placed upon this task which are discussed in the following paragraphs.

The device must be first of all be safe for use in the human body, the safety of the patient and operator is paramount and there is no compromise for safety in any medical device according to the standard BS:EN 60601-1, Medical electrical equipment, general requirements for basic safety and essential performance; the device must therefore conform to the appropriate medical safety requirements. The standard explicitly states several criteria including the allowable level of current leakage, as exposure to large leakage current is potentially very dangerous, and therefore must be kept below an accepted safety level so not to cause burns when inside the patient's mouth, oesophagus and stomach, nor must it endanger the operator. The device must be safe even in the event of electronic failure of any part of the device and so have appropriate design and fail safes so that although reliability and operation may be compromised, safety is not. The standard details a list of tests which must be performed such as leakage current testing and sharp object hazard as well as marking of equipment and buttons; the 384 page document is substantial and in some parts requires destructive testing to assess the safety of the device. A stipulation of the standard is that the device must still be safe to the patient with regards to leakage current and physical harm even if a fault occurs; this is termed *single fault safe*, if the device is still safe to the patient and operator even if a fault of any type occurs, anywhere in the device. Single condition failures include those which may cause further multiple failures are still considered single faults; such a failure of electronic components for example should mean that neither the patient nor operator is exposed to mains voltage. The chassis or other part of the device must also never become live in single fault condition as, due to the grounding of British mains power, may mean that the operator or patient is exposed to a large current (it is therefore advisable to use plastic or other non-conductive chassis and parts rather

than metal); in the case of an oesophageal catheter based device, the wet and delicate epithelium of the oesophagus is more susceptible to burns and damage from a low current than skin is. Leakage current is another significant section covered by the standard, with absolute values of acceptable current leakage for standard operation and single fault conditions. Faults are divided into three conditions, those which are so remote that they can be ignored, those which may occur and would constitute a single fault, and those which are so likely that they are to be considered a normal condition of operation. While it is required that single fault conditions are to be protected against, it is of course a minimum requirement, so double or redundant fail-safe protection may be used and is advised to produce a very safe device.

Tests for safety are to be performed in their standard operating conditions, or those which best mimic these conditions, for example, the standard operating condition of an endoscope is in extreme pH and aqueous solution and in some cases, high pressure, it must not produce a fault when subject to these conditions, therefore it should be acid resistant and waterproof as well as sturdy under pressures beyond the limits of human physiology.

Leakage current for any part of the device under normal operating conditions is 100 microamps and under single fault condition is 500 microamps; these correlate to the safest maximum current to which a person may be exposed to before burning or tissue damage may occur; earth leakage current is 5 milliamps and 10 milliamps for normal and single fault condition respectively.

A specific tool which is shaped like a small finger, tests the access of any parts of the device to leakage current of any of the open parts of the device, or those which can be opened without the use of a specific tool, for example button covers or connector ports.

Any medical device or apparatus must not endanger the patient for the period of time during or after the experiment if any parts of the device remain attached to or inside the patient. Checks for any such remaining apparatus which may present a potential hazard in any environment, such as in proximity to an MRI machine, must be checked for and removed if not passed through the digestive tract and out of the body

in good time. The current method of measuring the position of the SCJ, as discussed in the introduction chapter, is with fluoroscopy, a procedure which exposes the patient to a high level of dangerous radiation, so is therefore used for very small periods of time; this is not an acceptable level of safety for this device, therefore an additional safety requirement is that the patient or operator must not be exposed for radiation levels above background levels, other than for an initial validation against the gold standard.

2.1.7 Device requirements

The measurement device must be capable of reliably recording the position of the SCJ over extended periods of time; the tolerable level of accuracy of measuring the position of the SCJ to within 1 centimetre given the relatively small movements of the SCJ within the body and the large length of the oesophagus of up to 30 centimetres. Although displacement of the oesophagus in a hiatus hernia is typically 4 centimetres, it can be a separation of at least 3 centimetres or up to 6 centimetres. The more subtle movement of the SCJ during activities such as swallowing, breathing and during reflux episodes is significantly smaller, requiring a high precision measurement. The inherent resolution of the other upper GI investigation tools are limited to the separation between sensors; the solid state high resolution manometer having radial pressure sensors every centimetre means the longitudinal resolution rather than pressure accuracy along the oesophagus is every 1 centimetre. Similarly positioned pH sensors have also been employed so the current highest resolution of any internal upper GI medical device is 1 centimetre (Conklin et al. 2009). The output of these devices is often interpolated and displayed in a potentially misleading manner so that an operator may be unaware that the interpolation adds a source of error (Robertson et al. 2012; E. Robertson et al. 2011; E. V. Robertson et al. 2011), and that when movements of several millimetres are concerned, interpolation is not sufficiently accurate; a problem which may lead to misdiagnosis or incorrect research output. The interpolation may improve the visual aesthetics and

user interpretation but should be used with caution, and is it is being relied upon, thoroughly validated.

The device must also be compatible with other commonly used upper GI devices, as the position of the SCJ without other relative measurement offers little; the data is incredibly valuable however, when simultaneously used in conjunction with one or a combination of high resolution manometry, pH and or impedance tools. Because of the need for compatibility with said equipment, the devices must be combined together into one probe and passed together so relative position measurement is known; if the probes are not combined but passed separately or even allowed to move with respect to each other, then positional accuracy of relative positional and anatomical measurements is severely compromised.

The device therefore, must neither cause error to, by way of interference with, nor be the subject of interference from the associated devices when used concurrently in the same experiment.

The measurement accuracy of SCJ position should be at worst 10 millimetres and ideally 1 millimetre as desired by Prof McColl which would allow for very accurate measurements of SCJ position in the GI tract; this level of accuracy is much higher than that of the other devices, however the current gold standard of measuring the SCJ, fluoroscopy, has an accuracy of several millimetres, subject to interpreter variation, angle of image and reference position. Since 24 hour pH recordings are routinely made (Logan et al. 2002) the duration of operation of the probe should equal to this time period, however it is acknowledged that the practical limitation of study length may be imposed by and subject to medical ethical approval.

Ideally the device should have some inbuilt method for synchronisation with the other GI tools, which would allow the accurate investigation of various anatomical events for which timing is crucial. Fluoroscopy was calibrated using a marker visible in the video while simultaneously marked on high resolution manometry; it was observed that this technique had an error as high as several seconds, it is therefore imperative that this device does not have this problem, otherwise events which last all of several seconds could be completely misinterpreted or misdiagnosed. The device should also have a visual indication of the position of the SCJ for real-time

stand-alone use and have the ability to output the data to a computer or data logger for detailed post-experiment analysis with the other GI tools.

Use of this device will aid research in the Upper GI area, being predominantly used to explore TLOSRs, with the aim of recording for the first time, a full TLOSR and investigating how often they occur and what happens during the period of loss of sphincter tone.

2.2 Materials and Methods

2.2.1 Sensor and magnet arrangement

In order to develop a catheter based probe which meets the above requirements, a device was developed which consisted of an array of Hall effect sensors on a flexible circuit board which could be inserted nasally or orally into the subjects' oesophagus after a small magnet was endoscopically attached to the SCJ by a trained endoscopist, using the Olympus Endoclip as shown in figure 2.4, 2.9 and 2.10. This combination of sensors and magnet allowed detection of the magnet position along the oesophagus; the magnet position is directly associated with the SCJ position due to the close attachment. The array of Hall sensors was connected to a microprocessor and computer to facilitate position calculation based on the output from all the sensors.

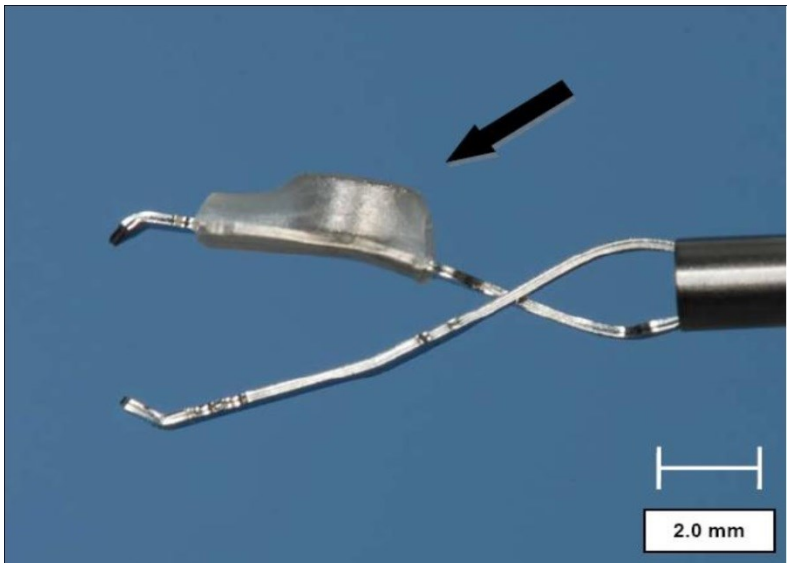

Figure 2.4 Customised Endoclip with magnet attached.

2.2.2 Stage 1 SCJ Locator

The specific Hall sensor used in the device was Allegro A1395 (Digikey, USA); a 6 pin, surface mount Hall sensor package which was 3.15 millimetres long by 2.15 millimetres wide by 0.8 millimetres tall (figure 2.8). The Hall effect sensors are linear with a sensitivity of 10mV/G, the package also contains in-built amplifiers with ratiometric output (Figure 2.6), meaning they can be connected to hardware directly, minimising the amount of external support electronics (figure 2.7).

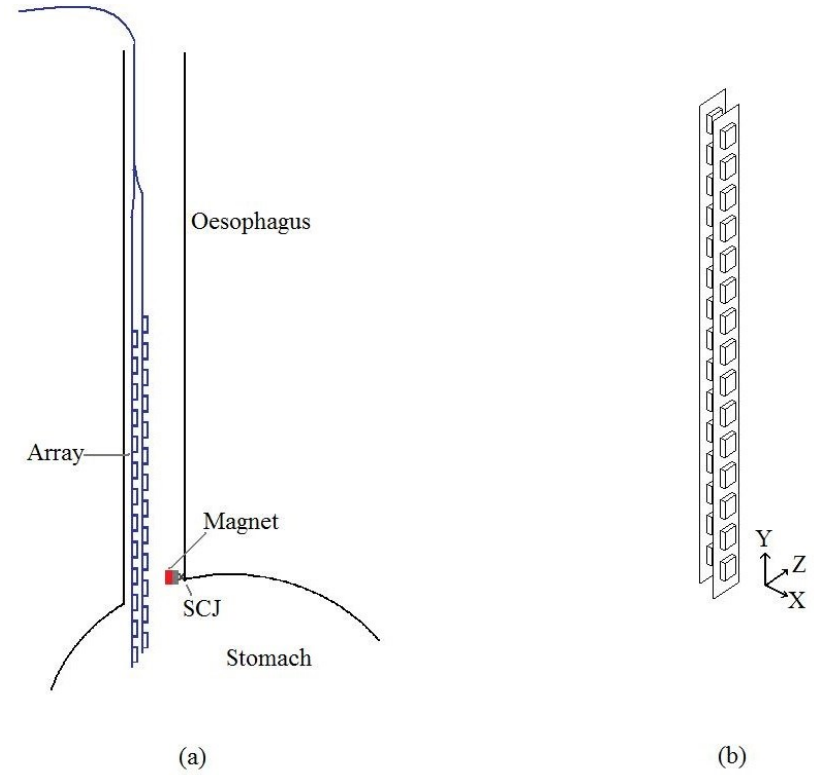

Figure 2.5 Stage 1 Squamo-Columnar Junction locator (in silicone, below). (a) shows the schematic of the device inside the body, with magnet attached to the SCJ. (b) shows the axis orientation with respect to the probe.

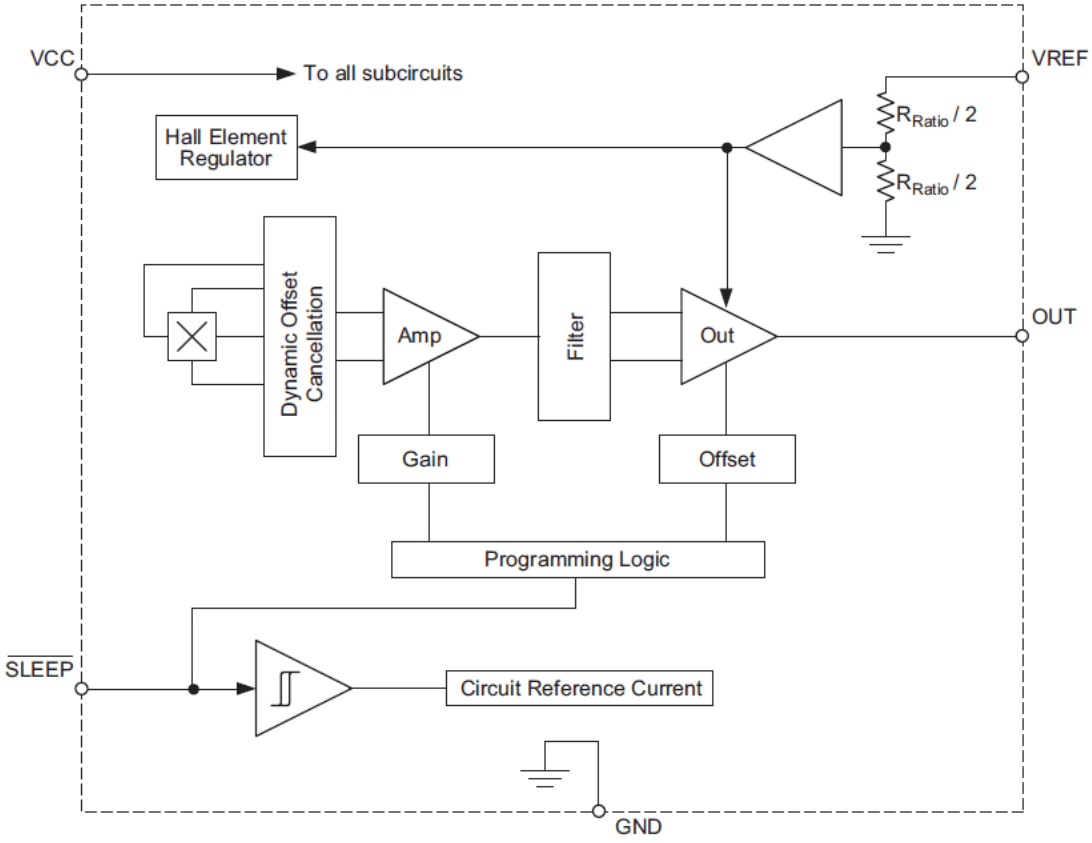

Figure 2.6 Allegro A1395 sensor functional diagram. Acquired from datasheet.

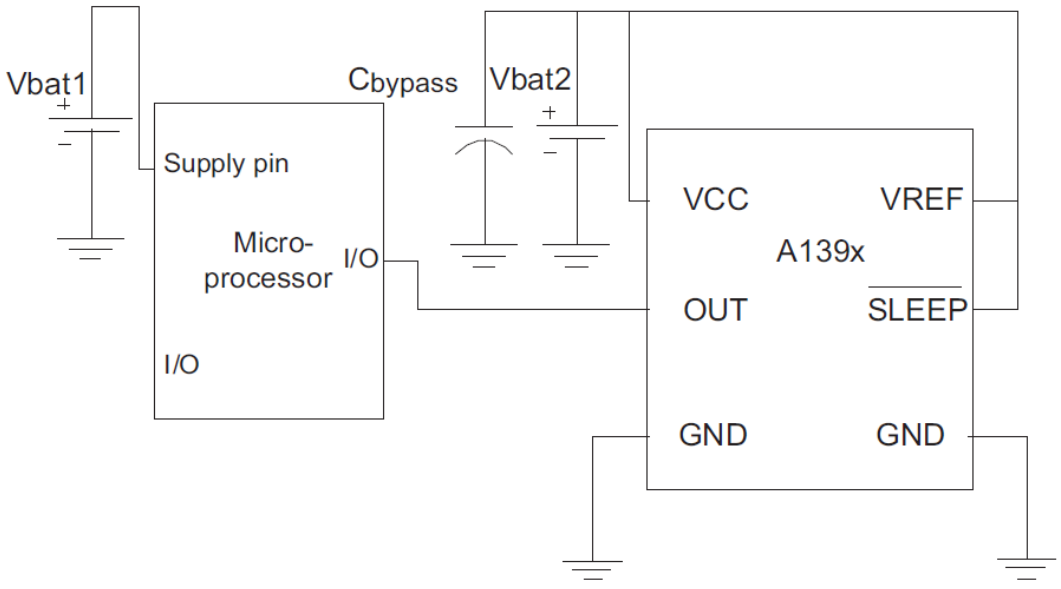

Figure 2.7 Allegro A1395 schematic with microprocessor. Acquired from datasheet.

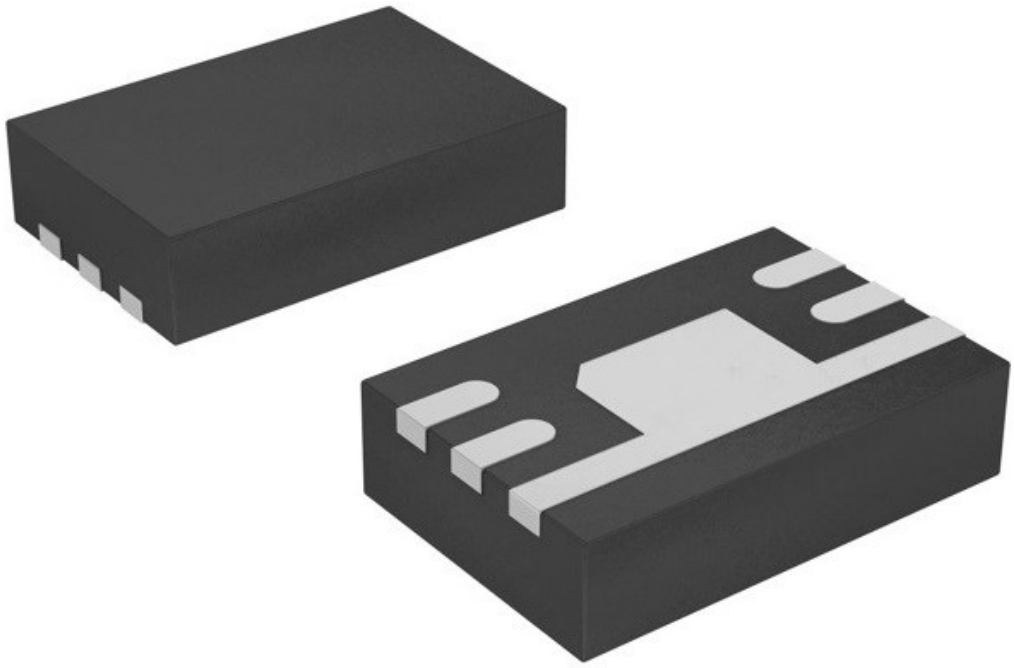

Figure 2.8 Rendered Allegro A1395 package

2.1.3 Magnet detail

A magnetic material must be used in association with the Hall effect sensors in order to allow for the designed system to function; the magnet strength must be such that it is detectable by the sensors at a range of at least a centimetre yet not saturate the sensor(s) at closer range. The magnet must also be safe for use in the digestive system and not cause physical or chemical damage to the body in any way. Another limitation of this system is that only one magnet may be used in an individual, as when the magnets are free in the digestive tract after the experiment has finished, multiple magnets may become attracted together; this causes a potential health risk if the magnets are in separate loops of the intestinal tract, which if become attracted may clamp a section of the intestine, which would cause necrosis and further associated complications as a result.

The magnet, as a marker of the location of the SCJ, must be locally attached to the SCJ; this is done using a standard Endoclip (Olympus, USA) (figure 2.10) which is

traditionally used for clamping shut gastric bleeds and ulcers, therefore is perfect for this system, as it is already accepted within the Upper GI fraternity and is safe for use in such an environment as well as having pre-existing attachment methods. The magnet is attached to the arm of an endoclip using heat shrink material such that it does not impair the firing of the attachment method of the clip and is as close as possible to the wall of the gastro-oesophageal junction.

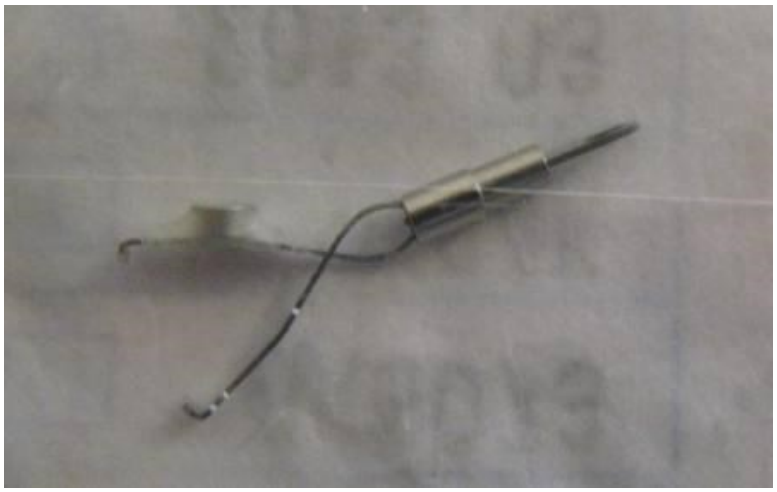

Figure 2.9 Olympus Quickclip Endoclip in firing device.

The method for attachment of the clip to the stomach or oesophageal wall is during endoscopic procedure; this is performed by a trained professional, whereby the endoscope is passed through a Lidocane-numbed oral cavity into the oesophagus and stomach. The SCJ is visible through the endoscope as a distinct change in tissue type and colour (Figure 1.2(a)); the clip is then attached to the SCJ by passing the magnet-clip arrangement through the working channel of the oesophagus attached to a firing device, which is employed when the clip's jaws are open and touching the SCJ. The position of the clip on the SCJ is then confirmed by the endoscope operator and the clip-firing device detached and withdrawn; some clips may have their jaws opened and closed multiple times in order to obtain a good position at the SCJ, however this feature is not available on all endoclips or their associated firing devices.

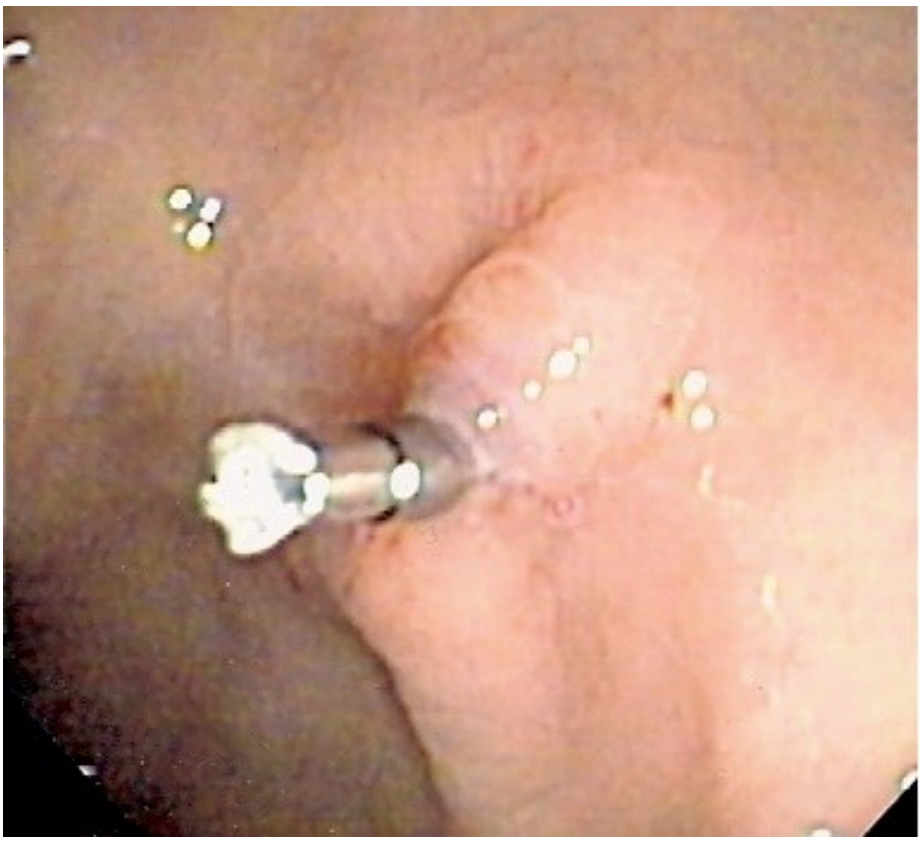

Figure 2.10 Endoclip with magnet attached, attached to the the gastric wall, as in standard use.

Due to the size and function of the oesophagus, there is a limit to the shape and size of the magnet such that it doesn't impede the GOJ closing nor obstruct a bolus of food matter passing into the oesophagus, therefore the magnet should be as small as possible while maintaining functionality; the magnet should also be free of sharp corners which could potentially damage the oesophageal lining. The strongest magnets available are those termed rare earth magnets, which are permanent magnets made from alloys of rare earth elements; the manufacture of these magnets allows for much stronger magnets than ferrite or alnico magnets of the same size. The two main categories of rare earth magnets are neodymium and Samarium-Cobalt; these magnets can be custom produced using either sintering or bonding processes to almost any custom shape and size, therefore due to the very high strength of these magnets per unit volume, and the customisability, they are the ideal choice for this situation. A magnet's field shape and strength are a function of its size and shape, therefore simulations can be produced which estimate these parameters which enable

the calculation of performance of a custom magnet. While custom magnets are significantly more expensive than rare earth magnets produced on mass, they may provide the only solution to a given situation. The ratio of elements within the magnet can be tailored so that the given size offers a precise strength; a feature which can be useful when trying to develop very small magnets which do not saturate sensors. With the first generation of SCJ locator probes, a small commercially available 2mm diameter and 1mm axial length disc or cylinder shape magnet was used, with both N42 Neodymium (B_r 12800 Gauss) and SmCo26 Samarium Cobalt (B_r 10300 Gauss) magnets tested in the above dimensions; the field strength graphs for each are produced in Figure 2.11, as measured by the Allegro A1395 Hall effect sensor.

For the third generation of SCJ locator probe, smaller magnets were needed for use with more sensitive sensors; these sensors were based on Magnetoresistance and are therefore susceptible to permanent saturation which severely affects their operation to the point that they no longer function within the system. A range of custom made and commercially available 1 millimetre diameter and 1 millimetre axial length rare earth magnets were manufactured in a varying range of strength material to test the optimum configuration of magnet-sensor strength and sensitivity. Although weaker magnets such as ferrite or alnico are available, it is not possible for them to maintain their magnetisation when manufactured in a size as small as required for this project. Samarium Cobalt and Neodymium magnets are currently used in the digestive system, specifically in orthodontistry, where they are used to maintain tooth alignment and maintenance of denture position; these magnets are relatively safe for use in this environment although Noar and Evans (Noar & Evans 1999; Noar et al. 2003) highlight the issue of long term corrosion of Neodymium magnets over a number of years. However, there is no issue for these magnets when used for a few days or weeks as with this application. The magnets used in the body are very weak, with a surface strength of 450 mT which decays to 4 mT at 5 millimetres and is nearly undetectable outside the body. However, the presence of a very strong magnetic field, such as that of a MRI machine, could potentially cause the magnet to move inside the body or even be pulled through the soft tissue of the gut to align with the external field. This is severe enough that after the experiments with the locator

probe is performed, the subject will return after 6-8 weeks for an abdominal x-ray in the posterior-anterior view in suspended respiration, to determine if the magnet is still present in the gut. Before which time the subject is told to avoid such environments unless absolutely necessary, whereby either upon request or if the magnet is still present upon scheduled x-ray, the magnet may be removed, or allowed to pass naturally and a repeat x-ray performed to confirm this after an extended period of time.

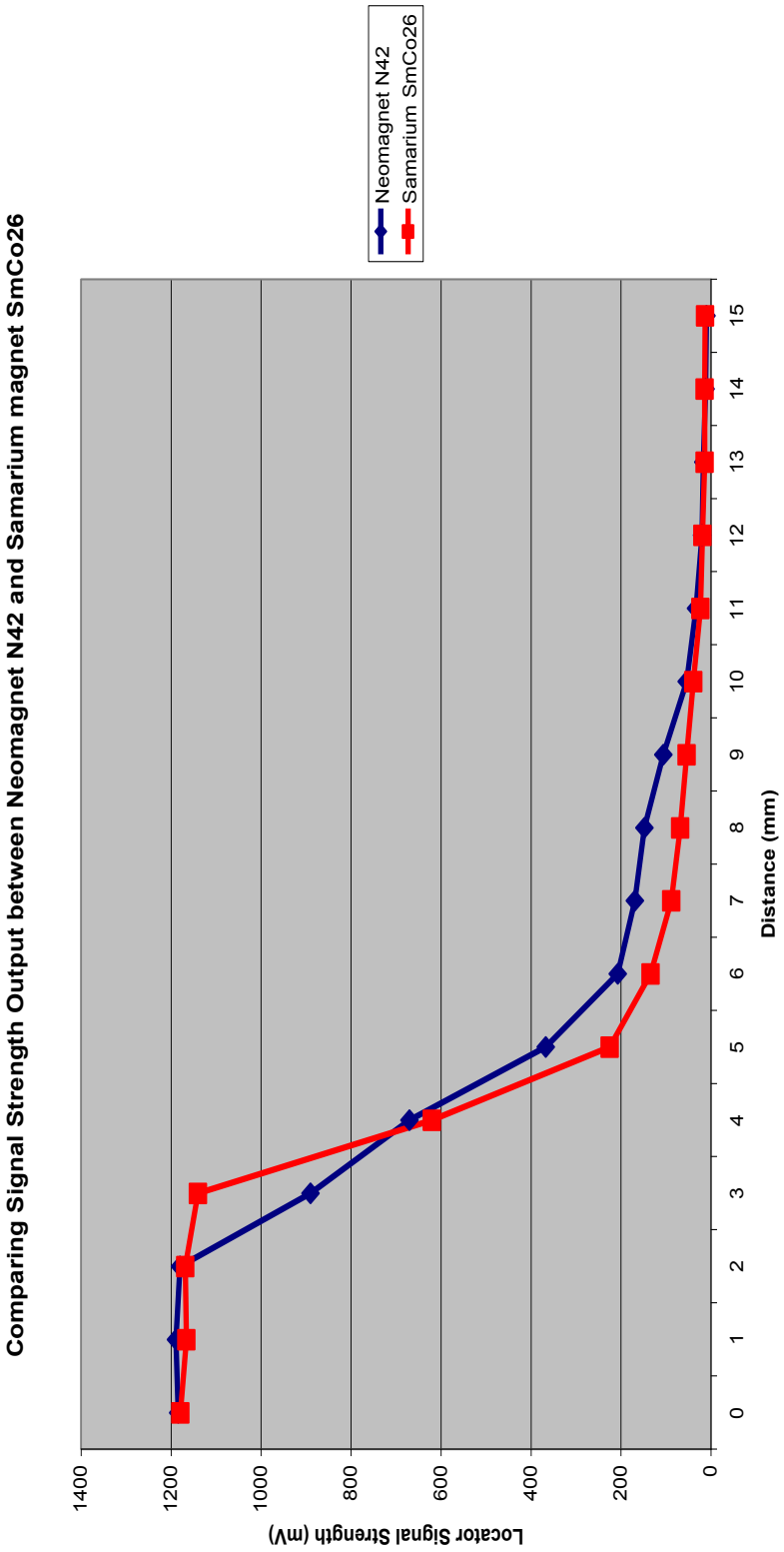

Figure 2.11 Field strength of 1 millimetre by 2 millimetre disc N42 Neodymium (B_r 12800 Gauss) and SmCo26 Samarium Cobalt (B_r 10300 Gauss) magnets.

2.2.4 Sensor arrangement/circuit board arrangement 1

There are several limitations with which the device has to cope in order to function appropriately and safely; one such significant issue is size, the probe must be able to be inserted into the patient via either the nose or mouth, without causing damage or significant pain, it must also not impede the action of the Upper or Lower Oesophageal Sphincters, swallowing or any other natural bodily function. The probe therefore must also be flexible enough to be inserted and allow some degree of free movement, while transversing the near right-angle section of the naso-pharynx. These limit both the size and material of the device as well as the design; with this in mind, a flexible printed circuit board (FCB) was produced which enabled 13 Allegro A1395 sensors to be placed along its length, as well as supporting electronics (shown in figure 2.12). The width of the FCB was limited to 3mm, due to the size of the oesophagus and GOJ; the sensors themselves are 2.15 millimetres wide, and each requires a smoothing capacitor close to the power rail of the FCB for accurate operation. The sensors were placed 1 centimetre apart for initial testing and to ensure adequate separation when soldering by hand or using machine placement, however it was quickly discovered that the spacing was too large and the magnet was not reliably detected along the full length of the sensor section. Therefore, 2 strips of sensors were placed on top of each other, with alignment in such a way as to enable 5 millimetre spacing between sensors, alternating between the top and bottom strip, as shown in figure 2.12. The output of each sensor was attached to a solder pad at the opposite end of the FCB, soldered to which was a wire in a multi-core cable, which in turn was connected to a multiplexer and microprocessor set up in order to sample each of the sensors' outputs in turn, and combine the outputs into useful information such as position of the magnet along the length of the probe and the strength of the field at the closest sensor (figure 2.14); this would enable the users to detect where the magnet was in the body and also ensure the magnet was being detected by a sensor. This information was both displayed on a LCD screen for stand-alone use (figure 2.13) and to a Polygraf machine which is a previously established PC interface for pH probes, but was adapted to allow the capture of the above values to a PC for later analysis. For in vivo use, all three generations of SCJ locator probe were

enclosed in a silicone tube (figure 2.5), as described in a later section. Once the device was produced, a set of initial validation experiments were performed in order to test the performance of the above device, the details of which can be found in the next section.

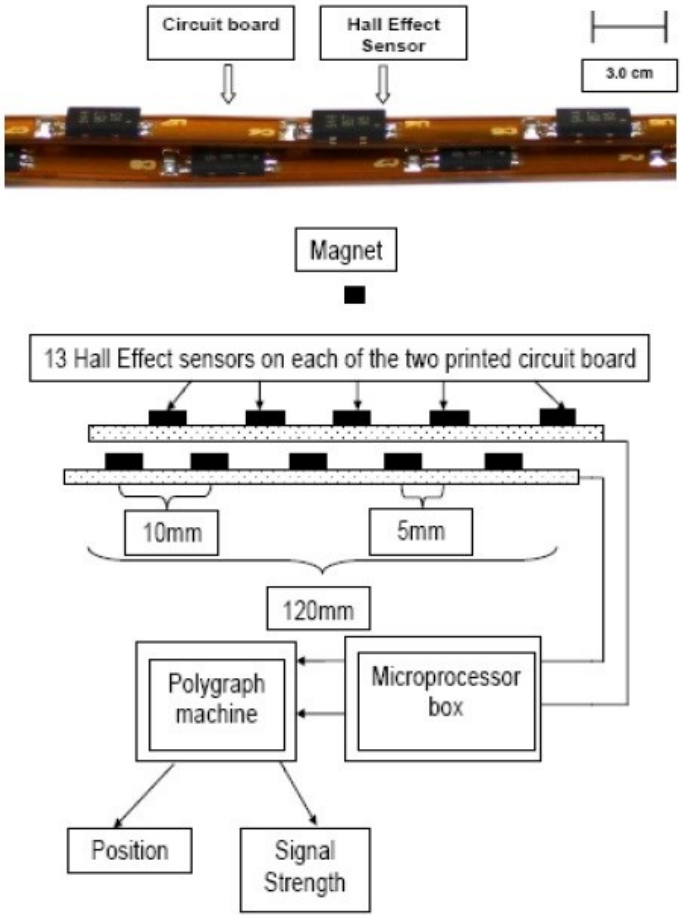

Figure 2.12 Schematic of connections with close up of flexible circuit populated with Allegro A1395 Hall effect sensors.

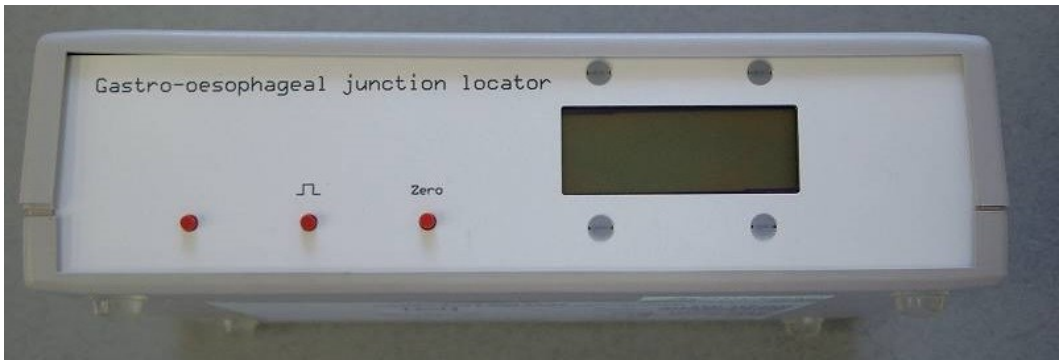

Figure 2.13 Microprocessor box with LCD output for immediate position display.

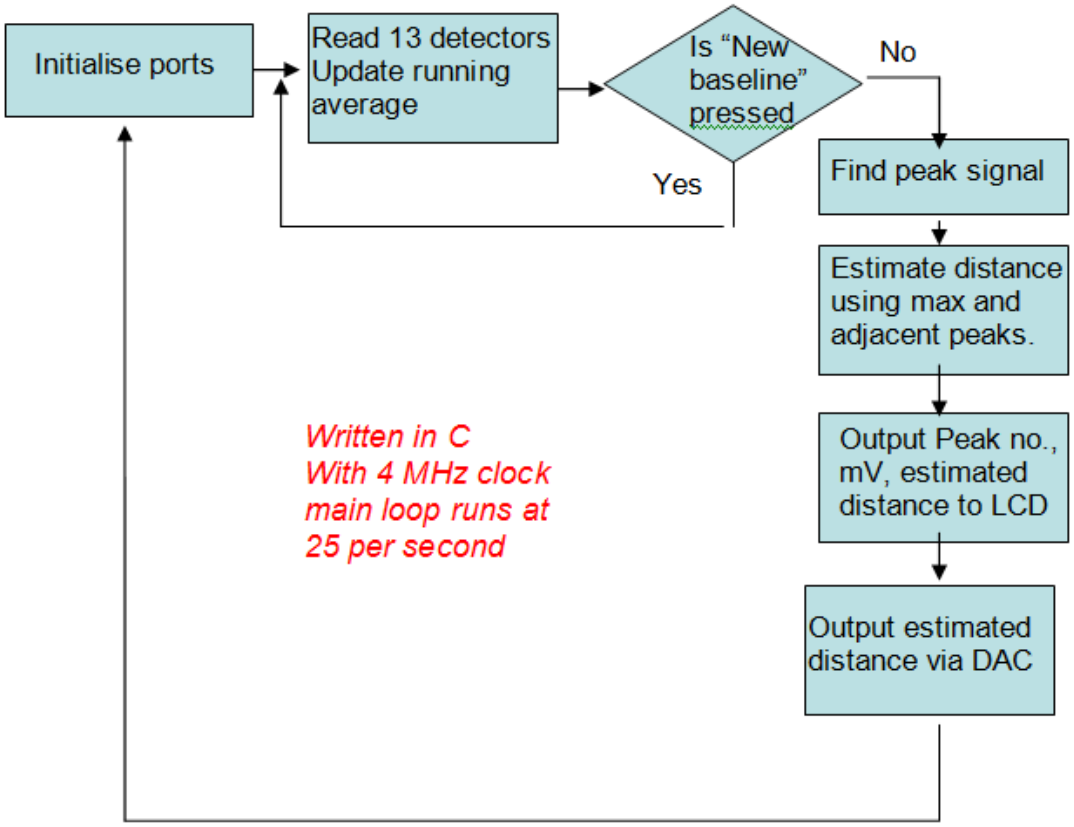

Figure 2.14 Microprocessor flow chart for sampling and outputting sensors, as used in all 3 stages of the SCJ locator probe.

2.2.5 Circuit board arrangement 2 "3D"

Validation experiments were performed to test the device's performance outside of patient contact, meaning all variables could be controlled and varied as required, in order to determine the potential weakest parts of the device's magnet detecting accuracy; these experiments were termed benchtop tests or experiments, to differentiate between *in vivo* or patient tests. As will be described in section 2.3, the benchtop experiments revealed the issue of orientation dependence with the sensors and magnet, this was thoroughly tested and showed that when the magnet was facing the side rather than the front of the sensor, the ability of the sensor to detect the

magnet was severely reduced. This flaw was also demonstrated *in vivo* by the loss of signal strength for a small percentage of time.

This provided a significant problem as signal could be lost during important anatomical events, meaning the device had to be rectified. The next generation of device therefore needed to ensure the was capable of detecting the magnet much more reliably without losing signal; the idea was developed to have two sensors at perpendicular orientation to each other to ensure that if one sensor was in a poor position to detect the magnet, the other sensor was able to detect it. The re-design also offered the chance to address the dual strip issue, by replacing the two strips with 1 dedicated strip with a large number of sensors, placed 7 millimetres apart. Due to the number of sensors and the limitation of size of the strip, a 3 layer FCB was designed and manufactured which allowed for the large number of outputs from the sensors; A custom multi-core cable was also manufactured to facilitate the connection to a multiplexer and microprocessor. The second generation FCB consisted of a main strip with 13 sensors and an additional tab for each perpendicular sensor (figure 2.15), which was flexible enough to bend at right angle and with the use of a custom jig, were glued in place to maintain the improved orientation. The sensors on the tabs had the same power and ground connection as the sensors on the main strip, which meant the output of each pair of sensors could be summated and used to calculate the position of the magnet. The solder strip of the FCB at the cable end was also improved by widening and having larger pads, so produce a more reliable connection (figure 2.16).

Figure 2.15 Circuit board for the “3D” locator probe showing the “tabbed” protrusions which are bent and secured at 90 degrees after population.

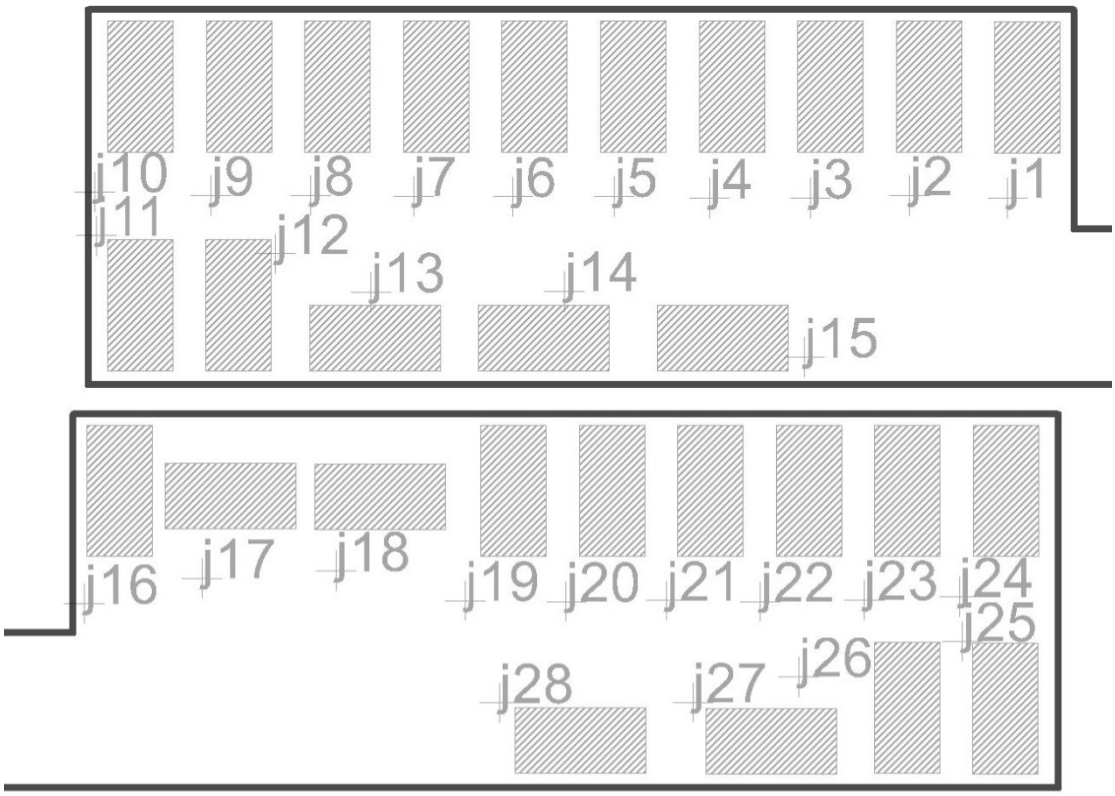

Figure 2.16 Circuit layout of multiple sensors and solder pads on widened end.

2.2.6 Circuit board arrangement 3 “MR sensors/I2C comms”

Initially there were promising results with the second generation of SCJ locator probes, with a better position measurement time throughout a whole patient study. The assembled probes themselves however only lasted about 10 studies before developing faults, which were mainly soldering based issues where the sensors were separating from the board due to stress from bending. It was summarised that although the second generation was less physically reliable, it was significantly better for in vivo use and allowed for more accurate and consistent recording of the position of the SCJ until failure. Another weak area of the previous generations was the requirement of a very large and heavy multi-core cable, necessary due to every sensor having an individual output; therefore there were over 20 wires attached to each strip. The heavy and thick cables caused issues as they would place stress on the soldered contacts which were on the fragile FCB; this was another weakness which

needed to be solved. Having therefore decided to develop a more reliable third generation of SCJ locator probes, in order to maintain the three-dimensional aspect of the second generation as well as minimise the number of solder contacts, dedicated three-dimensional magnet sensors with serial communications were sought; an digital address based sensor system with each sensor having a different address would allow communication to every sensor using the same input/output line. Initially there were very few sensors which suited the criteria, as often they would only have one address for all sensors from a manufacturer, presumably because they have to pay to obtain each address.

To check the compatibility of the digital communication method when used in conjunction with the manometer, a test experiment was designed, whereby a USB extension cable was manufactured with bare wire, which would be placed on both devices to detect any possible interference of the digital signal; the extension cable was two meters long and consisted of the four wires needed in USB communication At the end of the extension cable, a USB storage flash drive was attached, and via the cable, plugged into a laptop; to test the potential noise induced onto the HRM or pH devices or cables, a large 300 megabyte file was transferred to the USB storage device and the output of the pH probe and Manometer were recorded, after which the recording was maintained in order to provide a control of no noise. Since there was no noise on either the control or during transfer, it was deemed that digital sensors would have no noise effect on either device, therefore the digital sensor system for the third generation was developed.

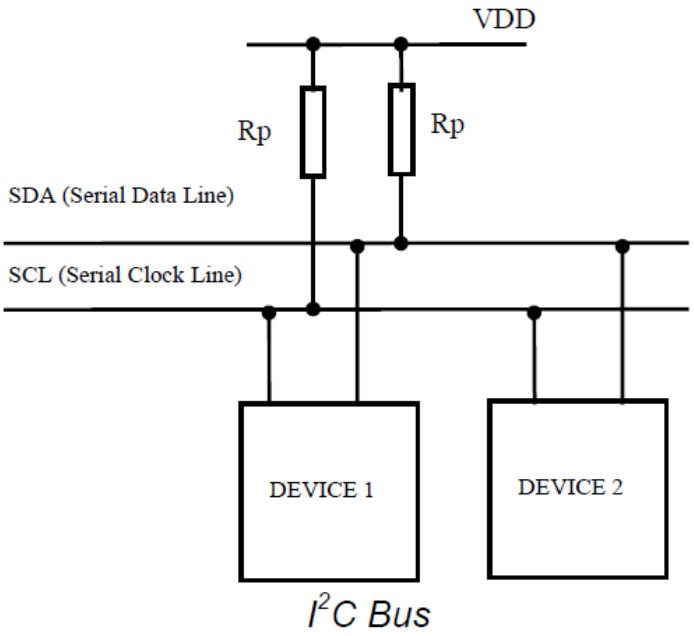

Number 35X	Part number	7bit I²C Address
350	MMC3280MS	0110000b
351	MMC3281MS	0110001b
352	MMC3282MS	0110010b
353	MMC3283MS	0110011b
354	MMC3284MS	0110100b
355	MMC3285MS	0110101b
356	MMC3286MS	0110110b
357	MMC3287MS	0110111b

Figure 2.17 Serial Bus with multiple devices, showing the different addresses for the Memsic MMC328XMS magnometer.

One suitable such sensor was found however, in early stage development, a three axis Magnetoresistive sensor was available, with Inter-Integrated Circuit (I2C) communications; the I2C technology is a multi-master serial single-ended computer bus developed by *Philips* that is used to attach low-speed peripherals (up to 400KHz) to a master device using one bus line (Figure 2.17). This technology would allow the use of a minimum of 4 tracks and contacts to which attach wires: Power, Ground,

Serial Data Line (SDA) and Serial Clock Line (SCL); the SDA and SCL lines are each connected to the power line with a pull-up resistor as the master and slave devices are only capable of pulling the data lines low. While the Clock line is controlled by the master, the data line is controlled by both master and slave, enabling bus control and communication with individual peripherals, or in this case, sensors. The Memsic MMC328xMS Ultra Small 3-axis Magnetic Sensor, with I2C Interface had been released during the search for a new sensor, with a 10-pin low profile LGA package (3.0 x 3.0 x 1.0 mm) and is capable of operating in temperature ranges of -40°C to +85°C (Figure 2.20). The sensor is capable of detecting magnetic fields within the range of +/- 8 Gauss, over which the sensor becomes saturated and remains in such a state until re-calibration is performed; this sensor is more sensitive than the previous Allegro A1395 sensor therefore a weaker magnet is required. The sensor itself has three axis measurement which is ideal for this application, and internal circuitry and analogue to digital converter (ADC) which digitises the output for each axis (Figure 2.18) and upon request, sends this information via the I2C bus to the master which in this case is a microprocessor. The sensor was available in 8 I2C addresses (figure 2.17) which meant that several banks of addresses were required in order to have enough sensors to have the required measuring section along the probe; this would increase the number of tracks and contacts for wires, but only by a few, which was more than acceptable considering the number of contacts that the previous generations required, 4 banks providing 32 sensors only requires 7 contacts (figure 2.19).

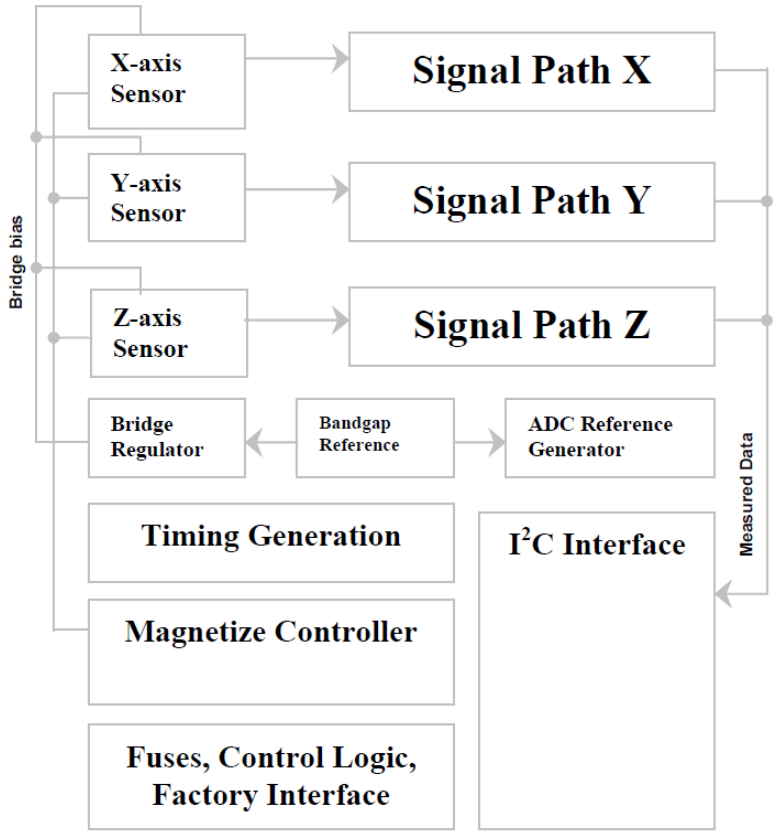

Figure 2.18 Internal schematic of Memsic MMC328xMS magnometer

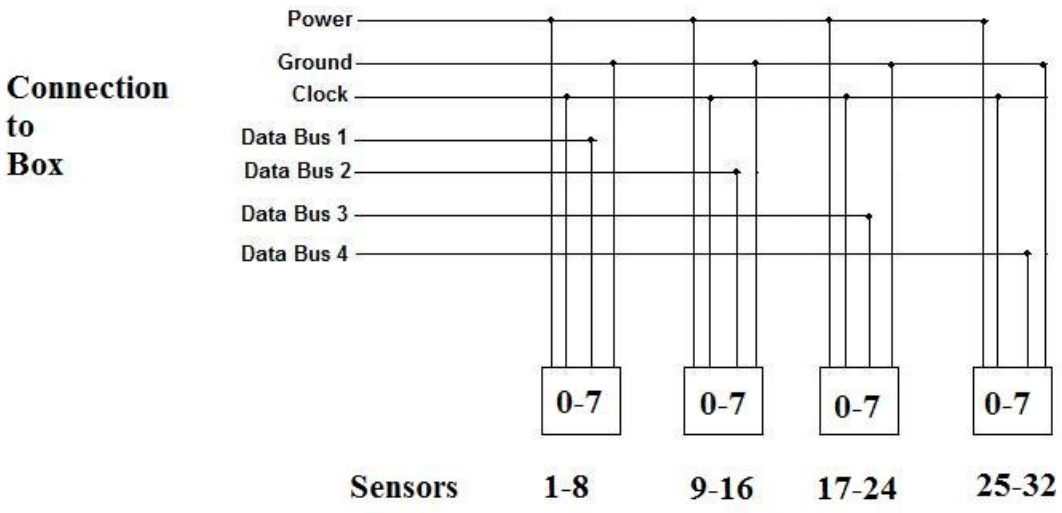

Figure 2.19 I^2C connection of 32 Memsic MMC328xMS sensors controlled with 7 wires.

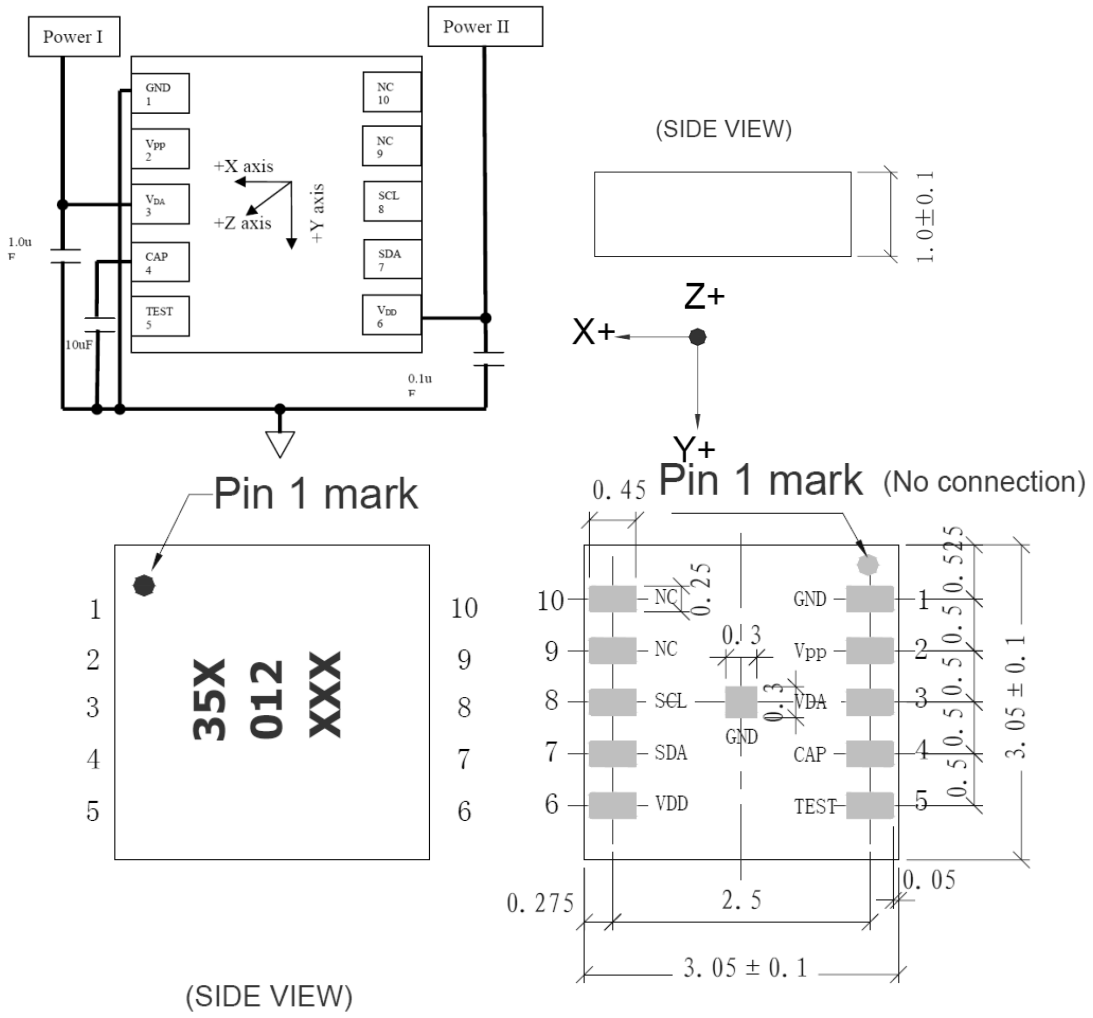

Figure 2.20 Memsic MMC328xMS connections and dimensions. Acquired from datasheet.

2.2.7 Initial Flexible Printed Circuit Board testing

As these sensors were more complex, both for hardware and communication software, as well as not knowing sensitivity performance with regards to magnet size and separation, it was proposed that a small rigid circuit board would be produced for the basis of a test strip for testing these sensors. Initially a rigid PCB was designed and manufactured as developing a rigid PCB is significantly cheaper than producing a flexible circuit board, and if the sensors were not suitable, would be a significantly larger waste of finances. The PCBs were produced on a panel to allow for sensor and passive component population, which were snapped apart and could be tested

individually; a 1.6 millimetre thick FR4 (composite material composed of woven fiber-glass cloth with an epoxy resin binder) 2 layer board was produced with soldermask, and the components placed by a Surface Mount Technology (SMT) pick-and-placed machine followed by reflow oven soldering. The boards contained one bank of 8 sensors, two capacitors for each placed near to the sensor, 4 solder contacts for wire and a FCB clip contact at the top to test a design which meant the FCB could be attached to a cable without the need for direct soldering. In addition to the above components, the board two pull up resistors for the I2C lines; all passive components were 0402 size (1 x 0.5 millimetre). Initial in vivo tests using a Memsic MMC328xMS three axis magnometer detailed the relative success of these sensors when measuring the magnet at the same ranges as previous generations were subject to, which would be connected to an I2C data system and it was decided that the third generation of SCJ locators would be produced on FCB, for which a custom FCB was designed, with a total of 32 sensors, connected on 4 address banks (figure 2.19) at a distance of 7mm apart. The total length of these boards was 649 millimetres, similar to the previous generations' FCBs, a limitation imposed by the maximum length of the panel from which the boards are laser cut; these boards were cut diagonally from the original panel to maximise the length available, an option suggested by the board manufacturer but not a normal option they offer. 32 sensors placed 7 millimetres apart offered a sensing section of 220 millimetres; the separation distance of 7 millimetres was chosen as this was the largest distance between sensors that could achieve reliable detection of a magnet placed in between two sensors, this was a trade off as the number of sensors is limited by the size of the board and number of solderable contacts (figure 2.21). An improvement on the initial design was made whereby the vias were moved from underneath the sensors, to next to them, as having the raised plated vias was believed to cause contact issues under the sensors, leading to a number of sensors which did not respond to microprocessor communication. The solder pads were larger than on the previous FCBs to minimise localised heat stress when hand-soldering the wires to the boards.

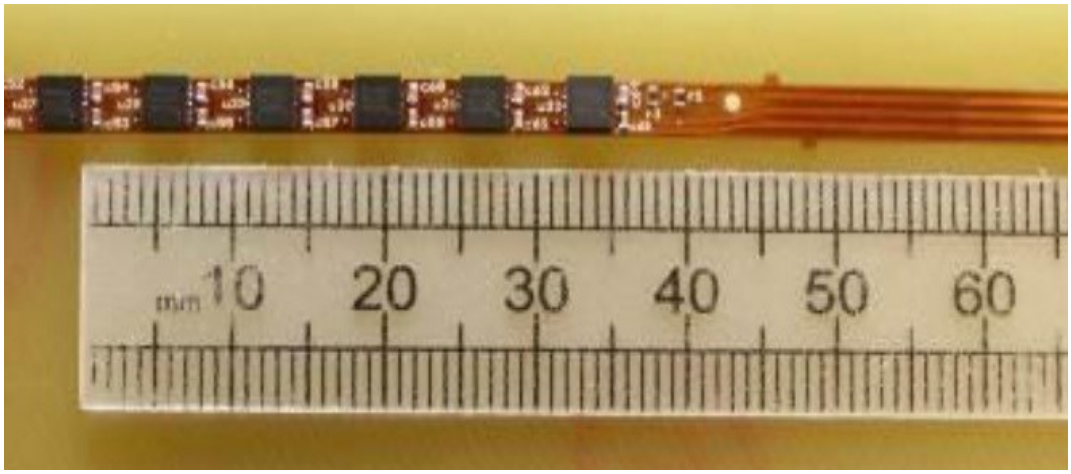

Figure 2.21 Stage 3 flexible circuit board populated with Memsic MMC328xMS magnometers.

The distance between sensors also had an impact on the flexibility of the whole probe, as the larger the bare patch of board between sensors or components, the more of the flexible board was exposed therefore allowing bending of the board without stress on the SMT solder contacts; there was 3.2 millimetres of bare board in between sensor and components. The reduction in the number of FCB tracks needed on the board allowed the increase of track width for better reliability; the new minimum track width was increased to 6 thou or approximately 0.2 millimetres, however most tracks were at least 10 thou. Thou is an imperial measurement and the British equivalent of one thousand of an inch; the American equivalent in circuit board design is mil, however to avoid confusion with mm, thou is used in this thesis. The 6 thou tracks were limited to such a size by the board layout and minimum size of vias and track-to-track gap; along the non-sensing portion of the board, the track widths were increased to 13.8 thou or 0.25 millimetres as these would be under regular bending stress at the neck and throat. Increasing the width of tracks on a FCB can affect the flexibility of the board, this effect is significantly exaggerated when two thick tracks are placed on the top and bottom layer overlapping; the total overlap of two tracks causes an I-beam type effect which essentially reinforces the FCB (Figure 2.22), therefore track overlap was minimised and eliminated where possible in order to maintain flexibility.

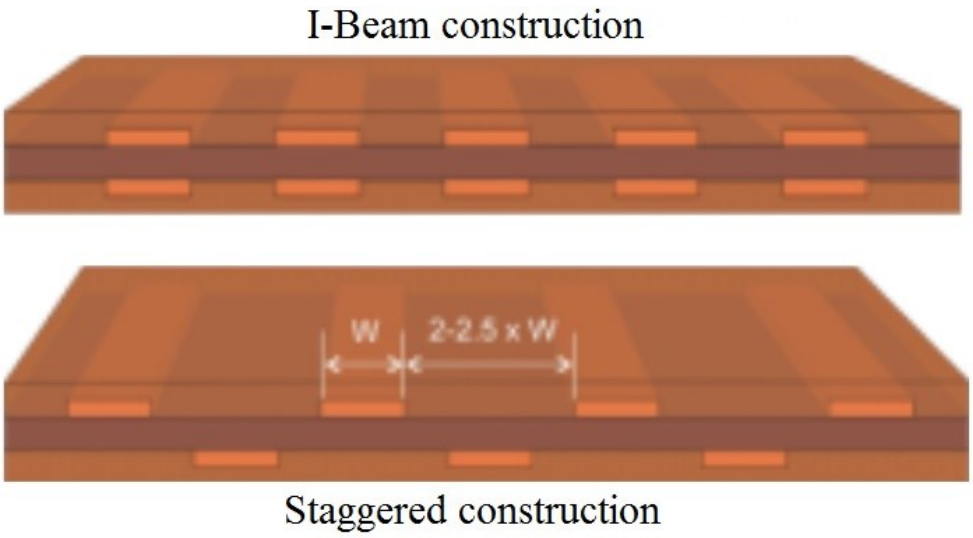

Figure 2.22 I-beam effect versus staggered design. Acquired from PCB3D (www.pcb3d.com/uploads/Flex_Design_Guidelines.pdf)

2.2.8 Encapsulation

For all three generations of the SCJ locator probes, the populated FCBs were passed down a hollow tube made from medical grade silicone which had an outer diameter of 4.8 millimetres and a bore of 3.2 millimetres; the tube was sealed at one end with a blob of silicone and allowed to set to produce a demi-spheroid tip for simple insertion). The other end of the tube was attached to the multi-core cable and kept in place with adhesive heat shrink material. This encapsulation maintained the barrier between electronics and patient, ensuring that the electronics were not damaged by the acid liquid environment of the upper GI tract and likewise the patient did not suffer any electronic current conduction *in situ*.

The electronics in the device, both the microprocessor and the FCBs were isolated via electronic safety mechanisms to ensure that if any leakage or other failure did occur, there was minimal and safe leakage to the subject within the legal requirements ascribed by *British Standard EN 60601:2006 Medical electrical equipment – Part 1: General requirements for basic safety and essential performance*. All generations of devices were tested by the Medical Electronics

department for NHS Greater Glasgow and Clyde who are responsible for the testing and regulation of medical devices within their catchment area, all devices were deemed satisfactory in accordance with the above standard in all areas tested.

2.2.9 Benchtop Validation

Before any device can be used in vivo, its performance must be tested and validated on the bench top; this minimises wasted time of a volunteer if the device doesn't perform adequately. It also decreases overall costs, as performing a procedure has significant costs for disposable equipment and expenses, and if the trial was unsuccessful due to an inadequately developed and validated device this leads to a waste of time and money. Another important reason for validation is for the scientific community; a device validation which has been published in peer reviewed literature leads to a quicker and stronger acceptance of a novel technology if peers can read about the validation and fully understand its performance and limitations. It has been seen on occasion, that a device which has been sold commercially, without appropriate published validation literature can be widely adopted, while still being inaccurate. This leads to a community of users, both research and clinical based, that are claiming accuracy which is better than the actual performance of the device; an example of such a situation is detailed later in chapter 3.

Initially, a single 1-D Hall effect sensor was investigated, and its output response to a 2x1 millimetre disc samarium cobalt magnet was investigated in order to determine the response of a single sensor in a variety of conditions. One of the most important factors is the distance at which the sensor can detect a given magnet, so an appropriate magnet may be chosen which does not saturate the sensor when too close, or saturate multiple sensors which would cause significant errors in accuracy, but most importantly can still be detected by the sensor at the working range of the device. Magnetic poles are directional, so a range of orientations is tested later. The inverse square law states that the magnitude of a signal, in this case the magnetic field strength, is inversely proportional to the square of the distance from the source of the field; monopoles are magnetic poles which follow this law, but as magnetic

monopoles only exist in theory or in artificial laboratory conditions and whose natural existence are still disputed as none have ever been found, the practical application of this law in magnetism is inaccurate.

As magnetic poles always exist in pairs, in the form of a dipole, or a combined north and south pole, the inverse square law never applies; if a magnet with a north and south pole are separated down the middle, the result is two smaller dipole magnets rather than individual monopoles.

These paired magnetic poles have two opposite polarities, north and south, their forces partially cancel each other because while one pole pulls, the other repels; the cancellation effect increases as the distance between the poles, l, decreases. This is known as the magnetic moment, M, and is demonstrated below, where ρ is the strength of the poles; l is a vector and points from south to north (equation 2.4).

$$M = \rho l \tag{2.4}$$

Due to the cancellation of the two poles, the strength of a magnetic field decays with the inverse cube of the distance (equation 2.5).

$$Magnetic\ manitude = {}^{1}/_{Distance^{3}} \tag{2.5}$$

In order to test the response of the sensor to a given magnet, an experiment was performed which measured the output of the sensor detecting the field from a small rod Samarium Cobalt magnet (E-Magnets, UK, 2mm diameter, 1 mm length) at several distances. As mentioned, magnetic poles are directional, so in order to test the inverse cubed response from the sensor, the magnet was placed in axial alignment with the sensor, and the north pole facing the sensor. The experiment was performed at 1 millimetre intervals from the sensor, ranging from 0 millimetres to 30 millimetres; this was done by mounting the magnet on an aluminium clamp stand, with a plastic ruler placed alongside the axis of the magnetic movement (figure 2.23). Plastic and aluminium were used as they would have no detectable effect on the magnetic field, unlike steel or other ferrous metals; any disturbance in the magnetic field would induce error into the experiment as the magnetically permeable material

would warp the magnetic field from the magnet, either increasing or decreasing the field strength at the sensor, and misrepresenting the in vivo effect of the device.

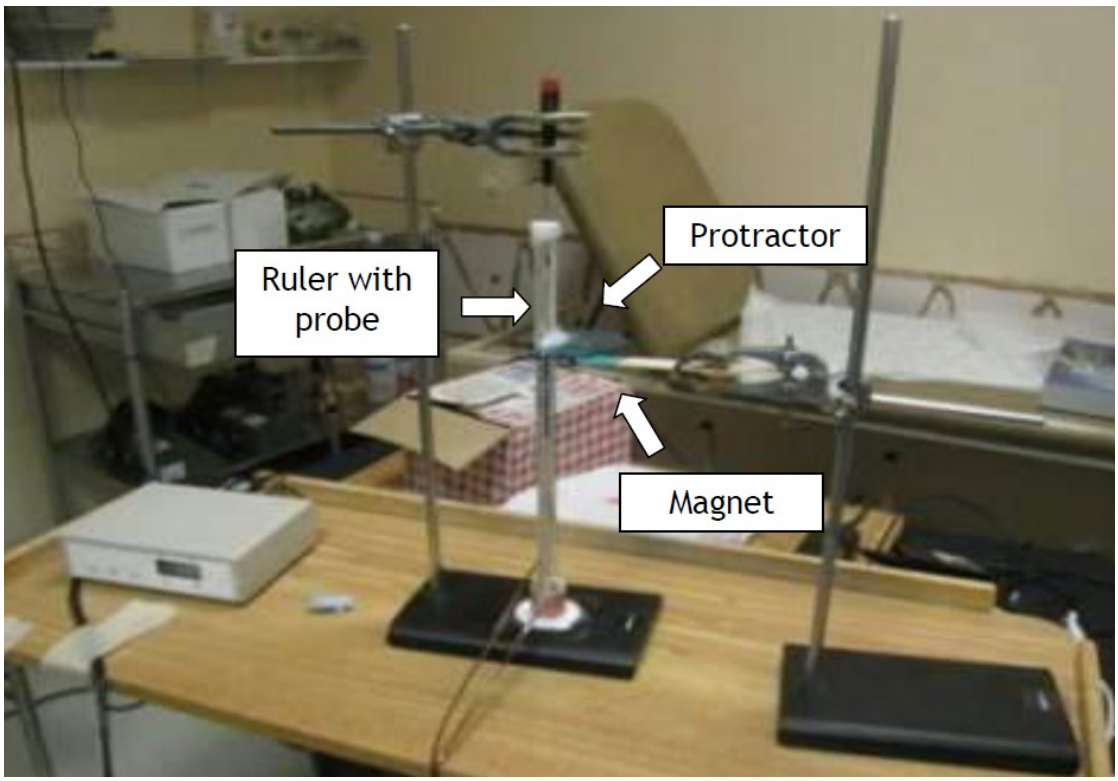

Figure 2.23 Benchtop experiment showing the sensor attached to a ruler, with magnet and protractor for angle measurement.

In order to fully test a practical Hall Effect sensor system, complete analysis must be performed in all possible positions and rotations. In the case of the two motile elements in this system, being the magnet and the Hall Effect probe, for the purpose of *in vitro* testing; one element, namely the Hall sensor probe, remains stationary and the magnet rotates and moves about and along the axes.

For the subsequent explanation, the following terminologies are used: *sensor* refers to a Hall Effect sensor, used for the detection of a magnetic field; *array* means a strip of flexible printed circuit board with 13 sensors along its length; p*robe* means two arrays laid overlapping on top of one another, in order to increase the resolution of the system as the distance between each sensor is reduced from 10mm to 5mm and *magnet* is a permanent rare earth magnet made from samarium cobalt, SmCo, (e-magnets UK Ltd, UK), a polar disc magnet with a diameter of 2mm and 1mm thick

(figure 2.24). For the sake of repeatability, when the magnet was rotated about the axis along the probe, the magnetic north was always facing the probe so as to minimise the variables with each experiment. As the magnet may rotate around the Hall sensor probe and about its own axes, as well as move parallel and change proximity to the probe, the definitions and results for these investigative tests are listed below.

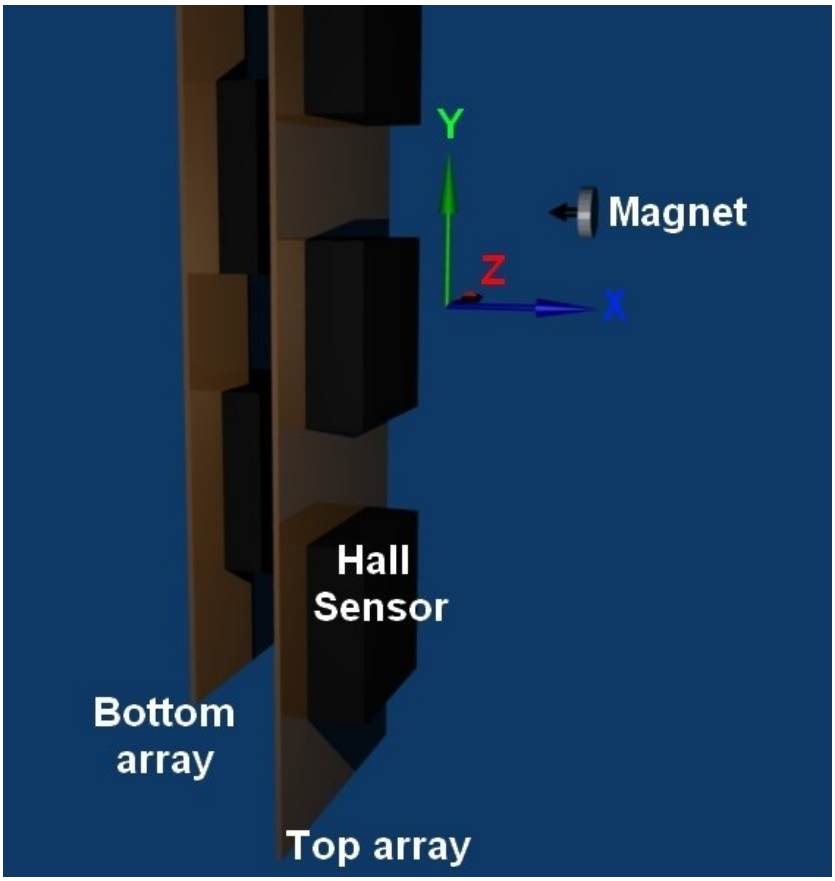

Figure 2.24 Illustration of system components

This test investigates the effect of rotation in degrees about the desired axis, from 180^{o} to -180^{o}. Values from 180 to 0 are a measure of the anterior signal strength, 90^{o} being directly in front of the Hall Effect array, which is the optimum operating criteria, to 0^{o} or 180^{o}, perpendicular on either side to the Hall Effect array. Likewise 0^{o} to -180^{o} is the measure of posterior signal strength with -90^{o} being directly behind the Hall Effect array. Each table is accompanied by a figure showing the rotation to clarify the orientation. In some positions, the movement from 0 to 90 degrees is

symmetrical to 90 to 180, and so is not included for simplification. Rotation of the magnet about its X-axis will not change the signal strength or position recordings as the magnet is symmetrical about this axis, and is thus not included in bench top results.

Proximity measurement is the direct distance in millimetres from the array's extremity in any direction, aiming to show the effect of distance on signal strength and position accuracy. This is included as the *in situ* distance will be unknown and is highly likely to change acutely, so the system must be capable of non contact position sensing in a dynamic human system. The distance at which the Hall sensors can detect the magnet's field is important as the magnet may not always be in close proximity to the array, either if the magnet is fixed deep within an oesophageal mucosal fold, during a large swallow or in the instance whereby the SCJ is pulled into the stomach by large distension and the system would ideally still be able to locate the magnet.

The array measures the magnet's position along its working length and the accuracy of the system is limited by the error in this positional recording. The Position error is the difference between actual position and the array's recorded position. Multiple readings were taken along the length of the probe, minimising local effects such as the arrays lying atop one another. The mean of the multiple readings are taken, with directionality of the error removed, providing a representation of the system's error in millimetres.

The probe was fixed motionless on a wooden table, the SmCo magnet was manually moved along the length of the probe in 1 millimetre increments, with distance along the probe was known and the voltage output from the probe recorded from the SCJ locator's output. This procedure was performed at 0, 5, 10 and 15 millimetres away from the surface of the probe and the magnet face; these experiments were repeated with the the magnet in several different positions relative to the direction of the sensors and with the magnet in a multitude of orientations in order to test the recorded signal strength of the magnet at these potential weaker orientations.

Initially the magnet was moved along the length of the probe in varying rotations; the rotations listed in the table are termed Rotation A (Figure 2.26), Rotation B (figure 2.27) and Rotation C (Figure 2.25). The spread of the error is shown in the position recordings, showing the fluctuations of the system, indicating its precision.

Signal strength is an important value for *in situ* testing as it confirms a valid magnet presence and indicates orientation and proximity. Signal strength lower than approximately 10mV can be attributed to electromagnetic noise as measured experimentally without magnet presence and/or calibration error and so a reported signal strength lower than this value may not be the magnet. Signals above this range, up to the maximum, confirm magnet presence and confirm valid position recordings. The data ranges from 0mV when calibrated, to 1200mV, with the latter showing the sensor has become saturated which occurs when the magnet is in optimum conditions, pointing a pole directly at the sensor surface. As the signal strength data is one-dimensional, it is unclear if distance or poor orientation is resulting in the signal strength fluctuation; however fluoroscopic in situ screening may reveal how much the magnet moves in orientation and proximity, to enable a better approximation as to the causes of any change. The saturation point to can be tailored to a certain degree, with different magnets and changing the calibration of the Hall sensors to maintain the best working distance as the oesophagus expands and moves during a swallow. For the few examples of negative or close to zero signal strength, no magnet was detected and any fluctuations can be attributed to local magnetic and electromagnetic noise, as well as minor calibration differences. Rotation about the probe's Z and Y axes for example are each symmetrical therefore only includes 90 to -90 degrees, however when the magnet rotates about its own (Y) axis, the magnet rotation is not symmetrical due to the polarity of the magnet. In some instances, large distance and acute rotations of the magnet from the probe mean no magnet is detected, an indication of no signal is outputted, and on these occasions no error can be recorded so these points are omitted from any graphs. All bench studies use a standard SmCo magnet described above moving along the middle portion of locator probe from the position of 50 to 70mm at 1mm steps per second. We also performed experiments looking at effects of recording at the ends of locator probe from the position of 100-120mm at 1mm steps per second. This effect was

important to study since there were more Hall Effect sensors in the middle portion of the probe compared to the end which may therefore affects signal strengths. A standard ruler (in mm scale) and a stopwatch were used during the experiments. All the different axes of rotation and all the different proximities mentioned above were tested in both positions of the locator probe. The position (mm) and signal strength (in millivolts or mV) readings were then extracted using the PolygramNET™ as described above.

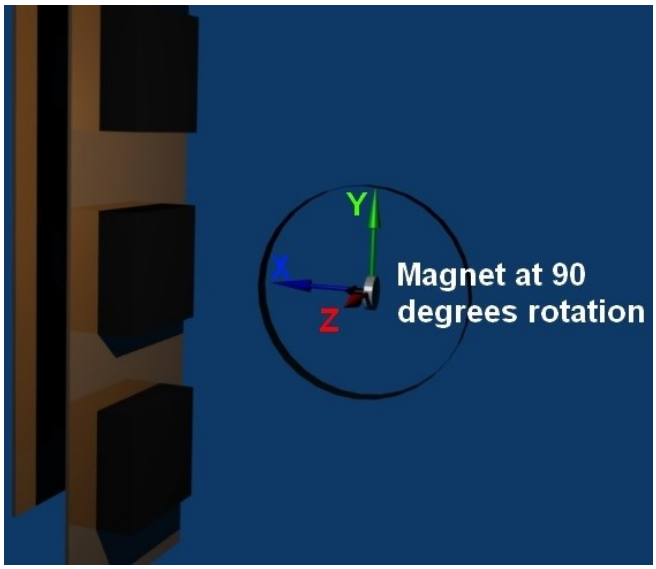

Figure 2.25 Magnet rotation about its own Z axis

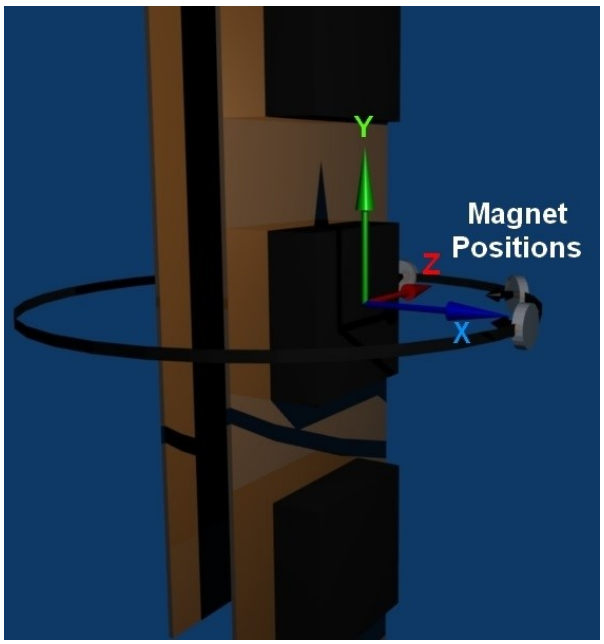

Figure 2.26 Rotation of the magnet about the sensors' Y axis

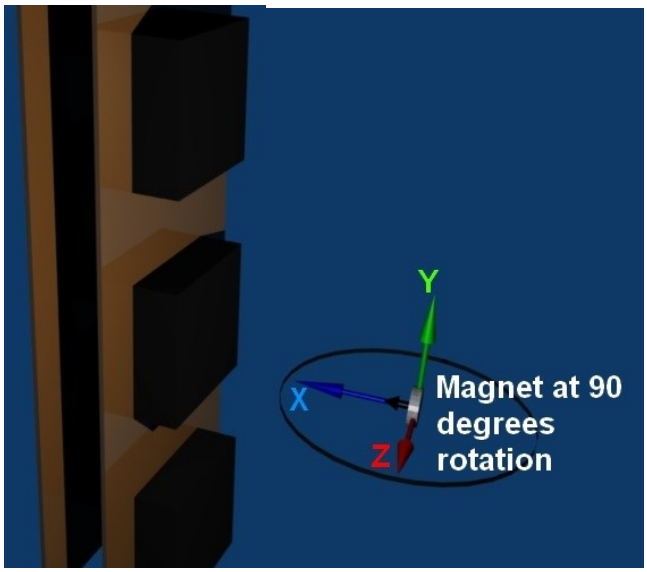

Figure 2.27 Magnet rotation about its own Y axis

2.2.10 Temperature effects on probe

Every transducer has the potential to be affected by a change in temperature due to the change in conductive properties at different temperatures. Hall Effect transducers are no exception, having metal or semiconductor elements which detect the presence of a magnetic field. This element is susceptible to heat and as the body's temperature differs from that of the room in which the bench tests were performed, it is important to investigate the effect of this change in temperature when the probe is used *In Vivo*. As the Hall Effect is the proportional voltage fluctuation of a semiconductor with the presence of a magnetic field, any change to the conductive properties of the semiconductor, for example heat, may invalidly change the output voltage. Practical Hall effect transducers can be affected by temperature in several key ways as will be explained in the following chapter.

There is no change of the signal strength of position when the probe is used and calibrated at the same temperature, however since the probe is being calibrated at room temperature and used at body temperature, the potential effect of this was tested. The following procedure was performed in order to test the aforementioned response of the system to a change in temperature. The tests were run at room temperature, which ranged from 16 to 25^{o}C, then testing at body temp and beyond, 37 and 40^{o}C respectively, noting any change in signal strength or position with the increase in temperature. A magnet was affixed to a given point along the probe, which was placed in a Stuart Scientific S.I.60 Incubator oven at room temperature and the incubator was heated to 37 ^{o}C; temperature inside the oven varied from that of the incubator dial by several degrees so an Ebro Logger EBI 20-TH digital thermometer was used to accurately control the incubator temperature by manually adjusting the thermostat on the incubator when required. Magnet is fixed and test performed as such because moving the probe will cause an undesired change in signal strength.

In order to appreciate the error induced as a result of change in temperature, drift over time must first be investigated, as any fluctuations over time could be misinterpreted as thermal drift. To test time drift, the same probe was placed in the

incubator at a fixed temperature with the magnet and probe stationary, recordings of signal strength, time and temperature were recorded every minute for an hour. Time drift experiments were performed at 18^{o}C and repeated at 33^{o}C, with high signal strength. To test the temperature change, the probe was placed in the incubator at room temperature, with the magnet in place and the incubator turned on, with recordings of temperature, signal strength and position taken every minute as the incubator's temperature rose to 40^{o}C.

The following procedure was performed in order to test the aforementioned response of the system to a change in temperature.

Each test was designed to investigate the effects of the change that occurs when a calibrated probe in inserted and used as designed in a human subject. The initial tests to be performed investigated signal strength drift over time at a fixed temperature, which would expose any drift of the system without an increase in time, in order to remove time as a variable in the experiments. Drift at both high temperature and low temperature were completed, keeping the temperature constant and allowing the probe to drift with time rather than temperature. The experiment was set up in the incubator and the magnet fixed in position as described above, with the signal strength, position and temperature recorded every minute. In order to appreciate the error induced as a result of change in temperature, drift over time must first be investigated, as any fluctuations over time could be misinterpreted as thermal drift.

To test time drift, the probe was placed in the incubator at a fixed temperature with the magnet and probe stationary, recordings of signal strength, time and temperature were recorded every minute for an hour. Time drift experiments were performed at 17^{o}C and repeated at 33^{o}C over a period of an hour, with high signal strength, as shown in figures 2.42 and 2.43 respectively.

To test the temperature change effect, the probe was placed in the incubator at room temperature, with the magnet in place and the incubator turned on, with recordings of temperature, signal strength and position taken every minute as the incubator's temperature rose to 40^{o}C. The ideal experiment would involve placing the probe directly into a heated environment, as this would more accurately simulate the in situ

operation. This is unfortunately not practical as moving the probe may cause the magnet to move with respect the transducers, giving changes in signal strength and position, masking as a change due to temperature, so the probe must be placed in a cool environment and heated to eliminate any movement artefact. As the output may vary depending on the initial conditions such as signal strength, two tests were performed, drift with increasing temperature with an initially high signal strength and an initially low signal strength. This was performed to investigate the change, to deduce if the fluctuation was indeed proportional to the change in temperature, and to test the system's validity *in vitro*.

Further to the report on heat test where the Hall Effect transducer appeared affected by changes in temperature, the question whether calibrating the locator probe at 37 degree Celsius may minimise the effect is investigated.

The locator was calibrated at room temperature as per protocol. Water bath was heated up to 37 degree Celsius. A beaker containing water was heated up until 37 degree Celsius and maintained at this temperature within the water bath. A magnet was placed on the locator using a clear plaster at a fixed position and low signal strength. The low signal strength is chosen since any effects in output would have been significant since signal strength is indicative of magnet's presence. The locator with magnet was then placed in the water beaker. Recording with Polygraf was started and continued over 1 hour.

2.2.11 Interference test with Manometer

Since the locator probe is useful in combination with the high resolution manometer (Sierra Scientific, USA), interference tests between the two apparatuses should be carried out to determine possible interactions. The manometer consists of 36 circumferential channels which are metallic in origin (copper). These channels with current flowing through may generate magnetic field that interferes with the Hall Effect transducers.

The locator probe was calibrated at room temperature as per protocol. Manometer was turned on and calibrated according to protocol. Water bath was heated up to 37 degree Celsius. A beaker containing water was heated up until 37 degree Celsius and maintained at this temperature within the water bath. The locator probe was combined with the manometer. A magnet was placed on the locator using microporus tape at a fixed position and low signal strength. The low signal strength is chosen since any effects in output would have been significant since signal strength is indicative of magnet's presence. Both the locator and manometer were then immersed into the beaker. Recording with Polygraf was started and continued over half an hour.

The locator probe was calibrated at room temperature as per protocol. Manometer was turned off and disconnected from its supporting machine. Water bath was heated up to 37 degree Celsius. A beaker containing water was heated up until 37 degree Celsius and maintained at this temperature within the water bath. The locator probe was combined with the manometer. A magnet was placed on the locator using microporus tape at a fixed position and low signal strength. The low signal strength is chosen since any effects in output would have been significant since signal strength is indicative of magnet's presence. Both the locator and manometer were then immersed into the beaker. Recording with Polygraf was started and continued over half an hour.

2.2.12 Interference test with 12 channels pH electrode

The 12 channel pH electrode (Synectics, UK), a monocrystalline antimony pH electrode is another apparatus beside manometer which will be combined with the locator probe to study the position of squamo-columnar junction. Any apparatus with current flowing may interfere with the output of Hall Effect transducers in the locator probe. Furthermore, the antimony within the pH electrode is a metal with possible diamagnetic potential. Since the pH electrode generates potential with a change in pH which raises the question whether the change in pH itself or the electrical

potential itself may interfere with Hall Effect transducers. The following experiments attempt to answer the above questions in a condition of low signal strength baseline since any effects in output would have been significant since signal strength is indicative of magnet's presence.

The locator probe was calibrated at room temperature as per protocol. Water bath was heated up to 37 degree Celsius. A beaker containing 100ml of pH 7 solution was heated up until 37 degree Celsius and maintained at this temperature within the water bath. A magnet was placed on the locator at a fixed position and low signal strength. The locator was then immersed within the beaker and Polygraf recording was continued for 10 minutes. A 10ml 1.0 M pH 1 solution (hydrochloric acid) was added into the 100ml of pH 7 solution. Polygraf recording was continued for a further 15 minutes.

The locator probe was calibrated at room temperature as per protocol. The disconnected 12 channels pH electrode was combined with the locator probe. Water bath was heated up to 37 degree Celsius. A beaker containing 100ml of pH 7 solution was heated up until 37 degree Celsius and maintained at this temperature within the water bath. A magnet was placed on the locator at a fixed position and low signal strength. The locator was then immersed within the beaker and Polygraf recording is continued for 10 minutes. A 10ml 1.0 M pH 1 solution (hydrochloric acid) was added into the 100ml of pH 7 solution. Polygraf recording was continued for a further 15 minutes.

The locator was calibrated at room temperature as per protocol. The 12 channels pH electrode was calibrated as per protocol. The connected 12 channels pH electrode was combined with the locator probe. Water bath was heated up to 37 degree Celsius. A beaker containing 100ml of pH 7 solution was heated up until 37 degree Celsius and maintained at this temperature within the water bath. A magnet was placed on the locator at a fixed position and low signal strength. The locator was then immersed within the beaker and Polygraf recording was continued for 10 minutes. A 10ml 1.0 M pH 1 solution (hydrochloric acid) was added into 100ml of pH 7 solution. Polygraf recording was continued for a further 10 minutes.

2.2.13 *In vivo* validation study for the locator probe

As the benchtop studies had demonstrated the huge potential for the accurate measuring the location of the SCJ in real-time, the next step was to test the device in human volunteers to evaluate its vivo use and validate it for future volunteer investigations.

As mentioned in the previous sections, the SCJ alone would be of little use, it becomes invaluable however when used in conjunction with the other upper GI tools such as a pH Probe or HRM; this will allow the device to provide useful and novel physiological measurement on the SCJ, GOJ and associated anatomy. Although the technology would be ideally combined in one slim catheter, this is far from the scope of this project and would require commercial collaboration, therefore the probes must be combined manually for each study, meaning the overall diameter may be uncomfortable or intolerable for some volunteers. The probe was combined with the other catheters required for the validation study, the pH probe and HRM using several rings of microporus tape along the length of the combined probes. The relative position of each probe could be recorded and tailored depending on the required insertion depth; something which varied from study to study. It was noted by medical colleagues that although using permanent medical safe glue would be an ideal solution to maintain the relative position of the probes, it was not possible as other studies required the use of only the manometer or other combinations of probes therefore the tape method was used.

The initial validation experiments were used with the custom 12 channel high-definition pH antimony electrode catheter with a diameter of 2.1 millimetres and the Manoscan High-Resolution Manometer, which has a diameter of 4.2 millimetres; later a new Slimline Manoscan HRM catheter was acquired which had a diameter of 2.7 millimetres making the overall diameter of the combined probes smaller and much more manageable.

All in vivo studies, both validation and further research trials, were performed by trained medical practitioners and with the assistance of a specialised GI nurse where

required. The validation studies required the volunteer to undergo several separate days of procedure to complete the trial; initially a breath test was required for detection of H. Pylori as a selection criteria for this validation and other research trials. H. Pylori negative subjects were then required to return to undergo clip attachment via endoscopy. A routine endoscopy was performed to detect a hiatus hernia, which if negative, allowed the patient to continue with the validation; with the endoscope still inside the oesophagus, the custom made magnet and endoclip was attached as described in the previous section. Before withdrawing the endoscope, visual inspection was performed to validate the attachment of the magnet-clip onto the mucosa at the SCJ. The subject would then either return another day, or continue with the study the same day, after a hour long period of rest after the endoscopic procedure.

Before the each part of the study, a volunteer was required to fast for a minimum of 6 hours prior to the onset of the trial; this ensured that the stomach was empty for endoscopy or probe insertion. Some trials required fasting from the night before the study, as they would investigate the effect of a meal on the GOJ and required the regulation of the stomach contents. The probes were combined on the day of the study and calibrated as required, with the three probes synchronised and set to record before intubation. The patient was required to sit at an angle of 60 degrees on a patient bed, after which their nostrils would be anaesthetised with the application of Xylocaine spray, similar to that used in endoscopy, and while waiting for the anaesthetic to take effect, KY jelly lubricant was applied to the length of the combined catheters. The combined lubricated assembly was then passed through the subject's nostril to the back of the throat, where it was passed into the oesophagus with the aid of some swallowing. As the assembly was passed slowly down the oesophagus, swallows would facilitate the passage into the stomach; the patient was aware that during any the part of the study they could cease the experiment should they feel too much pain or discomfort. Due to the nature of the intubation, gagging, watering eyes and nausea were common; although there were often minor incidences of the above most were associated with the intubation process and stopped as soon as the assembly had been passed into the stomach and secured in place using microporus tape at the nose. There were some instances where one nostril could not

manage to take the assembly, upon which the other nostril was anaesthetised and passage was attempted a second time, through this nostril; this often worked however there were some instances where patients could not tolerate the assembly through either nostril and were removed from the study. Oral intubation was potentially possible, however was more difficult due to the more acute angle between mouth and oesophagus; subsequent patient trials also required the subject to consume meals, something which would have been near impossible with oral intubation.

It was important to check that the depth of insertion was the same throughout the study or movement of the probe could lead to artefact which misleadingly appears as a movement of the GOJ. At the end of the study, the nasal tape could be removed and the assembly slowly removed; this stage was occasionally uncomfortable however in a small instance, withdrawal was followed by pain or nose bleeds in two cases but both ceased after a short period of time. The volunteers were paid per day and their travel expenses reimbursed.

The study was performed in adherence with good clinical practice and NHS ethics, predicated by the Declaration of Helsinki in 1964, which required the protection of human subjects in medical research. In Scotland, the Research Ethics Committee (REC) is the governing body in charge of reviewing, granting or rejecting ethical applications for human studies, protecting safety and well being of the volunteers in research. All human trials detailed in this thesis were reviewed and granted by the West Glasgow REC division. The REC references below cover the trials in all chapters in this thesis: 07/S0709/98 and 10/S0704/40.

As shown in the bench top study, the probe, like the manometer, is subject to inaccuracies when calibrated at room temperature despite being used at body temperature, therefore a calibration technique was developed which allowed the SCJ Locator probe to be calibrated at body temperature. The process was performed in a water bath which was set at 37°C, and checked using a thermometer; calibration was performed by using a button on the box containing the multiplexer and microprocessor, this button allowed for the zeroing of every sensor by reading its output voltage when no magnetic field was present, this also calibrated the sensor at the proximal 0mm along the sensing area, an identical magnet to that of the one

attached to the clip was placed on the most distal sensor, calibrating the maximum output and also the sensor at the most distal tip. The proximal and distal tip needed to be calibrated as such, as the computer via the Polygraf machine required calibration to the minimum and maximum magnet field voltage as well as the voltage associated with the length along the probe's sensing area; both of these were communicated to the Polygraf machine from the microprocessor's analogue outputs ranging from 0 millivolts for the minimum values to 1200 millivolts for the maximum values.

There are many separate systems used to investigate Gastroenterology in clinical and research practice; these devices can be physically combined into one assembly for intubation, however their outputs must correlate to the same time point, as differences between the devices can lead to severe misdiagnosis or a total misunderstanding of the anatomy and physiological events of the upper GI system. Thankfully, the output of the SCJ locator probe's microprocessor outputs analogue voltages which can be plugged into the Medtronic Polygraf machine; the USB based desktop PC Input/Output device also used for the custom pH probe, the two devices are inherently synchronised due to the sampling processes of the Polygraf system, however the other device which is used a lot within the GI field is the HRM system. The SSI high resolution manometer plugs into its own desktop PC Input/Output interface, which itself is connected to the PC via a USB connection. The desktop PC samples both of these devices with simultaneous programs, but the data that is recorded from both systems is not time correlated in any way, therefore an incredibly accurate method was developed to allow the synchronisation between these systems and indeed with the fluoroscopic video recorded for validation experiments; the alternative and less accurate synchronisation was to manually start both recordings with mouse clicks.

There are two conceptual methods of synchronising such systems, one is the implementation of a common signal or time stamp which is identical to both systems, the other being a common marker on all systems which is external and non electronic. The former method requires the inclusion of a time marker input on all systems, this may be an inbuilt feature such as those on multiple camera systems which record simultaneous using a common square wave or time signal sent to each

camera, allowing the precision synchronisation of every camera; the other method would be to simultaneously interrupt the input from the sensors in the devices themselves, however this may void device pH warranty and or disrupt the signal sampling, distorting the output from the sensors as some sensors may be in serial or parallel.

A simpler method is to mark the data as it comes into the PC in software form; the USB cannot be interrupted as loss of a portion of digital input would mean all further data would be misinterpreted. Instead, this must be performed in both systems' software, a feature which is thankfully present in both the Manoscan Acquisition Polygraf PolygramNET software. The data is often recorded using two separate computers, as they both need dedicated software which require significant proportions of the computer's resources therefore the sampling must be performed manually on separate computer interfaces, often requiring more than one person and a command to synchronise, which could be out be half a second or more due to many variables such as reaction times. Any synchronisation method should be performed both before and after physiological measurement, this is important as differences in computer clock speeds and sampling frequencies may lead to separation of the time in either system demonstrating temporal drift and the slow but steady severance of the two measurements. With the pre and post synchronisation points, any drift between the two time points allows the linear correction of this drift over time.

A far more simple method of synchronisation is a simultaneous influence on each sensor which allows for the change in data without any software or hardware modification, instead a stimulus on each sensor can be performed by a user and can allow the post processing correction by shifting the data until they are aligned by the concurrent stimulus. Often the bench-top synchronisation of these is difficult, as both a pressure, magnet movement and pH change is required instantaneously, which is difficult for one user to perform, and many to perform accurately; luckily there is a simple procedure which achieves for this. Physiological events such as a hard cough or a deep sniff not only increases pressure in the thorax, but also moves the sphincter upwards meaning both the magnet and pH step up point moves; the pH step up movement may be slower, but as the pH and SCJ locator both use the Polygraf

system, only one measurement of these is required to synchronise the system. Fluoroscopy is slightly harder to synchronise with this system, as often the machines do not have external trigger inputs and are subject to delay and ghosting effects when measuring anatomy. The best developed technique for synchronising fluoroscopy with the other systems is to use a very radiopaque marker in front of the body when recordings are being performed, and remove the marker very quickly whilst marking using the desktop software, the point in time when the marker is removed; in this instance, a thick metal wire was used which could be held by the operator who could simultaneously mark the Manoscan Acquisition software. Is is assumed that as the catheter systems are synchronised, that the fluoroscopy needs only to be synchronised with one of the catheter devices, and is therefore synchronised with all of them.

Other catheters or systems used in subsequent research studied included a respiratory sensor (Medtronic inc, USA) and an Impedance probe. These devices were attached to the Polygraf and HRM systems respectively, therefore did not need any extra synchronisation protocol.

For the studies requiring the use of the respiratory sensor, a small pressure sensitive pad is placed on the chest to measure thorax expansion. It was discovered that while placing the pad onto the HRM catheter before intubation, a simple sharp tap on the pad would also be transferred to the HRM, which was as good at synchronisation as the physiological measurement technique, so was used for simplicity in these studies.

The nutritional content of a meal has been the subject of many a study, with strikingly conflicting outcomes; it has been proposed that high fat meals worsen the effectiveness of the GOJ barrier, however this hypothesis has been both supported and refuted in many subsequent studies. It has been shown by Holloway (Holloway, Kocyan and Dent 1991) that a meal may trigger more TLOSRs, although it was suggested that gastric distension is the cause of the increased frequency, so the meal constituent debate continues. The consumption of a meal was used in validation and research trials involving the SCJ locator probe, this was to test the effectiveness of swallowing with the combined probe assembly and to test the Holloway hypothesis, respectively. Both liquid and solid meals were given to test the above, with Fortisip

(Nutricia Ltd, UK) and a fatty fish and chips meal consumed by the subject. The meal was consistent within each study, with measured portions for both.

Ten volunteers were recruited by means of an advertisement placed in a local newspaper. All screened subjects had their informed consent signed prior to study entry. Of these, six subjects successfully completed all parts of the study. The remaining four subjects were excluded due to problems with recording; three subjects were excluded due to the visible absence of magnet during fluoroscopy and the remaining subject was excluded due to oral intubation intolerance. The research in this thesis was approved by the ethics committee of National Health Service (NHS) Greater Glasgow and Clyde, covered by ref 07/20709/98 and ref 10/s0704/40; conforming to the declaration of Helsinki (1964) which safeguards human subjects in medical research The median age of the six successful subjects were 47.5 years (range 26 – 74 years old) where four subjects were males and two subjects were females. One male reported symptoms of gastro-oesophageal reflux and confirmed with presence of reflux oesophagitis on endoscopy. Both females had evidence of hiatus hernia during upper endoscopy but did not report any reflux associated symptoms.

For all medical proceedures, medical research professionals performed and assisted with the tasks, the author of this thesis did not participate in the studies involving patients and volunteers; those medically trained professionals were, in no particular order: Dr. Yeong Lee Yeh (Physician), Nurse Angela A. Wirz, Dr. Elaine V. Robertson (Physician) Professor Kenneth E.L. McColl (Physician).

All screened subjects fasted from midnight the day before the study and had a magnet attached endoscopically to the SC junction (Figure 1). The magnet was fixed using heat shrink material (PLK175, Plastronic PMG Co., UK), on a commercially available metal endoclip (model HX-606-090, Olympus UK), which is traditionally used for clamping and stopping gastric or oesophageal bleeds. The disc shaped polar magnet is made from samarium cobalt (SmCo) with a diameter of 2 millimetres and axial length of 1 millimetre (e-magnets UK Ltd, UK). The locator probe was calibrated at room temperature before being passed down through the nostril; the probe was cleaned before insertion with Tristol solution for sterilisation and the

patients' nasal cavity was locally anesthetised with Lidocane spray where required. The insertion continued until signals were seen on the computer display confirming the detection of magnet and sufficient insertion to ensure detection was possible with reasonable cranial or caudal movement of the magnet. A screening fluoroscopy was then performed at this stage to confirm and adjust where necessary, the locator probe until the desirable depth and position for subsequent screenings (Figure 2); at which point, the probe was fixed at the nose using microporous tape to minimise movement artefact. The setting for fluoroscopy machine was adjusted for correct dosing and was fixed for continuous screening at 5 frames per seconds (PV Pulsera, Philips, UK).

The volunteers were then allowed for a period of accommodation for about 10-15 minutes; this time allows the oesophagus and stomach to relax and accept the intubation without spasm. Subsequently, they were asked to perform a series of manoeuvres which were recorded simultaneously with fluoroscopy screenings which lasted between 15-20 seconds per series of manoeuvre. The manoeuvres performed included normal respiration, deep inhalation and full expiration, water swallowing and lastly withdrawal of probe out from the nostril. Total fluoroscopy screening was approximately 60-80 seconds for each volunteer. All images taken were then transferred and stored using Picture Archiving and Communications System (PACS) NHS however as previous experience had shown, in some instances, images were not transferred to this database, the fluoroscopic recordings were therefore recorded locally to provide a back-up using a DVD recorder; the successfully recorded video was then used for the following data analysis. The procedure for recording video directly from the Philips BV Pulsera C-Arm fluoroscopic device is as follows; attach the Video-Out via coaxial cable, to a Video Copy Box, attaching with a S-Video cable, the S-Video output of the Video Copy Box to the S-Video input of the DV/HDD/DVD, selecting the DVD recording format, the live video was monitored by connecting a JVC Cameron Systems monitor screen to the recorder using a coaxial cable; this is very useful in confirming magnet presence and appropriate intubation. Still images were taken frame-by-frame from the recorded video and were analysed using measuring tools built in the PACS software. Recordings from the locator probe were extracted from the PolygramNET™ software in ASCII

format/text format at 8 Hz and subsequently exported to Microsoft Excel 2007 for analysis.

All enrolled volunteers were called back after 6 to 8 weeks for a chest x-ray to ensure the magnet fell off. If the volunteer was required to attend an MRI procedure before the appointed dates then he or she had an earlier chest x-ray to document clearance of magnet. However all volunteers who turned up for the chest x-ray were confirmed to have no magnet in the abdomen. No volunteers reported any side effects from having the magnet in the gut.

The *in vivo* position of the magnet-clip was measured using fluoroscopy, a medical imaging device which allows real-time measurement of the body. X-Ray machines are sources of ionising radiation useful for imaging, as the radiation from the X-Ray emitter passes through different tissues and gets absorbed by others, allowing the imaging of sub-dermal organs and anatomy with a X-ray sensitive plate on the opposite side of the body. X-Ray images have been used in medicine since 1895, and have since been upgraded to include X-Ray sensitive cameras to produce fluoroscopic X-Ray videos.

Photons from X-Ray emitters can be very damaging to molecular bonds due to their high energy, and have the potential to disrupt DNA within a cell; if the radiation exposure is significantly high, cancerous cells can form. The extent of danger from the radiation is correlated by both strength of dose and duration of exposure; indeed Radiation Therapy uses concentrated high exposure X-Rays in an attempt to destroy cancerous growths, however radiation imaging requires vastly less radiation for an image or video. Although X-Ray radiation can be damaging to tissue, it is understood that in most applications, the risk from developing cancer from receiving an X-Ray is significantly lower than the requirement for imaging.

Due to the limits imposed on the study by the ethics board, in any of the upper GI studies performed in part or wholly for the validation of the SCJ locator probe, each subject may only be exposed to 90 seconds of fluoroscopic imaging, with the actual total duration lasting between 60 and 80 seconds, comprised of shorter near 30 second periods. The machine used in this study was the portable Pulsera C-Arm

Fluoroscope (BV Pulsera, Philips Healthcare, UK); for the 30 second imaging sessions, this system was set to continuous screening at 5 frames per second. As mentioned in the previous section, a radiopaque metal marker was used to synchronise the start and end of screening with the PolygramNet™ software; the magnet-clip was also relatively radiopaque which allowed for the measurement of the position and movement of the clip *in vivo*.

The images which had been transferred to PACS using the above method, allowed efficient and patient-doctor safe storage of the radiological videos; as well as storing various other imaging technique outputs such as MRI and Ultrasound, PACS is also equipped with specialised viewing software on certain computers connected to the network. The associated analysis with clip measurement for position validation was performed with these inbuilt tools; having such features as a measurement tool whereby the investigator marked two points on an image and could the distance between two points was calculated, also the software could calculate movement between two or more sequential images. The measurement was taken for each frame, relative to a known position on the assembly, as the Hall effect, HRM and pH sensors were all relatively radiopaque (figure 2.28). Although the analysis was time consuming, the data was tabulated and compared to the much simpler output from the SCJ locator probe.

Analysis of the position of the SCJ was performed with either Microsoft Excel 2003 and 2007 or Mathworks Matlab 2003 for graphical representation and Statistical Package for the Social Sciences (SPSS) version 18.0 for statistical analysis. The combined probes assembly outputs were extracted form each device in ASCII text format and plotted in a custom made software, which plotted pH data superimposed with the SCJ position, as well as un-interpolated, drift corrected HRM data together on one screen in the form of 2 graphs (figure 2.29). This graphical display allowed for the simple interpretation of a complicated combination of probes and their associated data; a TLOSR is visible in this example by a loss of sphincter tone in the HRM data, reflux in the pH data and most clearly by the upward movement of the SCJ. Outputs of the three devices varied in frequency so each was combined to form a new dataset at 8 Hertz. This required interpolation of the data to acquire a uniform

frequency; there is potential for inducing error into the system when doing this, but the movement of the clip is deemed too slow to cause any measurable error and ghosting effects on the X-ray images are a far greater source of error.

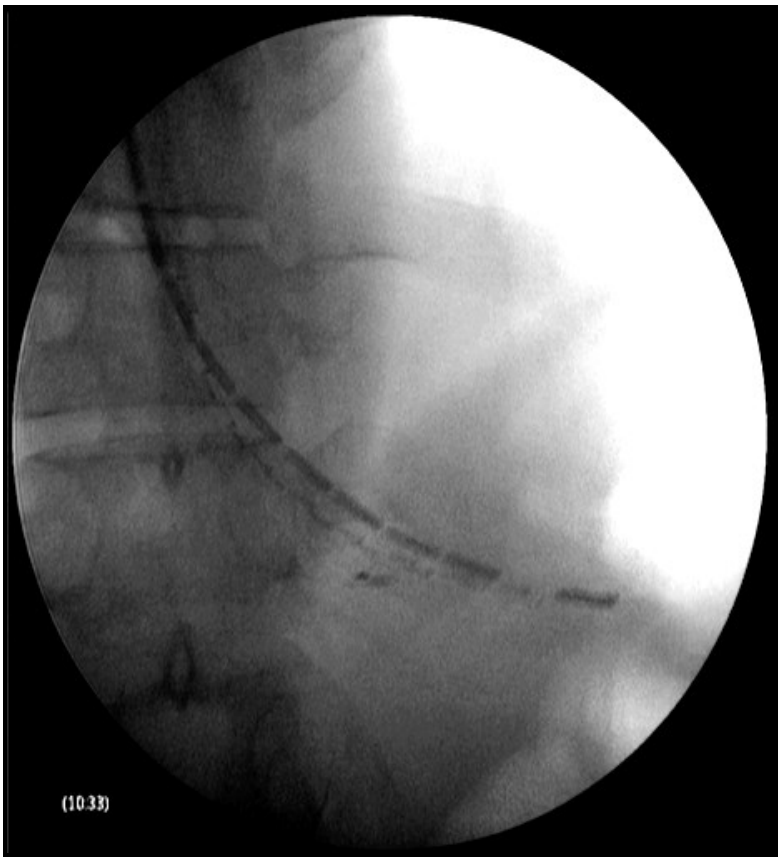

Figure 2.28 An example of the fluoroscope output showing clip position relative to the inserted probe. The Antimony sensors of the pH probe are most clearly visible, with the SCJ Locator probe and Magnet-clip somewhat visible, the HRM is not clearly visible.

2.3 Results.

2.3.1 Benchtop Experiments

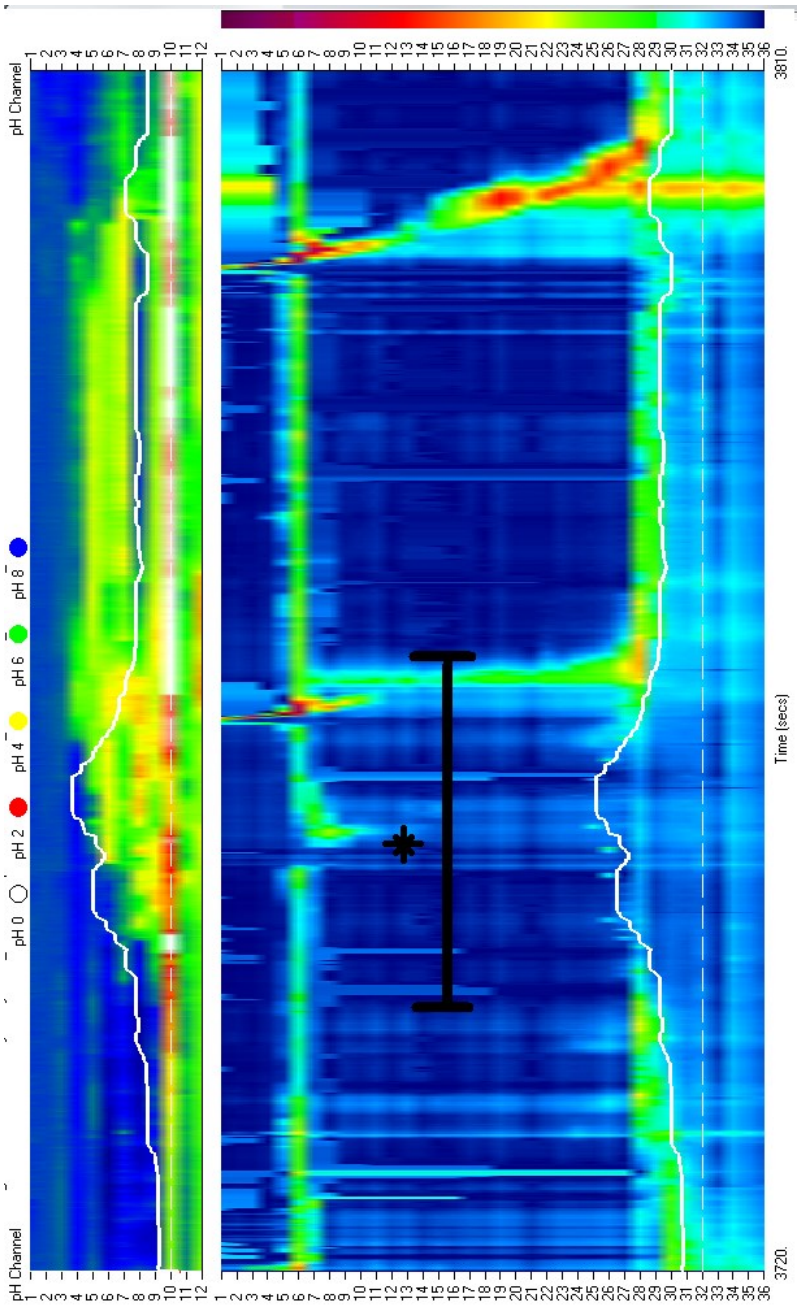

Figure 2.29 An example of high resolution colour plot displayed using the custom software. A TLOSR event is shown in this example*. The upper graphical display is a colour pH plot and the lower panel is colour manometric plot. Both graphs have the position of the SCJ output from the locator system superimposed in the form of a thick white line. Red is represented in the HRM and pH graphs as high pressure and strong acid respectively; blue corresponds to low pressure or neutral alkaline pH.

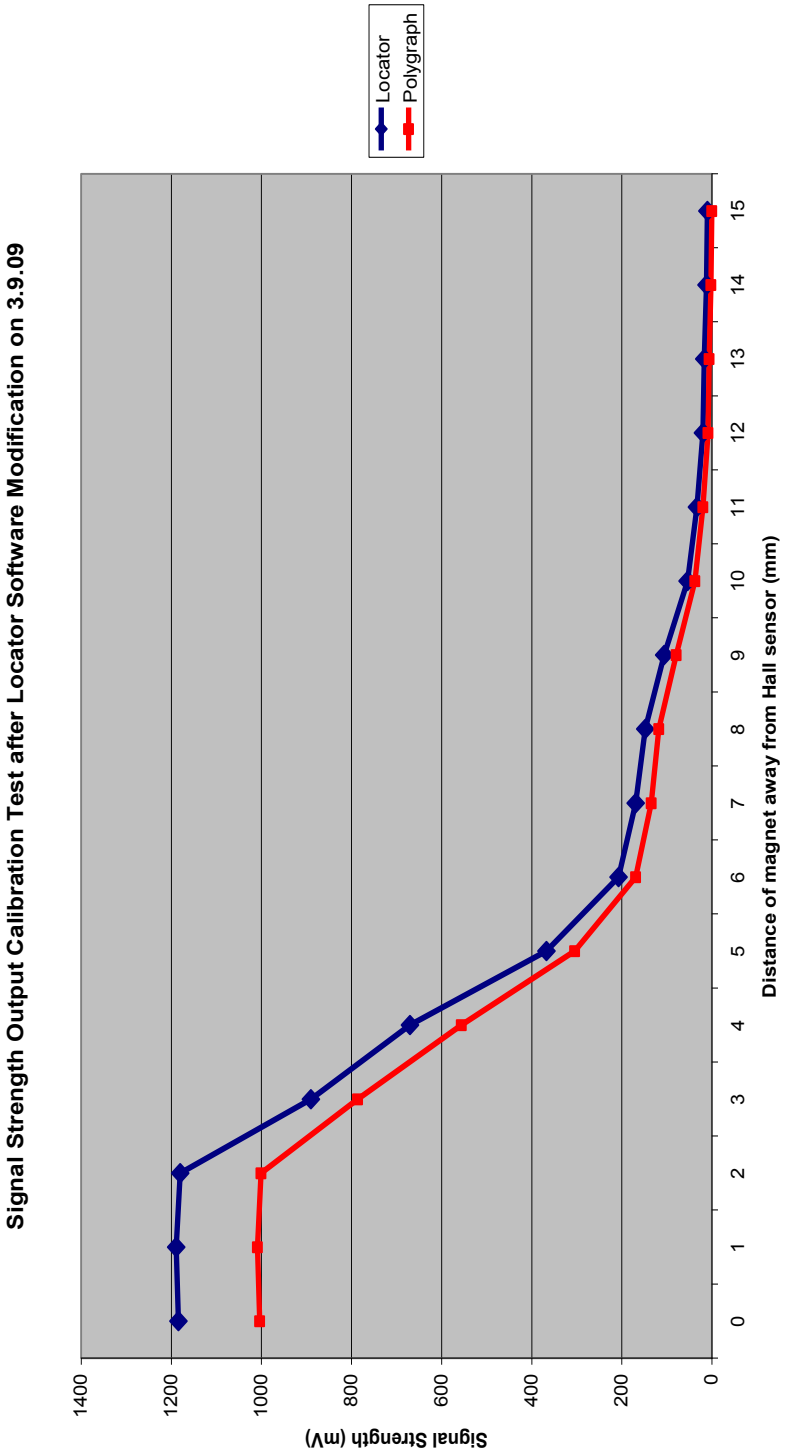

Figure 2.30 The signal strength output from the Polygraf machine matched with locator LCD.

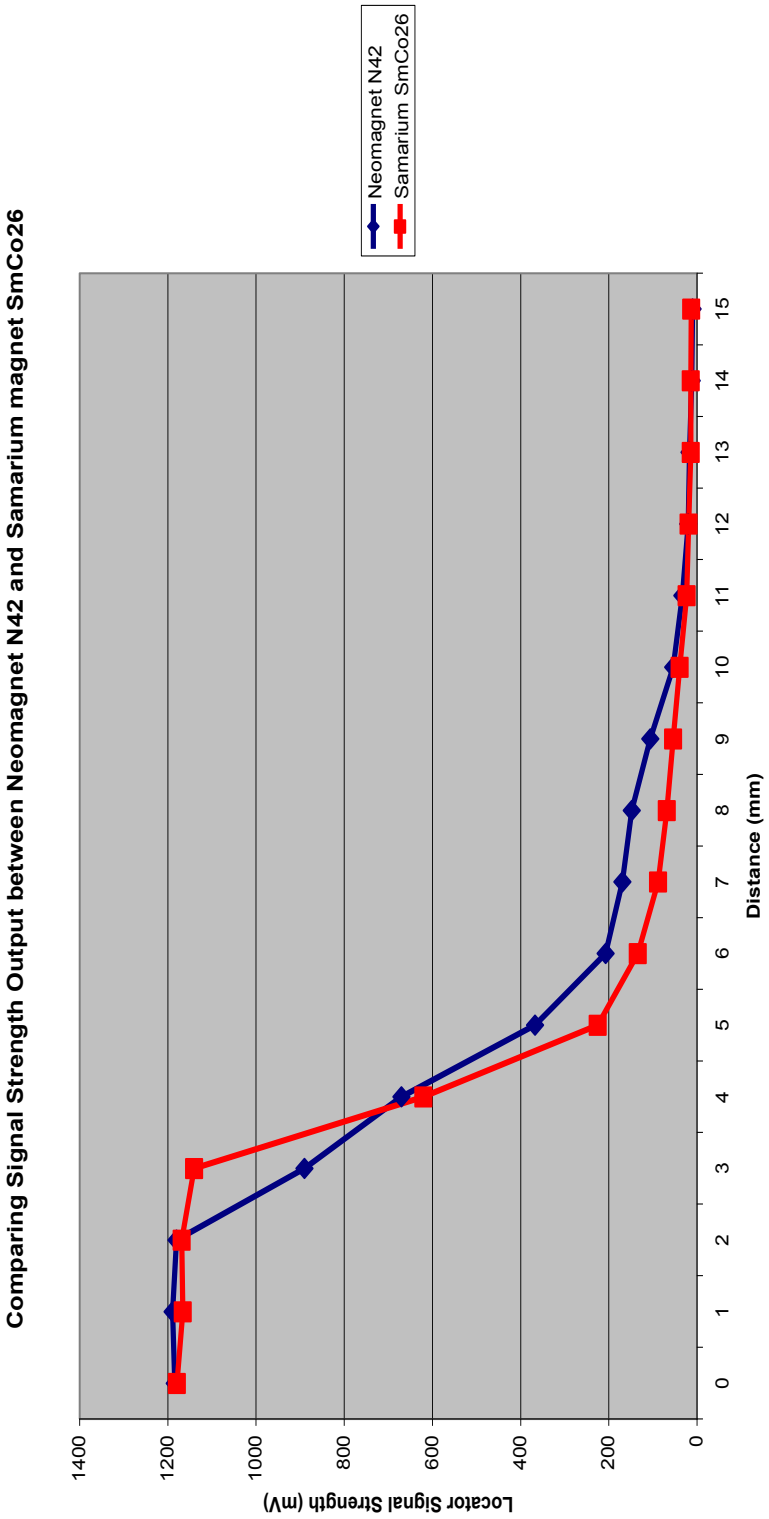

Figure 2.31 The Samarium-cobalt grade SmCo26 magnet output. It appeared to perform equally well in signal strength output with Neodymium grade N42 magnet with increasing distance away from the Hall sensor.

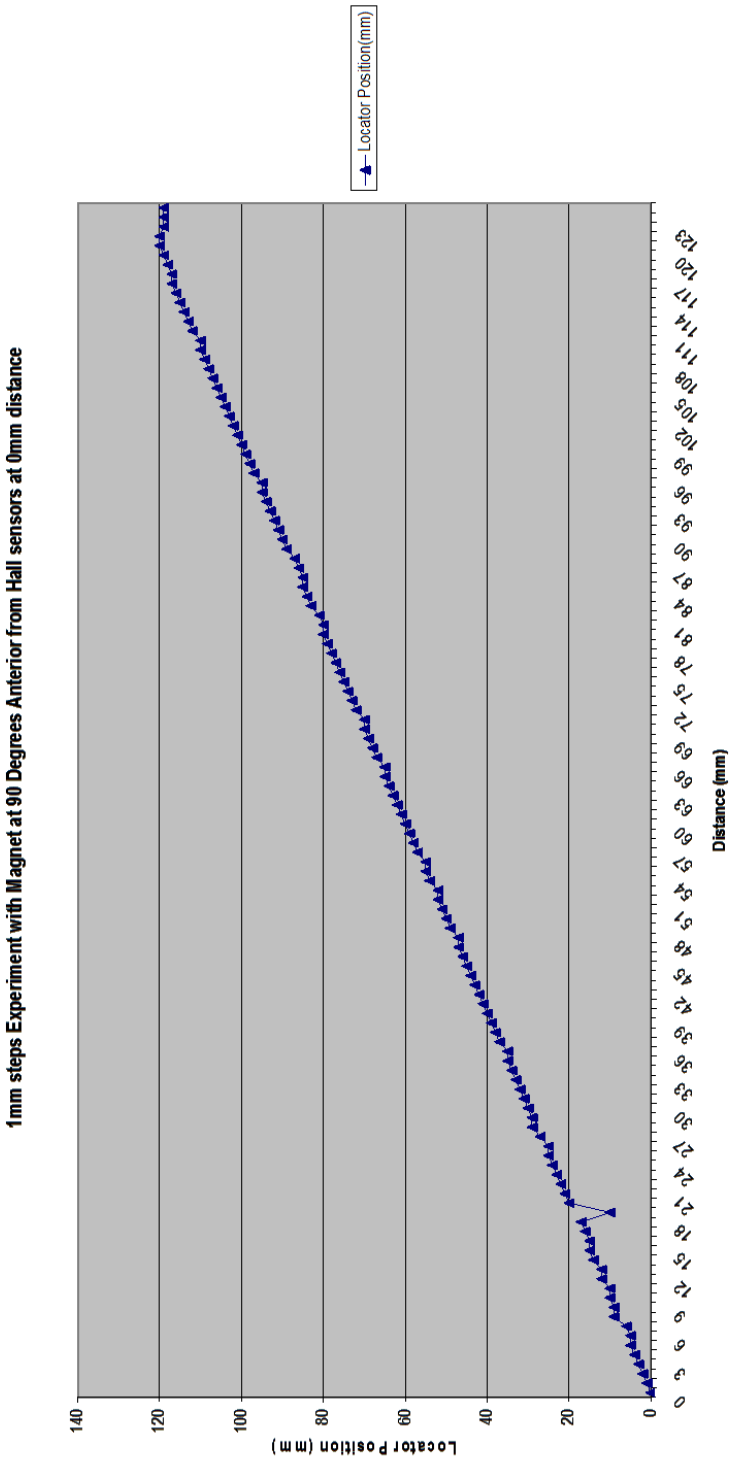

Figure 2.32 A smooth linear relationship was seen when a magnet placed 0mm away from Hall sensor array and moved along the length of the array

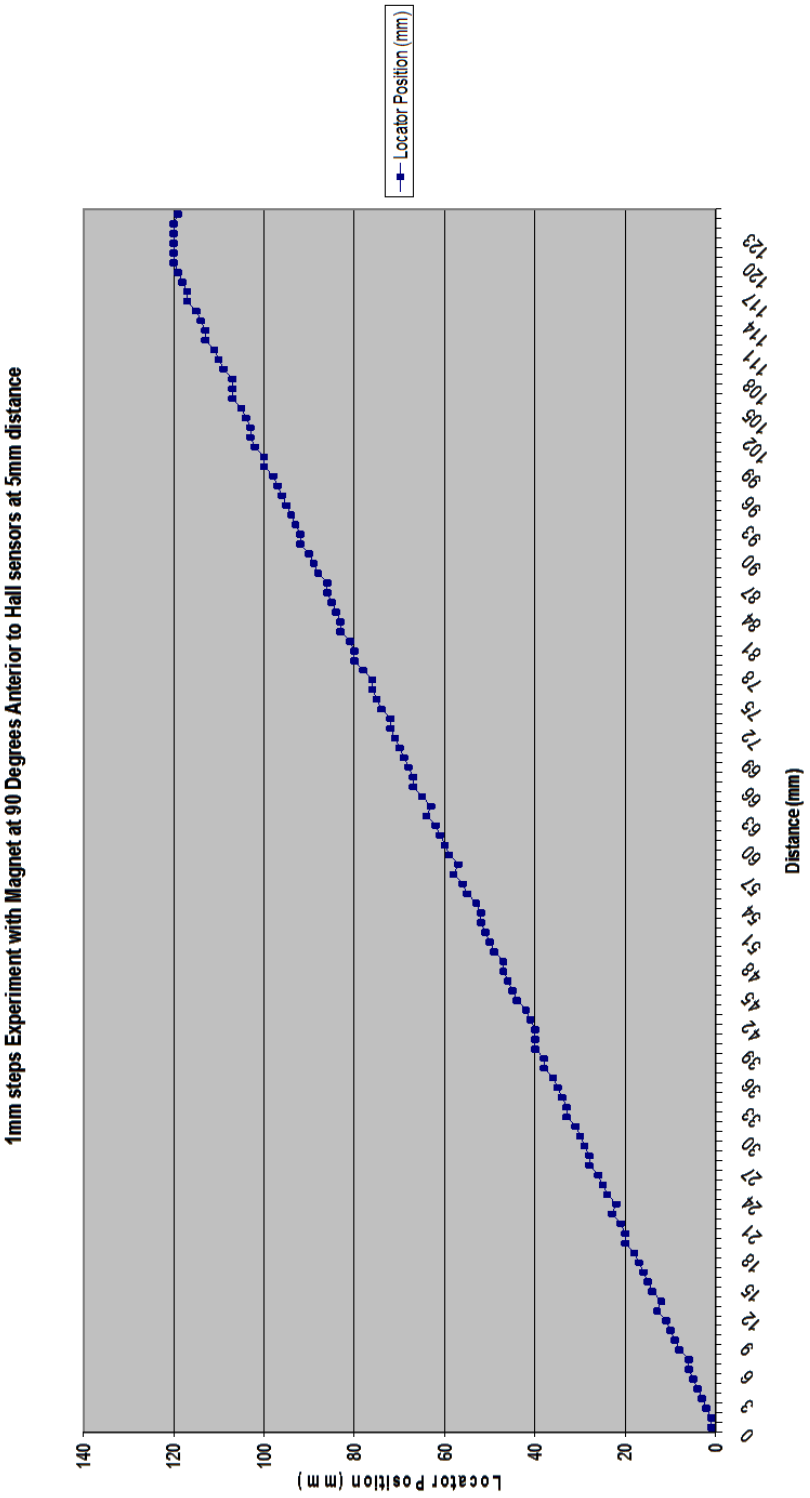

Figure 2.33 A smooth linear relationship was seen when a magnet placed 5mm away from Hall sensor array

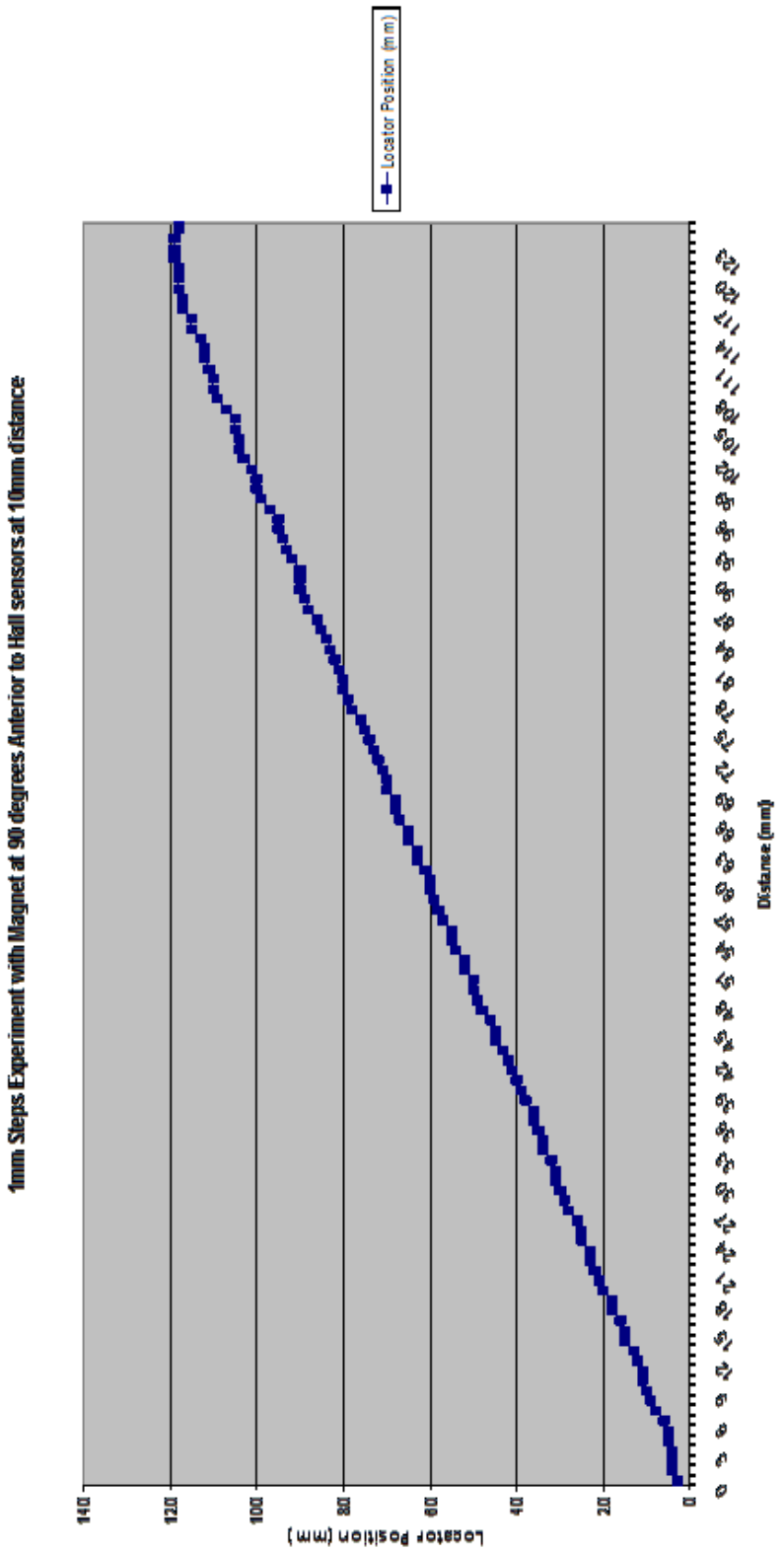

Figure 2.34 A smooth linear relationship was seen when a magnet placed 10mm away from Hall sensor array

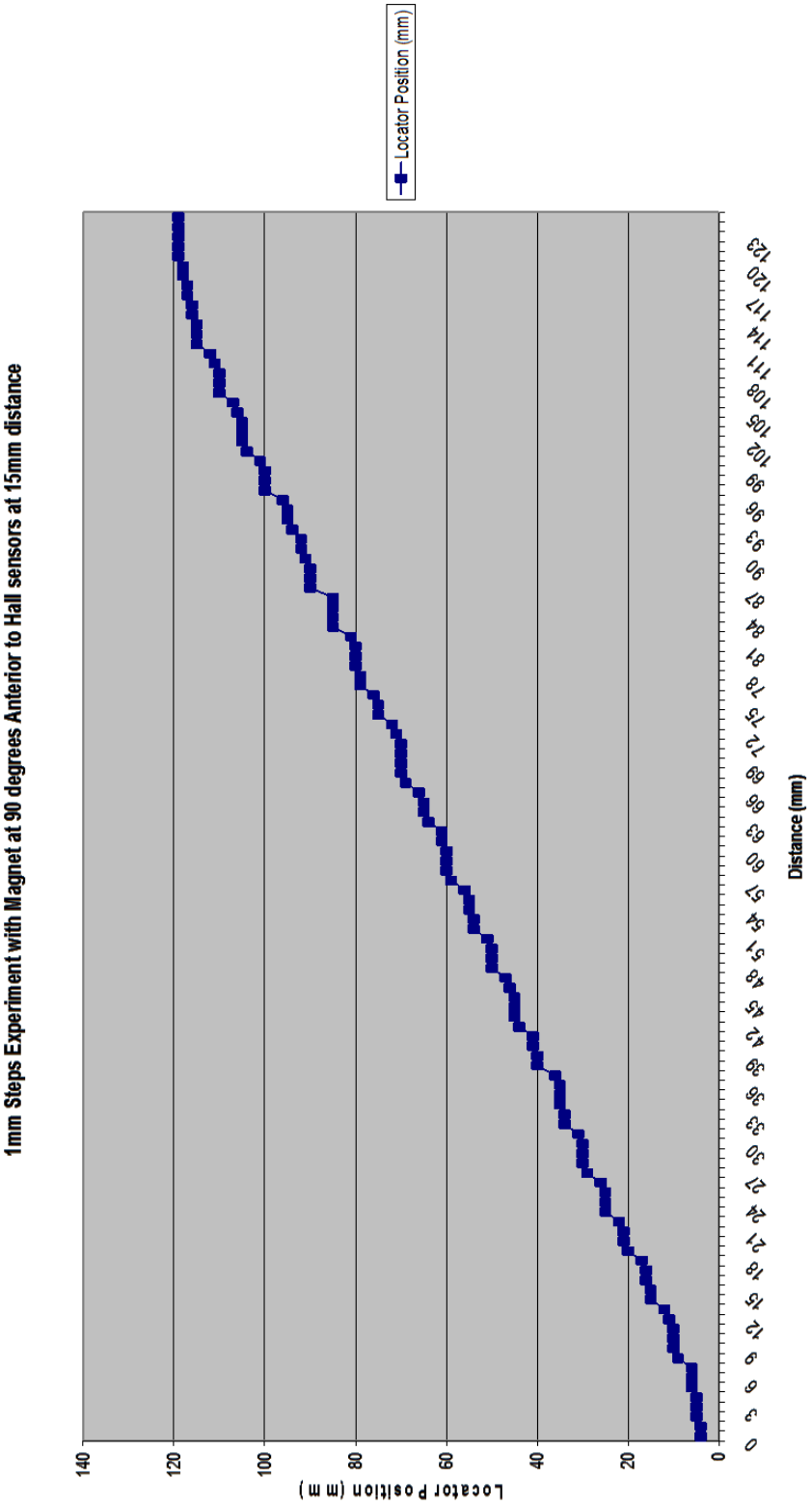

Figure 2.35 A linear relationship was seen when a magnet placed 15mm away from Hall sensor array

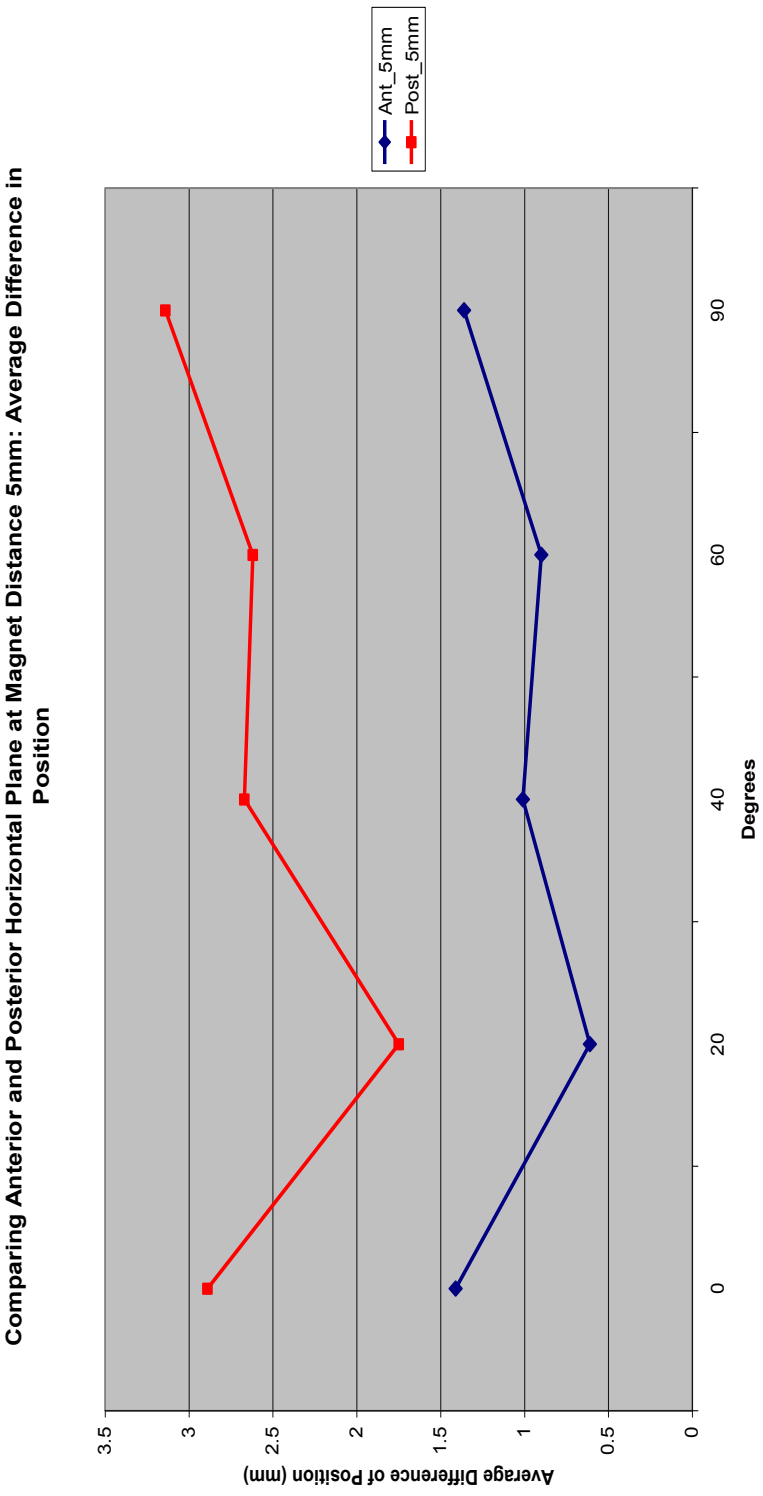

Figure 2.36 A magnet placed in the posterior-horizontal plane showed a higher mean position error compared to a magnet placed in the anterior-horizontal plane.

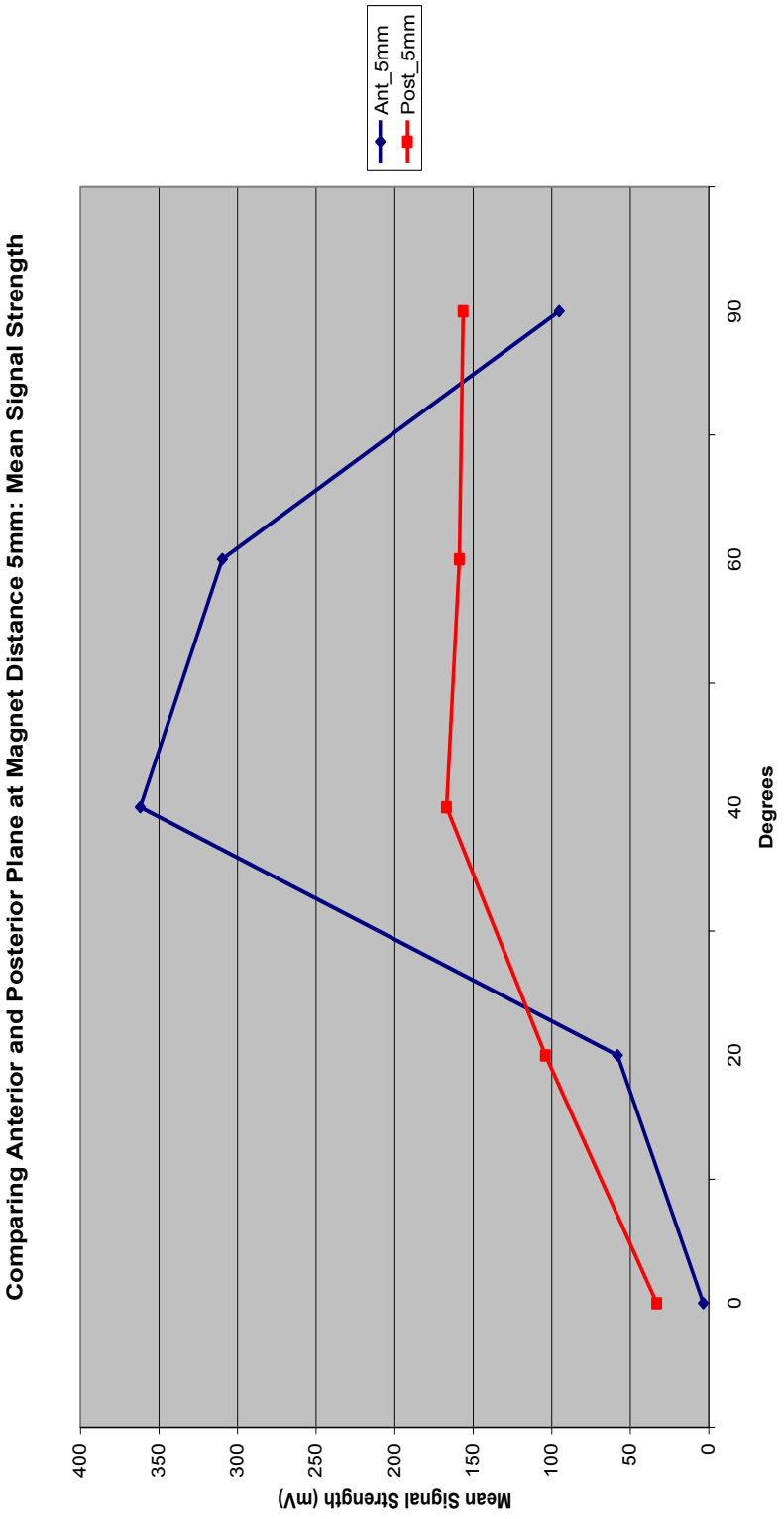

Figure 2.37 A magnet placed in the posterior-horizontal plane showed a lower mean signal strengths compared to a magnet placed in the anterior-vertical plane.

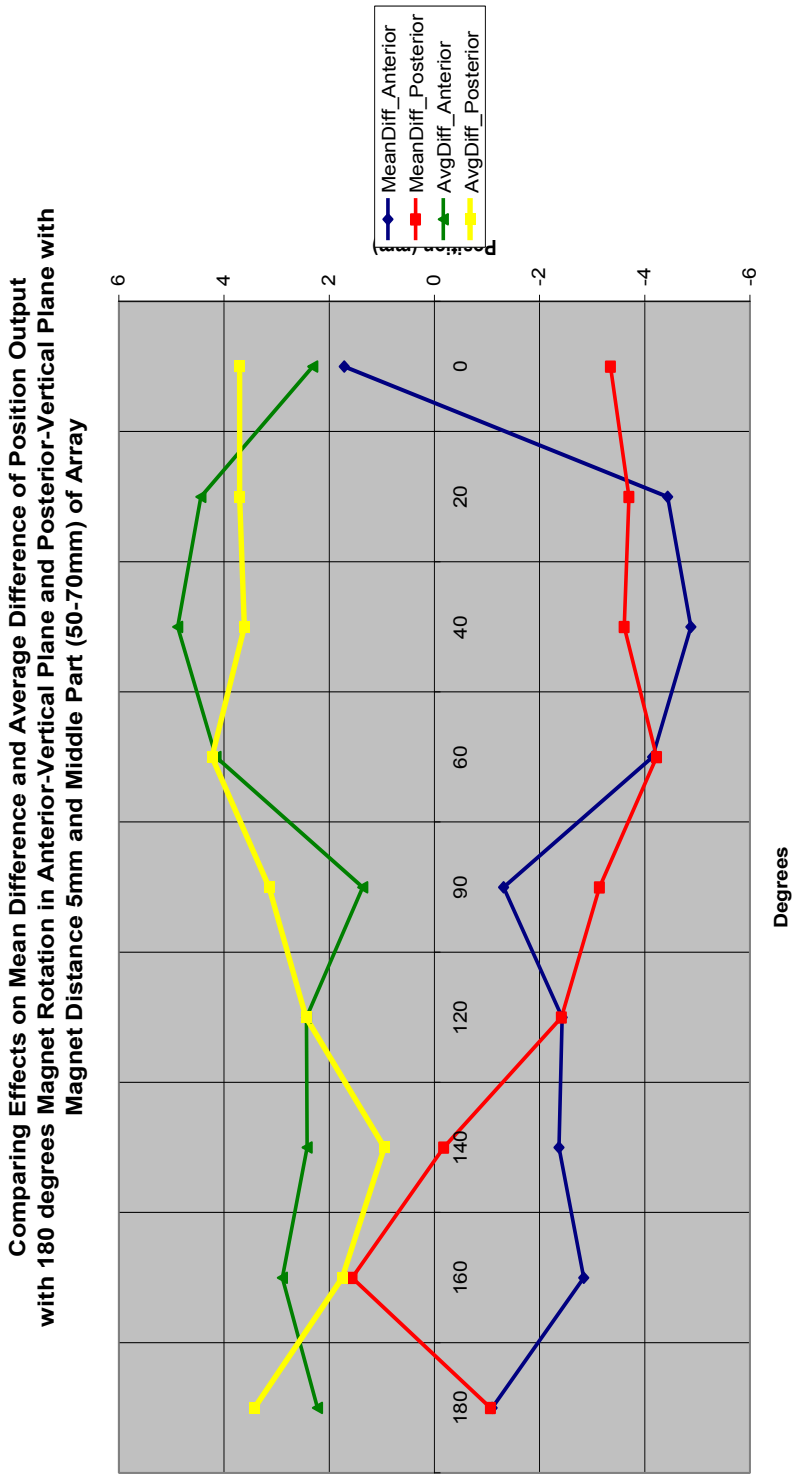

Figure 2.38 The mean and average (median) difference in position output in both middle part of anterior-vertical and posterior-vertical planes appeared comparable and low between 60 to 120 degrees. Both the ends of rotation arc (0-40 degrees and 140-180 degrees)

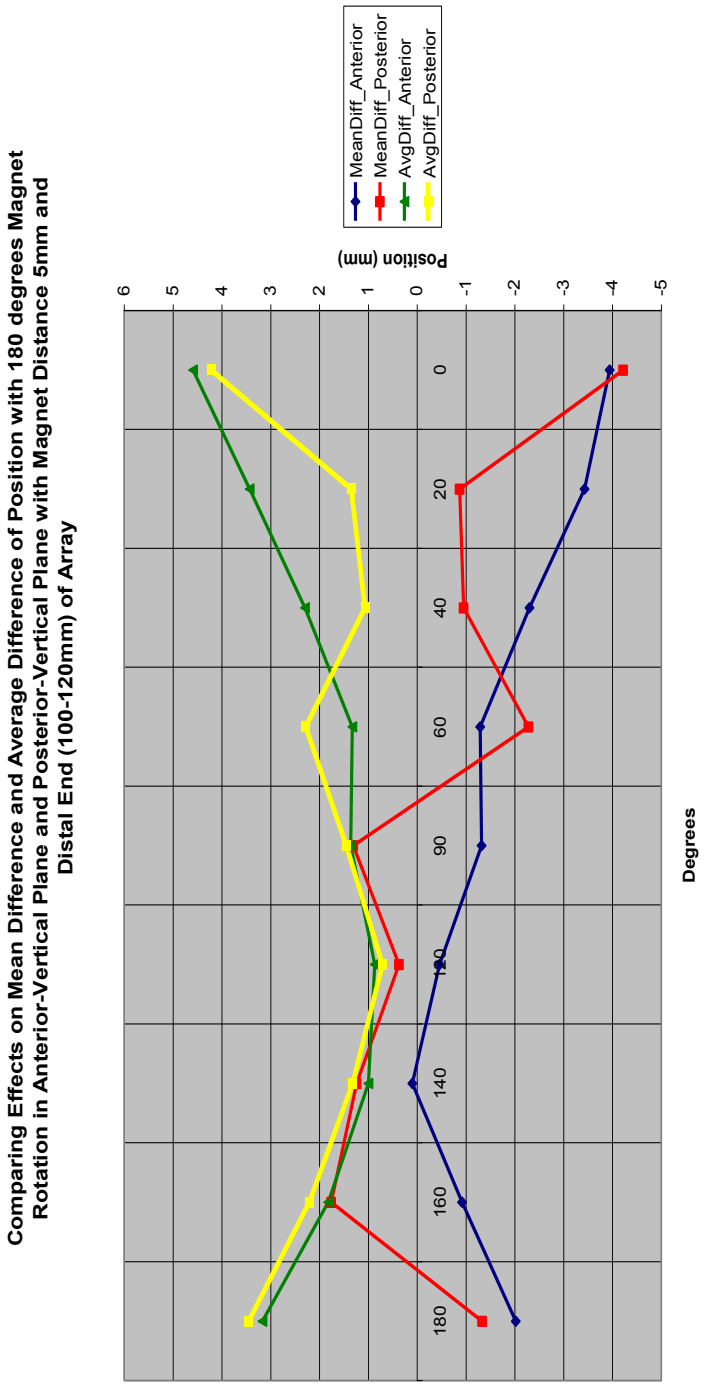

Figure 2.39 The mean and average difference in position output in both distal end part of anterior-vertical and posterior-vertical planes appeared comparable and low between 60 to 120 degrees. . Both the ends of rotation arc (0-40 degrees and 140-180 degrees) demonstrated a higher position error in distal end part of both planes.

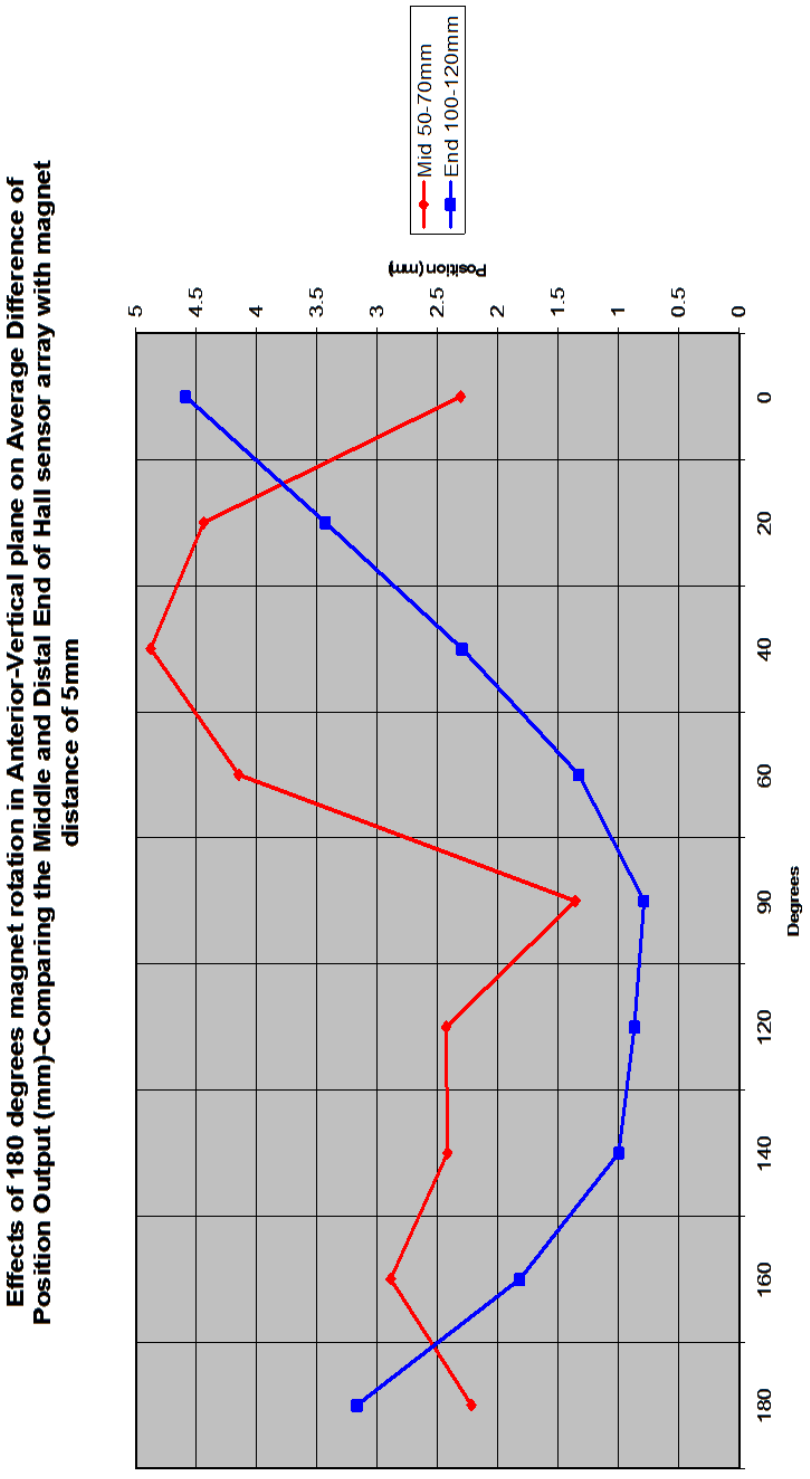

Figure 2.40 A magnet placed in the distal end of anterior-vertical plane showed a lower average difference in position output compared to the middle part. A higher average difference in position output was seen in rotation arc between 20-60 degrees of middle part compared to 120-160 degrees of middle part.

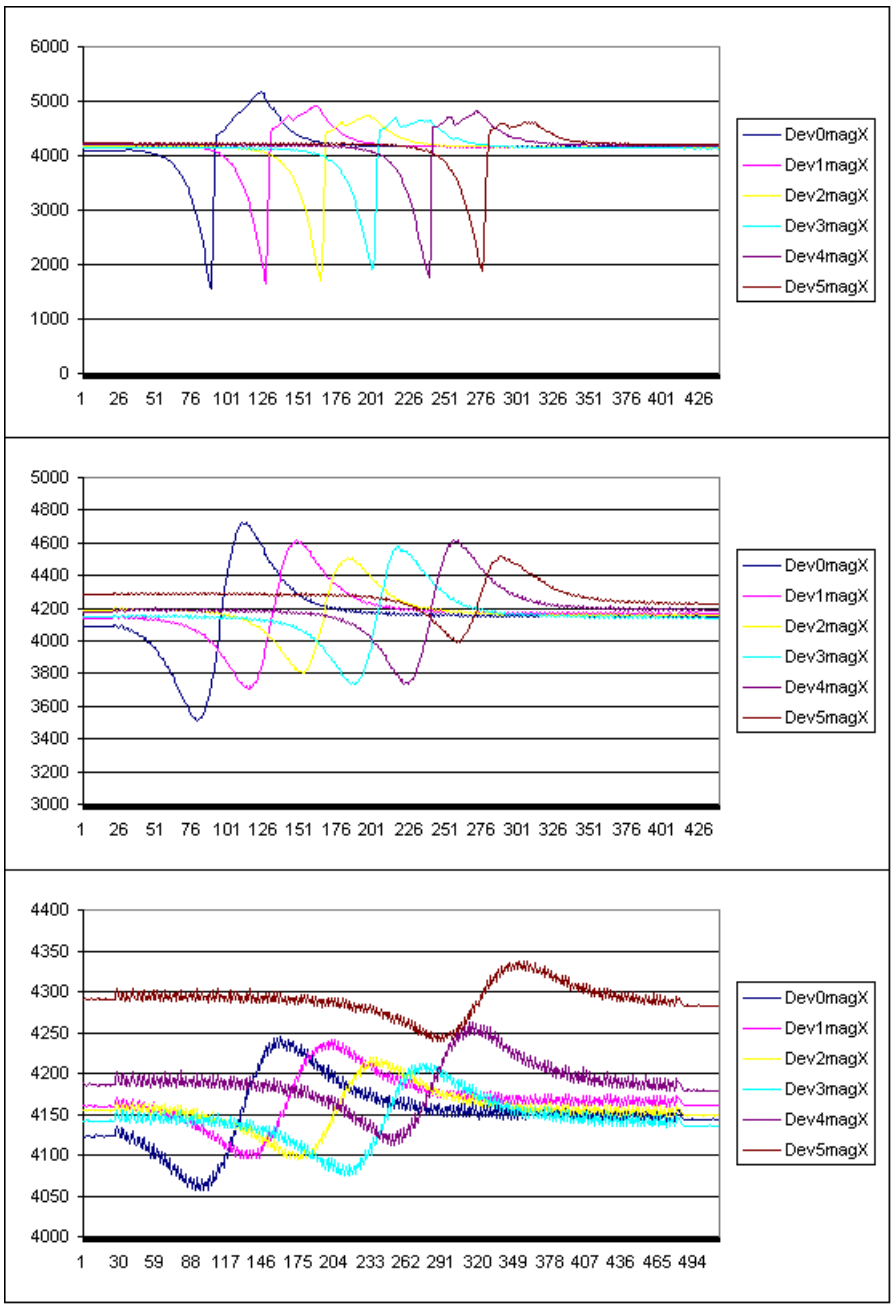

Figure 2.41 Validation of the third generation probe with Memsic MMC328XMS magnometers. The magnet was passed along 6 consecutive sensors at 0 mm distance (top), 5 mm distance (middle) and 10 mm distance (bottom).

It is worth noting that signal strength was lower at the very distal and proximal working ends of the probe, as fewer Hall sensors are present and does not allow for the desired interpolation of signal strength. The probe still works to the end, but although the most distal or proximal sensor can still detect the magnet, the magnet itself may be beyond the last sensor, and so when interpreting the data, it should be

noted that any position output of either 0mm or 120mm, could mean this has occurred.

When the experiment was performed in the rotation A arrangement, at distance ≤10mm an accuracy of 0 - 3.4mm was found for all rotations studied except for 0° at 10mm distance when studied signal strength was inadequate. At 15mm an accuracy of 1.2 - 6mm was recorded for all rotations except 0°, +20° and -20° when again signal strength was inadequate. The magnet was then moved along the length of the probe in the varying angles of rotation described as rotation B above. At distance ≤10mm an accuracy of 0.8 – 3mm was found for all rotations except 0° when signal strength was inadequate (Table 2.1). At 15mm the error was 2.1 – 5.8mm for all rotations except 0°, +20° and -20° when signal strength was inadequate.

Finally, the magnet was moved along the probe at different rotations described as rotation C. At distance ≤10mm the error was 0.6 – 7.6mm. At 15mm distance the error was 1.2 – 12.5mm for 0-160° and -90°. For 180°, -160°, -140°, -120°, -60°, -40° and -20° the signal strength was inadequate.

The accuracy was lower when the magnet was placed near to the end portion of the probe compared to the middle portion of the probe. For example, with an anteriorly placed magnet from the probe at 90° and 15mm distance, the error was 14.48mm when placed at the end compared to an error of 2.70mm when it was placed at the middle portion of the probe.

With a total of 108 studied orientations on bench, an error rate of less than ±10mm was achieved in 96.3% (104/108) of studied orientations up to a distance of 15mm between the magnet and the probe. The proportion of recordable signal strength below 10mV was 25% (27/108) during all studied orientations and proportion of studied orientations without any location recording due to unrecordable signal strength was 7.41% (8/108). Therefore there was a total of 32.41% (35/108) of studied orientations with significantly poor signal strength.

2.3.2 Temperature Effects on Probe.

There was no difference on low signal strength whether calibrating the probe at room temperature or at 37 degree Celsius (figures 2.42 and 2.43). Figures 2.45 and 2.46 show that when the probe is calibrated at room temperature and used at body temperature, there is a change in signal strength which is very undesirable.

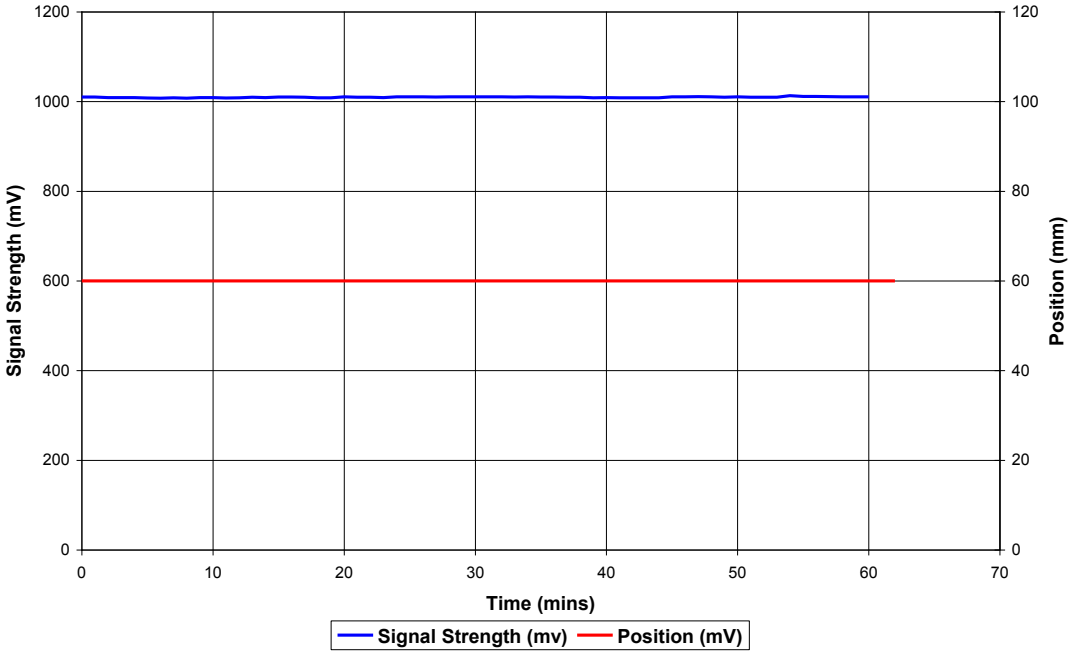

Figure 2.42 Signal Strength and Position at 17^{o}C, over time

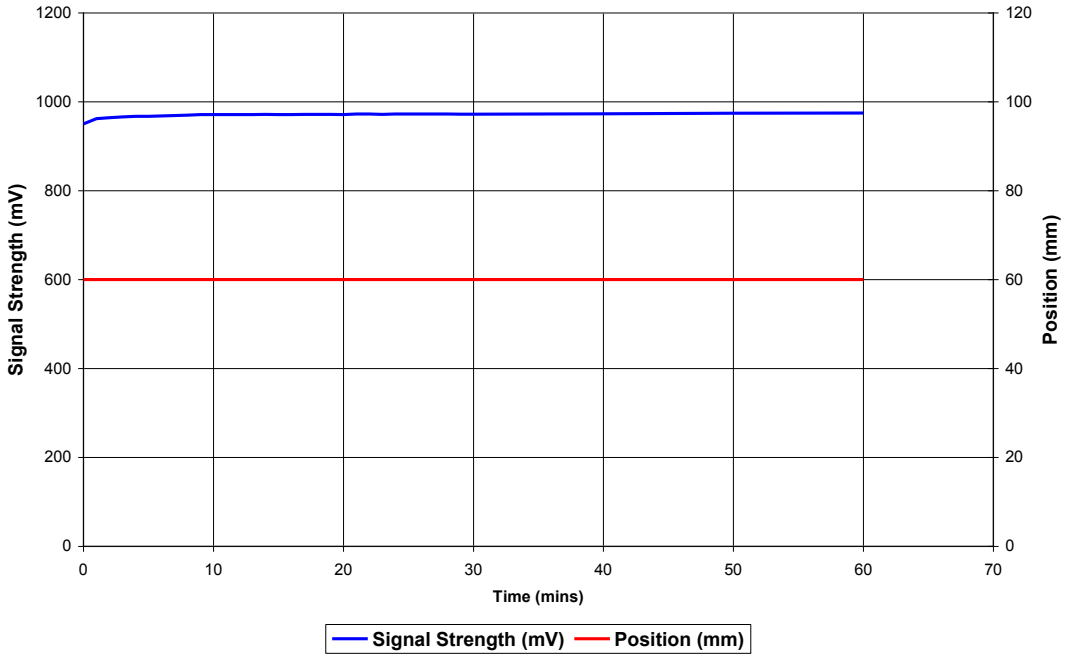

Figure 2.43 Signal Strength and Position at 33^{o}C, over time

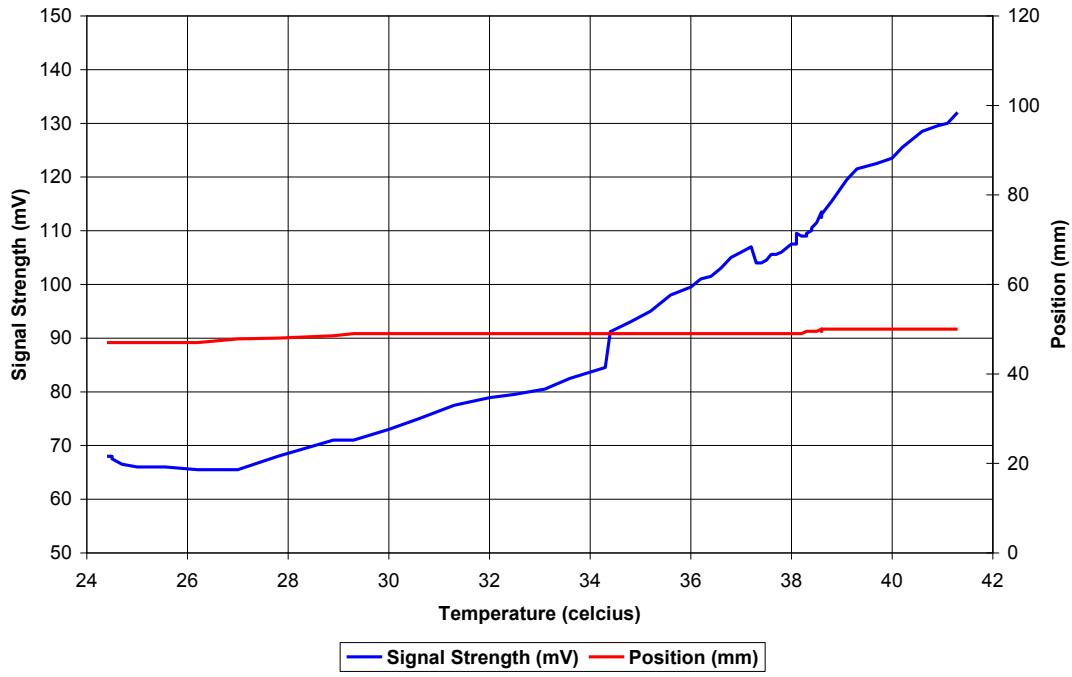

Figure 2.44 Signal Strength and Position Vs Temperature at initially low Signal Strength

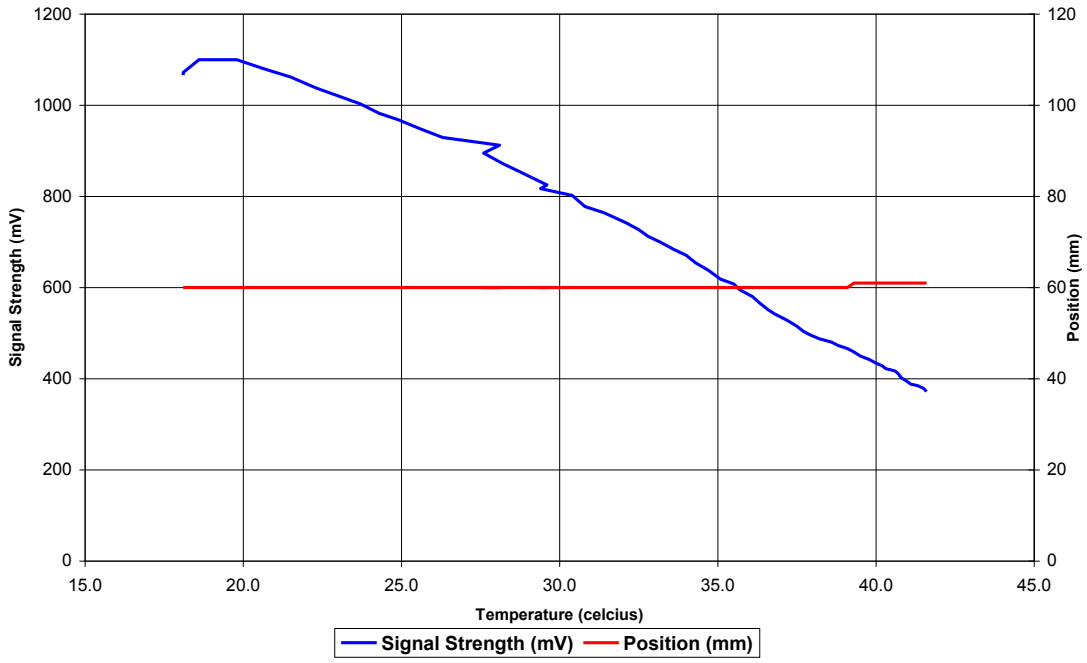

Figure 2.45 Signal Strength and Position Vs Temperature at initially high Signal Strength

2.3.3 Manometer compatibility

There was no interference between the locator and a connected manometer (figure 2.27). A connected manometer however caused an increase in signal strength output initially and peaked at 50s before tailing off by 500s and stabilised (figure 2.46). The position output did not show any interference. However this change can be potentially an artefact due to temperature effects or movement shifts or even real change due to enhancement of magnetic field as a result of metallic presence in the manometer. This experiment can be improved further by firstly, disconnecting (OFF) and connecting (ON) the manometer a number of times to confirm whether the change described is an artefact or real. Secondly, the combined connected manometer and the locator with magnet is exposed to a hydrostatic pressure of at least the lower oesophageal sphincter pressure (approximately 30mmHg). Figure 2.48 illustrated that whether connecting/disconnecting the manometer twice did not

replicate the change seen in the previous experiments suggesting that the earlier finding was an artifact.

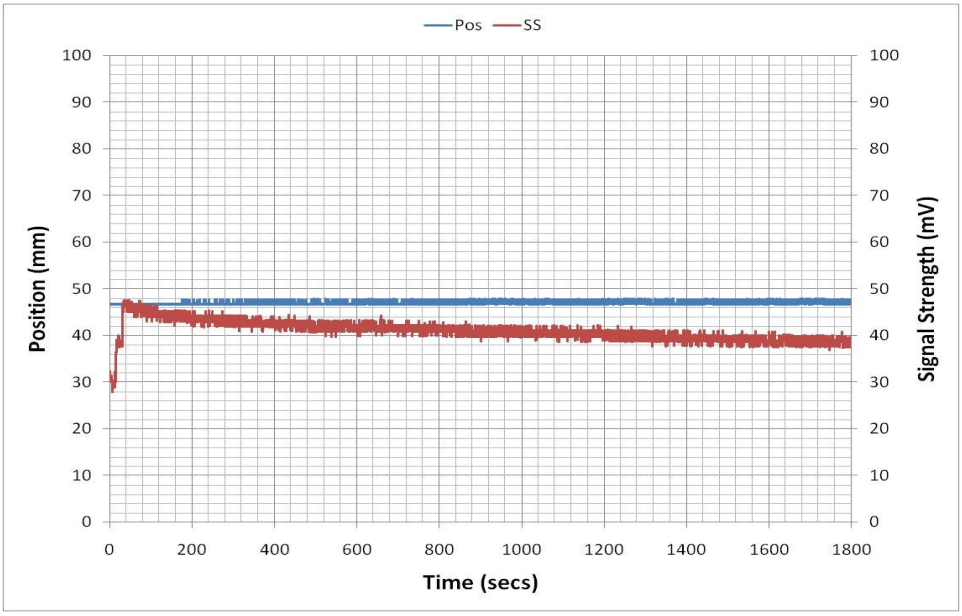

Figure 2.46 Locator probe combined with a connected manometer

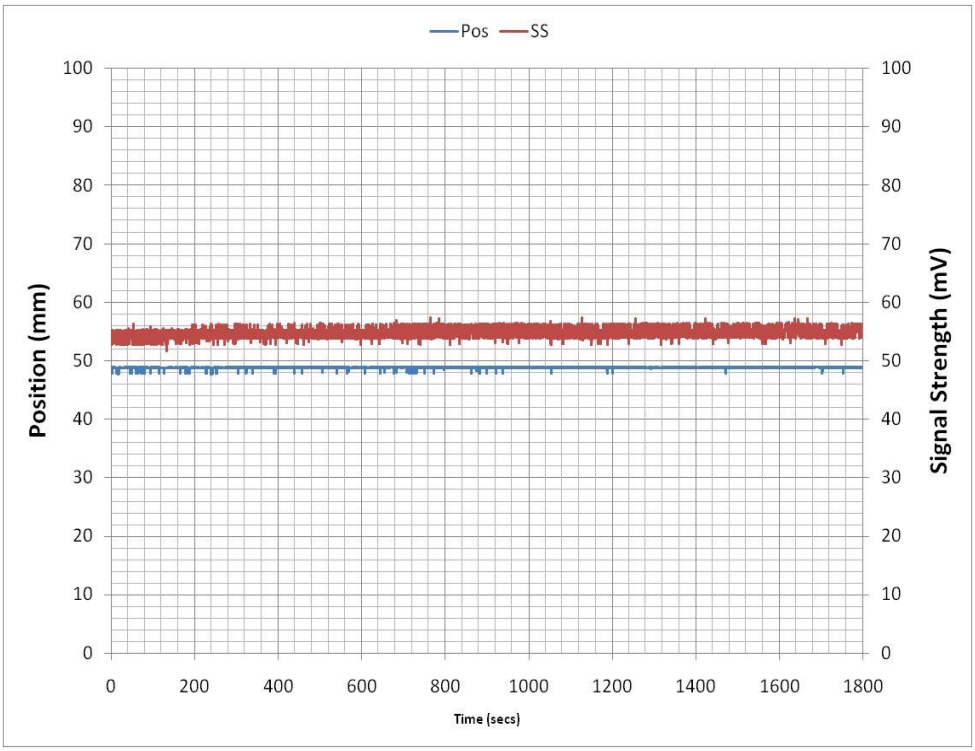

Figure 2.47 Locator probe combined with a disconnected manometer

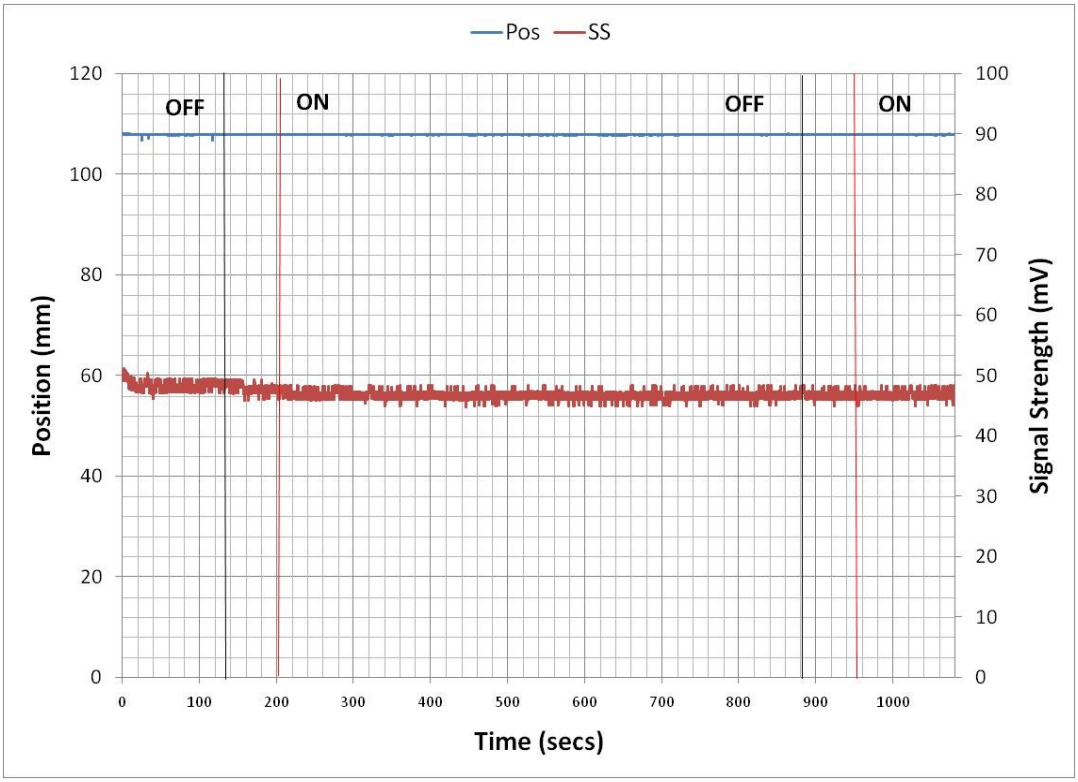

Figure 2.48 Locator probe with connected/disconnected manometer exposed to a median hydrostatic pressure of 25mmHg

2.3.4 pH probe interference

Experiments did not suggest any interference on the locator with a change of pH from 7 to 1 in the solution as depicted in figure 2.49 and 2.53. There were artefacts shown in figure 2.49 during the period of adding in hydrochloric acid solution. They are due to withdrawing of solution to prevent overspill out of beaker, movement shifts as a result of adding in solution and finally, a result of stirring to mix the solution. The signal strength was also reduced by approximately 5mV as a result of above artefacts.

Locator probe with a disconnected pH electrode also did not show any interference with a change in pH from 7 to 1 as shown in figure 2.50. Similarly there were artefacts as a result of movement shifts. Locator probe with a connected pH electrode showed a shift in signal strength of approximately 15mV as shown in

figure 2.51 but this shift was seen before adding in the hydrochloric acid solution and was associated with an artefact while preparing to add the acid as a result of movement shifts associated with withdrawal of solution, addition of solution and stirring of solution. However since the shift in signal strength was much larger. There did not appear to have any interference with signal strength between the locator probe and a connected pH electrode with an abrupt change from pH 1 to pH 7 as shown in 2.52.

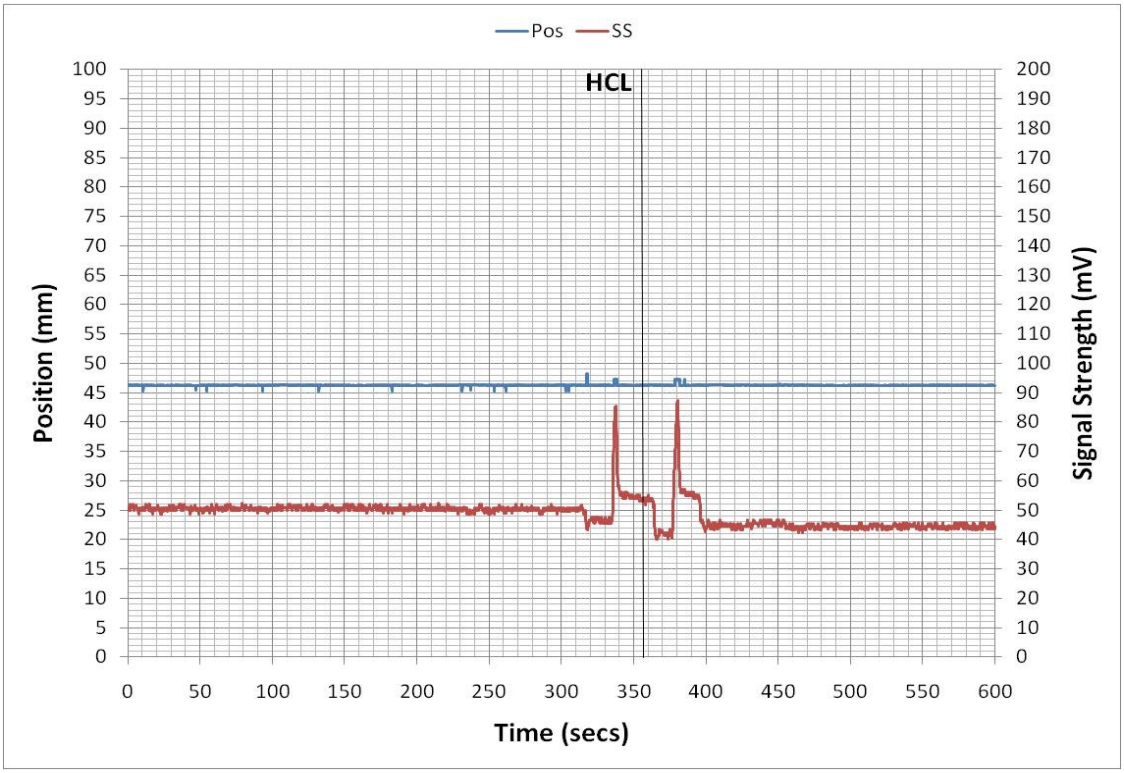

Figure 2.49 Locator only with abrupt change in pH

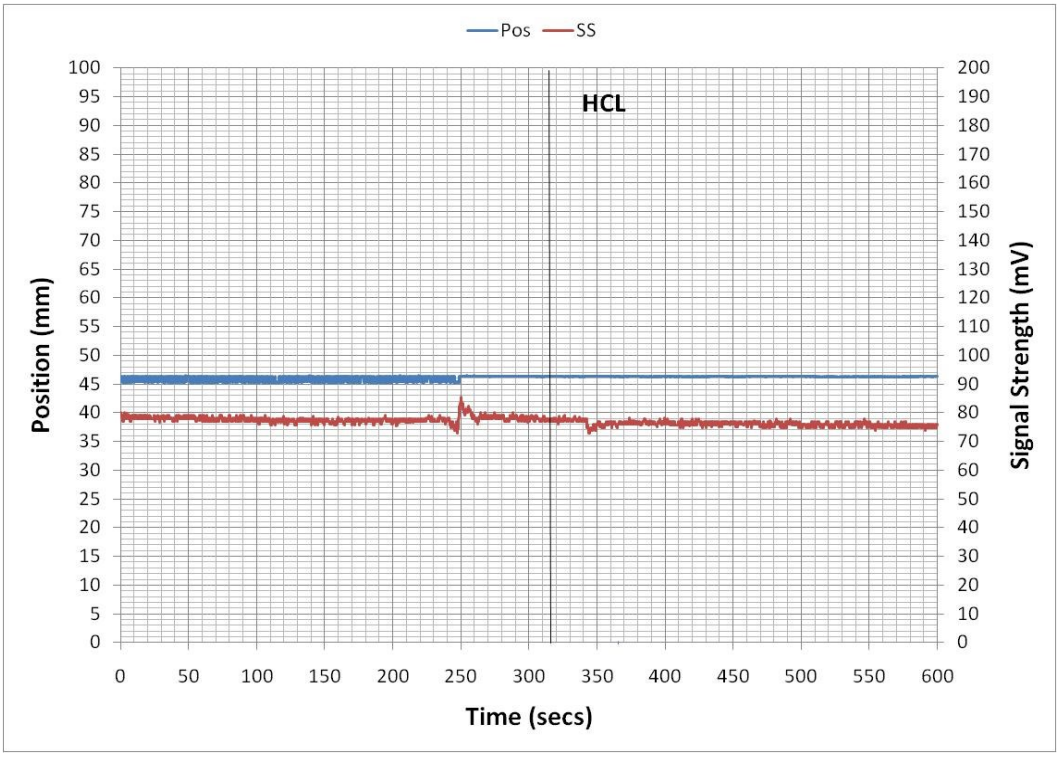

Figure 2.50 Locator and disconnected 12 channels pH electrode with abrupt change in pH

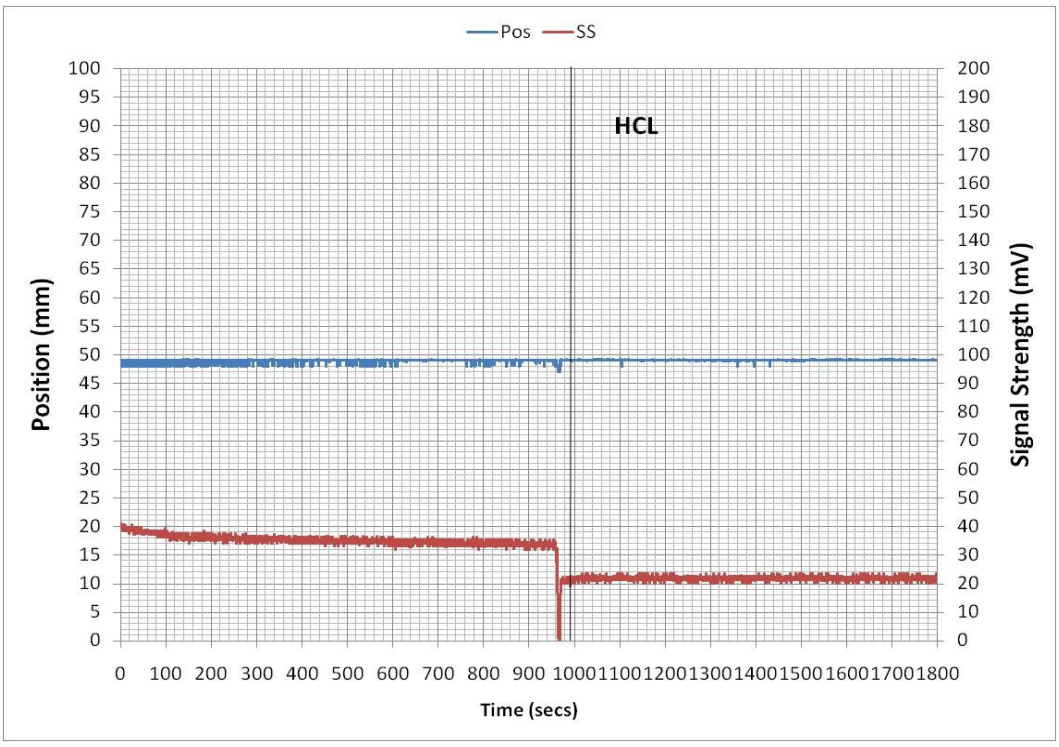

Figure 2.51 Locator and connected 12 channels pH electrode with an abrupt change in pH from pH 7 to pH 1

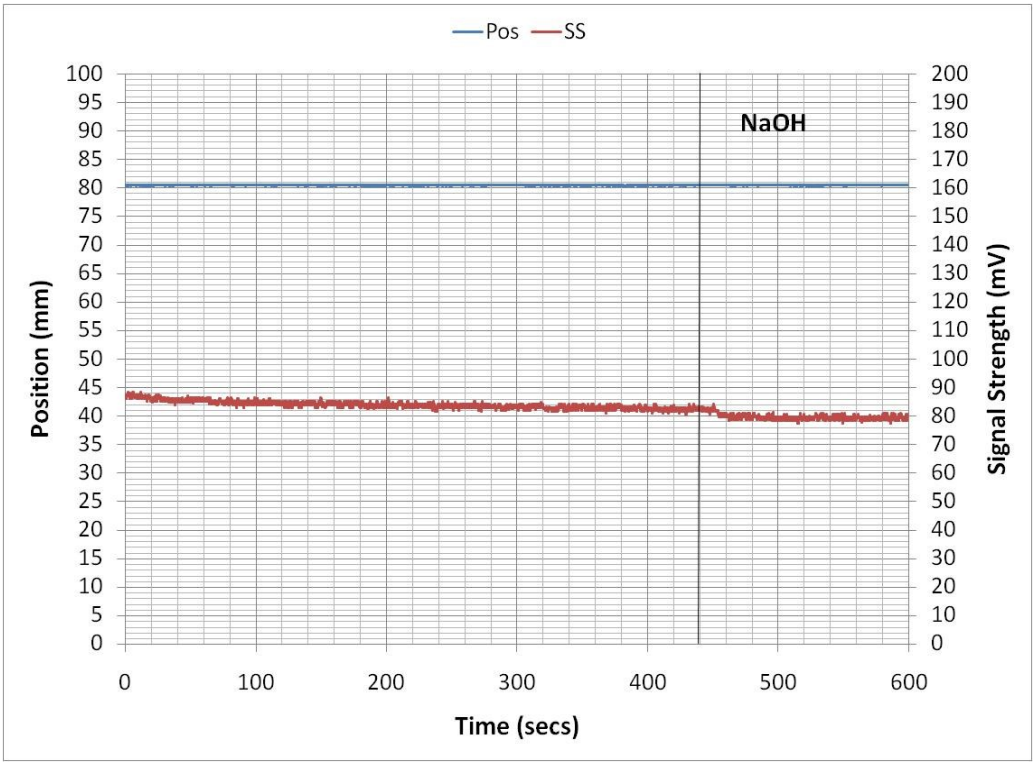

Figure 2.52 Locator and connected 12 channels pH electrode with an abrupt change in pH from pH 1 to pH 7

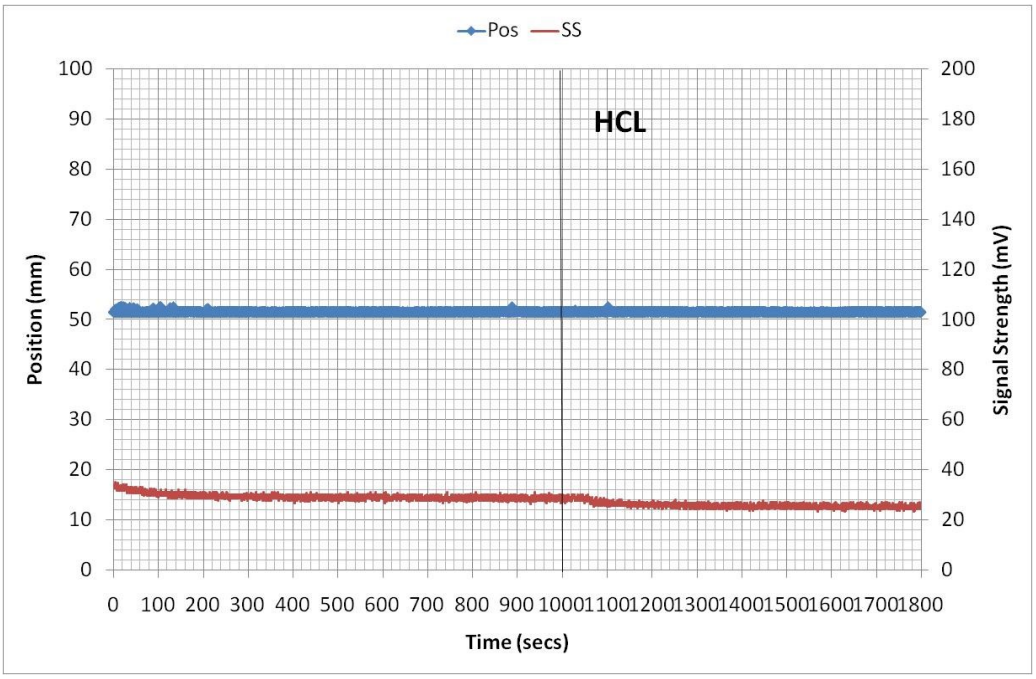

Figure 2.53 A repeat study of locator and connected 12 channels pH electrode with an abrupt change in pH from pH 7 to pH 1

2.3.4 In Vivo validation and results.

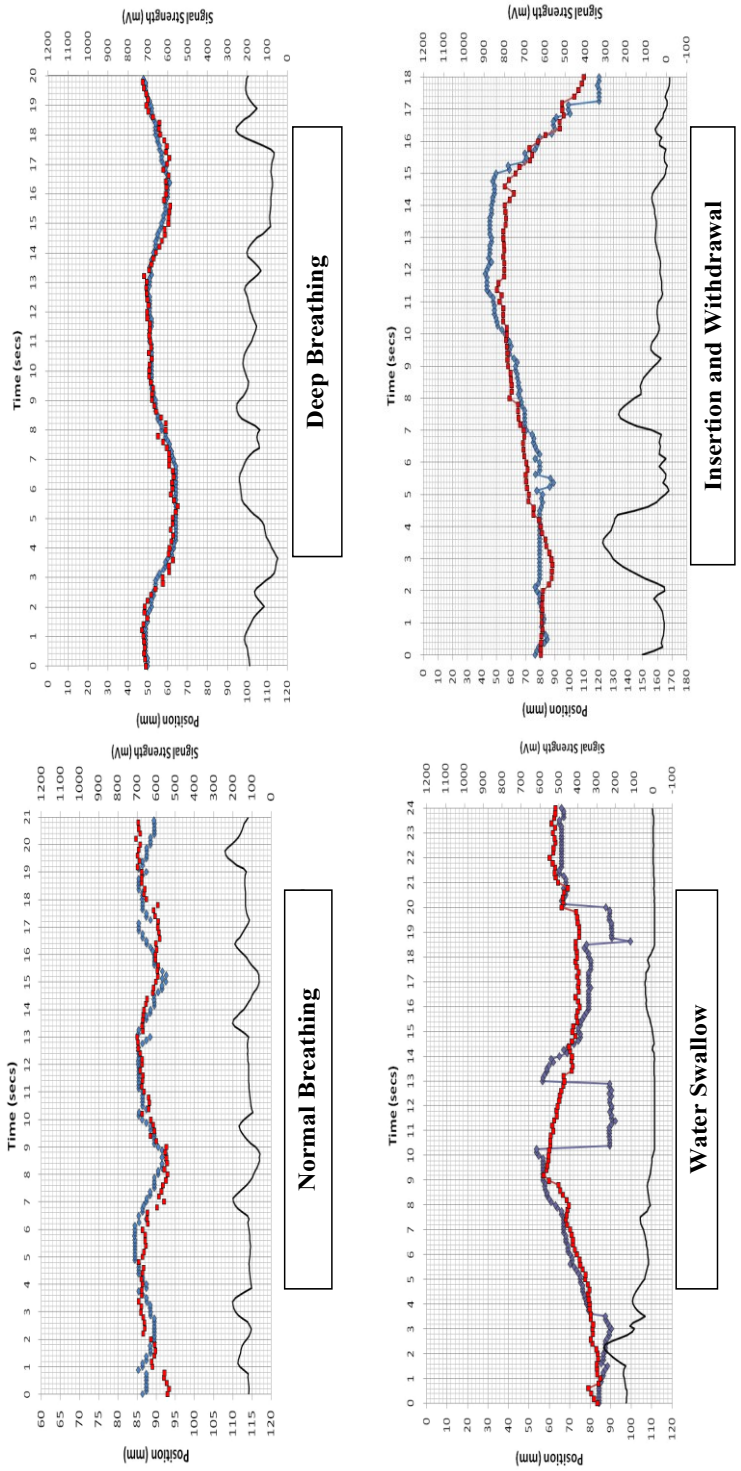

Figure 2.54 Examples of fluoroscopic validation of position as reported by the probe. Red markers are fluoroscopic clip position recordings, blue markers are the reported clip positions with the SCJ locator and the black line is signal strength.

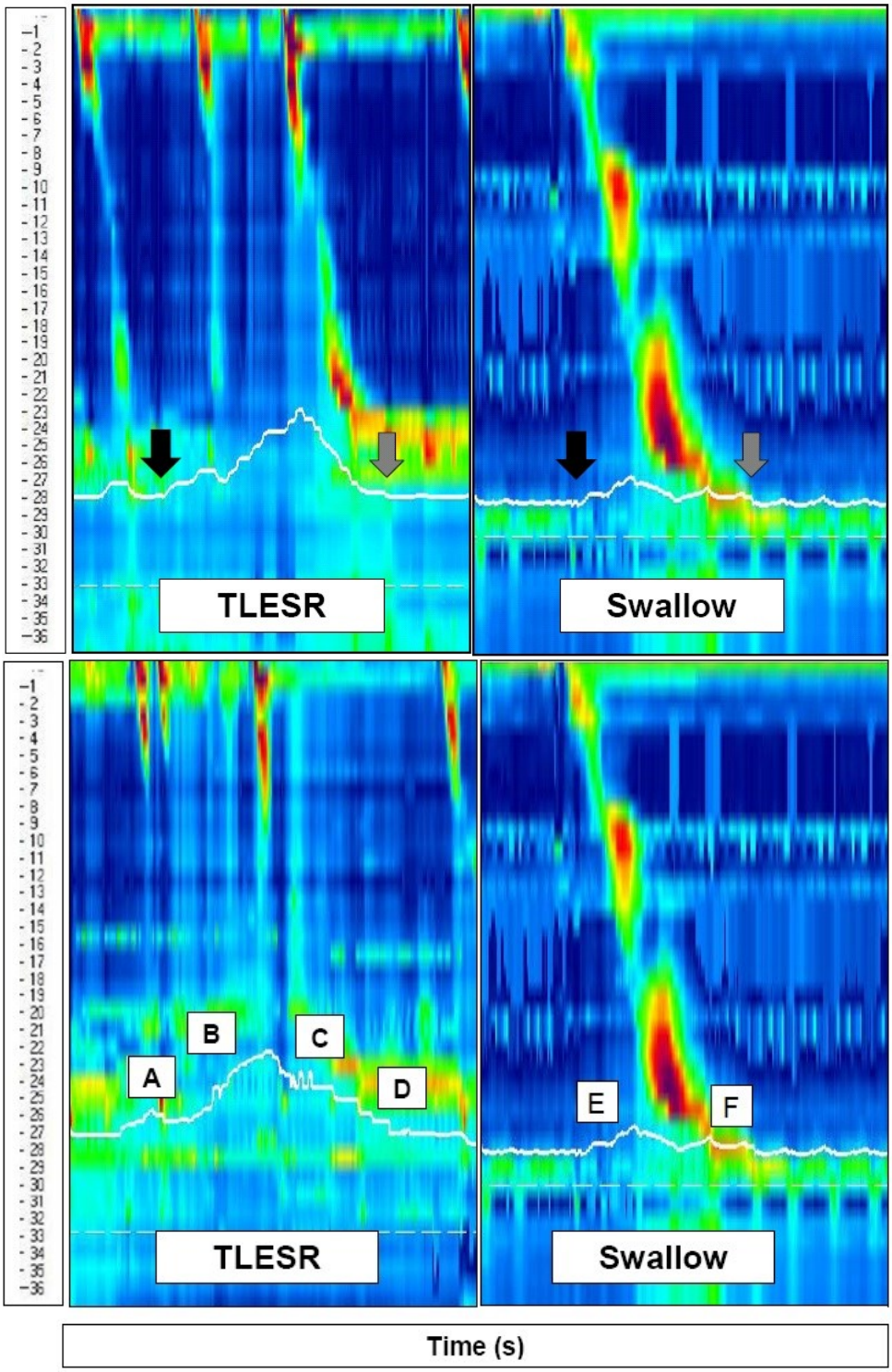

Figure 2.55 The movement of the GOJ as measure by the probe (thick white line) superimposed on colour contour manometry plot. Examples of characteristics of GOJ movement during TLOSRs (left) and swallows (right) are shown. The black and grey arrows indicate the start and end of the GOJ movement respectively. A, B, C and D indicate phases that occur during TLOSRs; D and E indicate swallowing phases.

2.4 Discussion

2.4.1 Benchtop validation

The sensor's ratiometric output is as expected, proportional to the inverse cubed of the distance to the magnetic field. the two different types of magnet, the SmCo and NeFeB magnet followed this law, with similar responses, however the N42 Neodymium magnet induced a higher output in the sensor at greater distance while producing a lower output than the Samarium Cobalt magnet at distances less than 4 millimetres. Both magnets saturated the sensor at distances of 2 millimetres or less (figures 2.30 and 2.31. The above experiment was performed using the north pole of the magnet pointing directly at the sensor; the saturation of the sensor is not an issue as it recovers as soon as the strong field is below the saturation threshold without any lasting effects and performs as normal after saturation. The sensor appears to not be able to detect the magnet at a distance of 15 millimetres, this is due to the field being so small, it is lost in background electromagnetic noise and the Earth's magnetic field; this quality is called the sensor's range, the limit of the distance at which the sensor can detect the magnet.

The discrepancy between a smooth response and the inverse cubed curve is most likely due to the inaccuracy of the position measurement, performed with a plastic ruler, meaning that if measurement of the distance of the magnet to the sensor's face was not precise there would be a variation in the output of the sensor as it is sensitive enough to detect the small difference in magnetic field between 1.1 and 1.0 millimetres. This hypothesis is confirmed by the re-testing of the experiment with a much more accurate linear motor track, which is capable of making movements to the degree of micrometres, meaning the distance from the sensor is more accurate than when performed manually. The only source of error could be due to misalignment of the axis along which the magnet is moved, however this appears to fit the inverse cubed curve very accurately so is presumed to be very well aligned (figure 2.31).

The oesophagus is made up of mucosal folds when not passing food; the folds have a very small diameter, estimated to be 10 millimetres, so the sensor's range of 15 millimetres was considered acceptable to proceed with development. The development of the circuit and the associated microprocessor hardware was performed, which allowed for the calculation of the magnet's position along the working 22 centimetre sensing range of the probe, the response of the microprocessors interpolation algorithm is shown in Figures 2.32, 2.33, 2.34 and 2.45, at distance of 0, 5, 10 and 15 millimetres respectively; the experiment was performed by manually moving the magnet along the length of the prototype SCJ locator probe in steps of 1 millimetre. The very smooth linear response of the interpolation algorithm can be seen at distances of 0 and 5 millimetres, as the magnetic field is strong at this distance; with increasing distance from the probe, the interpolation algorithm becomes less accurate, which can be visibly seen by the jagged step-like graph at 15 millimetres. This inaccuracy is due to the very low magnetic field from the magnet being lost in background noise; the step-like output derives from the fact the sensors are placed 5 millimetres apart, meaning that although the field is still detectable if a magnet is placed directly in line with a sensor, as it progresses along the probe, it moves parallel such that the field is pointing at the gap in between two sensors, resulting in a very weak field at each sensor.

The magnet may move a significant amount *in vivo*, as it is only attached to the mucosa at the small jaws of the endoclip to which the magnet is fixed; the jaws of the endoclip are clamped onto the soft mucosa and can rotate about the point of attachment, therefore experiments were designed and performed to test the response of the device to a variety of rotations and directions such that any potential system weaknesses can be identified and reviewed.

As expected, the sensor is very directional, with the angles perpendicular to the magnet outputting the lowest voltage at a given distance, although this is expected when working with the Hall effect, as the sensitive Hall effect element is directional to a magnetic field; the output of the sensor when the magnet was placed exactly behind the sensor was similar to that of the front, however with a weaker output

(figures 2.36, 2.37. 2.38, 2.39 and 2.40), however this is most likely due to the increased distance to the sensing element which is placed at the front of the package, as well as the integrated circuitry and flexible circuit board in between the element and magnet distorting the field. It is evident from the direction and rotation experiments (tables 2.1, 2.2, 2.3, 2.4, 2.5, 2.6, 2.7, 2.8, 2.9, 2.10, 2.11, 2.12, 2.13 and 2.14, in appendix 1) that the direction of both the magnet and its attitude respect to the probe is important, with several orientations decreasing the working range between device and magnet. It is important to test and validate this device *in vivo*, after having highlighted several orientation issues, to review if they affect the ability of the device to reliably detect the magnet and hence SCJ position. The magnet may be free to rotate but potentially more importantly the oesophagus can dilate to allow the passage of a bolus during swallows, relaxation of the oesophagus during belching or TLOSRs, meaning the radius of the oesophagus may be larger than 15 millimetres; as this has not been measured due to the difficulty of doing so, it is unknown that this will be an issue during probe use.

The accuracy of the device as reporting the position of the magnet along the probe is tested against the known position of the magnet moved along the sensing range in 1 millimetre increments, the below errors are derived by producing a mean of errors along the length where the error is the difference between the actual position minus the reported position; this error is distance and angle dependant. The error at 0 millimetres was often less that 1.5 millimetres and ranged from 0.03-2.72 millimetres. The error at 5 millimetres was often less than 3 millimetres and ranged from 0.04-4.44 millimetres. The error at 10 millimetres was often less than 4 millimetres and ranged between 0.07-7.58 millimetres. At 15 millimetres, occasionally the magnet was not detected in certain orientations, so are excluded from the error measurement as no position was recorded; the range when the magnet was detected at 15 millimetres was often less than 10 millimetres, ranging between 0.32 to 19.28 millimetres. An error of nearly two centimetres is rather large, however this is because of the low signal to noise ratio of the magnet and the fact the magnet was pointing at a different sensor due to its rotation; the accuracy at 15 millimetres is not ideal however it was noticed that the output from any sensor was often less than 10 millivolts, so whenever the output from the highest sensor is less than 10

millivolts, the position of the magnet is deemed inaccurate or invalid, as this could mean significant misrepresentation of SCJ position. Importantly the position of the magnet and hence SCJ was often within 4 millimetres and occasionally less than 1 millimetre; the errors were both negative and positive however in order to calculate the mean, the magnitude of error was taken (described as average difference in the tables). The high accuracy orientations often correlated with a substantial signal strength from at least one sensor, meaning the output of the microprocessor which showed the value termed Signal Strength, a value calculated from the relative outputs from sensors near the magnet, could also be used to demonstrate accuracy confirmation when used in the in vivo environment, as the actual position is not known when used inside the body without the validation of fluoroscopy. Signal Strength also correlated highly with distance to the sensor; as the magnet neared the probe the signal strength increased proportionally, subject to rotation.

There is a very similar output of the SCJ locator used when looking at the LCD display and when using the direct output to the Polygraf, meaning the data can be trusted as recorded by a PC using this method; the only discrepancy is due to the difference in maximum outputs in the display and the voltage limitations on the Polygraf inputs, however this is negligible.

It is worth noting that accuracy at the most distal and proximal ends of the sensing range was marginally worse, this is due to the lack of sensors with which the interpolation algorithm can calculate the output; it is unavoidable therefore positional outputs at either the maximum or minimum of the probe's length must be interpreted with knowledge of this problem. The placement of the SCJ locator probe within the oesophagus and stomach may be as such to ensure that the SCJ may move up and down without reaching either end of the sensing range; without testing, it is unknown the extent of SCJ movement however it is suggested that initially the centre of the sensing range be placed in the LOS so that 10 centimetres or so of sensing region remains either side of the LOS borders, allowing for any potential movement.

The accuracy of the third generation probe was confirmed on the benchtop as shown in figure 2.41, where the new sensors are at least as accurate as the previous model, with several added advantages are due for *in vivo* tests soon.

2.4.2 Temperature effect on probe

The signal strength from the sensors varies up to 0.4% between each extreme with a standard deviation of 1.04% over the period of an hour, however any slight rise is most likely the result in the gentle rise in room temperature over this time due to the building's central heating system. At 37^{o}C the results are similar, with very little change in signal strength, 2.4% with a standard deviation of 4.45% which can be mainly attributed to the gentle increase in temperature of the incubator. Once the temperature factor is removed, a standard deviation of 1.01% is achieved. A promising result is that during both of the time drift tests the position recording never fluctuates more than 1mm, which is the resolution of the output.

The outcome of this test is the evidence that there is minimal drift in signal strength over time, even at higher temperatures, this drift is mainly the result of change in environment temperature. The constant position recording too is a good indication that the probe performs consistently over time, as the magnet does not move during this experiment.

Change in temperature does have a significant effect on the signal strength and the change appears to be dependent on the initial signal strength, the evidence for which can be seen in figures 3 and 4, where initially high signal strengths decrease and initially low signal strengths increase. The latter may be a problem if the signal strength is so low it could be a result of electromagnetic noise from the room or any equipment used in conjunction with it. This could result in a signal falsely attributed to the magnet, giving anomalous position values. In figure 2.45 the signal drops approximately 40mV per degree Celsius or 3.6% of original signal strength per degrees Celsius, so when the system is calibrated at a room temperature of 17^{o}C, the signal strength may reduce by 36% when used in the body, with the 20^{o}C increase. A signal strength value of 400mV is still a high signal strength so the position recording can be assured, however when the signal strength is initially lower there may be a problem with a signal strength drop. Concurrently in figure 2.44, a signal strength increase is observed, which as previously mentioned can give a false position recording, and changes approximately 2.5mV per degree Celsius, or 2.5% of

original signal strength per degree. This is obviously a lower percentage change than that shown in figure 2.45, but it could have repercussions when interpreting position validity at lower signal strength.

Although it appears that the ratiometric output of the Hall effect sensors changes with varying temperature; importantly it doesn't show any signs of drift with temperature, unlike the HRM demonstrated in the previous chapter. The sensors appear to act predictably with temperature, meaning that the increase from room temperature to body temperature will have a known and correctable effect. Having established the extent of this temperature dependant output fluctuation, it was decided to test the sensors while calibrating them at body temperature in a 37^{o}C water bath, when tested at body temperature they showed no change, suggesting that a calibration at body temperature when using the probe *in vivo* will successfully and accurately compensate this for temperature dependence. In these experiments there may have been some minimal artefact, such as expansion of the silicone tube in which the sensors and FCB are encased, which would mean the magnet was moved slightly further away from the sensors.

Importantly, there is no change in the calculated magnet position despite the change in sensor output; it may however affect the range at which the magnet can be detected therefore body temperature calibration is strongly recommended.

2.4.3 Manometer compatibility

Any ferrite or magnetic permeable material within the manometer, be they pressure sensing components or associated circuitry, has the potential to distort the magnetic field form the magnet-clip, this may noticeably affect the performance of the SCJ locator probe by increasing or decreasing the detected signal strength. Similarly electric current flowing through wires in the connected manometer may cause interference via an electromagnetic force, an output which may vary dependant on the output from the sensor and therefore from a change in hydrostatic pressure. It was therefore vital to check the potential interference between the manometer and the

SCJ locator, with both high and low hydrostatic pressures on the bench top before using the devices together *in vivo*. The results suggest there is negligible effect of the manometer on the SCJ locator probe, when neither connected nor disconnected; the disconnected experiment showed that the metal section of the HRM had little effect on the SCJ locator and the connected experiment showed that the current flowing through the sensors had only a slight effect on the SCJ locator. The SCJ locator demonstrated a mean drop of 5mV when the manometer was switched on, however this is well within acceptable levels and is constant when the manometer is on. Changes in hydrostatic pressure could not be checked as changing the pressure on the dual probe set up would have undoubtedly moved the magnet, probably by decreasing the cross section of the hollow silicone tube to which the magnet was attached, therefore the SCJ output would have increased significantly more than any effect from the HRM.

The only affect that caused issues was the occasional tendency that the magnet became attached to the metal sensors, causing a very small spike in pressure readings at that sensor; the magnet was slightly attracted to the sensors and this was noticed on the bench top, however the attractive force was so minimal that it would not inhibit movement of the SCJ in vivo. The slimline HRM which was later acquired showed absolutely no attraction between the magnet; as it was significantly smaller and easier to intubate when in a multi-catheter assembly, it was used for all subsequent in vivo studies after the validation.

There appears to be several limitations in the bench top studies, demonstrating artefact, which when repeated were not present; these artefacts may make it difficult to interpret results, however they were explainable in the form of temperature effects and movements of the assembly or magnet. The repeated experiments confirmed the phenomenon were in fact artefact rather than interference between probes. The experiment also shows that the Hall effect sensors are not sensitive enough to detect current changes in the manometer in the experimental set up, although there is a very minimal change of the signal strength output after switching the HRM on, it is so minimal that is very unlikely to affect the performance of the SCJ locator in any way.

The experiments showed there was no interference between the manometer and the SCJ locator, as neither device was affected when used together.

2.4.4 pH Catheter compatibility

It appeared that all experiments on possible interference between the acidic or alkaline environment, 12 channel pH electrode and locator probe did not suggest any interaction. Even though combining the locator probe and 12 channel pH electrode for in-vivo study may theoretically create electrical interference but current bench experiments did not suggest that it is so.

The results of bench experiments were not without problems of interpretation, especially with the presence of artefacts. However It has been realised that these artefacts were movement-related as a result of adding, stirring and withdrawing of solution. Beside artefacts, movement may have caused a change in signal strength but as shown in graphs, the change was usually small at approximately 5mV. Therefore by repeating some of these experiments and reducing movement artefacts, the results were more interpretable. Even though the results appeared to show there was no gross interference, a small interference may still be possible since the system is not sensitive or designed to detect such interference.

As a summary, there did not appear to have any gross electrical interference between the 12 channel pH electrode and the locator probe from bench studies. Like the manometer, both magnetically permeable materials and current flow has the potential to interfere with the output of the SCJ locator, and likewise the SCJ locator and magnet has the potential to interfere with the pH catheter. Antimony in the sensors is slightly diamagnetic, meaning it creates a small field in opposition to an externally applied field, therefore could repel the magnet; this was tested on the bench top and no effect was found, presumably to the relative weakness of the magnet and the small amounts of antimony in the sensors relative to the strength of gravity.

The limitation in accuracy for these tests is the fact that adding either acid or alkaline liquid to the measuring column in which the assembly was placed, often moved the

magnet, producing significant and abrupt changes in measured signal strength, due to changes in magnet position. Several experiments were repeated in order to confirm that the outcomes were artefactual rather than interference. These artefacts are shown in figure 2.49 and figure 2.51 are uncharacteristic changes in SCJ locator signal strength; when repeated they are not present, this is because every care was taken to minimise magnet movement due to the adding of alkaline or acid, which swirled in the column. The magnet was placed toward the bottom of the container so as not to be directly in the stream of added liquid; the liquid was also added more slowly than in the initial experiments.

There appears to be very minimal interference between either probes when these artefacts are removed, such that there is a small signal strength decrease of up to 2 millivolts when adding either acid or base, suggesting that there is minute interference from the pH catheter on the sensors of the SCJ locator.

This is most likely due to the change in current along the device, similar to the effect of switching the HRM on; a change of 2mV is very unlikely to affect the performance of the device, only at very low signal strength is it able to cause issues. The pH catheter experiences no change in pH measuring when used in conjunction with the SCJ locator, nor does the magnet affect the pH sensors output. Ultimately the device remains unaffected by either probe and even though minor changes of variation are reported, the magnitude is so small that the device can operate as normal, with the orientation and attitude of the magnet to the SCJ locator far more important when limiting the effectiveness of the SCJ locator's performance; the position does not change with the minor effects of combined usage, therefore is deemed compatible with both devices.

2.4.5 *In Vivo* validation

The measurement of the SCJ has been shown in the in vivo validation experiments; the recording of the SCJ position is shown in figures 2.54; in one example the SCJ locator data has been overlaid on the manometry and pH data in figure 2.55 which allows for useful analysis of a very complex area. This figure shows the SCJ position

when inserting and withdrawing the probe approximately 60 millimetres, this should simulate significant movement such as that of a TLOSR; the position of the SCJ output (blue dots) is similar to that of the fluoroscopically recorded and interpreted data (blue dots). The signal strength, shown as a solid black line, fluctuates quite markedly; the areas of variation between the fluoroscopic data and the SCJ locator data seems to coincide with the periods of low signal strength, suggesting that this is the cause of the variation.

Very similar data is presented in normal breathing, with fluctuations in signal strength coinciding with phase of respiration; possibly due to the changes in pressure between the abdomen and thorax resulting in relative movement of the SCJ and GOJ. It is known that the sphincter pressure changes with the phase of respiration, hence this could be exerting forces on the clip to change its position.

Even more closely matched is the data for deep breathing, which is almost identical throughout the breath cycle, the difference between this and normal breathing is the movement; also the signal strength is higher for the slow breathing, suggesting that signal strength could be affected by the speed of movement of the magnet. The alternative answer could be that the magnet is in a better orientation at different stages of the study, although without knowing the three dimensional position of the magnet and SCJ locator, it is almost impossible to speculate on this, as the fluoroscopy data is merely two dimensional and substantially noisy.

The swallow maneuver shows a potential black spot for the SCJ locator, demonstrated by the sudden jump in position; this occurs twice during the example swallow. The most probably cause of this is the distension of the oesophagus to allow the bolus of water to pass through, thereby increasing the distance between the magnet and closest sensor; this combined with a poor orientation would mean the magnet was outside the detection range. The second loss of signal is probably associated with distension of the secondary swallow, often present only in the distal oesophagus following the initial peristalsis for the function of fully clearing the oesophagus of remaining bolus contents and saliva. Other than the periods of loss of magnet, which coincide with periods of zero signal strength, the detailed position is relatively close; without fluoroscopy, the invalid positions can be identified using a

signal strength of less than 10 millivolts, and noticing the severity of change between two data points, much greater than any physiological measurement.

Subsequent studies recorded the movement of a physiological TLOSR, detailing the proximal movement followed by return of the SCJ and hence GOJ; this was subject to statistical testing, suggesting that presence of this movement was the best indicator that a TLOSR had occurred, more so that pH or manometric data. As demonstrated by Lee et al (Lee et al 2013), the movement of the SCJ is clear and substantial; acid is clearly visible above the SCJ towards the end of the TLOSR event, as acid of pH 4-6 remains above the line indicating the SCJ position. The LOS sphincter appears to close around the SCJ, which traps acid above the LOS and SCJ, exposing the sensitive oesophageal mucosa to gastric acid; this clearly shows that TLOSRs are important in reflux based diseases and could explain why so much acid reflux measured at the traditional 5 centimetres proximal to the LOS is missed. TLOSRs are evidently important in short segment reflux.

HRM demonstrated the loss of LOS tone, which occurred during the relaxation but also occurs during swallows, meaning it was not a totally reliable indicator for LOS relaxation; acid reflux was very similar in nature when using pH data as a TLOSR indicator, it too was therefore not as reliable as the SCJ locator probe.

96% of the time recording a signal strength of above 10 millivolts. During the valid magnet position periods, the magnet showed statistically significant correlation (p-value=0.001) with the fluoroscopic data with accuracy ±10 mm over 88.9% of the time.

It was noted that when recording the position of the clip using fluoroscopic data, that there would undoubtedly be some error induced into the output, as the clip was at times barely visible and ghosting effects caused movement artefact in the video which was manifested by a slight delay in movement, or blurring at relatively faster velocity of clip or probe movement. This ghosting has undoubtedly accounted for some of the difference in position measurement, which although appears to suggest the SCJ locator is not precise, actually means that the data merely shows the relative difference rather than the error of the SCJ locator itself. There could also be a

discrepancy between the two datasets, as the magnet clip moves and rotates on the mucosa; the clip which is barely visible may appear to move significantly, when the magnet which is close to the mucosa is not moving as much, thereby creating a difference between visually identified position and actual recorded position.

The second generation device uses two Hall effect sensors orientated perpendicular to each other to compensate for the directionality of the sensors; this showed much improved results when tested in vivo. The percentage of time the magnet was detected was improved over the initial generation (98%) and the percentage of time the signal strength was greater than 10 millivolts was also much improved, suggesting that the two sensor set up offered significant advantages.the distance between the sensors was also reduced, increasing accuracy of ±7mm The design and complexity of the second generation was however a limitation; the device was much more delicate and the number of studies performed with this iteration was much less, as the board and sensors were more fragile and would bread down after 15 to 20 in vivo tests. Although repairs were made, the design was an issue, with sensors becoming detached from the board at various places.

Having got promising data from the second generation of SCJ locators, it was decided that instead of producing more devices which were similarly weak and almost semi-disposable, as the cost per device was too great, the three dimensional concept would be redesigned using brand new sensors which had inbuilt three axis magnetic measurement. The sensors also used digital bus technology meaning that with multiple addresses available in I2C compatible devices, several devices could be attached to the same output, significantly reducing the number of solder connections to the FCB, which was a limitation of the previous generation. The device was designed initially on a rigid board which produced the confirmation that these ICs were sensitive enough to detect a magnet in vivo; the FCB board was then manufactured and assembled using precise industry based companies with the equipment and expertise to do so. The devices were tested on the bench again, to confirm that the device was capable of measuring the magnet, before being tested in vivo.

It is worth noting that throughout the three generations of devices, the signal strength is always significantly lower than that expected from the bench top experiments, suggesting that the orientation of the magnet is a significant factor in loss of magnet detection, working range and reliability, therefore the magnet size could be increased to a certain degree; a limit on size must be considered, as a large magnet may have a counterproductive effect on the function of the GOJ during magnet-clip attachment.

The validation data has been compiled into published literature, presented at the British Society of Gastroenterology in 2011 (Y. Y. Lee et al. 2011; Y.Y. Lee et al. 2011), and as a paper in the Medical Engineering and Physics Journal (Yeong Yeh Lee, Seenan, et al. 2012). After this validation, the device has since been used in several cutting edge studies, including accurately measuring TLOSRs for the first time. This research, published in the Journal of Neurogastroenterology and Motility (Y Y Lee et al. 2012)(Yeong Yeh Lee, Whiting, et al. 2012; YY Lee et al. 2012; Y Y Lee et al. 2012; Lee et al. 2013), expands on Pandolfino's paper (Pandolfino, Zhang, et al. 2006) which used fluoroscopy to intermediately measure the GOJ movements during TLOSRs, however fluoroscopic studies were limited to duration of recording with the X-ray based fluoroscopic devices, and had to rely on HRM to detect the onset of a TLOSR by loss of sphincter tone, inevitably missing the first few vital seconds of the GOJ movement; this also would have had position errors caused by the aforementioned ghosting. The SCJ locator probe developed here has undoubtedly allowed the first accurate recording of a full TLOSR due to the ability to continuously measure the SCJ position. The device was then used to classify the characteristics of a TLOSR and the extent of movement; this was briefly mentioned in Pandolfino's paper however there were many limitations to the method which meant that full recording was not performed and the number of transients recorded was significantly less than with the SCJ locator probe. The important highlights of this paper showed that the GOJ moved up 25 millimetres in most instances, however the proximal movement reached as much as 85 millimetres in one volunteer. The GOJ then returned to its original distal position, however the speed of GOJ restitution varied between subjects; this interesting finding, coupled with the manometric and SCJ locator data similarities between TLOSR-based SCJ movement and that of a hiatus hernia sparked the thought that TLOSR proximal movement and

frequency led to the development of a hiatus hernia. Research was performed using the SCJ locator investigated the similarities between the two phenomena (Lee et al. 2013; YY Lee et al. 2012) concluding that due to stretching of the Phreno-oesophageal ligaments with large TLOSR-based GOJ SCJ movement, a hiatus hernia was actually the progression of a severe, chronic relaxation of the LOS.

The improved reliability and simplicity of the third generation of SCJ locators now facilitates the investigation of the upper GI tract like never before; in addition to the slimline HRM, custom pH catheter and the addition of other GI tools such as Impedance catheters, significant contributions to the understanding of many diseases and motility disorders can be fully investigated continuously over long periods of time. The implementation of the SCJ locator removes the X-ray exposure health risk with fluoroscopy and allows safe recording as well as vastly reducing the labour intensive and time consuming data interpretation associated with the previous gold standard. The development of custom software which superimposes the squamocolumnar junction position onto accurate and drift-corrected high resolution manometric and pH colour plots enables for simple visual interpretation of a very complex and dynamic system with a large number of measured variables.

Chapter 3

High Resolution Manometry- calibration, drift and other error.

3.1 Introduction

3.1.1 Pressure sensors in medicine.

Pressure sensors are used widely throughout medicine, from manually measuring blood pressure to more sophisticated inter-arterial catheters. Specifically, capacitive sensors have been used in medicine for over a century, with Cremer using the catheter based technology to measure amphibian cardiac activity as early as 1907 (Abele 1989), and more recently to measure the oesophagus for digestive motility (Logan et al. 2002).

One such oesophageal motility measuring device is the SSI high resolution manometer (Formerly produced by Sierra Scientific Instruments, CA, USA, which was acquired by Given Imaging LTD, Yoqneam, Israel, in 2010) shown in full in figure 3.1, a relatively new technology used to detect pressure at a multitude of points in the oesophagus and stomach; based on solid state sensors (figure 3.2) rather than the more traditional perfusion systems it offers the advantage of being very simple to use and outputs the data as a easy to interpret colour contour plot. This device is used clinically over short periods to investigate a range of oesophageal motility abnormalities; these procedures can be performed for relatively short periods of time, approximately 20 minutes. Research studies have been performed using HRM for up to 2 hours, when accommodation and insertion/withdrawal are included, it is vital therefore that the device works as accurately for 20 minutes as it does for 2 hours. If the device is inaccurate or drifts over time, then both clinical and research outcomes may inaccurate for diagnostics and research output; it has been noted by colleagues that during tests of over an hour, the device has drifted significantly, despite staff following the manufacturer's calibration guidelines. To this end, the

accuracy and long term stability of multiple SSI high resolution manometers was tested. After an initial literature search, it was very unclear as to the technology used in these devices, so after more thorough tests, including investigating the manufacturer's website, press releases and finally patent a search, it was eventually found in the latter that the company had filed several patents detailing the use of capacitive sensors for high resolution manometry (Parks & Son 2005); this was different to the common assumption by Conkin et al. (Conklin et al. 2009) that the sensors were based on a strain gauge technology.

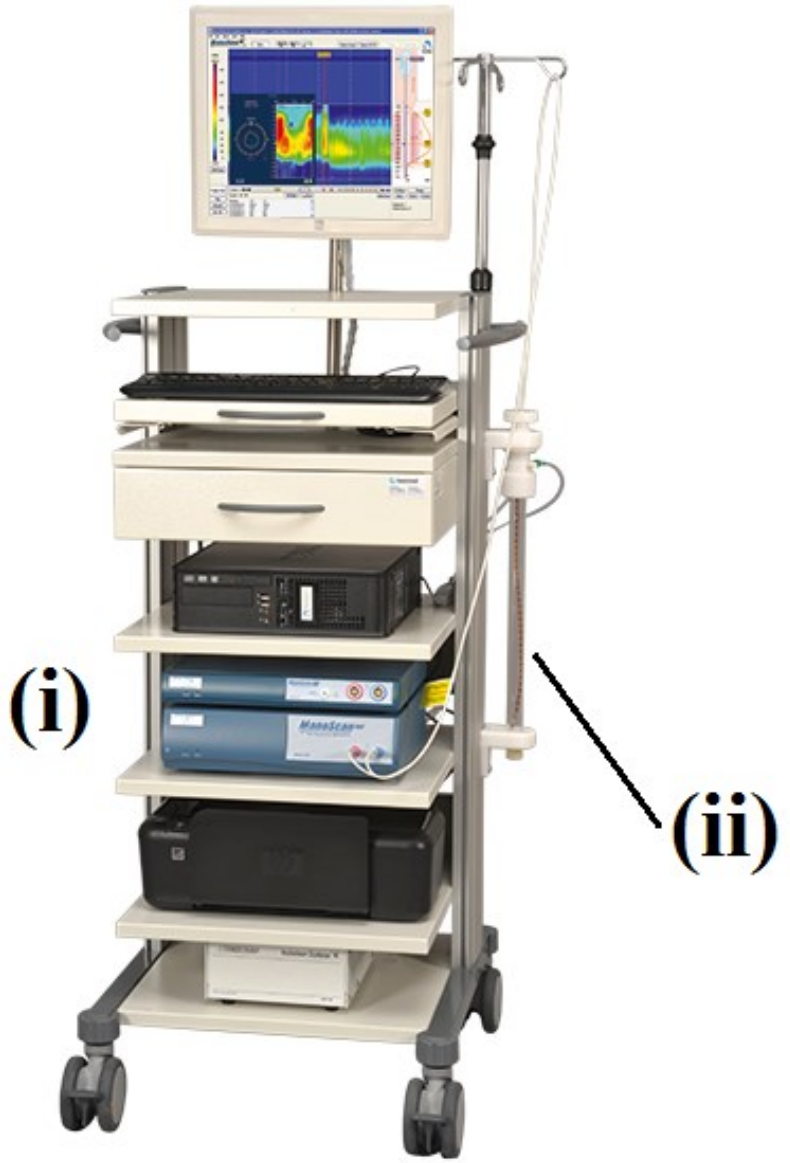

Figure 3.1 Manoscan HRM computer system (i) and pressure chamber (ii) system. (www.givenimaging.com)

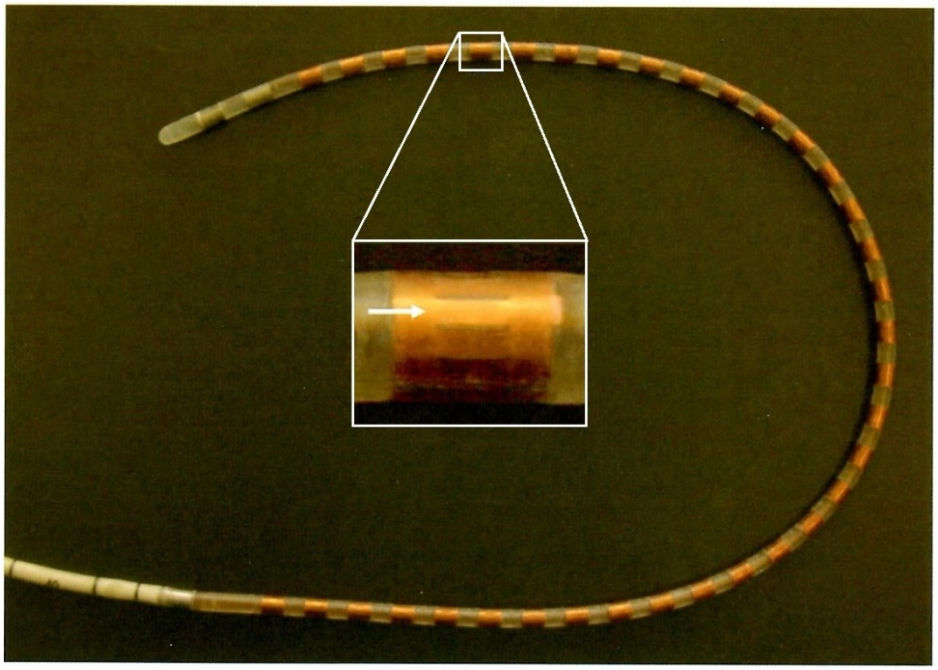

Figure 3.2 Illustrating the radial sensors (close up) in the catheter. (Conklin et al. 2009)

Although the Manoscan HRM is a system which is very widely used, there is little published work on performance validation. One study published in 2009 by Ayazi et al compared the ability of HRM system with the conventional pull through water perfusion system in the measuring of the lower oesophageal sphincter (Ayazi et al. 2009). The authors showed a significant difference in lower oesophageal sphincter variables between the two manometry devices, concluding that solid state HRM overestimates sphincter length and pressure; these comparative differences although interesting could arise from inaccuracies between tests rather than necessarily indicating a vast difference between accuracy, however it leads to the question of validity with the unvalidated Manoscan HRM system.

3.1.2 Capacitive sensors

Capacitive sensors are based on capacitive coupling, whereby two conducting plates placed either side of an insulating dielectric material, which can also be air, will hold a capacitance proportional to the surface area of the plates divided by the distance between the plates (equation 3.1).

$$C = \frac{A\,\varepsilon}{d} \tag{3.1}$$

Where C is Capacitance, A is the surface area of the plates, ε is the absolute permittivity of the dielectric material and d is the distance between the plates.

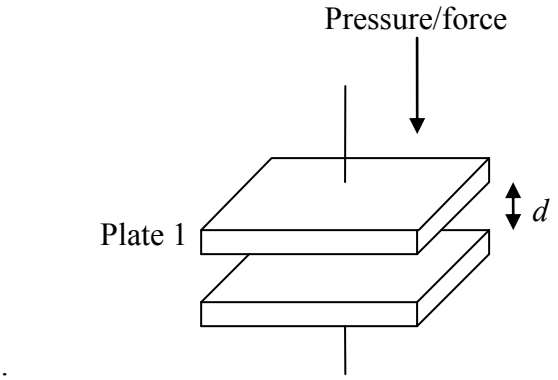

Figure 3.3 Geometry of a capacitive sensor

For a pressure sensor illustrated in figure 3.3, the distance between two plates varies with applied pressure, producing a change in capacitance which corresponds to the value of the applied pressure. The sensitivity of the sensor is defined as the proportion of capacitance change with a change in applied pressure, there are many sources and causes of error for capacitive sensors as discussed below. Offset error occurs when a constant value is added to the output value, effectively shifting the baseline and all other values. Temperature change is the main contributor to this error, which can be reduced by calibrating at the temperature in which the sensor is to be used.

All material exhibits expansion or contraction when exposed to a change in temperature, which may result in a physical change in gap size (Baxter 1996), as

well as change the conductive properties or dielectric permittivity ε, of the materials used in the sensor, which is yet another source of error. The accuracy of the SSI HRM is 2 mmHg peak to peak, meaning the sensor may vary by +/- 1 mmHg from the actual value, as stated in user guide.

The shape and planar geometry of the plates play important roles in the sensor's performance (Heerens 1986), the deformation due to pressure may warp the flat surface of the sensor, and the contour of deformation may be different for similar pressures, questioning the repeatability of a flexible plate capacitive sensor (Puers 1993). The deformable plate problem is highlighted in Figure 3.4, the fixed plate capacitive sensor shown in (a) will deform to the same gap d_2, where the deformed plate is very dependent on where the force is applied, which is illustrated in the difference between (b) and (c), given the same input pressure, p.

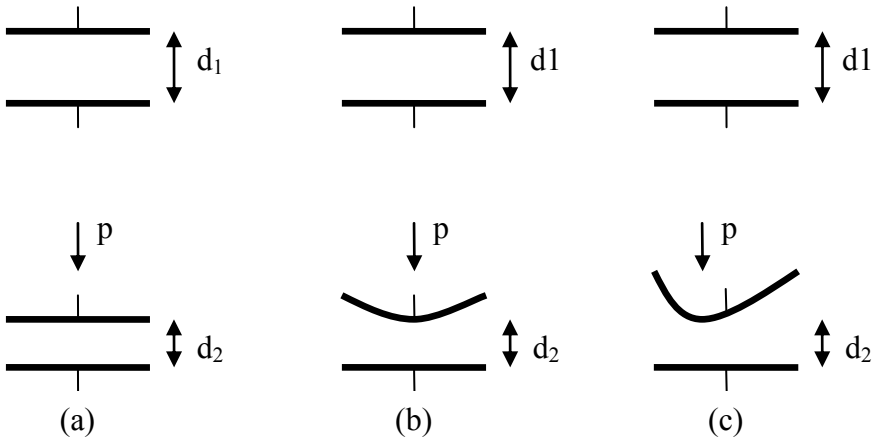

Figure 3.4 Rigid plate versus deformable plate capacitors (a) A rigid plate capacitive sensor and uniform deformation. (b) A deformable plate capacitive sensor deforming as expected. (c) A deformable plate capacitive sensor deforming not as expected.

Rigid plate capacitive sensors will deform uniformly and repeatably over time as a given force anywhere on the surface of the sensor will deform it equally; the deformable plate capacitive sensor is much less repeatable, as the distance and plate profile changes depending on where the force acts upon the plate (figure 3.4), meaning that a known force or pressure may produce a different output when tested

multiple times. Manufacturing tolerances and inhomogeneity in each sensor may lead to different sensors giving substantially different outputs for the same force. According to the device's patent (Parks & Son 2005), each sensing unit, located every centimetre uses several small sensors placed radially around the sensing unit; this will generally minimise the difference between each sensing unit as each sensing unit averages out the multiple sensors. The interpolation between each sensor is also inaccurate as the sensors have a certain width over which they measure, this will mean that measurements of several millimetres along the length of the probe are not accurate as they have been averaged out by each sensing unit. Creep is a physical phenomenon whereby a material may deform under the influence of stress, for example when an external pressure is applied. This may result in a measured change in pressure over time as experienced *in vivo*, leading to the observed drift. The sensors under higher pressure would tend to deform further. Material hysteresis, that is the material not returning to its original shape, may exaggerate this error. As the sensor is non-ideal, leakage current flows across the plates through the dielectric material over time, which causes gradual drift however this leakage is approximately linear.

Change in humidity within the probe and gradual ingress of dirt and other impurities in the probe itself will change the dielectric permeability, but the weekly thermal calibration will go some way to counteract this; as the probe should be hermetically sealed this should not be much of an issue, although wear and bending associated with use and cleaning, may over time cause micro-tears and deplete the hermeticity of the seal. The sensors used in SSI's high resolution manometer consist of several of the above sensors placed radially along the manometer's length as highlighted in figure 3.2

3.1.3 Temperature calibration compensation

As with all solid state transducer based systems, the Manoscan manometry probe (figure 3.2) is susceptible to thermal drift (figure 3.5) however the manufacturer includes some compensation for the change in temperature. This temperature

calibration is typically performed weekly in a fixed temperature water bath at 37 degree Celsius prior to use; this supports calibration relative to elevated temperatures and increased pressure environment of the body; this calibration is then applied automatically while the probe is in use at elevated temperature and withdrawn when the probe is removed from the body. While this calibration is included, it is minimal and only acts to zero the offset of each sensor at body temperature and atmospheric pressure and does not correct for a slow time dependent drift which occurs. This compensation is saved for the week and applied to the recorded data. Even though this may work for most clinical uses which last less than an hour but with the extended period of use within the research environment, the compensation method outlined above does not adequately compensate for drift. This has been noticed before by our research group during a research study when, once removed the manometer still displayed significantly high pressures of 40-60 mmHg despite being in air as observed by clinicians and demonstrated in figure 3.5; it was highlighted accidentally in a validation bench study where clinicians noticed that there was an evident and progressive pressure drift over an extended period of time. These pressures were very high, and often twice the expected LOS pressure; if the zero pressure value was higher than in vivo pressures, sphincter pressure could be incorrect by a significant amount demonstrating significant invalidity for any pressure measured using this device. Bench tests were then designed and performed in addition to an in-vivo experiment to determine the characteristics and more importantly the effect of this temperature drift on the practical use of this device within the medical community.

3.1.4 Consequences of uncompensated temperature drift

Within our research group, there is a need for extended periods of use of the solid state manometer which if the temperature drift is not compensated for adequately will leads to overestimation or a false positive error of sphincter pressure and sphincter length analysis by up to 60 mmHg for an hour study based on observations (figure 3.5); this is significantly important and has severe implications and

consequences for all clinical and research uses, as error in these measurements can lead to misdiagnosis or incorrect conclusions from research about the very functionality of the digestive system.

Tests were designed to determine the characteristics of the drift to establish if it was for example linear or if it settled over time, these are described below in the methods section 3.2. This experimentation also tested each sensor to establish inter and intra sensor variability and drift characteristics; following this experiment, compensation may be applicable if the drift is predictable or can be compensated for afterwards, promoting more accurate results.

It is clear from figure 3.5 that the high resolution manometer demonstrates a severe degree of thermal drift, up to 60mmHg overestimation after 2 hour of intubation; while the LOS pressure is typically 40 mmHg as previously stated, this could mean that diagnoses based on upper GI tract pressure profile, such as hiatus hernia or dysphagia, could be misdiagnosed. It can clearly be seen in a 2 hour study, after the extubation period, all pressures should be equal to atmospheric pressure and represented by the blue colour in the colour contour scale. However in some sensors the recorded atmospheric pressure is between 40 to 60mmHg represented by the green/yellow colour in the pressure scale. This discrepancy demonstrates the magnitude of baseline or thermal drift in a prolonged study; the potential for misinterpretation of HRM results is significant, when some sensors record atmospheric pressure as higher than that of the LOS. Although it is clear to see at the end of a study, many researchers or clinicians may be unaware of this error as they may ignore pressure recordings after extubation, this belief is supported by the omission of any such observations in HRM literature; the fear is that the error, while unknown among peers, may mean totally incorrect conclusions leading to inaccurate assumptions of the upper GI tract are being deduced on a daily basis.

The following sections document the result of collaborative investigation into the accuracy and time dependent drift properties of the Manoscan 360 high resolution manometry system. The experiments were designed and work undertaken with a research group in the Gastroenterology department at Gartnavel General Hospital under supervision of Professor Kenneth McColl of Glasgow University. Those

researchers involved included in no particular order: Elaine Robertson, Yeong Yeh Lee, Angela Wirz and Mohammed Derakhshan and Professor Kenneth McColl.

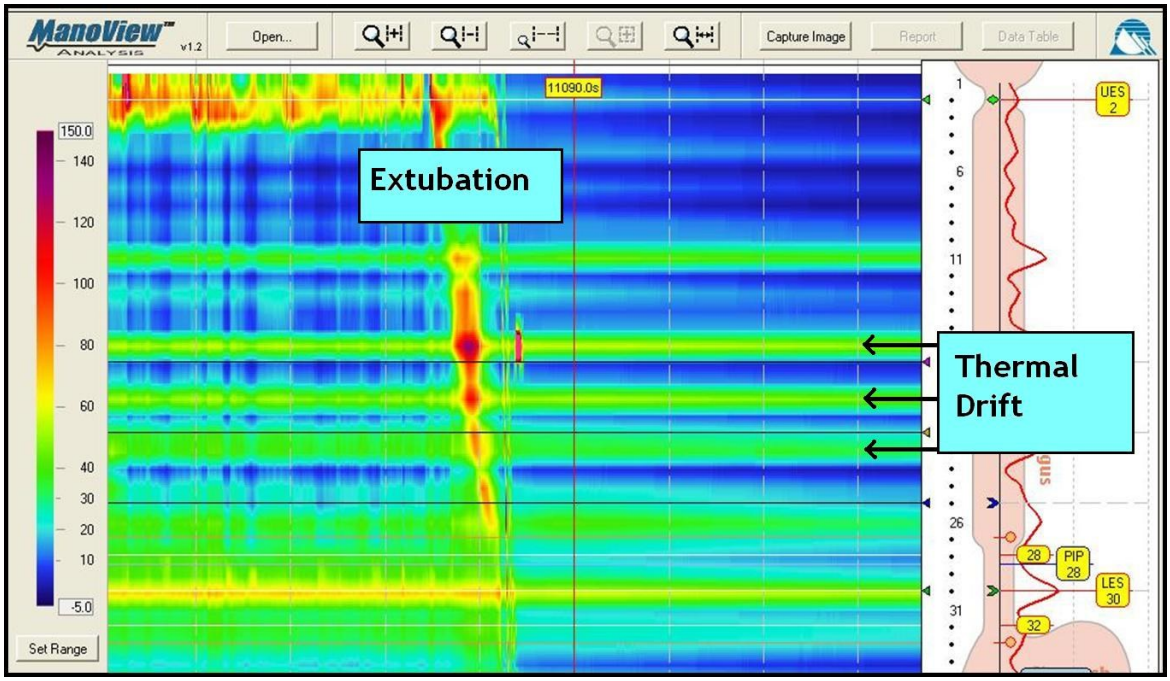

Figure 3.5 The high resolution manometry catheter data at the end of a study having been removed from the patient and held aloft, demonstrating post-study error. The colour contour plot describes the pressure along the probe (inside the upper GI tract). The Y-Axis represents the oesophagus, with the top at the upper oesophageal sphincter leading down to the stomach at the bottom. The X-axis represents time, and can be scaled for interpretation. After extubation the sensors are hanging freely in air, so should all display 0 mmHg (dark blue) but clearly some are still displaying pressures of up to 60 mmHg (yellow) some examples are indicated, therefore some sensors are displaying significantly incorrect large pressures meaning LOS, gastric and intra-sphincteric pressures could be wildly inaccurate.

3.2 Methods

3.2.1 Manometer in an aqueous environment at 37 degrees Celcius for over one hour

The manometer was calibrated for pressure as per the manufacture's protocol, which applies a multitude of fixed pressures from 0 mmHg to above any possible biological pressure via barometric chamber (figure 3.1.ii) during automatic calibration. A 2 litre column beaker was filled with warm water and immersed in a temperature controlled water bath (Grant Instruments, UK) (figure 3.6, left); this ensured the water was 37^{o}C throughout the experiment; when the temperature in the beaker had equalized with the surrounding water basin, the manometer was immersed into the beaker for a period of 1 hour. Before, during and after the submersion, the pressure was recorded using the associated Manoscan Acquisition software. Every 5 minutes the HRM was removed from the water and held still in the air without any contact to the sensors for 30 seconds before being re-inserted into the beaker; at the end of the study, the probe was held in this manner for 60 seconds, after which, the recording was ceased. Hydrostatic pressure for each sensor was calculated with respect to its depth and removed from the outputted data.

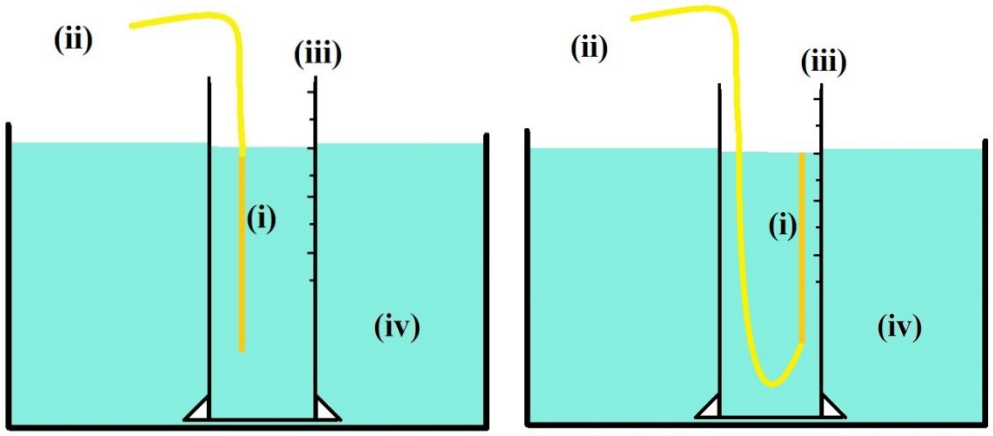

Figure 3.6 The manometer (i) submersed in a beaker of water (iii) in a temperature controlled water bath (iv)connected to the recording apparatus (ii). Left image shows the set up used in section 3.2.1 and the right image shows the set up used in section 3.2.2.

3.2.2 Manometer in an aqueous environment at 37^{o}C for over one hour with sensors in reversed position

This experiment was then repeated at a separate day with sensors in the reversed position; sensor 36 was now at the top and sensor 1 was at the bottom of the 40 cm long column beaker (figure 3.6, right). This reversed repetition was necessary because the sensors at the bottom were exposed to a higher hydrostatic pressure than those at the top of beaker (a pressure difference of 30mmHg due to the water column). By reversing these sensors would mean that all sensors were exposed to a similar hydrostatic pressure of 30mmHg and also allow comparison for different hydrostatic pressure between the top and the bottom of the beaker. Sensors in the body are exposed to different pressures, for example those that are subject to sphincter pressures of 30 mmHg or more for extended periods of time; it was useful therefore to investigate if the sensors experiencing higher prolonged pressure equal to that of the SCJ were subject to more drift. This experiment was performed as in section 3.2.1, only with the modification that the probe's tip was at the top of the water rather than at the bottom. Hydrostatic pressure for each sensor was calculated with respect to it's depth and removed from the outputted data.

3.2.3 Manometer in an aqueous environment at 37^{o}C for over four hours

To further understand the nature of the evident drift, a prolonged experiment was performed in a similar manner to the previous experiments, however the duration of catheter submersion for this experiment was for 4 hours, in upright condition (3.6, left). Hydrostatic pressure for each sensor was calculated with respect to its depth and removed from the outputted data.

3.2.4 The immediate effect of temperature change.

After the initial tests mentioned above, in order to fully understand the difference between each sensor when placed under the same pressure, the following test was performed. A shallow temperature controlled water bath (Grant Instruments, UK) was used without the inclusion of a column beaker. The experiment was designed to determine the initial effect of placing the probe from room temperature into body temperature

A water bath was set to 37 degrees Celsius, with a digital thermometer (HI 98509, Hanna Instruments RI, USA) added to ensure the temperature of the water bath, providing visual feedback which allowed the manual adjustment of the water bath's thermostat if the temperature fell or rose due to inaccuracies of the analogue temperature control of the whole water bath, the water bath was filled with a shallow volume of water of a height of 2 centimetres; the temperature was generally very constant after an initial adjustment. Pressure recordings were captured using of the Manoscan Acquisition software version 1. After manufacturer's calibration described in section 3.1.3, the probe was immediately held in air for a period of 60 seconds where it would measure atmospheric pressure at room temperature. The recording was continued, while the manometer was placed directly into the body temperature water bath where another 60 second recording was made. For each sensor, the difference between the pressure recorded at room temperature and body temperature of 37^{o}C was calculated. The associated hydrostatic pressure of 2cm water is 1.47 mmHg and this was subtracted from the measured pressure difference in air and water; the remaining pressure was therefore the direct result of warming the probe from room to body temperature. This experiment was repeated 6 times in order to average individual experiment error and to provide enough data for statistical analysis.

3.2.5 Measurement of a constant pressure at 37^{o}C and 20^{o}C.

In order to fully assess the stability of the baseline pressure with temperature and time, bench top experiments were designed and implemented. A temperature controlled water bath was prepared with water heated to and maintained at 37^{o}C; the depth of water was 10 centimetres, a pressure of approximately 7.4 mmHg. The HRM catheter was immersed in the water bath and secured in position. For each repetition the catheter was taped in the same position at the non-sensing section and all thirty six sensors were stationary and immersed in the water at the same water depth; there were 6 repetitions. Thereafter the catheter was left undisturbed for a two hour period whilst pressure recordings were captured using Manoscan Acquisition software version 1. Since the depth of water and catheter position remained constant, the pressure each individual sensor was exposed to was constant, therefore any change in measured pressure was interpreted as a change in the baseline of the sensor. This protocol was replicated but with the water bath heated to and maintained at room temperature of 20^{o}C, as it was suspected that the increased temperature of the human body may exacerbate any drift phenomenon. This experiment was repeated 6 times in order to remove individual experiment error and to provide enough data for analysis. The results are displayed in table 3.2.

3.2.6 Developing a thermal drift compensation algorithm

To investigate the manufacturer's thermal compensation procedure, measured pressures at the end of each two hour study were taken as the thermal compensation values for each sensor. These values are subtracted from the pressure readings taken at five minute intervals to produce corrected values. For each corrected pressure reading, the difference from zero was considered an error (eq 3.2).

$$error = p_{actual} - p_{measured} \tag{3.2}$$

After the drift shown in 1 hour experiments was observed as linear (figures 3.8 and 3.9) and had linear sections in the 4 hour experiments (figure 3.10), a correction algorithm was developed, as the manufacturer's algorithm appeared ineffective. Each sensor's beginning and end atmospheric pressure body temperature value was used to calculate a straight line graph or what should be zero mmHg; as the drift was linear, these lines very closely followed the drift, and using the graph's equation of an individual sensor, that sensor could be corrected at every time point using equation 3.3; this processing was performed using custom software developed by Dr Andy Kelman, a mathematics and software modelling researcher at the University of Glasgow, it also displayed the colour contour plot without any interpolation or colour smoothing between sensors, allowing for much more accurate diagrammatic representation. Later versions of this software superimposed pH and SCJ locator probe data for a complete graphical display of any Upper GI equipment used (figure 3.7).

$$p_{corrected} = (correction\ constant \times time) - measured\ pressure \quad (3.3)$$

Linear correction was applied to each of the 216 pressure time graphs tested, with deviation from zero considered an error. For the correction processes results for uncorrected and corrected data were compared for hypothetical studies of 15minutes, 30 minutes, 60 minutes and 120 minutes and analysed using the Mann-Whitney U test; this would highlight the importance and severity of error with given study lengths.

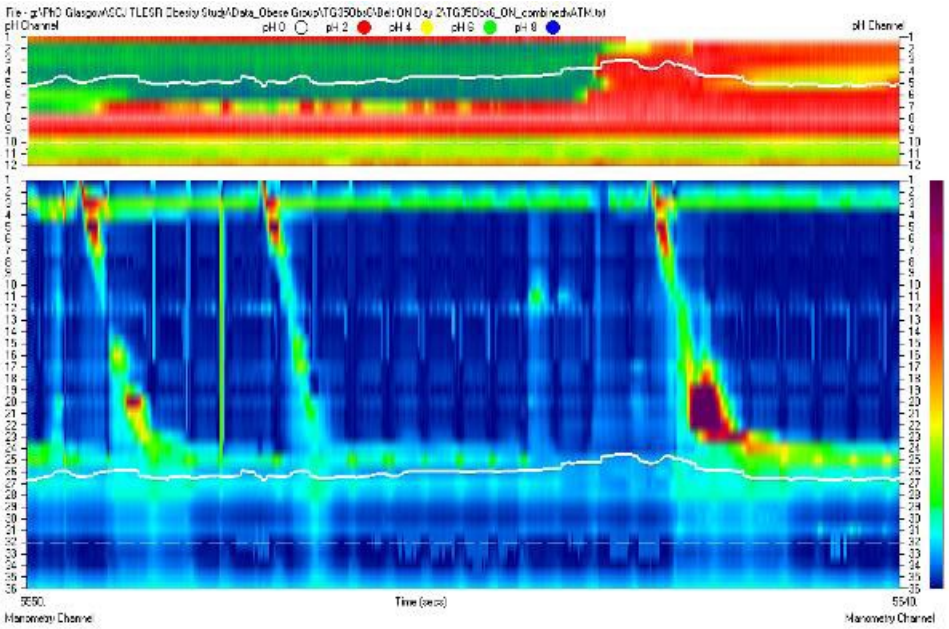

Figure 3.7 An example of colour contour plot using the custom software mentioned above. This output applied the linear correction. In addition to the correction, the software adds other data, if measured, such as pH and SCJ locator data. The thick white line represents SCJ position. The top colour plot is the pH data from a multi sensor pH probe and the bottom colour plot is the pressure topography profile.

3.2.7 *In Vivo* validation of thermal drift compensation algorithm

Our research group has access to three Manoscan HRM probes, and for the 6 *in vivo* studies a probe was chosen at blinded random, but with each probe being used twice and the probe number being noted by an independent member of staff.. For each study, the time point immediately after probe removal was selected when the probe was free of external pressure being held at the non-sensing section but still at body temperature in order to assess the accuracy of the earlier studies and investigate if there was any other factors influencing drift that could be accounted for in ex-vivo studies. Actual pressure values were recorded for each sensor and corrected as part of the post-study analysis. As part of the standard medical investigation protocol for prolonged studies using the HRM, pressures are recorded at conditions of 37^{o}C and no applied pressure at the start of each study prior to intubation. Based on the demonstrated linearity of the results of the previous bench top experiments, it was

hypothesised that the drift of the baseline during the in vivo study had also been linear. Interpolation and subsequent drift gradient calculation was therefore possible between the start and end values for each sensor within each. This gradient-based correction algorithm was developed and shown to be accurate in the bench top experiments, which is independent of study duration and allows comparison between in vivo studies of different length and with the bench top data. The cause of error could be inferred from this data, as drift varied from probe to probe, sensor to sensor and reported pressure both increased and decreased from the actual pressure measured.

While comparison was made between the probe used in the bench top experiments, and the same probe tested in vivo, each of the three probes were also compared to each other to determine the degree of inter-probe rather than inter-sensor variability; these results were summarised as median and inter quartile range and compared using Mann-Whitney U test in section 3.3.5.

Ethics approval covering Upper GI catheterisation for research purposes was granted by West Glasgow Research Ethics Committee, with REC references 07/S0709/98 and 10/S0704/40. The present author was not involved in the human trial testing, but was an invited observer and collaborated with device evaluation, design of tests, analysis of data and subsequent correction.

3.3 Results

3.3.1 Thermal drift investigation

During the initial three experiments, the manometer was exposed to a column of water, all sensors were exposed to a different hydrostatic pressure with sensors towards the bottom being exposed to higher pressures. In the 2 Litre column of water, the sensors at the bottom were exposed to a pressure comparable to that of the lower oesophageal sphincter, approximately 30mmHg. From experiment 1, all sensors appeared to demonstrate different pressure drifts independent from each other but all drifted in a linear fashion upward in the same direction, as shown in figure 3.8.

For clarification and consistency, sensors were numbered with the most distal sensor at the tip being 36 and the most proximal sensor labeled 1; the sensors in between are labeled in progression between these outer limits. This nomenclature is the same as that used by the Manoscan system, as displayed on the right hand side of the colour contour plot (figure 3.5). It appears that the error as calculated by equation 3.2, is similar and always positive. The error increases over time and appears linear (figure 3.8). It is also worth noting that, despite using the manufacturer's standard calibration in the pressure chamber, there is still an offset of up to 7 mmHg, which shouldn't be present if the sensors were properly zeroed. The offset ranged between 0 and 7; the offset seems to be greater with sensors towards the proximal portion of the probe. The last data point on each graph decreases, this is due to the removal of the sensor from water, however this return to room temperature should see the sensors returning to their original value; it does not. There is a trend to the sensors under more pressure, those at the bottom of the water column, to drift to a greater extent; the drift for sensors in the first 5 centimetres of water (sensors 1-5), drifted up to 6mmHg over an hour, while sensors in the deepest part (sensors 31-36), under 36 cm of water, drifted up to 11 mmHg. There was a large overlap between adjacent sensors however, which suggests that the variability between sensors is a larger factor in drift than pressure.

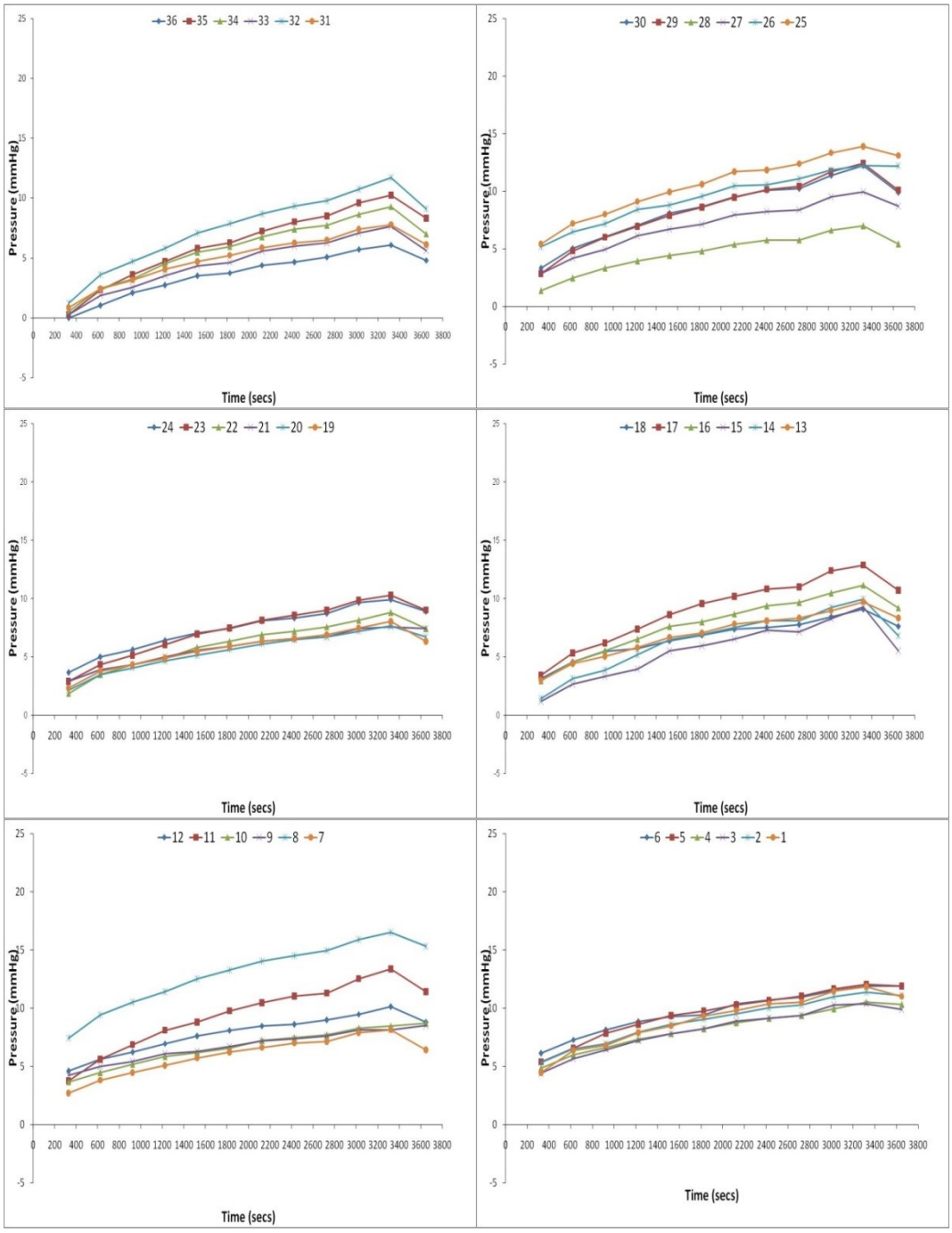

Figure 3.8 Intermittent pressure reading drifts over 1 hour at 37^{o}C for all 36 sensors of the manometer in an aqueous environment at body temperature; data shown is from an individual experiment. Each sensor was corrected for the hydrostatic pressure it was experiencing.

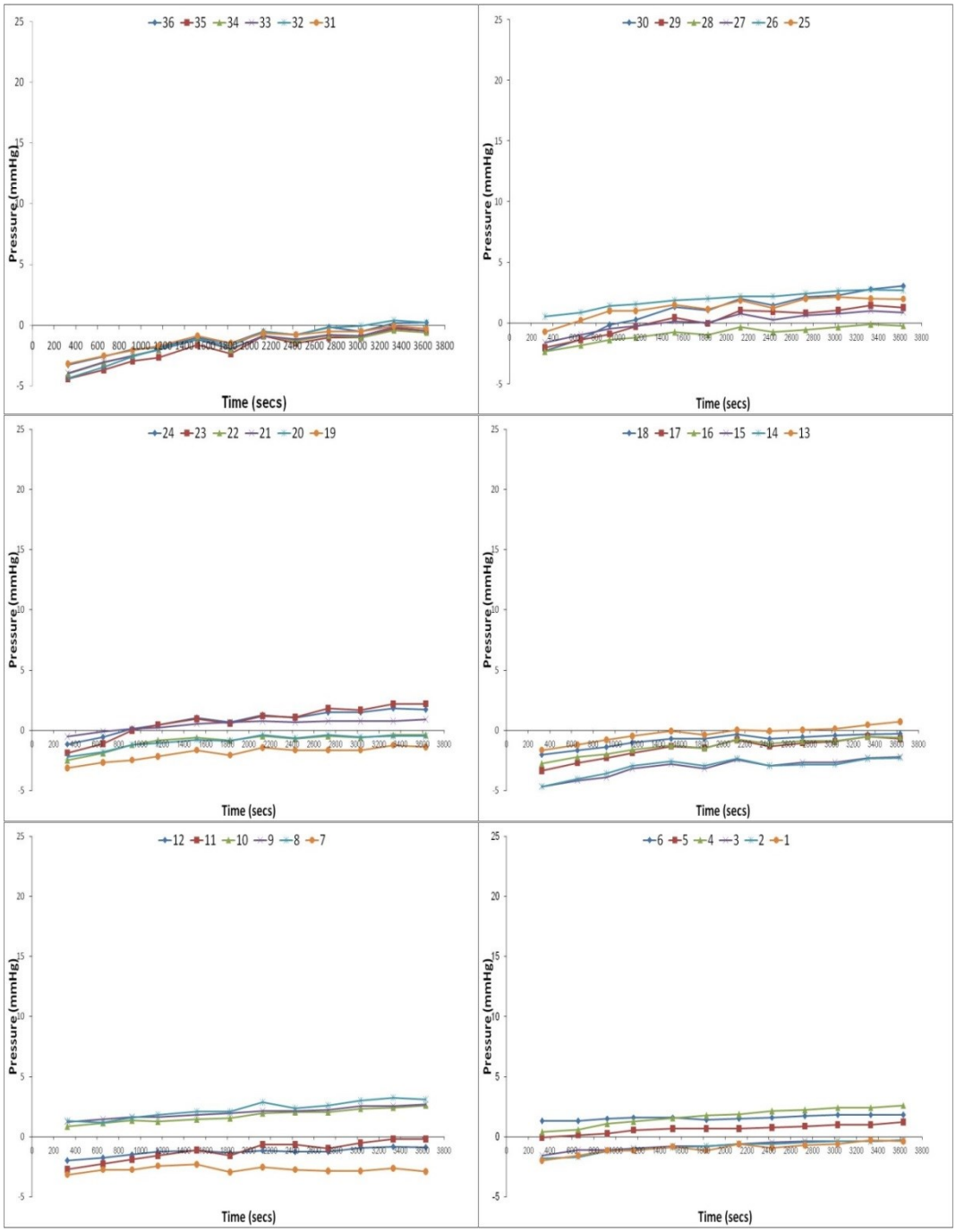

Figure 3.9 Intermittent pressure reading drifts over 1 hour at 37^{o}C for all 36 sensors of the manometer in an aqueous environment at body temperature; data shown is from an individual experiment. Each sensor was corrected for the hydrostatic pressure it was experiencing.

The trend for drift when the sensors were placed upside down in the water column is positive, however the drift is noticeably less and occasionally negative. The error range was between -1mmHg and 3mmHg. When removing the probe from water there was very little decrease in pressure, possibly due to the lack of drift. It is worth noting that the offset is between -5mmHg and 2mmHg; this is the same magnitude and therefore precision, as with the previous test however the accuracy is better. The manufacturer's calibration is performed at weekly intervals and had been performed 2 days prior to this test, whereas the test performed with the sensors the right way up (section 3.3.1.1) was performed 6 days after the manufacturer's calibration. This suggests that while the manufacturer's calibration compensates drift to a certain degree, by zeroing the sensors, it becomes less accurate over a number of days and that it is not performed often enough.

The drift over 4 hours is significant to the point that sphincter pressure is present on sensors who have very little pressure; potentially leading to total misdiagnoses. The offset is at most 2mmHg as manufacture's calibration had been performed several hours before this experiment was performed. The range between sensors had expanded significantly after 4 hours, up to 9mmHg difference between the most and least drifted sensors. An artefact had occurred to sensor 1 after 8000 seconds resulting in a significant jump in pressure; while it was not know what caused this error, the probe was sent to the manufacturer who explained the sensor was faulty and needed to replace it. It highlights the possibility of sensors to significantly change pressure without the software drawing attention to it. The research group experiences faulty sensors at a rate of 1-2 a year and while this sensor is unlikely to cause misdiagnosis based on its position, a more positionally important sensor could cause misdiagnosis or require repetition of the procedure at a later date and require fixing at a cost of several hundred pounds per sensor malfunction. After the probe was removed from the water bath at the end of the study, there was no decrease in pressure. Even though the manufacturer's calibration procedure had been performed hours before, this experiment highlights the drift still occurring over long periods. Even after an hour, almost all sensors had drifted by 5mmHg.

Manometric data for each of these experiments was exported from the Manoview Acquisition software in raw ASCII text format and plotted in Microsoft Excel; statistical processing was performed in SPSS software (IBM, USA), this allowed the analysis the drift and attempt to derive and apply a correction. All data from the studies were subject to the manufacturer's in vivo calibration process but not to any additional correction other than those mentioned.

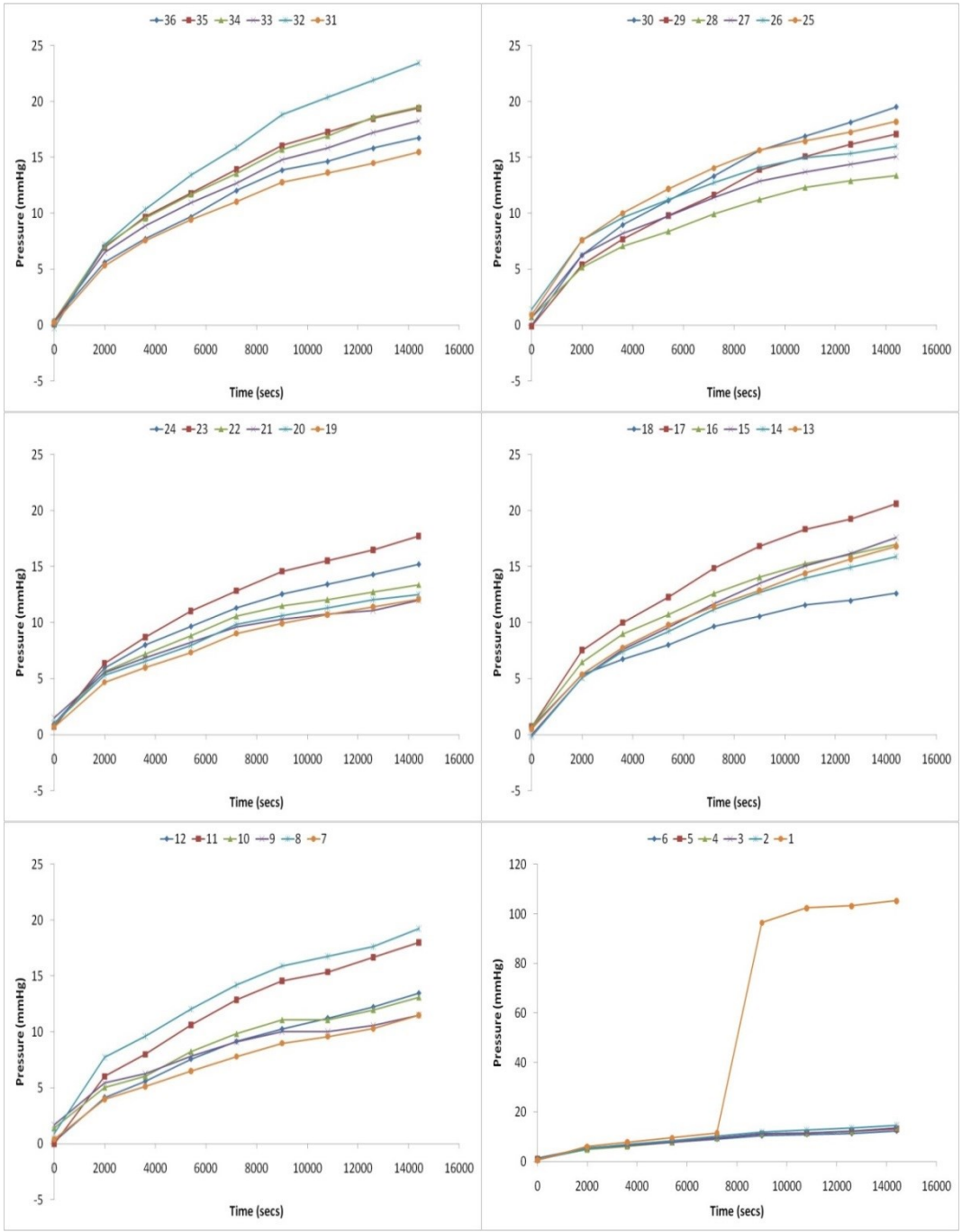

Figure 3.10 Pressure reading drifts over 4 hours at 37^{o}C for all 36 channels of the manometer in an aqueous environment at body temperature; data shown is from an individual experiment. Each sensor was corrected for the hydrostatic pressure it was experiencing.

3.3.2 The Immediate Effect of Temperature Change

The immediate response to the temperature change for each sensor was summarised as a median pressure error (table 3.1), comparison was drawn between sensors with the Kruskall-Wallis test for non-parametric data. The magnitude of any drift-like effect of temperature with time was calculated as the difference between the last recorded pressure for each sensor and the pressure recorded at 60 seconds into the experiment. The 60 second values were taken rather than zero to differentiate from the initial temperature effect. Pressure change was calculated as a median for each sensor and sensor characteristics were compared using the Kruskall-Wallis test. Results for the difference between room and body temperatures tested were compared using a Mann-Whitney U test.

To establish the nature of a prolonged pressure change with time, pressure was plotted on the y axis in mmHg against time on the x axis at five minute intervals. For six experiments with thirty-six sensors this process produced 216 graphs for each temperature tested. Each graph was analysed by linear regression to ascertain the association between pressure and time for each temperature.

As shown in figure 3.11, the variability for each sensor is very small; from 6 repetitions, the spread of response for an individual sensor is small, suggesting that each sensor's immediate response to change in pressure is repeatable and predictable. There is a large variability between sensors (table 3.1, figure 3.11), while some sensors demonstrated a decrease in pressure, almost all of the sensors showed an increase between 5 and 10 mmHg. The median immediate pressure change for all 36 sensors was 7.0mmHg (IQR 3.8), there was a large and statistically significant variability between sensors ($P \leq 0.0001$); the inter-sensor range was -3.3 to +9.9mmHg.

Table 3.1 Median pressure error due to immediate temperature change

Sensor number	36	35	34	33	32	31	30	29	28	27	26	25
immediate pressure change (mmHg)	8.5	8.5	9.9	4.1	8.1	3.4	8.9	9.3	6.7	7.2	7.3	7.4
Sensor number	24	23	22	21	20	19	18	17	16	15	14	13
immediate pressure change (mmHg)	6.2	5.8	7.5	9	5.9	2.8	5.9	2.9	4.7	-3	-0	8.2
Sensor number	12	11	10	9	8	7	6	5	4	3	2	1
immediate pressure change (mmHg)	6.8	2.2	-2	6.2	8.6	8.3	4.9	5	8.7	8.5	7.5	9.2

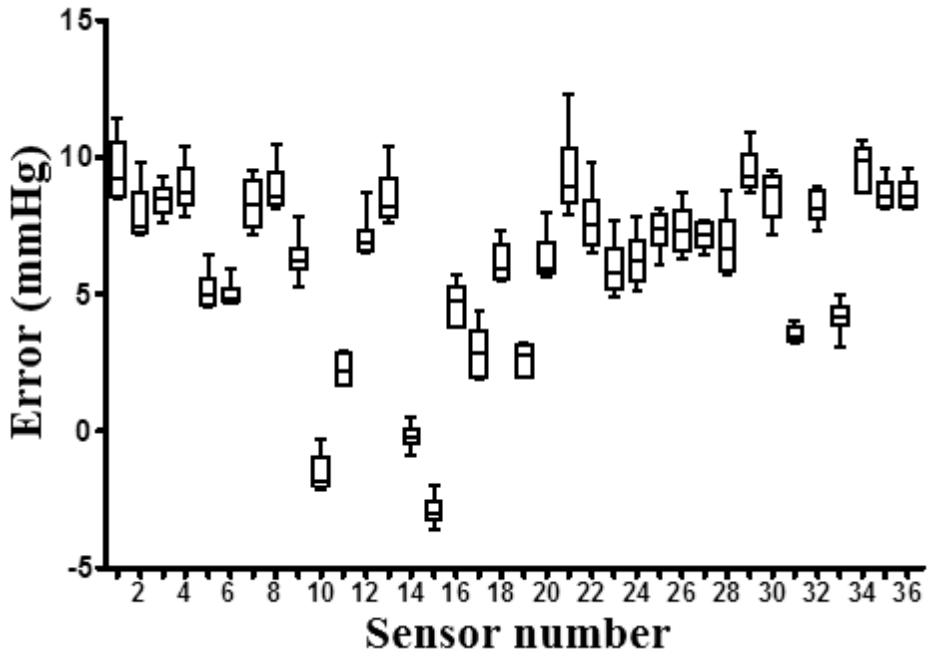

Figure 3.11 The median immediate pressure response of thirty-six sensors exposed to a temperature of 37^{o}C when repeated 6 times.

3.3.3 Measurement of a constant pressure at 37°C and 20°C.

For this two hour experiment performed at body temperature, the median pressure change between the beginning and end values was 11.1mmHg (IQR 9.9mmHg). The magnitude of the effect varied among sensors with a range of 3.0mmHg to 33.2mmHg. (p=<0.0001) (Figure 3.12) For an individual sensor there was variation in the degree of pressure between studies (Table 3.1). With the water temperature maintained at room temperature (20°C) rather than 37°C, there was still a noticeable increase in median pressure at 4.8mmHg overall (IQR 4.8mmHg), however the magnitude of this change was significantly less than at body temperature (p= <0.0001). Each of the 216 pressure versus time graphs obtained at body temperature was inspected to verify the pressure and time correlation. Thirty-six example pressure time graphs are shown in (Figure 3.13), for a certain sensor within a given experiment the change in measured pressure was linear. The R-squared value was calculated for each of 216 pressure-time graphs; in all of which R-squared was over 0.85.

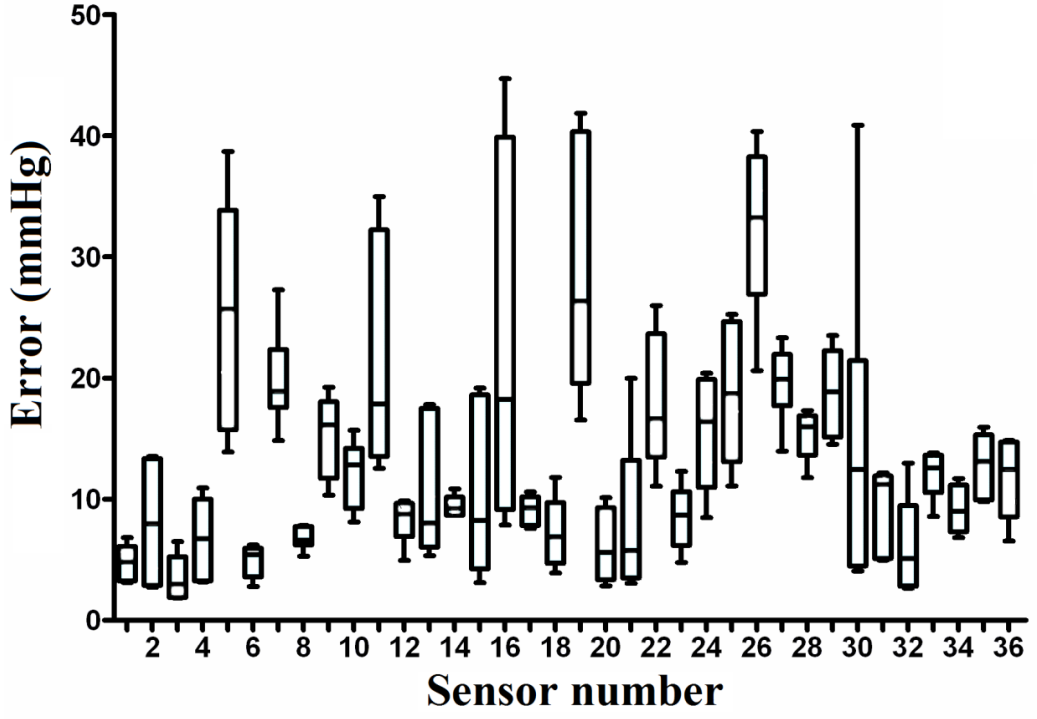

Figure 3.12 The magnitude of pressure change at 37°C after two hours for each sensor following removal of the immediate temperature effect.

Table 3.2 Comparison of median pressure error at 20°C and 37°C after 2 hours.

Sensor number	**36**	**35**	**34**	**33**	**32**	**31**	**30**	**29**	**28**	**27**	**26**	**25**
Pressure Drift (37°C)	12	13	9	13	5	11	12	19	16	20	33	19
Pressure Drift (20°C)	5.6	5.6	4.3	4.2	3	3.1	3.7	5.3	4.9	5.9	9	5.7
Sensor Number	**24**	**23**	**22**	**21**	**20**	**19**	**18**	**17**	**16**	**15**	**14**	**13**
Pressure Drift (37°C)	16	8.7	17	5.8	6	26	6.9	9.3	18	8.3	9.2	8
Pressure Drift (20°C)	4.6	2.5	6.2	2.1	2	9.8	3.7	5	7.9	4	4.5	3
Sensor Number	**12**	**11**	**10**	**9**	**8**	**7**	**6**	**5**	**4**	**3**	**2**	**1**
Pressure Drift (37°C)	8.8	18	13	16	7	19	5.4	26	6.7	2.9	8	4.8
Pressure Drift (20°C)	4.1	6.6	5	4.3	4	3.9	3.1	5.2	4.5	2.9	5.3	3.2

Table 3.2 shows that drift is emphasised by the sensors being at body temperature rather than room temperature in 35 out of 36 sensors, with the remaining sensor's drift being the same at both temperatures. The median difference between the errors was 7.15mmHg; one instance of 24.2 mmHg difference between drifts at 37 and 20 degrees Celsius was observed, highlighting the severity of drift inside the body rather than at room temperature where calibration occurs.

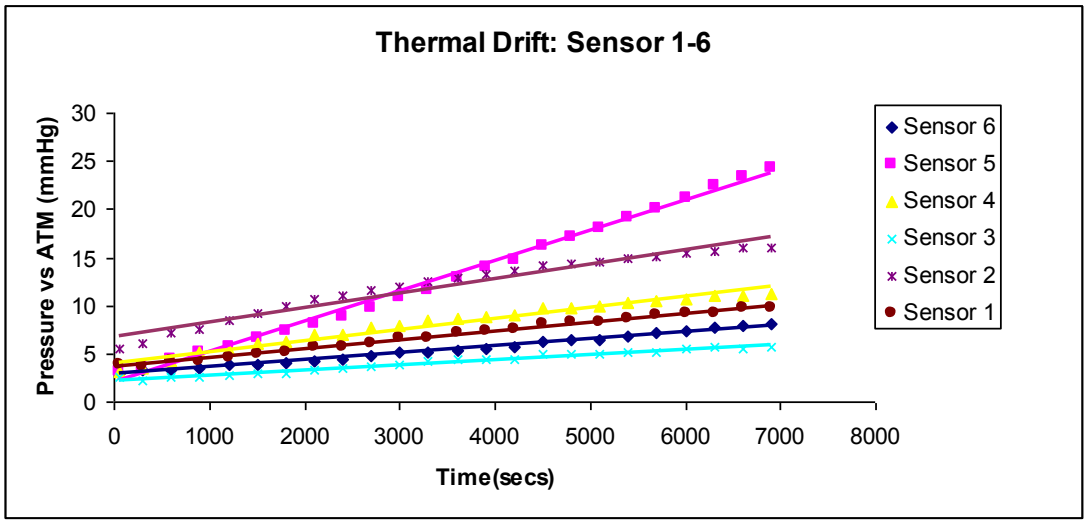
Thermal Drift: Sensor 1-6
Pressure vs ATM (mmHg)
0
5
10
15
20
25
30
0
1000
2000
3000
4000
5000
6000
7000
8000
Time(secs)
Sensor 6
Sensor 5
Sensor 4
Sensor 3
Sensor 2
Sensor 1

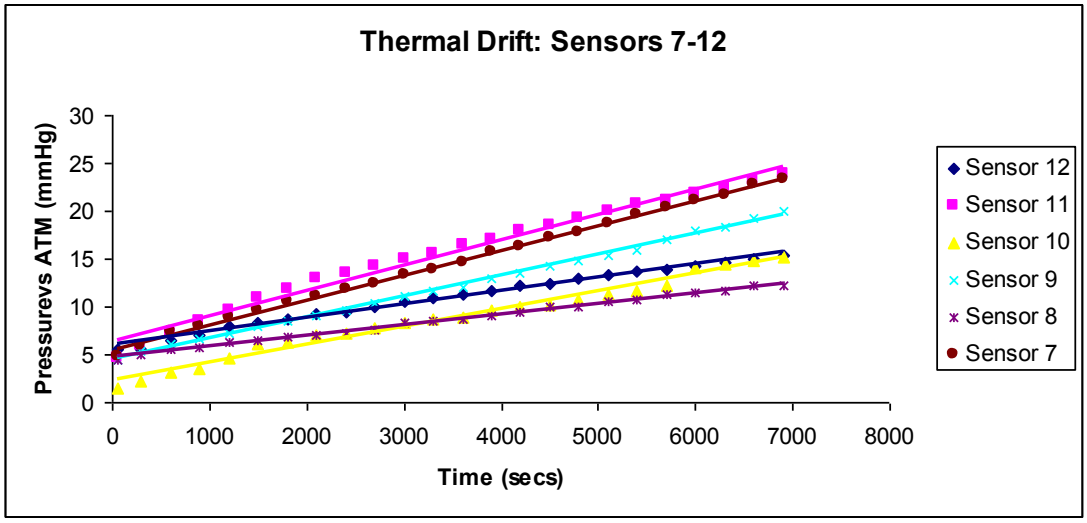
Thermal Drift: Sensors 7-12
Pressurevs ATM (mmHg)
0
5
10
15
20
25
30
0
1000
2000
3000
4000
5000
6000
7000
8000
Time (secs)
Sensor 12
Sensor 11
Sensor 10
Sensor 9
Sensor 8
Sensor 7

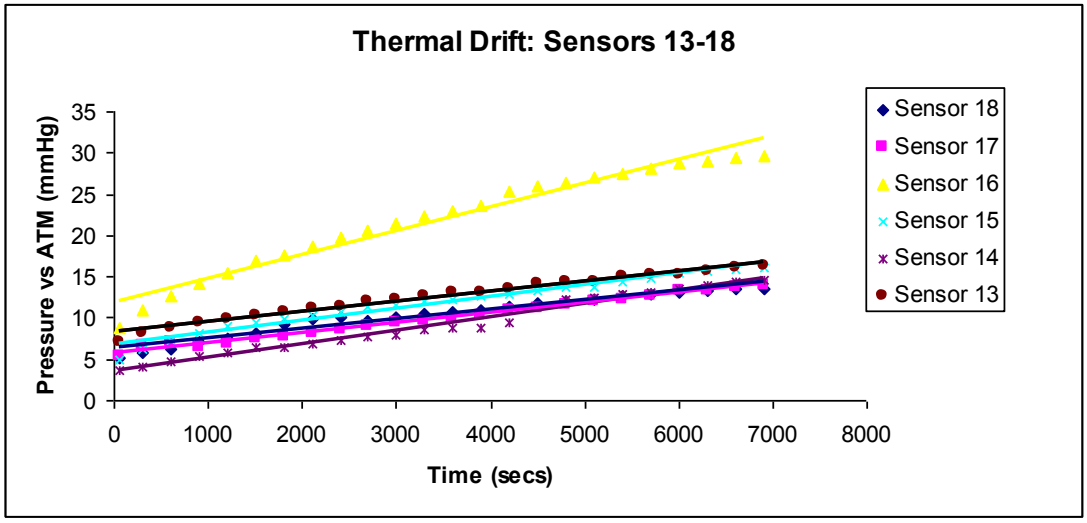
Thermal Drift: Sensors 13-18
Pressure vs ATM (mmHg)
0
5
10
15
20
25
30
35
0
1000
2000
3000
4000
5000
6000
7000
8000
Time (secs)
Sensor 18
Sensor 17
Sensor 16
Sensor 15
Sensor 14
Sensor 13

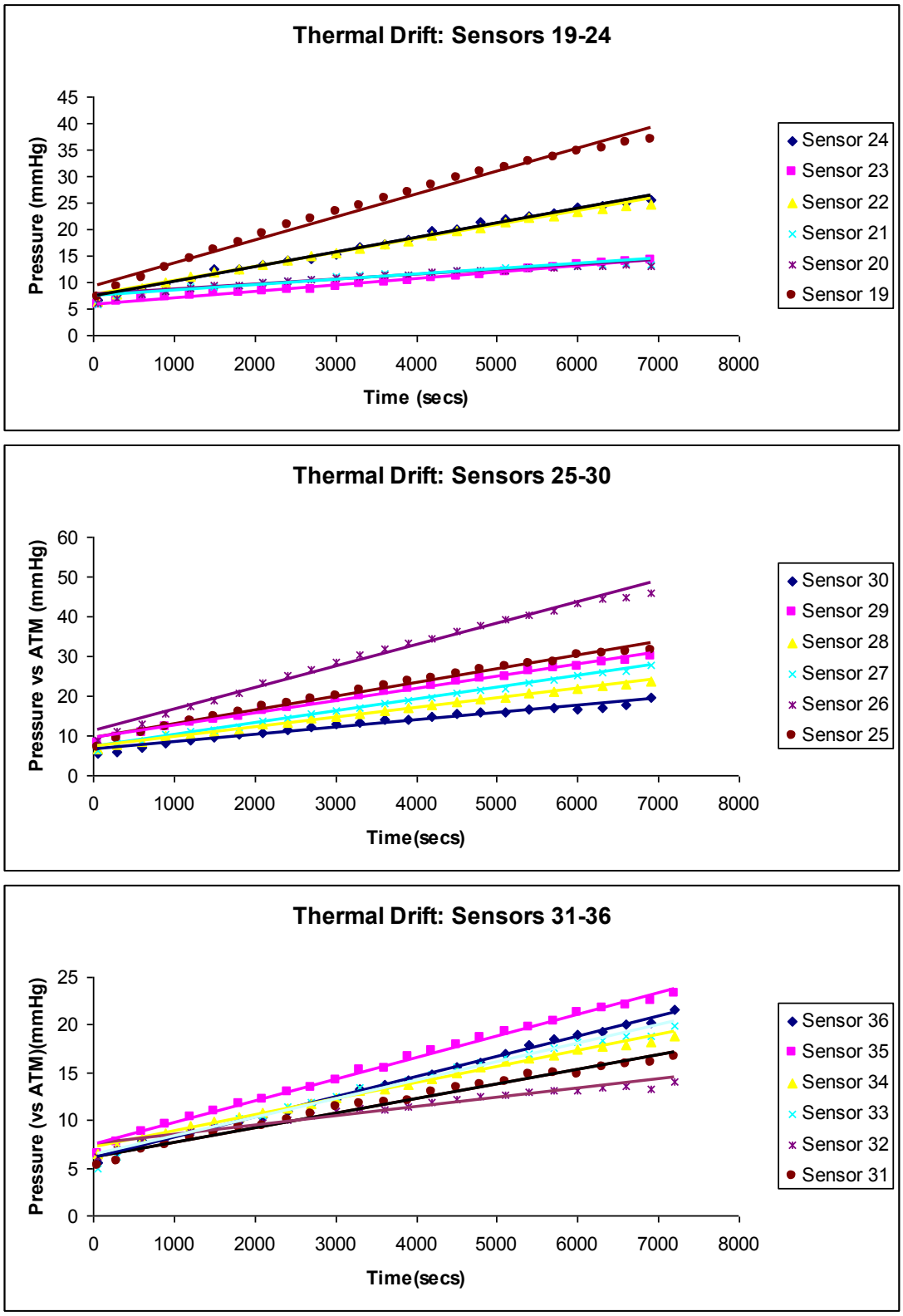

Figure 3.13 Pressure change over a period of 2 hours from a single experiment charting all 36 sensors. This demonstrates the drift effect over a period of 2 hours, trend lines are added to each sensor, highlighting the linearity of drift over time.

3.3.4 Developing a thermal drift compensation algorithm

For data corrected by the manufacturer's thermal compensation method (detailed in section 3.1.3) the error varied by study duration. At fifteen minutes into the study the median error for all thirty-six sensors was 1.2mmHg (IQR 1.2mmHg at thirty and sixty minutes were 2.9mmHg (IQR 2.5mmHg) and 5.4mmHg (IQR 5.2mmHg) respectively. The error with study duration is shown in Figure 3.14.

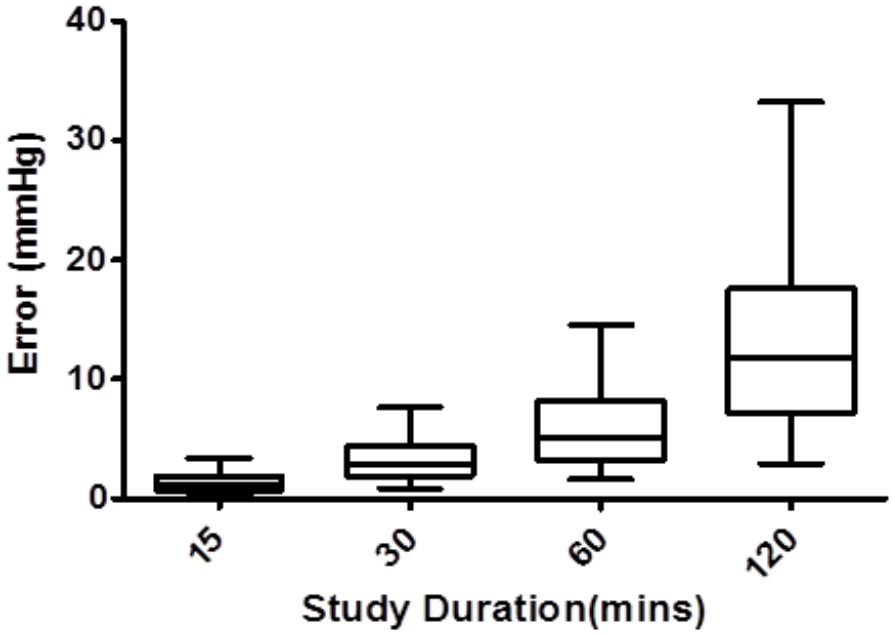

Figure 3.14 Median error of all 36 sensors when using the manufacturer's calibration method with respect to time.

3.3.1. *In Vivo* validation of thermal drift compensation algorithm

After application of our suggested linear correction, as described by equation 3.3, the median error for a 15 minute study was 0.2mmHg (IQR 0.3mmHg). For a thirty and sixty minute study median error was 0.2mmHg (IQR 0.2mmHg) and 0.3 (IQR 0.4mmHg) respectively. The error was compared for the manufacturer's and linear correction and the differences were highly significant with P values of <0.0001 for all study durations tested. (Figure 3.15). The median line gradient for probe A was 0.10mmHg/min (IQR 0.08) equating to a baseline drift of 12.0mmHg in two hours. For probe B and c gradients were 0.05mmHg/min (IQR 0.05) and 0.10mmHg/min

(IQR 0.06) respectively. The median line gradient for probe A on the bench top was 0.10mmHg/min (IQR 0.09) which was not significantly different from the in vivo gradient. (p=0.91) For individual sensors in vivo there was considerable variability in the extent of baseline drift indicated by variation in line gradients (p=<0.0001), however this did not appear exaggerated in sensors exposed to the high pressures of upper and lower oesophageal sphincters (Figure 3.14). In vivo probe behaviour was similar between probe A and probe C. (p=0.71) Probe B showed significantly less drift than either of the other two probes. (p=0.0001) (Figure 3.16).

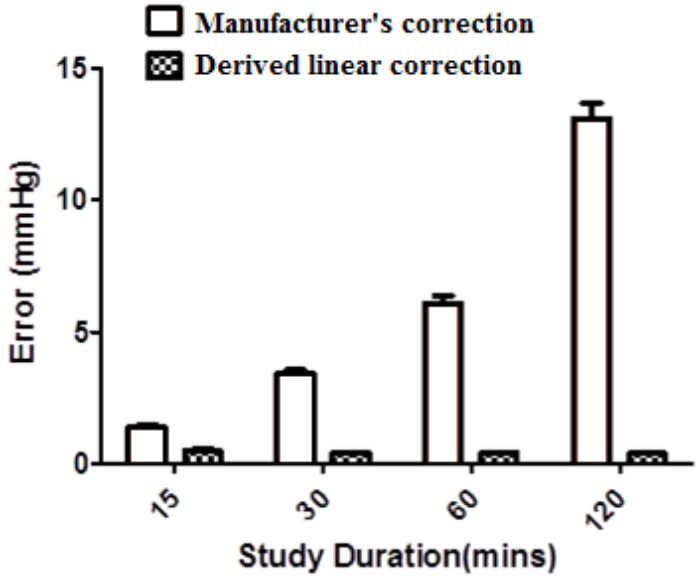

Figure 3.15 Comparison of residual error after linear and standard correction.

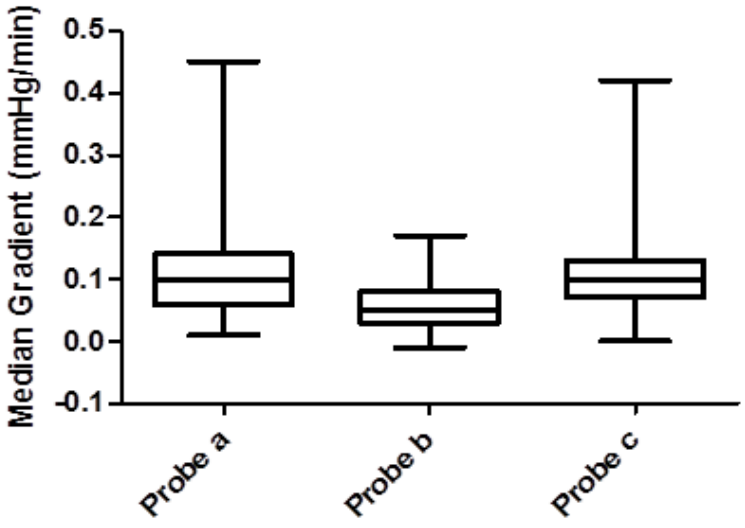

Figure 3.16 Comparison of median, inter-quartile range and range for each probe tested in vivo.

3.4 Discussion

3.4.1 Thermal drift investigation

In experiment 1, the small but visible differences from linearity may be due to water temperature fluctuations, as the water basin was accurate to several degrees and the water close to the heating and sensing element was more accurate than the water farther away, this may be the same for other experiments performed in this manner. The drop of pressure for each sensor at the end of the experiment shows the atmospheric pressure (figure 3.8), this is higher than that at beginning and shows the severe extent of drift with this device. There is an initial difference for each sensor despite the recent calibration, this may be due to the hydrostatic correction to some extent, however there is a similar phenomenon in experiments where each sensor is experiencing the same hydrostatic pressure, yet there still appears to be an initial difference; this suggests that even when calibrated as suggested by the manufacturer, some degree of error remains; observed as high as 7mmHg, the effect is worsened with increasing time from manufacturer's calibration. While the manufacturer's calibration correction is performed weekly, in situations where it is not performed weekly, the offset error may be even higher; as a LOS pressure step up is defined as 2mmHg, this could produce an significant error in measurement of LOS length.

The negative initial pressure in figure 3.9 may be due to the hydrostatic correction, as it appears to be consistent in this experiment and appears to show the opposite of figure 3.9, when the device was placed upside down in the column beaker. An alternative explanation could be that the experiment in figure 3.9 was performed less time after the manufacturer's calibration, therefore increasing accuracy while not affecting precision of the pressure measurements. In both experiments, the direction of the drift is positive.

Figure 3.10 again shows a constant and positive drift however the drift appears linear initially, but after a number of hours, starts to flatten out, suggesting that the drift is not linear during extended studies. This initial finding could be mean that an

extended study may not be correctable if the drift varies from linear; however further experiments will investigate this phenomenon. The Manoscan device was on and powered up and recording for several hours before the test, so it is highly unlikely that the electronics were warming up to a stable temperature. The drift could be limited by capacitance leakage or voltage limitations in the hardware. It is evident that staggering drift occurs where after 4 hours, there is up to a 23 mmHg difference in one sensor from start to finish; this poses a significant issue when measuring the SCJ which could be as low as 20mmHg. One sensor appears to malfunction mid study, which although is uncommon, does occur and requires maintenance by the manufacturer; it is unclear why such malfunctions occur as the manufacturer offer little feedback as to the source of error.

3.4.2 The Immediate Effect of Temperature Change

The initial or immediate thermal effect varies between sensors although for a given sensor is consistent. The sensors employed in this technology use capacitive sensing (Parks & Son 2005) which measures the change in distance between two opposed sensing plates caused by applied pressure. Change in temperature can affect the properties of the metal plates or of the material in the intervening space and reset the baseline (Puers 1993; Baxter 1996).

The area of the sensing plates is fixed, this in turn means that the spacing between the plates, d, would have to change. Since this is how the sensor responds to pressure, with d changing under pressure, this will be read as a capacitance proportionate to pressure change and should be of the order of a few millimetres of mercury (mmHg). The observed error is termed ‘offset’ and is likely to underlie the observed immediate thermal effect. The immediate behaviour of an individual sensor when exposed to a temperature of 37oC is reproducible shown by a narrow range in Figure 3.11. This means that the standard ‘in vivo compensation’ process performed weekly is likely to encounter similar values and correct the data appropriately. Therefore based on our findings thermal effect is likely to be well compensated in the current operation of the system.

The baseline drift is best understood as a progressive upward change of the baseline or zero pressure with time. This effect varies markedly between sensors (inter-sensor variability) and for a given sensor between experiments (intra-sensor variability). For a given sensor within an experiment the effect is highly linear. Capacitive sensors are liable to 'current leakage' which may contribute to this observed phenomenon. In this process current flows from one sensing plate to another via the intervening material (Baxter 1996). Over time this can produce a change in the output and may produce a linear drift in the baseline; Also, the sensors' amplifier circuit and interface circuitry could be a source of drift, showing the constant rise/baseline drift..

This could be because the amplifiers power supply drifts, causing a proportional drift. Also the internal amplifier circuit may be liable to drift due to ambient temperature changes around the amplifier or due to differences in heat dissipation (Bonnelycke 1972).

3.4.3 Measurement of a constant pressure at 37^{o}C and 20^{o}C

The extended room temperature experiment shows a baseline drift of all sensors (figure 3.12) which may be due to the aforementioned creep and capacitive leakage. The initial pressure change in the room temp to body temp can be explained by an increase in the offset error as a direct result of the dielectric permeability changes and plate expansion or contraction which changes the capacitance. The increased drift exhibited when a probe calibrated at room temperature is exposed to pressures at body temperature (table 3.2) (in the water bath), is the result of the combined initial thermal offset (figure 3.11) and the steady baseline drift (figures 3.8, 3.9, 3.10) showing an exaggerated thermal drift (figure 3.13).

3.4.4 Developing a thermal drift compensation algorithm

As the observed error is linear throughout the extent of a 2 hour pressure measurement (figure 3.13) it is possible to correct for this error by measuring the gradient of drift for each sensor, and correcting for drift at any point in time by using

the gradient and initial offset and correcting each point in time for each sensor; although this takes time to process as well as certain requirements before and after experiments. It is obvious from figure 3.15 that the error is significantly reduced and does not increase with time, unlike with the manufacturer's standard correction. It was expected to see from the study that some sensors near high pressure zones show greater drift, demonstrating a higher creep based drift from the sensors under higher pressure, however this was not so. There is also a difference between the Manoview Acquisition and Analysis software, so real-time and post analysis can provide different results, as the Analysis software interpolates between the sensors, meaning the graphical plot which although looks near, is actually misrepresenting the data which can lead to incorrect analysis, research conclusion or diagnosis.

While the company provide a thermal compensation on request, it merely removes the initial thermal offset. To correct for the ongoing thermal drift however, we suggest employing the linear gradient correction method as discussed in section 3.2.4, using equation 3.3 applied to all datapoints, in studies more than 15 minutes; the error using standard correction and the new linear correction are compared in Figure 3.15, even though for a 15 minute study the error is still higher using the standard correction, it may be acceptably low, especially when remembering the complexity of taking the required pre and post pressure measurements and then applying the correction. While the specific cause of this is attributed to the capacitive sensor, poorly designed electronic circuit could also be a contributing factor; with the correction applied, accuracy was high and the drift was eliminated, therefore the cause was deemed irrelevant by the medical practicioners.

This work appears to be the first and only systematic attempt to characterise the behaviour of the solid state high resolution manometry system with temperature and time. Biphasic system characteristic has been demonstrated; an initial effect associated with the change to in vivo temperature and an ongoing pressure change with time. To differentiate these effects we propose the terms 'thermal effect' for the initial effect of temperature and 'baseline drift' for the ongoing effect. Therefore our initially proposed term 'thermal drift' is misleading and should be avoided.

3.4.5 *In Vivo* validation of thermal drift compensation algorithm

It is impossible to fully duplicate the complex and dynamic in vivo condition of the human digestive tract on the bench top, however in order to address this we inspected six in vivo studies from each of three probes available to the research group. The magnitude of the baseline drift was similar for the probe tested on the bench-top and used for extended in vivo studies. There was also no clear exaggeration of the baseline drift in sensors exposed to the upper and lower oesophageal sphincters, which agreed with the bench top experiments which showed despite some sensors being exposed to higher pressure, all sensors drifted a similar amount with no correlation between hydrostatic pressure and drift magnitude. This suggests that the baseline drift severity is primarily a temperature phenomenon rather than the result of pressure. It is clear however that the device drifts significantly more when exposed to body temperature than room temperature; this suggests that although there is a constant baseline drift, it is exacerbated by higher temperatures. The baseline drift at calibration temperature could be the result of capacitive leakage or any other factor suggested in the introduction to this chapter, however it is difficult to determine the cause.

Comparison between the three available probes from the in vivo data suggests a there is a variation in tendency to baseline drift. From both bench top and *in vivo* results it is apparent that there is marked variability in the degree of baseline drift between individual sensors, this is demonstrated in figures 3. 8, 3.9, 3.10, 3.11, 3.12, 3.13 3.16, and table 3.2. Since a probe is a collection of thirty-six sensors with independent baseline drift characteristics it is understandable that the baseline drift profile will vary from probe to probe, dependant on the sensors within the probe; this poses a quality control problem for manufacturers. The present method to correct for baseline drift is to subtract a measured pressure from every sensor, taken at the end of a clinical study after extubation from the in vivo pressures; this basic correction will simply shift the pressure-time line down the y axis but without addressing the gradually increasing drift. This does not correct for individual sensor variation, but may be adequate for a very short study however unacceptable with longer studies as

the overall error with time, indicated by the gradient of the line will be unchanged. Given the time dependant and linear nature of baseline drift we have suggested an algorithm where time compensation may be employed as the basis of the correction process. We have tested a linear correction on our bench top data with an overall error of 0.3mmHg independent of study duration. Comparisons suggest that this type of correction is superior in reducing the error for all study durations with a P value of <0.0001. It is strongly urged therefore, to implement this type of correction in clinical and research settings where the HRM is the mainstay of research. Unfortunately the discovery of this highly significant and large source of error may mean that every study and clinical investigation of over 30 minutes would be inaccurate. The definition suggested by (Pandolfino, Ghosh, et al. 2006) of a 2 mmHg step up point of the LOS could be wildly inaccurate unless this compensation is employed; it has been shown in the above results that two adjacent sensors can drift such that their baseline is up to 10 mmHg apart, an error which completely overshadows the small measurements which the HRM is being used for. The basic error of each sensor is +/- 1 mmHg even when accurate and calibrated, therefore if one sensor has +1 mmHg of error and the adjacent sensor experiences -1 mmHg error, the step up point as defined by Pandolfino will be inaccurate anyway; the 2mmHg step up point is therefore naturally flawed when used with the solid state HRM technology, however although untested, the accuracy of the more traditional water perfusion manometers may be sufficient for this degree of accuracy. Implications in research into upper GI disease could be incorrect using this method, as over or under estimation of LOS length and pressure can occur, leading to knock on effects in clinical diagnosis. Diseases such as hiatus hernia and dysphagia are often based on manometric output, therefore any inaccuracies in the measurement could produce misdiagnoses, with potentially severe repercussions on patients who are misdiagnosed or require alternative or repeat investigations, which as also costly to the health services.

Following the preliminary results shown in figures 3.8 and 3.9,we communicated directly with the manufacturers, Sierra Scientific Instruments, USA, and were advised initially dismissed, with the company citing misuse, lack of calibration or faulty probes for our results, having investigated further and presenting the

remaining results in this chapter, we were eventually advised of an alternative protocol for prolonged studies. This protocol does allow the application of a linear correction for each sensor from the in vivo calibration values to the set thermal compensation values and extrapolating from our bench top data will dramatically reduce the error associated with baseline drift. However at present this protocol has to be locally enabled in the program files by the manufacturer and as it is not mentioned in the standard operating instructions. When suggesting to the manufacturer that this severe error should be publicised by the manufacturer and the correction sent out to all HRM users, the company declined to comment and ceased communication with our group. Unfortunately it requires awareness of the problem on the part of the user before being able to employ the correction, therefore this issue was presented by Dr Elaine Robertson at both the British Society of Gastroenterology 2011 in Birmingham (E. V. Robertson et al. 2011) and Conference on Digestive Disease Week, Chicago 2011 (E. Robertson et al. 2011); many attendees watched the oral presentation, with a large number of medical practitioners and researchers admitting they had the same error but upon contacting the manufacturer were told that the error was introduced by the users rather than a flaw in the device. Having spoken to the attendees in question, it was clear that this issue needed publication, so a paper was drafted and published in Neurogastroenterology and motility (Robertson et al. 2012). Although this correction removed a significant amount of error, it also necessitates performing and recording *in vivo* calibration at the start of each prolonged study which is more laborious and cannot be applied retrospectively to data sets for those who have collected data without following this protocol.

Based on the results of the collaborative bench top experiments we would suggest that the current correction process be replaced by our suggested linear correction algorithm, as this is already within the capability of current software, as demonstrated by the manufacturer's linear correction which needs a personal request to receive. This could be done by interpolating between stored in vivo compensation values collected weekly and the set thermal compensation values specific to each study rather than at the end of each study; this would considerably improve the accuracy of the HRM system, would allow its use for prolonged studies without

additional hardware modification and would not impact on ease of use. It is believed that the manufacturer knew about this problem, as it already had developed its own correction algorithm, however was reluctant to publicise the error or release the correction as this would mean admitting that every experiment previously was inaccurate and therefore invalid. It is obvious from the data presented in figure 3.17, that uncorrected data is wildly different to corrected data, this image enforces the importance of accurate and representative measurement using medical devices.

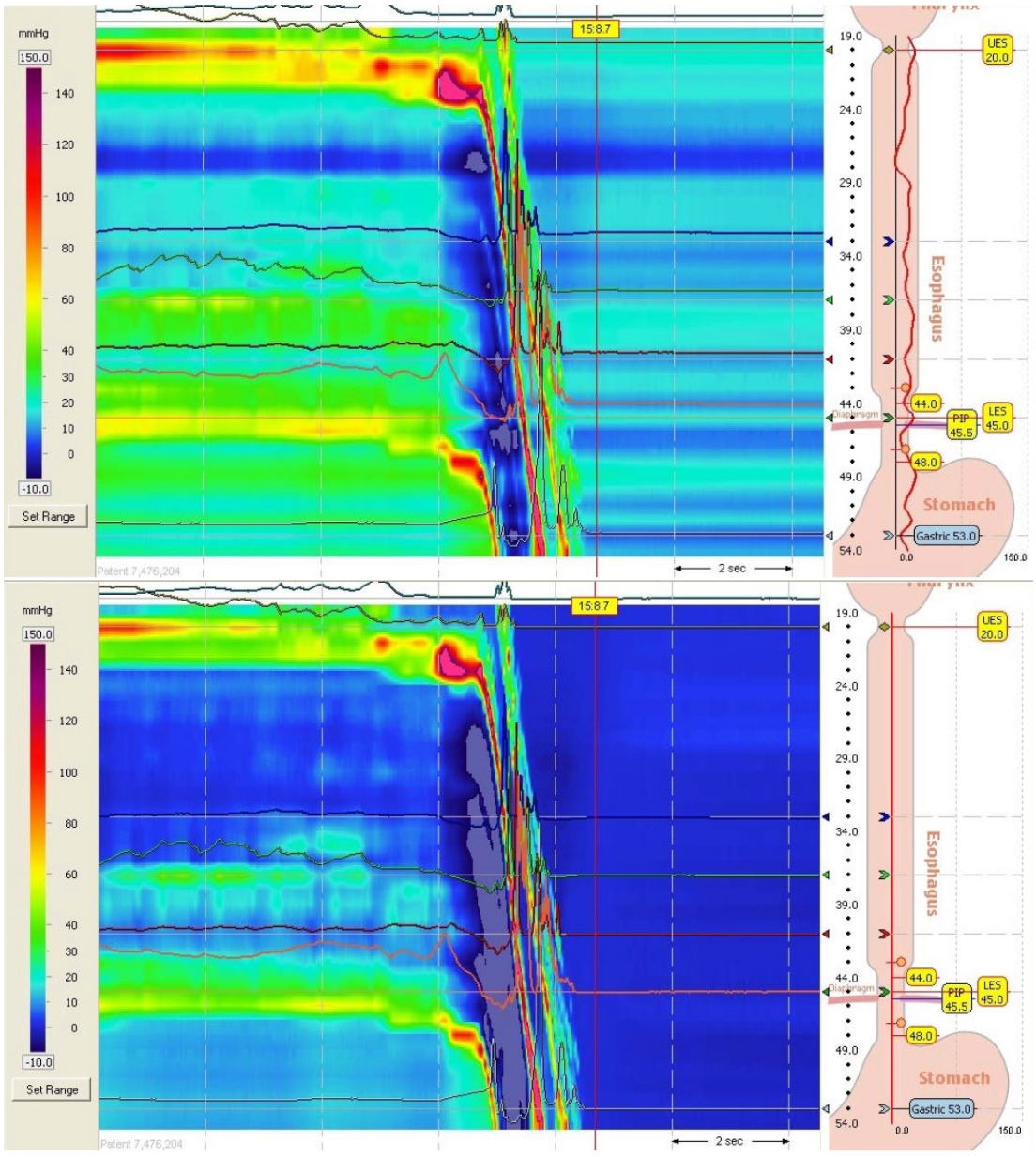

Figure 3.17 Comparison between uncorrected data which has drifted (above) and corrected data which shows very minimal drift (below).

In conclusion these experiments have quantified and classified the behaviour of the HRM system with temperature and time. There is an immediate thermal effect which is well compensated and an ongoing baseline drift which is not well recognised or addressed. The error associated with this phenomenon could be reduced by applying a linear correction. Ultimately this would be best incorporated into standard software so that ease of use is maintained. This observation represents a quality control issue for the manufacturer as well as setting a challenge to all manufacturers of similar technologies. Thermal effect and baseline drift must be considered, documented and addressed.

While the above conclusions are striking and important, it is worth noting that the significant changes with time and temperature exposed in this research are exclusive to the Manoscan high resolution manometer; other manometry devices are available, both solid state and perfusion based and it is not known what levels of drift these systems are subject to.

Chapter 4

Development of a minimally invasive device capable of accurately measuring the position of the SCJ from outside the body.

4.1 Introduction

4.1.1 Why measure the position of the SCJ externally

Initially Nagler et al (Nagler & Spiro 1963; Nagler et al. 1960) published work detailing the increase of reflux incidence induced by prolonged upper GI intubation, deducing that the pressure of a catheter in the throat, oesophagus and stomach, caused by its presence, increased the number of reflux episodes. This rather important fact was much ignored or forgotten since its publication, as many medical researchers publishing oesophageal or gastric pH or pressure data do not cite or even mention this significant phenomenon.

Nearly three decades later, a paper was published by Mittal et al., detailing the effect of a catheter in the pharynx on the frequency of TLOSRs, showing strong causal evidence supporting Nagler's original hypothesis that catheters cause an increase in reflux incidents (Mittal et al. 1992).

Mittal's method of action suggested that pharyngeal stimulation triggered relaxation of the LOS via the efferent pathway of the vagus nerve, similar to when swallows are initiated, however these LOS relaxations occur without any peristaltic action. The method offered by Mittal explains that TLOSRs may be induced by triggering the vagal nerve in the pharynx; the technique used a sleeve perfusion manometer across the LOS inserted via gastrostomy, to measure the LOS pressure in order to identify TLOSR events as they happen. This allowed the manometric identification of complete and incomplete LOS relaxations tested in 6 subjects repeated with and

without a pharyngeal catheter present. TLOSR frequency was higher in every subject when the catheter was present in the pharynx. Statistical testing showed 72% of the TLOSRs were associated with the presence of the catheter, a significant increase and likely to skew any catheter based testing. The paper concludes that pharyngeal stimulation is certainly responsible for the increase in TLOSR frequency; Mittal concludes that while increased, TLOSRs are still likely a real physiological action without any catheter present, in such events as belches or swallowing. This paper does explain Nagler's findings of increased reflux during catheterisation as TLOSRs are often associated with or followed by gastric reflux. Noordzij, Mittal et al published a follow up paper 8 years later, describing a similar experiment in which they tested the pharyngeal mechanoreceptor's ability to stimulate TLOSRs by using bursts of air from an endoscope on different sites in the nasopharynx (Noordzij et al. 2000). The investigative technique also uses manometry to detect TLOSR events, as well as monitoring several physiological parameters; the catheters were inserted nasally for this experiment despite previously showing statistically significant data that pharyngeal intubation induces TLOSRs.

The paper did conclude that pulses of air triggered TLOSRs at all three sites in the pharynx after between 5 to 20 seconds of pulse; increased duration of air pulse at a particular site correlated with an increased likelihood of a TLOSR event. It was noted that although the LOS relaxation was triggered by the air pulses, neither the catheter nor air pulses caused relaxation of the crural diaphragm. In both papers, there was pressure across the LOS due to the presence of a catheter used to detect TLOSRs, however this was mentioned in neither, despite the potential that the presence of a catheter in the LOS may itself cause the sphincter to relax. Mittal's initial paper suggested that 72% of the TLOSRs recorded were due to the presence of a catheter in the pharynx, however the follow up paper ignores this initial conclusion and performs experiments with a catheter present. Due to the inconsistency of Mittal's claims and the undeniable fact that if Nagler and Mittal's findings have merit, then all clinical investigation and research related to reflux, motility and the upper GI tract using any sort of catheter has the potential to be misinterpreted; the very nature of measuring the oesophogastric area may cause phenomenon as a direct consequence. This important flaw in all experiments may lead to the

misunderstanding of GI motility and disease, as well as causing misdiagnosis based on erroneous data. The new gold standard as developed and proposed as part of this thesis is also subject to this flaw.

Due to the internal nature of the anatomy, it is currently impossible to detect TLOSRs without catheterisation; even with MRI, the anatomist is barely able to detect the presence of a much larger hiatus hernia, and is unlikely to detect the marginal opening of the LOS during full relaxation and unable to determine incomplete TLOSRs.

It was therefore decided to develop a totally novel and ground breaking medical device which is capable of measuring the position of the SCJ without catheterisation; this device could then be used to fully confirm or refute Mittal's hypothesis. The device, as well as answering Mittal's question once and for all, should allow the prolonged SCJ position measurement subsequent detection of TLOSRs; although many studies use 24 hour ambulatory pH monitoring, the current limit of trials using larger manometry equipment is ethical approval regarding patient comfort, therefore the non-catheter based measurement of the proposed technology is a huge advantage. This technology allows the subjects to continue their daily lives, more so than 24 hour ambulatory pH, and potentially for much longer duration. The nature of this device would be non-invasive during its measuring period, however may require endoscopy or other intubation before recording; the lack of any pharyngeal or LOS stimulation should detect only true TLOSRs, assuming they are not artefactual.

The local pH could be simultaneously monitored without catheterisation with the concurrent recording using the Bravo Capsule, clipped to the oesophageal wall and transmitting the pH data to an external device without the need for a catheter; it is unclear whether a Bravo Capsule in the oesophagus could itself trigger TLOSRs, however this could be tested using the proposed device.

4.1.2 Problems of increased distance

The sensitivity of the currently used for internal SCJ position measurement magnet sensors (Allegro A1394) is not adequate enough to detect the existing magnet from outside the body; the field is too weak at this distance (approximately 0.03 gauss)

and would require very expensive and bulky machinery to be able to detect it such as a SQUID system . MRI and SQUID sensors may be sensitive enough to measure the relatively weak field from outside the body, however this is not only very costly but requires the subject to be lying recumbent for the duration of the study, for which the study would be limited to less time than adequate to allow statistical testing.

If a device is to be able to detect the magnet outside the body and investigate the number of TLOSRs it must be small enough to allow the patient to undergo extended studies due to the frequency of TLOSR events being as low as one per 30 minutes. Ideally the device would be portable allowing ambulatory studies to be performed, which could be used to investigate motility disorders and when combined with the Bravo capsule, acid reflux; the limit to this device's use would then be battery life which is simple to overcome and patient conformity. While there was a limit of size of device due to limits of intubation through the nose and oesophagus when measuring the SCJ using a catheter probe, there is no longer such a significant limit when used externally. There is another important limitation placed onto the proposed technology however, if using the well established magnetic sensing technique, the weaker field at this distance means equipment sensitivity and magnet size and strength need to be redressed. As shown in figure 4.1, there is a significant distance between the oesophagus and the skin; the oesophagus is approximately in the centre of the chest cavity, anterior to the spinal column, posterior to the lungs and heart. The oesophagus is marginally closer to the back than the front chest wall, and is estimated to be between 8 and 10 centimetres from the skin, subject to the person's size and subcutaneous fat levels.

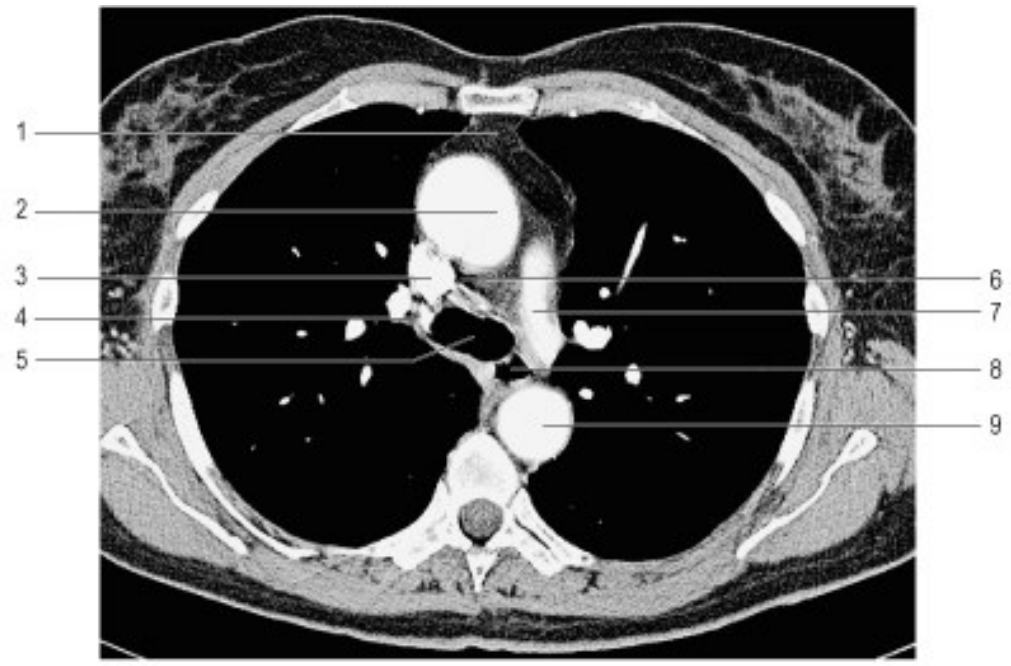

1. Anterior junction. **2.** Ascending aorta. **3.** Superior vena cava. **4.** Right para-tracheal space. **5.** Carina (bifurcation of trachea). **6.** Superior pericardial recess. **7.** Left pulmonary artery. **8.** Oesophagus. **9.** Descending aorta.

Figure 4.1 Transverse plane image of the body with the white arrows showing chest anatomy including the oesophagus in front of the spine (8).

4.1.3 Magnetic properties of the body

Magnetic permeability of a material is a measure of its ability to support a magnetic field, which in essence describes its magnetisation from an external magnetic field. Should the human body or tissues be more or less permeable than air, the range at which the magnet can be detected will either increase or decrease respectively. Henrys per meter (Hm^{-1}) is the SI unit for magnetic permeability however Newtons per Ampere squared (NA^{-2}) are also used. The permeability constant (μ0), otherwise known as the magnetic constant or the permeability of free space, is the measurement of the amount of resistance experienced when forming a magnetic field in a vacuum, with a value of $\mu_0 = 4\pi \times 10^{-7}$ Hm^{-1}. The magnetic dipole of a material B, is proportional to the strength of external magnetic field **H**. magnetic

permeability μ, is the proportional factor, demonstrated in equation 4.1, μ, is a scalar if the medium is isotropic or a second rank tensor for an anisotropic medium.

$$\mathbf{B} = \mu\mathbf{H}, \tag{4.1}$$

The magnetic constant μ actually varies with humidity and temperature, as well as the frequency of the applied field, leading to frequency dependant magnetic constants μ_f. Relative permeability μ_r, is the ratio of the permeability of a specific material to the permeability of free space μ_0, shown by equation 4.2. This is calculated to demonstrate and facilitate the comparison of different materials' permeability to that of a vacuum, where μ_r of a vacuum is 1, and air is 1.00000037. More magnetically permeable materials such as steel and ferrite have relative permeability of 100 and 640 respectively while less permeable materials such as water and superconductors have μ_r is 0.999992 and 0 respectively.

$$\mu_r = \frac{\mu}{\mu_0}, \tag{4.2}$$

There is a little data on the permeability of tissue, human or otherwise; papers that mention the use of magnetic fields in the body use μ_0, the magnetic permeability of a field through a vacuum (Wu et al. 2005; Weitschies et al. 1994; Guo et al. 2008) or air (Sinatra 2010; Wang et al. 2006), with Wang et al, stating that the permeability of the body is similar to that of air, without including a reference or evidence to back this claim up. The permeability of air is $1.2566370614 \times 10^{-6}$, while the permeability of a vacuum is 1.2566371×10^{-6}, a marginal difference, but when large errors are introduced such as those used by the above papers' modelling, this could account for a small percentage of this. More importantly the human body is 50-65% water and water is less permeable than both air and a vacuum; permeability of water is 1.2566270×10^{-6}, again a small change, but an error none the less. The few papers which describe a specific and measured magnetic permeability detail the permeability of bone (μ_r=0.99999156) (Hopkins & Wehrli 1997) and blood (μ_r=0.99999153) (Weisskoff & Kiihne 1992) respectively, equating to a permeability of $1.25662645 \times 10^{-6}$, very similar to the permeability of water. The minute difference in permeability of air versus the body is negligible; the distance over which the system is to be measured is significantly higher limiting factor. The effect of blood,

which is a paramagnetic fluid, may have an effect on magnetic fields, as it is detectable in an MRI machine, however Sinatra describes a technique whereby blood is passed in between a magnet and magnometer (Sinatra 2010); when the blood was pulsed through the passage having been exposed to a high magnetic field, it still did not present a magnetic field to the sensor, concluding that blood will not have an effect on a magnometer unless it is sensitive enough to detect the electron spin such as that in an MRI machine.

4.2 Methods and Materials

4.2.1 Different/more sensitive sensors

The issue of measuring an internal magnet from outside the body allows the solution of some issues while it also causes other issues: with the luminal catheter based SCJ locator, the size was the largest constraint on the technology, as it must be able to fit comfortably through a subjects nose and not interfere with the functioning of the LOS, also the distance over which the sensors needed to detect the magnet was at worst approximately 2 centimetres during swallowing. The issue of size is totally reduced when the internal criterion is removed, therefore meaning the electronic component count and complexity can be increased and the need for a delicate flexible circuit board is removed. The distance over which the sensor must be able to measure is a lot greater, with figure 4.1 demonstrating the distance over which the magnet must measure: this poses the greatest limitation on the equipment, therefore a sensor or system must be much more sensitive in order to facilitate the longer range magnet measurement.

Several high sensitivity magnetic sensors were tested with a simple DC supply according to the manufacturers' recommended power and current requirements in order to establish the most sensitive sensor. These sensors are compared the Allegro A1395 sensor used in the previous chapter in order to provide the basis comparison.

4.2.2 Constant current supply

Previous work (chapter 2) led to the development of a high-resolution Hall effect sensor based catheter probe consisting of an encapsulated array of A1395 Hall effect sensors (Allegro Microsystems, USA) placed on a flexible printed circuit and external microprocessor which measured the magnet from in the oesophageal lumen with an accuracy of 1 centimetre (Yeong Yeh Lee, Seenan, et al. 2012). This technology allowed the user to accurately measure movement of the SCJ due to

breathing, swallowing and TLOSRs over extended periods, both pre and post-prandial.

Recent papers by Mittal have suggested the very presence of oesophageal luminal devices affect the behaviour of the sphincter and may artificially induce extra TLOSRs by way of laryngopharyngeal mechanoreceptor stimulation. As a significant number of reflux events occur as the result of TLOSRs, the therapeutic objective is often to minimize the number or TLOSRs (Mittal et al. 1992), however since the presence of an intraluminal probe increases the frequency of TLOSRs, the focus of this research is towards developing a non-luminal tool which measures the movement of the SCJ. This device is required to operate from outside the patient or volunteer, to avoid increasing TLOSR frequency due Mittal's mechanoreceptor event, and provide a tool capable of reliably measuring TLOSRs without triggering them.

Sensitivity is an accurate term for describing sensor efficacy, however in this application, the important factor is range; the distance over which the magnet can be detected, as the magnet is merely a marker for the SCJ, therefore although the sensitivity is increased, this paper will use range to describe the sensor. For the purpose of clarity, all bench-top tests will use a 1789 Gauss Samarium Cobalt disc magnet of 3mm diameter and 2mm length, in ideal orientation.

Due to the increased distance involved, higher sensitivity magnometers were required, so several Hall effect sensors were tested, which enabled an initial increase in range, demonstrating an increase of range from the commercially available Allegro A1395, used in previous generations, to the more sensitive AHS P15A. the range using a standard power supply was increased from 15 millimetres to 24 millimetres simply by changing the sensor. This range increase was still limited by noise, therefore a Constant Current circuit was developed to supply the power for the Hall effect sensor. An initial Direct Current (DC) system was developed for use with the P15A sensor (figure 4.2), which had no internal circuitry or amplification; showing high levels of noise and drift due to internal heating due to a noisy environment and high current respectively. Therefore a regulated 5 Volt constant current source of 5 milliamps was used to supply the Hall effect sensor; this was

prescribed by the manufacturers, AHS, in the datasheet. This increased the sensitivity by reducing internal heating therefore thermal drift and with the addition of shielding, decreased noise greatly.

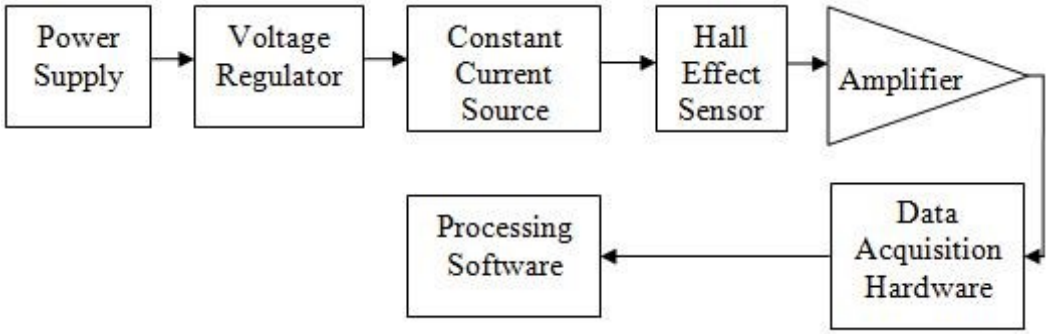

Figure 4.2 Direct Current voltage regulated system with data acquisition.

4.2.3 Increasing sensitivity with alternating Current supply

In order to advance the current SCJ locator probe technology (Yeong Yeh Lee, Seenan, et al. 2012), the equipment must be redesigned in order to measure the magnetic clip externally, which provides new problems whilst removing others. Where the luminal probe was severely restricted by size, both of the sensors and the flexible circuit board on which they were mounted, the new non-luminal probe will have no such restraint, as it will not be employed nasally, therefore resolution and complexity may be significantly improved. This is fortunate, as the distance over which the magnet needs to be detected increases significantly with the new design criteria. In order to further the device, a range of high sensitivity Hall effect sensors were tested and the AHS P15 GaAs sensor (AHS, UK) was used to improve the overall performance where a DC driving circuit was employed.

4.2.4 Methods of increasing Hall Effect Sensor Sensitivity.

The limiting factor of Hall Effect sensor sensitivity for large signals is the transduction ratio (Leroy et al. 2006) as seen in equation 4.3. Where S_A is the sensor sensitivity, V_H is the Hall voltage, and B is the component of magnetic induction.

$$S_A = \left| \frac{V_H}{B} \right| \tag{4.3}$$

Therefore there methods of increasing sensitivity are to both reduce the output noise for example with good conditioning electronics, and amplify the measured field without adding noise. The output noise N_{VH} is determined by the low frequency noise N_{VH}^{LF} and the thermal noise N_{VH}^{th} as seen in equation 4.4.

$$N_{VH} = N_{VH}^{LF} + N_{VH}^{th} \tag{4.4}$$

Thermal noise is dependent on the sensor itself and becomes the limiting factor when low frequency noise is significantly reduced. Equation 4.5 describes the output of a sensor as a function of current and carrier density; this equation demonstrates the sensitivity of a sensor and what factors determine it.

$$V_H = -\frac{IB}{Ned} \tag{4.5}$$

Where I is the current flowing through the sensor in amperes, B the external magnetic field, N is the charge carrier density in carriers/cm^3, *e* is the charge on an electron (1.6×10^{-19} C) and d is the thickness of the conductor. As the electron charge is fixed throughout physics, the charge carrier density is fixed for a given sensor Hall element; the rest are variable. The magnetic field can be increased with decreasing distance between the sensor and magnet, or alternatively by increasing the strength or size of the magnet; the shape of the magnet may also affect the size of the field at a given distance. The thickness of the sensing element, d, also plays an important part in sensor sensitivity, however this is fixed when the sensor is produced; the thickness of the sensing element and the conductor make-up which determines the charge

carrier density, in combination, establishes the sensitivity of a Hall sensor given the same power input, the likely cause of the difference between tested sensors.

The final variable in equation 4.5 is the current flowing through the conductor; the higher the current the more voltage is produced for a given field. While the current can be increased to allow a better sensitivity, there are manufacturers' limits of current flow through the sensing element, often set by internal conditioning circuitry. The Hall element sensors which are essentially just a sensing conductor in a packaging with pins, have no conditioning circuitry so are therefore may be subjected to increased current; the manufacturers of such sensors often place limits of current flow on these devices, as the sensing elements themselves have a limit to the maximum current that can flow through them before damage occurs. Increasing the direct current through the sensor will also inevitably cause internal heating; this will increase the drift and hence reliability of any sensor, so the maximum current value must not be exceeded.

While direct current supplies are limited, the use of alternating current (AC) supplies for the sensors are less limited as current is not constantly flowing through the sensors, rather it is alternated; this allows a much higher peak current through the sensor with a significantly reduced heating effect.

The ability to drive the sensor with an alternating current is also useful for noise reduction; with noise being predominantly at the low frequency end of the spectrum, with 60 Hertz mains noise contributing, a high noise-free frequency can be used as the sinusoidal alternating frequency for the sensor, with all other frequencies being removed, significantly improving signal to noise ratio. The use of analogue circuits and operational amplifiers allow the design of custom alternating current and associated filtering and amplification to allow the sensitive detection of a small magnet at the large distance associated with measuring the magnet from outside the body.

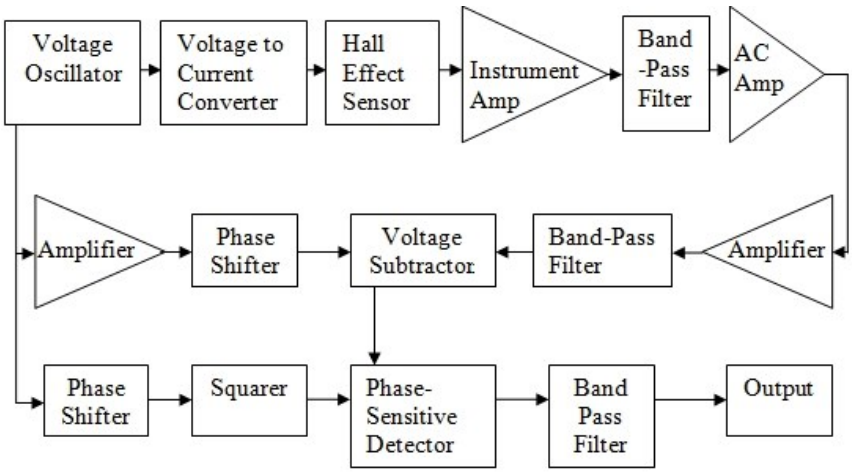

Figure 4.3 AC Circuit block diagram

In order to drive the Hall effect sensor with an alternating current, a bespoke circuit was designed; the concept of which is shown in figure 4.3 and will be discussed below. A voltage oscillator will create a fixed frequency sine wave output, as the current is the main factor for sensitivity, this voltage oscillation will be converted to a current oscillation directly connected to the Hall effect element; the differential output of the Hall effect sensor will then be amplified by an instrumentation amplifier and band pass filtered to remove any noise. The output will then be amplified and AC coupled and potentially band pass filtered a second time. The output of this section will be a sinusoidal voltage proportional to the product of the AC input to the sensor and any magnetic field the sensor is subject to. In order to remove the sinusoidal current component, a Subtractor circuit will be used; the same voltage oscillator will be amplified and phase shifted such that it exactly matches the output from the band pass filter and amplifier portion output when no external magnetic field is present on the sensor. The two matched outputs will be inputted to the voltage Subtractor, producing a 0 volt DC output when no magnetic field is present; the output from the Subtractor will still be sinusoidal when a magnetic field influences the sensor, therefore further steps must be produced to accurately measure these small sinusoidal voltages. The same voltage oscillator will undergo phase shifting and squaring to provide an in phase and frequency matched reference voltage for a phase sensitive detector (PSD); the PSD or Lock-In Amplifier, is a circuit that is capable of detecting very small sinusoidal voltages which are of a

given frequency and phase, even when said sine waves are hidden in a noisy environment. The PSD effectively multiplies the output from the voltage Subtractor with the reference square wave, and any random or non-matched noise cancelled out, with the output being a rectified sine wave; this rectified wave has an output proportional to the magnetic field on the sensor, which when low pass filtered, is effectively a AC amplitude to DC converter

This circuit will effectively increase the system's magnet detecting range, an Alternating Current (AC) driving system was designed, as the above specifications. The system works by supplying AC to the Hall sensor at 1.59 kilohertz, the output of which is proportional to the product of the AC and the presence of a magnetic field. The output is amplified and band-pass filtered at the driving frequency then subtracted from a phase matched driving AC signal, producing a sine wave with amplitude proportional to the magnetic field. A Phase-Sensitive-Detector (PSD) is employed to accurately measure this sine wave. The increased sensitivity Hall effect sensor will be employed, with several calibrated sensors along an array connected in parallel; the output of each of these sensors placed externally but aligned with the oesophagus, will be recorded by a microprocessor and calculated into an output, detailing the position of the magnet along the array and the signal strength of the magnet, much like the catheter based SCJ locator probe. This similarity will allow the current users of the SCJ locator to use and interpret data with no extra training.

4.2.5 Noise reduction

Initially after producing a simple DC power circuit for use with the Hall sensors, it was noticed that there was a lot of noise on the output voltage; a Fast Fourier Transform was performed to analyse the noise, highlighting any significant sources. There was a significant level of noise at 60 Hertz, which is associated with the mains power interference, in addition to mains noise, there was apparent random noise in the system, which varied in frequency and was not always present. This noise was tracked down to a neighbouring room, with high power servo-motor based equipment, which produced a high level of noise which was picked up by the circuit.

Having highlighted the sources of noise as external to the circuitry, all wiring and circuit boards were shielded with grounded coaxial wire and noise shielded box respectively. This significantly reduced the external noise which produced a much cleaner signal, however there was still a small amount of noise due to the unshielded Data Acquisition ribbon cable and break-out board; the length of this cable was kept as short as possible to minimise noise.

4.2.6 Passive magnetic field amplification

The noise-equivalent magnetic induction (NEMI) spectral density is defined as the output noise to absolute sensitivity ratio as shown in equation 4.6. The smaller the NEMI spectral density, the smaller the magnetic induction the sensor can detect.

$$S_{NEMI}(f) = \frac{N_{VH}(f)}{S_A} \tag{4.6}$$

Another way to improve the resolution of the sensor is to amplify the magnetic field in proximity of the sensor by a combination of increasing the gain of the magnetic field $G_{magnetic}$ and conditioning electronics $G_{electronics}$, with respect to the overall noise output of the system, effectively increasing the signal to noise ratio as seen in equation 4.6.

$$S_{NEMI} = \frac{N_{out}}{G_{magnetic} \cdot S_A \cdot G_{electronics}} \tag{4.7}$$

Increasing $G_{magnetic}$ would increase the sensitivity and range of the sensor by increasing the magnetic field, B, and decreasing noise-equivalent magnetic induction according to equation (4.7). Passive amplification of the magnetic field will be detailed in section 4.2.19.

4.2.7 Voltage Oscillator

In order to create an alternating current driven circuit, an oscillator must be designed, built and tested; the circuit will create a tuneable custom oscillating

voltage. The peak to peak voltage will be then, with the use of a voltage to current converter, create the alternating current used to drive the Hall effect sensor. In order to develop the desired sinusoidal voltage, a sine wave generator integrated circuit will be used in conjunction with passive components such as capacitors and resistors; it is the values of the passive components which will determine the frequency, magnitude and offset of the sin wave output. A Monolithic Function Generator IC was used in order to crease the oscillating voltage, the EXAR XR-2206 (RS Components, UK) was used as demonstrated by figure 4.4; this IC is capable of creating high quality sine, square, triangle, ramp and pulse wave forms of high stability and accuracy. The output waveforms are modulated by an external voltage driven by passive components. The frequency of operation can be controlled using said components between 0.01 Hertz to approximately 1 Megahertz; timing resistors and capacitors control Voltage-Controlled-Oscillators and Current Switches to modify the output to the desired waveform, frequency and magnitude. The package used here is the 16 lead PDIP package, which can be mounted in a socket for ease. The waveform variables are customisable as variable resistors have been used in the design where resistance value determines the shape and size of the voltage output; the chosen frequency for initial design is 1600 Hertz due to the fact that it is well above mains and local low frequency noise sources, while being well below computer frequency, meaning that with band-pass filtering, most sources of noise can be removed. The voltage oscillation was simply converted to current oscillation in order to drive the Hall sensor with an alternating current.

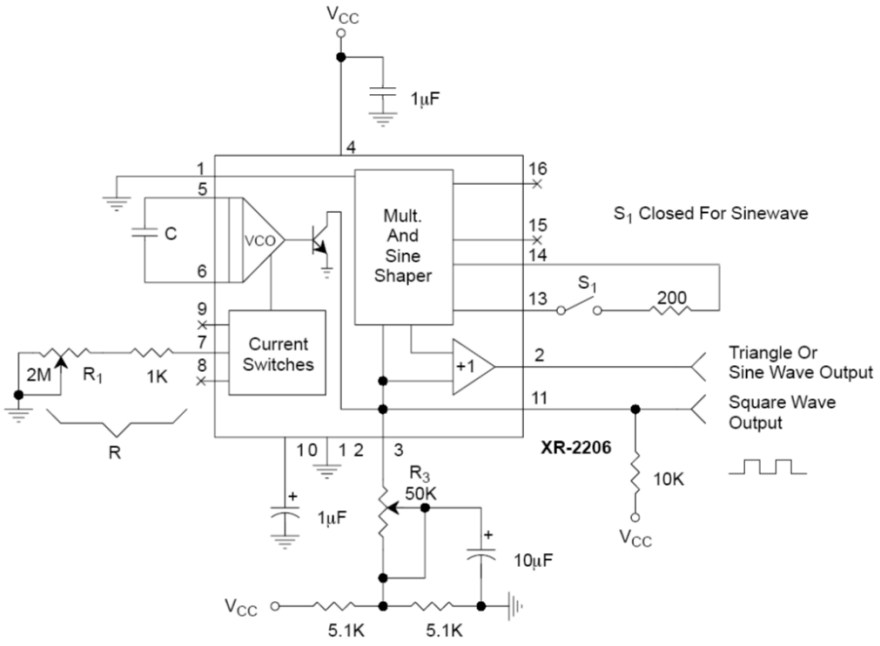

Figure 4.4 Sine wave generator circuit. Acquired from datasheet.

The Loop gain Aβ is determined by equation 4.8, and when $R_1C_1 = R_2C_2 = R_3C_3$ reduces to equation 4.9: the frequency of the sine wave produced is simplified to equation 4.10, so using a 10 nF capacitor and 10k resistor, the frequency becomes 1.59kHz.

$$A\beta = \left(\frac{1}{R_1C_1 j\omega}\right)\left(\frac{R_3C_3 j\omega + 1}{R_3C_3 j\omega\left(R_2C_2 j\omega + 1\right)}\right) \tag{4.8}$$

$$A\beta = \frac{1}{\left(RCj\omega\right)^2} \tag{4.9}$$

$$\omega = \frac{1}{RC}, \qquad \text{Freq (Hz)} \;\; F = \frac{1}{RC\pi 2} \tag{4.10}$$

4.2.8 Voltage to current converter.

The voltage to current converter (figure 4.5) facilitates the driving of the Hall element with a precise alternating current determined by the voltage from the oscillator where R_G determines the gain, G (equation 4.11): current is determined by

R_1 and the alternating voltage from the oscillator in equation as shown in equation 4.12. Accuracy of the circuit is determined by the quality of components used.

$$G = 1 + \frac{50K\Omega}{R_G} \tag{4.11}$$

$$I_o = \frac{V_{IN}}{R_1} \cdot G \tag{4.12}$$

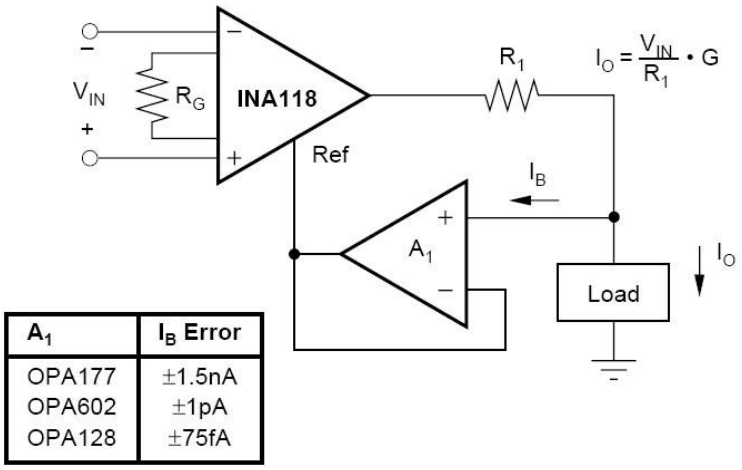

A_1	I_B Error
OPA177	±1.5nA
OPA602	±1pA
OPA128	±75fA

Figure 4.5 Voltage to current converter. Acquired from datasheet.

4.2.9 AC coupled amplifier

The AC coupled amplifier acts in a very similar way to a normal operational amplifier, with the addition of capacitive coupling providing an inherent high pass filter, as shown in figure 4.6. The cut off frequency is described by equation 4.13 and again the resistor being variable provides a tuneable cut off frequency.

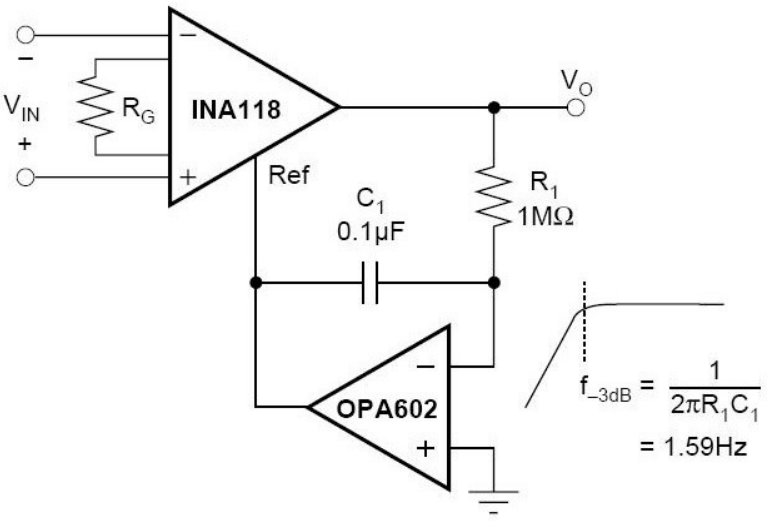

Figure 4.6 AC coupled amplifier using a OPA 602 operational amplifier and INA118 instrument amplifier. Acquired from datasheet.

$$f_{-3dB} = \frac{1}{2\pi R_1 C_1} \tag{4.13}$$

4.2.10 Instrument amplifier

The output from the Hall sensor when using the basic Hall element, is a differential voltage; a differential voltage differs from a simple voltage-referenced single wire output, it has two output connections, where the output from the sensor is the difference between these two outputs, which doesn't require a ground reference. Differential outputs have very good common-mode rejection, that is the ability to reject external noise as both outputs have the same noise, in opposite magnitudes, which is removed when amplified by a suitable operational amplifier

Instrumentation amplifiers are capable of detecting very small differential voltages and accurately amplifying them using a combination of internal operational amplifiers. The INA118 is a low power medical instrumentation suitable instrumentation amplifier, with current feedback input circuitry providing wide bandwidth and high gain from laser trimmed circuitry. The INA118 (figure 4.7) is available in an 8 lead DIP package, which, like the XR-2066, can fit into a suitable socket, allowing simple construction. The INA118 has a variable gain set by a single

resistor, which for this purpose is a variable resistor, allowing easy and swift gain changes.

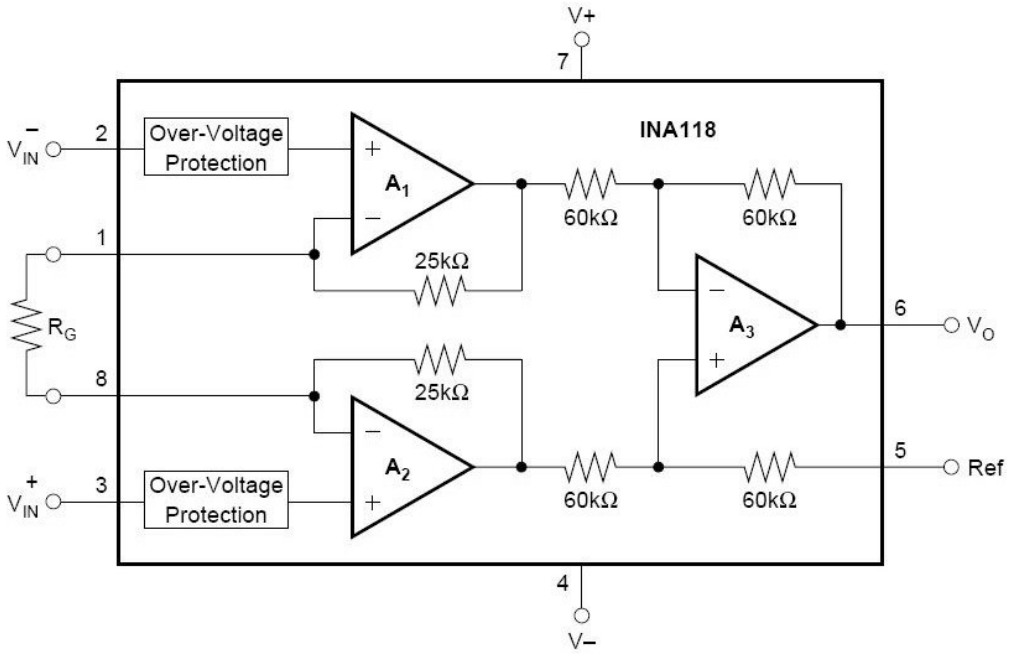

Figure 4.7 Instrument amplifier INA118 internal diagram and external components. Acquired from datasheet.

RG determines the gain according to equation 4.14 In this instance R_G is a variable resistor producing variable gain, so when R_G = 5K, G=11.

$$G = 1 + \frac{50K\Omega}{R_G} \tag{4.14}$$

4.2.11 Band Pass Filter

In order to remove the unwanted noise and interference from the sinusoidal output of the Hall effect sensor, an electronic device called a filter must be used; A filter is a combination of components that allows passage of electric signals at certain frequencies or ranges, while preventing the passage of undesired frequencies. Filters are common-place in analogue electronics, as frequency is important in such applications as telecommunications or analogue signal processing. While passive

components can be produce a filter without any powered components, a better filter can be produced using an operational amplifier with these passive components. Low or high Pass filters are filters which allow either low or high frequency signals to pass, the cut off frequency, set by the component values, determines the frequencies which are passed and filtered. while filters are analogue, they do not act as ideal filters, and do not remove all frequencies outside of the cut off range, but suppress them; the closer the frequency to the cut off, the less it is suppressed. Higher complexity filters require more components, leading to higher order systems which are better filters; a 4^{th} or even 5^{th} order filter will act more like an ideal filter than a 2^{nd} or 3^{rd} order filter. Band pass filters such as those described by figure 4.8, allow only a certain range of frequencies to pass while filtering frequencies either side of the upper and lower cut off borders. Band stop or notch filters do the opposite of band-pass filters, allowing all but a defined range of frequencies through, often used to filter out a constant frequency such as mains noise.

For each filter type, there are several optimisations, based on different design constraints; where several have been tested in this work, only the best performing design will be detailed, unless more have unique characteristics allowing for better performance. For the band pass filters in this system narrow band filters were used as they perform better noise rejection. The method of narrow band-pass frequency calculation is shown in appendix 2.

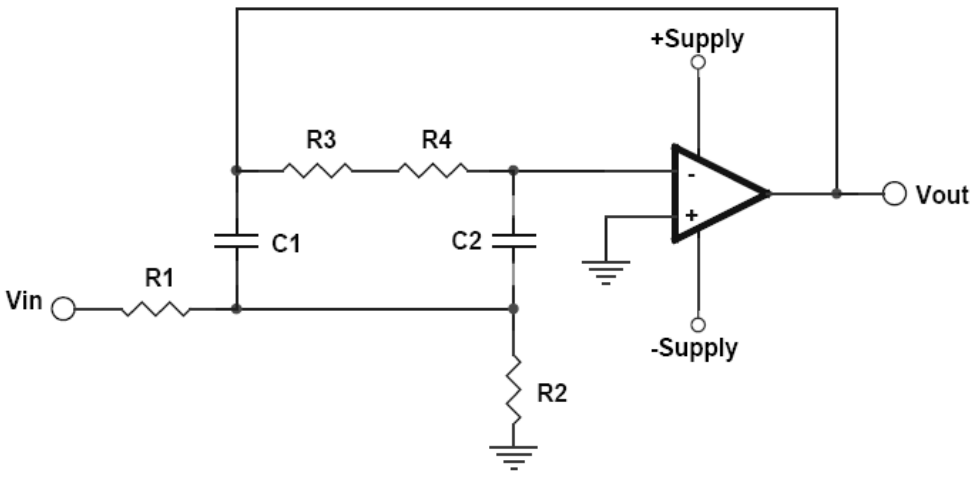

Figure 4.8 Narrow band pass filter (for +/- supplies).

4.2.12 Operational Amplifier

In order to allow for the system to work, simple operational amplifiers must be designed which allows the signal to be amplified for desired analogue processing. The amplifier is a simple non inverting operational amplifier based design; the gain of the circuit is determined by the feedback loop and voltage divider therein (see equation 4.15 and figure 4.9). The use of a variable resistor for either resistor allows the change of amplification as desired.

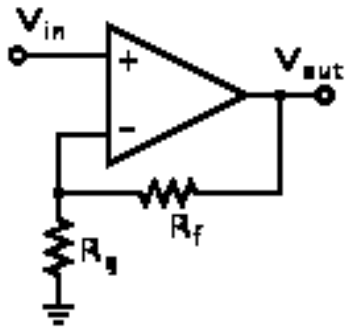

Figure 4.9 Non-inverting operational amplifier.

$$G = \frac{V_{\text{out}}}{V_{\text{in}}} = 1 + \frac{R_f}{R_g} \tag{4.15}$$

4.2.13 Phase Shifter

In addition to band pass, band stop etc., there are filters that do not filter any frequencies of a complex input signal, instead they just add a linear phase shift to each frequency component, thus contributing to a constant time delay. These are called all-pass filters. The act as phase shifters which allows for the matching of two signals; the inclusion of an operational amplifier in a circuit will be associated with a given delay or phase shift of that signal, therefore in order to match two signals out of phase, an all pass filter must be used which can be trimmed to allow the two signals to be brought into phase. The all pass filter uses an operational amplifier,

resistors and capacitors to complete this task, however one fixed value resistor is replaced by a trim-potentiometer which can be tailored to the circuit, allowing precise phase matching. The circuit is designed as in figure 4.10, with output described by equations 4.16 and 4.17. So varying (R1.C1) will vary phase. As it is easier and cheaper to use a variable resistor, the capacitor will be fixed at C=10nF.

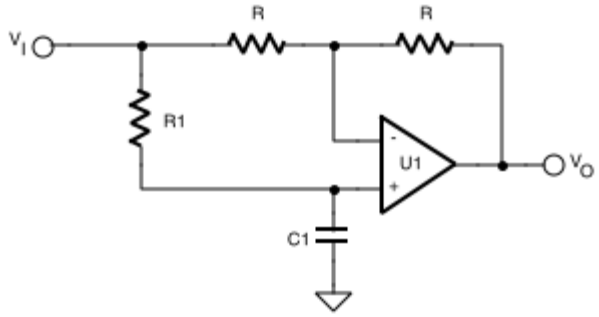

Figure 4.10 Phase shifter circuit diagram.

$$\frac{Vo}{Vi} = -\frac{s - \dfrac{1}{R_1 C_1}}{s + \dfrac{1}{R_1 C_1}} \tag{4.16}$$

$$Phase(rad) = \tan^{-1}\left[\frac{\dfrac{2\omega}{R_1 C_1}}{\omega^2 - \left[\dfrac{1}{R_1 C_1}\right]^2}\right] \tag{4.17}$$

4.2.14 Subtractor

The output of the Hall effect sensor is proportionate to the current flowing through it and any magnetic field present; the current in this case is a sinusoidal wave, which means the output is a sinusoidal wave, whose magnitude is increased by a field. in order to remove this sinusoidal component, after it has been amplified and band passed, the initial voltage must be matched using the phase shifter mentioned above, and a Subtractor circuit. The Subtractor circuit is a simple operational

amplifier in differential amplifier arrangement; the output of this circuit as shown in figure 4.11. When the sensor is not subject to any magnetic field after calibration, the output of the sensor is zero volts, however when there is a magnetic field present on the sensor, from an external magnet, the output is a small sinusoidal voltage proportional to the field alone; calibration is performed manually, using an oscilloscope to match the phase and amplitude of the two inputs to the Subtractor.

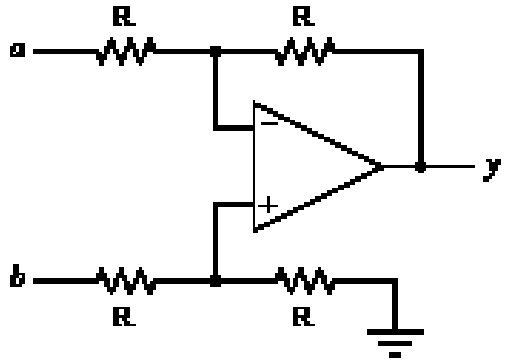

Figure 4.11 Subtractor circuit. Where the output y = b – a.

4.2.15 Phase sensitive detector

A lock-in amplifier is capable of measuring small sinusoidal signals at known frequencies, which may be hidden within comparatively larger noise. A Lock-in amplifier accomplishes this by detecting only the components which are in-phase and of the same frequency as a reference signal, thereby excluding a significant proportion of noise, effectively increasing the SNR to detectable levels.

Any signal can be mathematically determined by a combination of a finite number of sinusoidal waves at different frequencies. The product of two sinusoidal waves of different frequencies is a wave of mixed frequencies and amplitudes, the product of two sine waves of the same frequency is always a sinusoidal wave unless the waves are exactly out of phase, in which case the product will be a flat line with a given offset. It is these sine product laws which enable the low pass filter to remove all but the dc offset from the output of the lock in amplifier, where the output is then

proportional only to the magnitude of the input signal, which is itself proportional to a magnetic field acting on the Hall Effect sensor.

After the output from the Subtractor, any minute changes in magnetic field will affect the output such that a small sinusoidal voltage may be present when a small magnetic field is present, making the sensor much more sensitive by increasing the current it can pass and increasing the effective output sensitivity. These minute changes are detected by the lock in amplifier or phase sensitive detector; the PSD required a timing square wave in order to function. This square wave is exactly in phase with the subtracted output; the PSD effectively multiplies the small sine input by the square wave, rectifying it if it is in phase, after being low pass filtered, the average DC component of the rectified wave becomes the output from the PSD. The magnitude of the sine wave is proportional to the output from the low pass filter, meaning the PSD and LPF act as a sine magnitude to DC converter; albeit a very accurate and sensitive one. The main advantage of a PSD over a simple RMS to DC converter is that it is far more sensitive, although requires much more complex calibration; the PSD rejects signals which are not sinusoidal or in phase with the reference which mean the device can effectively detect a small sine wave hidden in a mix of larger magnitude wide frequency noise. The concept of the phase sensitive detector or lock in amplifier can be seen in figure 4.12, with all components included, extracting a small signal hidden within noise, with the circuit diagram shown in figure 4.13.

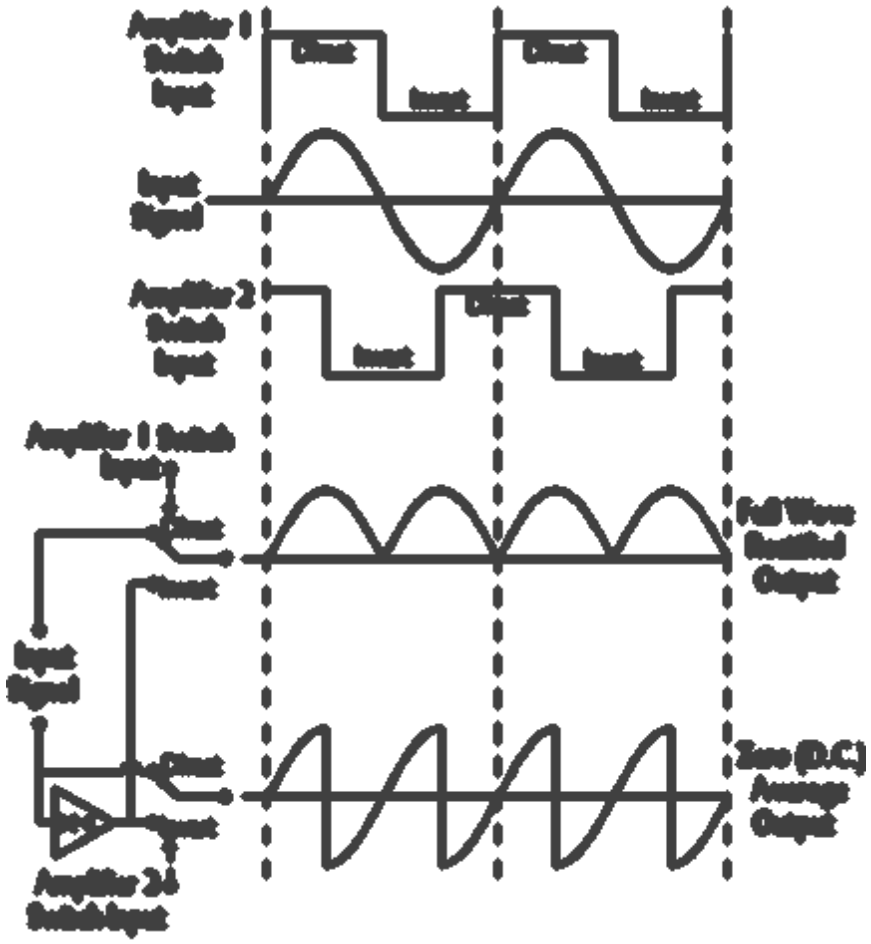

Figure 4.12 Concept of a lock-in amplifier. The addition of a low-pass filter produces a voltage offset proportional to the amplitude of the input wave if it is in phase and of the correct frequency. Acquired from Cairn Research. (http://www.cairnweb.com/manuals/patchman/mcm2.html).

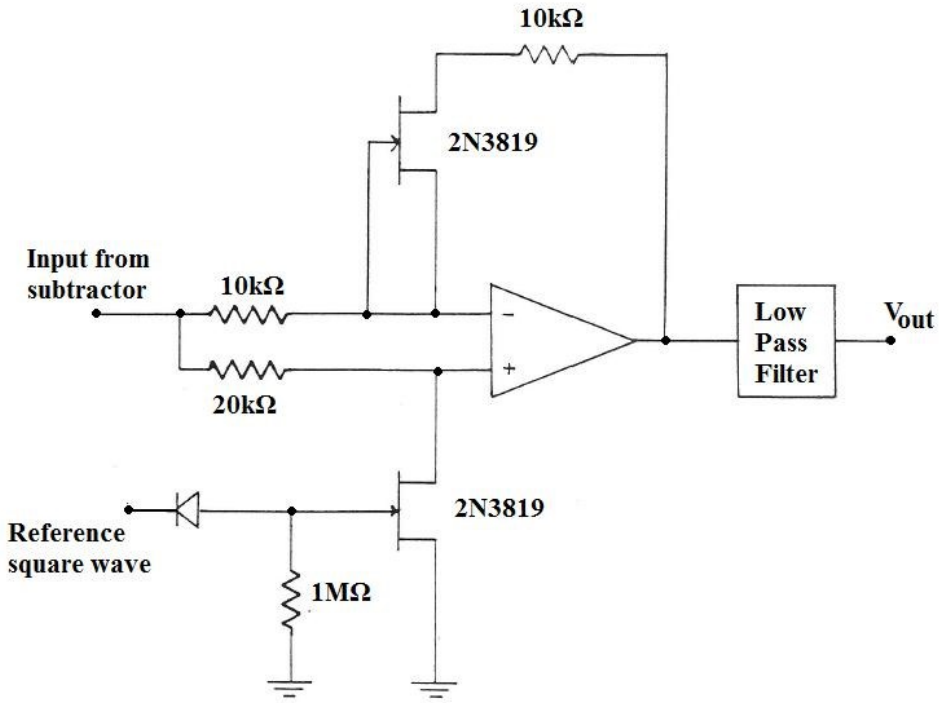

Figure 4.13 Phase sensitive detector circuit diagram

4.2.16 Sine to square wave converter

As mentioned above, the PSD requires an in phase and frequency matched input reference signal, therefore a sine-to-square wave converter was designed and built which take the output of the Oscillator, as it is at the exact frequency of the system, and converts it to a square wave. This wave is phase shifted to match the output phase of the Subtractor; the sine to square wave converter is essentially a a non-inverting amplifier circuit acting like a comparator, which switches to detect which input is larger; in this instance there is a threshold on one of the inputs which is fixed and set to enable the output switches whenever sine changes from positive to negative, shown by figure 4.14.

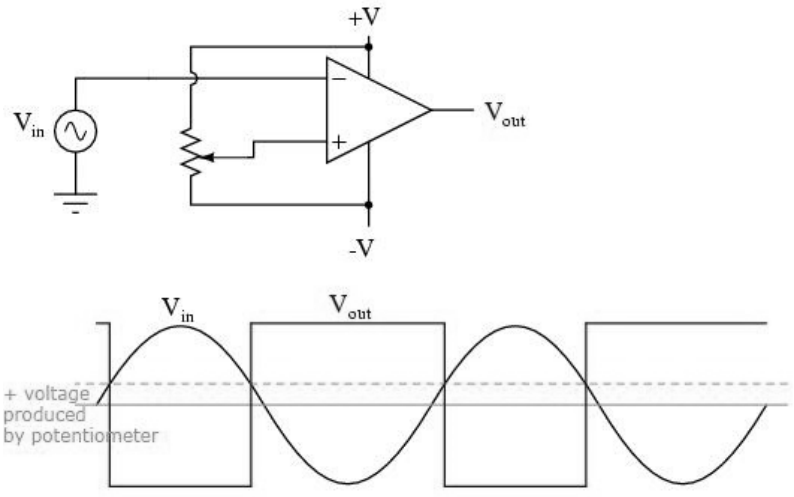

Figure 4.14 Sine to square wave converter circuit and output.

4.2.17 Low pass filter

The low pass filter is vitally important in converting the PSD output into a measurably DC output rather than a rectified sine wave; this is a simple 2nd order low pass filter in Sallen-Key configuration (figure 4.15) based around an operational amplifier and passive components. The filter is set to have a cut off frequency of 10 hertz, which allows the change of output with a detected magnet without delaying the change in amplitude, while removing all of the sine component, producing a DC component proportional to the peak of the rectified wave. This output can then be sampled to digital by an analogue to digital converter and processed via a microprocessor.

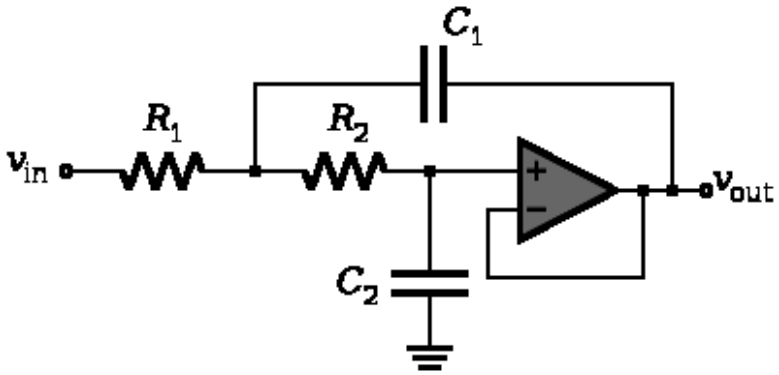

Figure 4.15 Sallen Key second order low pass filter Circuit diagram.

$$f_c = \frac{1}{2\pi\sqrt{R_1 R_2 C_1 C_2}} \quad (4.18)$$

With R1 and R2 both 16 Kilo Ohms and both capacitors 1 µF, the cut off frequency is 9.947 hertz; more than suitable to cut off any remaining oscillation from the phase sensitive detector. The cut off frequency is calculated using equation 4.18.

4.2.18 Voltage rail

The sinusoidal wave ideally should be AC coupled and have a positive and negative component, therefore all operational amplifiers and other ICs in this system must have a dual supply of positive and negative 9 volts. A voltage inverter was used to invert the positive power input to the system, be that from a 9 volt battery or mains input 9 volts from a medical grade transformer. The inverter created an opposite and equal voltage with reference to ground, thereby creating a dual supply power rail for the system ; this circuit as shown in figure 4.16 uses an Intersil ICL7660 IC in an 8 lead PDIP arrangement for socket mounting.

The combined circuitry for the AC system is shown soldered onto custom designed 2 layer printed circuit board in figure 4.17.

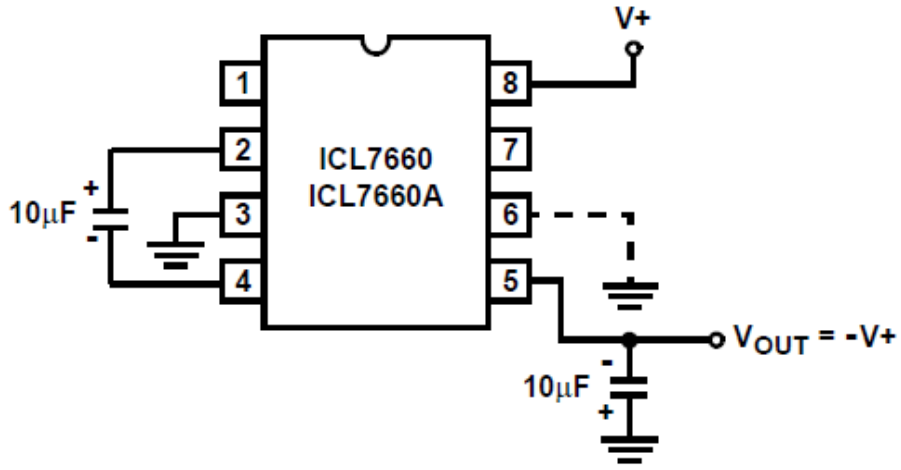

Figure 4.16 Voltage rail circuit diagram.

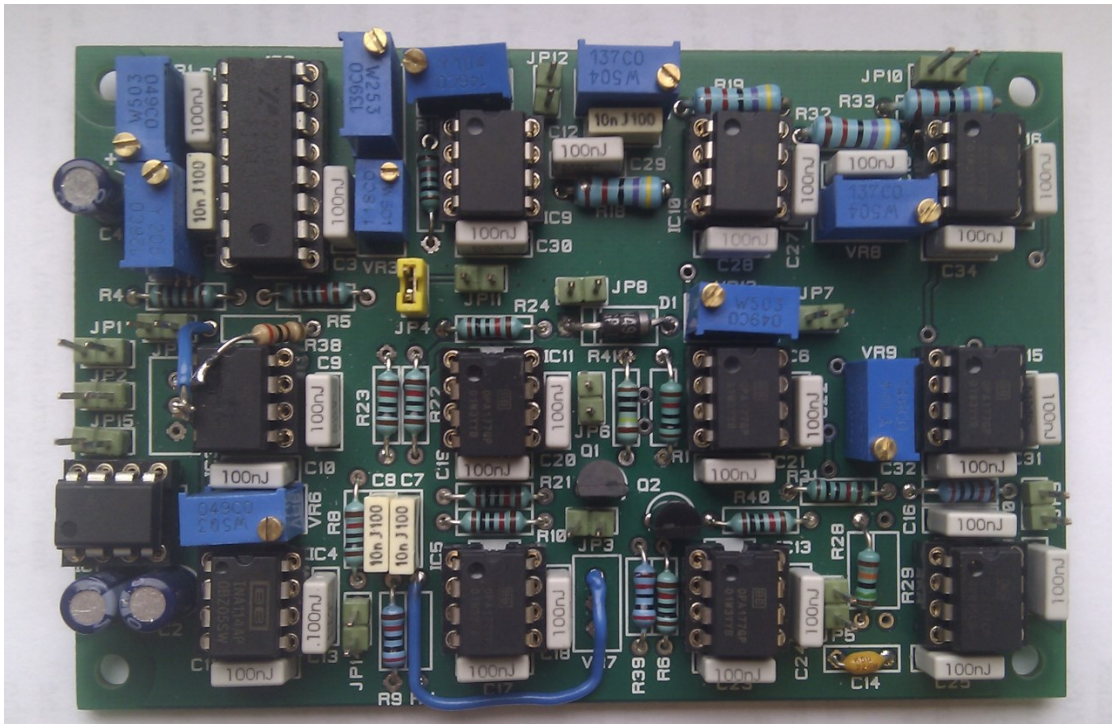

Figure 4.17 AC circuitry with components.

Calibration of the AC circuit as shown in figure 4.17 requires complex set up, which is why the circuit contains a lot of trimmable potentiometers. The potentiometers in the circuit set, in no particular order, the frequency, amplitude and phase of the initial sine voltage, the gain of each amplifer, the phase for each phase shifter, the cut off frequencies for the filters and the symmetry of the square wave. Thankfully the calibration of the AC circuit is only required upon initial set up.

4.2.19 Passive amplification of the magnetic field with Flux concentrators

In order to increase $G_{magnetic}$, flux concentrators can be employed, whereby a ferromagnetic material is placed in-between the sensor's Hall element and the magnetic field source, amplifying the magnetic field at the sensor.

The amplification of the magnetic field for magnetic sensors was first detailed in a US patent filed in 1982 (Pitt et al. 1983), where Pitt et al detailed the manufacture of small Hall effect sensors with integrated metallic element which was designed to

decrease hysteresis and concentrate the magnetic field; this patent did not claim that the magnetic elements could amplify or increase the external field, instead they described the benefits of including such a material. In 1986, Pitt and Extance filed a United States patent entitled Hall Effect Device with Overlapping Flux Concentrators, detailing the addition of a flux concentrating apparatus to a standard Hall effect sensor (Pitt & Extance 1986). The patent highlighted the benefits of having an integrated material which is highly magnetically permeable in order to amplify the external magnetic field; it is believed that this sparked the research into magnetic flux concentrators, which due to the development of improved designs, now significantly amplify weak magnetic fields.

A review of Hall effect sensor technology was published in Sensors and Actuators by Popovic in 1989 (Popovic 1989), which detailed the current technology and problems associated with accuracy and linearity; this paper has a small paragraph in which the author mentioned the potential for the technology to be used with "magnetic flux concentrators", however it appears that the author included this paragraph with a view to overcome the above inaccuracies with the technology rather than amplifying magnetic fields. Popovic appears to coin the phrase Flux Concentrator (FC) in this paper, and goes on to be a leader in the field of FC research.

A doctoral thesis was submitted by Blanchard in 1999, who, under the supervision of Popovic, performed cutting edge work into the development of FCs (Blanchard 1999); detailing the relative importance of shape, thickness, orientation and gap between FC pairs when used in conjunction with Hall effect sensors.

In 2001, Popovic published a paper detailing a fully integrated Hall effect device containing several Hall effect elements and a pair of flux concentrators (Popovic et al. 2001); these concentrators were used to orientate the field, however it was pointed out that when aligned such that the gap between two ferromagnetic flux concentrators was small and placed on top a Hall effect element, the field in the gap was up to five times stronger than the external field upon the sensor; the first mention of the application of FCs as passive magnetic field amplifiers.

A year later, Drljaca published a paper with Popovic et al, describing the design of planar flux concentrators with which to increase Hall effect sensor's sensitivity (Drljaca et al. 2002). This paper went into significant detail regarding the design of FCs; the shape of FC pairs is important for field amplification, with Tanga pairs (figure 2.18) calculated as providing the best amplification of field. The amplification of a 5 mT field with the traditional bar-shaped FC pair was 10 fold, to 50mT, whereas the tanga-shaped FC pair amplified the same field to 120mT. The paper describes that for both simulation and experimental FC pairs, the gap width is important, with decreasing gap size leading to larger amplifications; the limit of gap manufacture in the experimental set up was approximately 2 micrometres. The use of two pairs of FCs, a micro and macro pair, ensured the correct alignment of FCs to the Hall effect sensor. With regards to amplification saturation, Drljaca showed via simulation that although the FC pairs could significantly amplify an external magnetic field, above 5-10 mT, the amplification became saturated and was not linearly correlated with field strength beyond this limit. As a final note, the author reminded the reader that optimal design was a trade-off between sensitivity and saturation, as amplification was saturated at a given design of FC pairing, and that the application may lead to saturation of the FCs and Hall effect sensor if too strong a field is present.

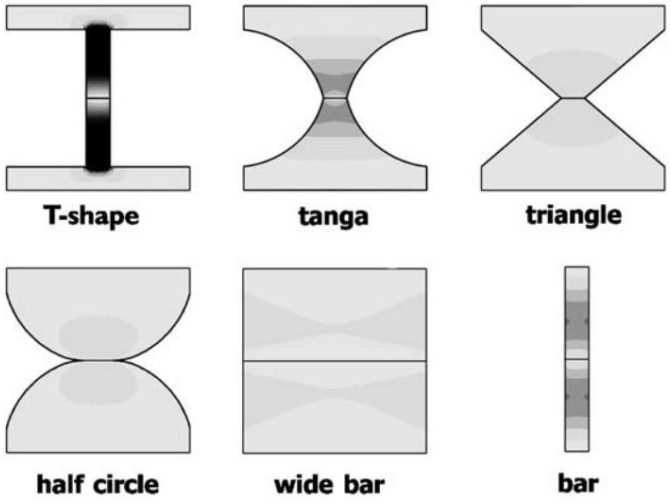

Figure 4.18 Flux concentrator shapes in literature. (Drljaca et al. 2002)

That same year, Edelstein published a paper detailing the use of permalloy FCs to reduce 1/f noise in magnometer applications (Edelstein & Fischer 2002); this paper shows the onset of high permeability materials as flux concentrators, while the author was researching noise reduction as an application as opposed to amplification, it shows the use of Permalloy rather than the ferrite based FCs as traditionally used. Permalloy is a nickel-iron magnetic alloy (80% nickel and 20% iron content) with a very high magnetic permeability. Frequency dependant magnetic permeability is important for concentration of electromagnetic fields for such applications as passive RFID tags, where frequency specific ferrite cores concentrate EM waves from the reader in order to charge a capacitor for data transmission.

For angle based magnetic field detection, FCs were also developed (Demierre et al. 2004), which facilitated the angular measurement of a magnet based on a cross-shaped FC and multiple Hall effect sensors; demonstrating the increase in FC research and development for commercial application.

A matrix of 16 High sensitivity FC based Hall effect sensors were used by Stathopoulos in 2005 to measure the passage of a 6 millimetre diameter by 7 millimetre long magnet through the stomach and intestinal tract. The desire of this paper was to track a magnet to a rough area rather than know its precise location, therefore the position error was acceptable although it would not be acceptable when measuring the position of the SCJ.

A paper by Leroy et al published in 2006 described in great detail, the work performed by their group into simulations to improve the amplification of magnetic fields using flux concentrators (Leroy et al. 2006). The paper featured rod concentrators, in between which a magnetic sensor was to be placed; this work derived many equations and deduced several important conclusions for the design of FC pairs. Length to diameter ratio is very important with regards to rod shaped FC pairs, as narrow regions need to be a minimum length in order to maintain flux. A length-to-diameter ratio of between 100 and 500 provides optimal design, although the application can limit the FC length; the range is given as increasing magnetic permeability of the material allows for increased gain with longer length, when lower permeability materials may not.

The important factors for the novel design is concentrator length, radius and cylindrical-shape regions, extending beyond the limiting factors of material permeability. The magnitude of magnetic permeability can vary significantly, ranging from basic ferrite ($u_r=10^3$) to magnetic irons ($u_r=10^6$), with the higher the permeability the better the gain for a given FC design. The airgap, or gap between FC pairs where the magnetic sensor would sit, is a factor when deducing the limit of the system gain, with the gain increasing exponentially as gap width decreases below 0.4 millimetres; unfortunately the use of a magnetic sensor in the gap between FCs often limits the practical width, otherwise gains of several 1000 can be achieved. In addition to the above factors, it is explained that amplification can be increased beyond that limited by relative permeability of FC material, with geometry of FC extending the amplification; in this case cylinders with conical end and blunt tip, much like the shape of a blunt pencil, provided the highest simulated gains. Ferrite cores are often cast into desired shapes but they can also be ground by specialised material; the cost for producing custom shapes is high due to detailed manufacture techniques, minimum order quantities and tolerance levels. The brittleness of ferrite means it often shatters when trying to produce custom shapes without said specialist equipment.

In 2009 a paper published by Griffith, describes the testing of ferrite and mu-metal flux concentrators (Griffith et al. 2009); the rod ferrite and triangle mu-metal FCs have relative permeability of 6000 and 30000 respectively, with a gap of 2 millimetres in between which a vapour cell is placed. The paper shows the simulation and testing of such FCs for a specific application, however this experiment investigates the relationship between frequency and sensitivity, showing that although the materials have frequency dependant permeability, they still offer sufficient amplification across a wide bandwidth.

It has been demonstrated in the literature that a weak magnetic field can be amplified greatly with the use of carefully designed flux concentrator pairs; the relative permeability of a material can, along with geometry, increase the gain of a magnetic field significantly. The gap between FC pairs is often limited by placing a sensor in between them, however if the gap can be minimised, the gain will be higher. It was

also noted that several papers briefly mentioned pair alignment, with misalignment of FC pairs, significantly reducing their amplification ability. It has been proven that FC facilitated the detection of a magnet in the digestive tract, from outside the body, albeit at low precision; the inclusion of Flux Concentrators combined with high sensitivity Hall effect sensors for this doctoral work is vital in order to minimally invasively measure the position of the SCJ accurately.

4.2.20 Magnetic field simulation

In order to test novel designs of flux concentrator for this application, ViziMag 3.17 was acquired; ViziMag is a Windows-based software, designed specifically to provide efficient and accurate visualization of magnetic circuit field lines and flux density. The software was constructed with the objective of intuitive and rapid model creation, with both calculation and display of field lines and flux density in line, graph or colour contour visualisation. The software enables the user to design and calculate complex two dimensional magnetic constructs based on permanent magnets and magnetically permeable objects; ideal for the testing of design and calculation of magnetic field amplification using magnetically permeable FCs and a small permanent magnet at large distance. The user is required to graphically set up the magnetic flux and permeability regions to scale, after which the simulation and calculation can be run; the mouse can then be moved over any region of the line or colour contour plot to determine the magnetic field at any location within the field of view.

The limitations of the software are the two dimensional calculations and the ability to construct only polygons with straight lines rather than curves, however accounting for these limitations, the software still provides an incredibly useful insight into the magnetic gain ability of flux concentrators.

4.2.21 Flux concentrator amplification with differing shape and size

As the literature suggests different shapes for optimum design, notably triangular or cone shape FC pairs, these are compared against square and rectangular shaped FCs,

both in pairs or individually either in front of or behind the sensor. Also gap distance and alignment are examined in detail to the practical level, in order to validate previous findings. The output of the calculations allows the visualisation of the magnetic field along the magnetic axis, which shows the relative amplification when using FCs as a line graph plotted with field strength against distance pointing along the North pole, towards the FC and sensor. The colour contour plot is also included which allows for very clear visualisation of the field amplification around the magnet and FCs; the gain at the sensor point is also tabulated, as this is the important factor in determining FC efficacy. The shapes tested are tabulated in table 4.2, results can be seen in figure 4.33 and 4.34.

4.2.22 Practical flux concentrators

Following simulation which validated the findings in literature with regards to shape and pairing, the next step was to manufacture the FCs for experimental bench top validation. There were several constraints to producing said FC designs; the two dimensional nature of the software calculations meant it was unclear if the FCs should be rectangular in nature or cylindrical. The permeability of a FC in the software could be designed and tailored by simply entering a different value for relative permeability, however the range of relative permeabilities in manufactured material was somewhat limited. The frequency dependant nature of permeability was often tailored to high frequency applications such as transformer cores or RF inductor centres, meaning sometimes there was only data for high frequency relative permeability rather than at very low or permanent magnet frequency.

The most commonly available FC material was ferrite in the form of rods, used for RFID cores; the ferrite rods had relative permeability of between 100 and 600, similar to that used in the simulations. The rods were tested using a 2mm diameter 1 mm long N42 magnet fixed in position at a given distance from the sensor or FC, if one was placed in front of the sensor. The field strength was measured with the constructed and calibrated AC. The zero was performed with the apparatus set up and no magnet present; a control measurement was taken with the magnet at a fixed

distance from the sensor, for comparison when calculating the gains using the variety of FCs.

The Ferrite rod shapes were the only commercially available form of high magnetic permeable material (Dexter magnetic technologies ,UK); the other mu-metal type materials were not available in anything but vast quantities and were therefore not viable. Custom designed ferrite shapes were available, however these were produced at vast cost to the buyer and since the application was small, with each shape demanding a large fee, the custom design was not financially workable. In order to test conical or triangular shapes, the rods were machined by a trained workshop engineer; the shapes were limited by fragility and size of the rods, however a method was developed by grinding the tips of the rods down producing the pencil shapes mentioned by Leroy et al. The variety of shapes were tested and compared versus those simulated shapes where similar; the results of which can be seen in the associated section below.

4.2.23 Size and shape of internal magnet

Upon testing the fully calibrated sensor system with the magnet used with the internal SCJ locator probe, it was clear that the maximum effective range was too small, and even though in some people, the magnet could be detected given ideal alignment and orientation, it would be on the edge of the detection range, making the external locator unreliable. According to the Hall equation, the output of the sensor was proportional to both the current through the system, and the magnetic field to which it was subjected; since the current had been increased such that the output was as high as it could be, the magnetic field is the only other parameter which could be increased. The increased sensitivity is directly proportional to the effective magnet detection range, therefore by increasing a magnetic field, the distance at which that magnet could be detected increases. A magnet's strength is predominantly determined by the material it is made out of and the volume of said material; the shape of a magnetic field outside the magnet is also influenced by its shape. There are other factors which affect a magnet's field strength, such as temperature, but as these are essentially fixed within such conditions, they are assumed to be constant.

The magnitude of a magnetic pole is determined by the material due to the magnetization properties of said material; Magnetic susceptibility is a dimensionless proportionality constant, indicating the extent of magnetization of a given material when exposed to an external magnetic field. A related term is magnetizability, the proportion between magnetic moment and magnetic flux density. A similar parameter is the magnetic permeability, discussed above, which expresses the total magnetization of material and volume. There are more magnetically susceptible materials, which produce stronger permanent magnets when exposed to a strong magnetic field; ferrite magnets are fairly strong, however proprietary rare earth magnets have higher magnetic susceptibility, producing the strongest magnets per size. Since the current SCJ locator probe magnet is a 2 millimetre diameter by 1 millimetre long disc shaped Samarium Cobalt rare earth magnet, other than investigating stronger grades of rare earth magnets, which require custom production, the size must be increased in order to obtain a stronger magnetic field to enable the detection of the magnet at a greater distance.

4.2.24 Orientation

Since magnetic sensors are directional, due to the directionality of the north-south pole principal of a magnetic field, if the internal magnet rotated away from the sensor, it would provide a much weaker field, so the magnet inside the body must be oriented towards the sensor for maximum sensitivity and range. This can be done using another external magnet, which if placed on the opposite side of the body and of sufficient strength, would orientate the internal magnet while not saturating the sensor.

As has been shown in a previous chapter, the Hall effect sensors are very directional and the direction of the north-south pole has significant bearing on the ability of the sensor to measure the magnetic field. The internal magnet is not as close to the sensor as in the catheter based SCJ locator probe; while the orientation of the magnet was not much of an issue when the magnet was within 10 millimetres of the probe due to the relative field at this distance, the external locator is must more susceptible to misalignment of the poles to the sensor. Benchtop tests, investigated the issue of

alignment of the magnet to the sensor, measuring the output when a magnet was displaced along both parallel axes from an original starting point directly over the magnet. Also rotation of the magnet away from an individual sensor was performed, which would determine the importance of magnet orientation towards the sensor. It was evident from the results that small displacements or rotations severely inhibited the sensors output and therefore detection range; a technique was designed and developed which maintains the internal magnet's alignment with the sensors outside the body, minimising the issue of magnet rotation.

4.2.25 Alignment technique

Two separate magnets have polar opposite attraction, that is, two magnets will align and attract with each other subject to distance between them, their magnetic field strengths, weight and other factors. The alignment force comes into effect before attraction, at the fringe of the field; this is why compasses align with the earth's magnetic field as the relative attraction between them is weak at this level, but while suspended on a medium in which they can rotate with low friction, the magnetic needle of the compass aligns with the relatively weak surface field of the Earth's magnetic field. Magnets exert forces and torques on each other due to the laws of magnetism, for small fields the interaction can be modelled using the equation 4.19,

$$F = \frac{\mu q_{m1} q_{m2}}{4\pi r^2} \tag{4.19}$$

Where F is force in newtons, q_{m1} and q_{m2} are the magnitudes of magnetic poles, μ is the permeability of the intervening medium and r is the distance between the two poles. The force between two magnets is directly correlated with the ability of two magnets to alighn, however the force must be sufficiently great to overcome any forces opposing rotation or movement; such forces may be friction from the surface on which the magnet is lying or gravity. The force between the magnets is essentially determined by the strength of both magnets and the distance between them; the distance is a strong determinant as it is a squared factor, however this is fixed for this environment, or at least for an individual. Again the permeability of the intervening tissue; as detailed by the literature, the permeability of the body is similar to a

vacuum (Wu et al. 2005; Weitschies et al. 1994; Guo et al. 2008) or that of air (Sinatra 2010; Wang et al. 2006), both of which are very similar indeed, and when used in this context, the difference between the two becomes highly insignificant when compared to large values of the magnitude of the poles and the distance between them. The remaining variable in the formula is the magnitude of the two magnets; the higher the strength of the magnets, the greater the force at a given distance. As one magnet is placed inside the body, at the SCJ within the oesophagus, its size is limited; the magnet may be increased in size from the one used currently but it is important not to increase the size to such a degree that it may inhibit swallowing, LOS competency or other motility aspect. The remaining factor therefore is the strength of the external magnet; this magnet can be made sufficiently large that it may orientate an internal magnet from outside the body. The magnet must also not inhibit the movement of the internal magnet, otherwise it will be invalidating any readings made; a long bar magnet was used to ensure the magnet could move up and down without any friction from the magnet, as the bar magnet is magnetised such that the north and south poles are magnetised on the face of the magnet. The magnet used for external orientation was a Neodymium N42 Bar magnet of 50 x 25 x 10 millimetres (EP648, eMagnets, UK); this gives 5 centimetres of axial movement, however if required, either custom magnets can be developed giving longer axial length and movement, or multiple magnets of the same type can be held together end to end to double the axial length.

The small internal magnet is also attached to the SCJ via a clip, as this procedure is well established with the current SCJ locator probe; the orientation of the magnet may be somewhat limited by the ability of the clip to rotate about the mucosa to which it is attached, a property which is determined by the amount of mucosa within the endoclip jaws, something which is highly variable. The friction from the sphincter, if the SCJ is within or near the LOS, may also limit the alignment movement and rotation; it was therefore decided to develop a method of attachment which would allow the complete and low-friction rotation of the magnet within the oesophagus to facilitate the optimal orientation from the external magnet. Redeployable clips were used as they could be repositioned if clipping was not satisfactory in the first instance.

4.2.26 Magnet Orientation

In order to determine force required to orientate a magnet using another magnet or magnetic field, the attracting/repelling force must be established to explain the relationship between two magnets at distance. The magnetic flux density very close to each pole, in T, is represented by equation 4.20. The force between two magnetic poles is simply represented by equation 4.21, where F is force, N, q_{m1} and q_{m2} are the magnitudes of magnetic poles, A/m, μ is the permeability of the intervening medium, r is the separation.

$$B_0 = \frac{\mu_0}{2} M \tag{4.20}$$

$$F = \frac{\mu q_{m1} q_{m2}}{4\pi r^2} \tag{4.21}$$

This is a good approximation while the two poles are close however for a large separation, the equation must be expanded to the following. The force between two identical cylindrical bar magnets placed end to end is approximately (while x is large), is shown in equation 4.22.

$$F = \left[\frac{B_0^2 A^2 \left(L^2 + R^2\right)}{\pi \mu_0 L^2}\right] \left[\frac{1}{x^2} + \frac{1}{(x+2L)^2} - \frac{2}{(x+L)^2}\right] \tag{4.22}$$

Where B_0 is the magnetic flux density very close to each pole, in T, A is the area of each pole, in m^2, L is the length of each magnet, in m, R is the radius of each magnet, in m, and x is the separation between the two magnets, in m. The above equation allows calculation of the force from two identical magnets and can be broken down into two main components, the attraction component, F_a, which describes the interaction of the magnets as determined by their surface strength, and dimension (equation 4.23) and the distance (equation 4.24) component, F_d, which is a power-law scaling factor for the force equation over given separation. For 13mm x

13mm samarium cobalt magnets over a separation of 10cm as an example, the force output is 0.35 Newtons, the equivalent of 35 grams.

$$F_a = \frac{B_0^2 A^2 (L^2+R^2)}{\pi \mu_0 L^2} \tag{4.23}$$

$$F_d = \frac{1}{x^2} + \frac{1}{(x+2L)^2} - \frac{2}{(x+L)^2} \tag{4.24}$$

Assuming this is enough to orientate a magnet, the force between two magnets can be calculated. The attractant component is a more complicated version of $\mu q_{m1} q_{m2}$, and compensates for the dimensions of the magnet. The simplification of the attractant part is allowed due to the identical nature of the magnets, so the following was performed to allow the calculation using different size magnets, resulting in equation 4.25.

$$\frac{Bo_1 Bo_2 A_1 A_2 \left((L_1 L_2)+(R_1 R_2)\right)}{\pi \mu_0 (L_1 L_2)} \tag{4.25}$$

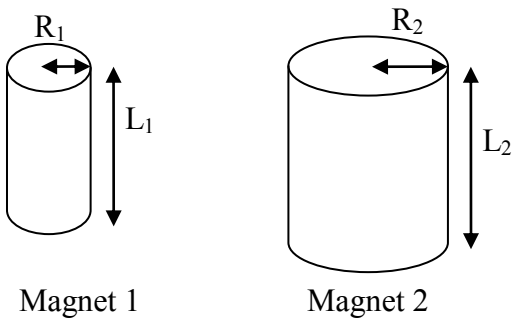

Figure 4.18 Magnet length and radius demonstration.

So for A_1A_2 to equal A^2, if A_1 is halved in size, A_2 must be doubled. For a 2x2mm magnet the other magnet must be 50x50mm in order to have the same force, this principle is shown in figure 4.19.

Experiments were performed to determine the force needed to orientate a small magnet using a larger magnet against the force of gravity, as shown in figure 4.20. Force can be calculated from the separation at which the smaller magnet pivots to become orientated, as both magnet sizes and strengths are known. While the main force opposing the magnet alignment here is gravity, it is possible that the friction of

a tight sphincter could also inhibit magnetic rotation, therefore this force is a minimum, and where possible would be greater than this value. The external magnet would have a maximum size, so not to attempt to pull the magnet towards it and through the patient; likewise it would not want to inhibit axial movement.

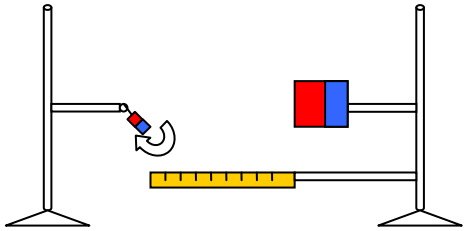

Figure 4.20 Experimental set up to measure the magnetic force required for alignment between a small magnet and a large magnet at distance.

4.2.27 Encapsulation

Initial testing on bench top, showed that the bar magnet could orientate a small magnet at a large distance; this experiment was performed such that the opposing force of the magnet was simply gravity. It is evident that within the LOS or oesophagus, the forces acting against the magnet's rotation will be greater than this, however it is almost impossible to measure the force against which a magnet can turn; the force is also augmented by the endoclip attachment to the oesophagus, which can limit the rotation of the clip and hence magnet. The force of the LOS varies, with an average of 35 mmHg; it is safe to assume that this force, acting on a magnet, is sufficient to hold the magnet in place rather than letting it rotate with an external magnetic field. The force opposing rotation is likely to be large, therefore in order to overcome this issue, a magnet encapsulation method was designed and developed, which allowed the low friction movement of a magnet inside a solid capsule, which could be attached to the SCJ via the traditional clip method. The solid capsule will allow rotation of the magnet in all angles, allowing the small internal magnet to be aligned with the external bar magnet, despite all forces pressing against the solid capsule. There are a number of constraints on the capsule design, firstly it must not be hazardous to the subject, be it through sharp edges nor poisonous or toxic material; secondly the capsule must be sufficiently strong to withstand pressures of 40 mmHg or above, while still allowing the magnet to rotate; thirdly the

capsule must have in place a method of attachment and detachment to and from the mucosa of the oesophagus. Initially it was proposed that a small cylindrical magnet could be placed inside the capsule, however upon further investigation, spherical magnets were found and purchased, around which the capsule could be made, while allowing very low friction movement. The material choice of the capsule, was investigated, with several safe plastics being highlighted but the cost of manufacture of custom three dimensional plastic parts was significant when injection, blow or compression moulding were used; the cost was increased by the small complex nature of the designs. An alternative low cost manufacture process was therefore desired, with three-dimensional printing or rapid prototyping an obvious choice, however the cost for several small hollow spheres, produced in halves so that the magnet could be encapsulated, was over several hundred pounds; the structure of rapid prototyped plastics are weak as they are manufactured a layer at a time, which causes issues when the magnet needs to be attached using a reliable method. Finally, a polymer called Polycaprolactone (PCL) was discovered, it is a biodegradable polyester with a low melting point of 60^{o} Celsius. This material is perfectly safe for use within the gastrointestinal tract, as it has previously been used for encapsulating drugs for targeted delivery, therefore the breakdown of PCL within the body is safe. The low melting point of this polyester means it is easy to work and can be moulded by hand; initially several prototype designs were hand moulded around a magnet, with increased reliability and repeatability with gained experience. The hand moulded capsules allowed the rotation of the magnet within; this was confirmed by shaking the resolidified capsule, with a rattling noise confirming the freedom to rotate. In order to attach the capsule to the LOS, the capsule had small protrusions on opposing sides, with small 1 millimetre diameter holes drilled through, which allowed the threading of surgical suture strand; the strands were tied in the form of a large individual loops. The magnet and capsule were passed into the oesophagus on the end of a long catheter, in parallel to an endoscope, through the working channel of which, a standard endoclip and firing device was passed; the clip was positioned such that a loop of suture was caught in the jaws of the endoclip, which was then attached to the SCJ using the normal firing technique. The process was repeated with the other loop, ensuring the magnet and capsule didn't move from its position

straddling the SCJ. The biodegradability of the capsule and suture materials meant that the clip wouldn't stay attached for too long; the issue of permanent magnet attachment was raised in a previous chapter, so this problem could be avoided without the requirement of magnet removal surgery. PCL is biocompatible however its degradability is increased when mixed with starch, a process which could be employed in future clips, should the clip not fall off within the required time; the amount of starch in the mixture could be tailored to provide a more repeatable degrading and hence detachment time, best suited to the requirements of the experiment. The magnets chosen for spherical nature, size and strength were a 6.4 millimetre diameter N38 Neodymium sphere magnet, with a 2.5 kilogram pull force, stronger than the magnet tested meaning it should be more likely to align, with the added benefit of being detected at a greater range when used with the AC Hall effect device. The overall size of the magnet and capsule was approximately 10 millimetres across; a sufficiently small size not to interfere with the LOS action, nor will it cause issues for motility, as the larger Bravo Capsule is used in the oesophagus with little ill-effect.

4.2.28 Attachment method

The capsule has a small tab through which a hole is drilled, and attached are to two small loops of surgical suture thread: a detachable tube with the magnet at the end will be inserted through the mouth during endoscopy, one or two clips will be deployed through the working channel of the endoscope and be closed around the loops of thread and the wall of the SCJ, anchoring the magnetic encapsulation to the SCJ for measurement. The biodegradability of the PCL and the surgical suture should ensure that the magnet falls off within a few weeks, and usual magnetic screening will take place, like with the smaller magnet used in conjunction with the luminal SCJ locator, to ensure complete passage.

4.2.29 Medically safe power supply

As required, the safety of this device for use in human subjects if paramount; the safety standard BS:EN 60601 set by the Medical Device Directive requires certain

criteria for safe and failsafe operation of medical electrical equipment. In accordance with the required standards, a medical grade power supply was used with this device, which for patient testing will be plugged directly into a Residual Current Device, designed to act as yet another level of safety if the device starts to become unsafe, offering greater protection than fuses or circuit breakers. The device will require microprocessor, and as a precaution, the hardware not in contact with a volunteer will be electrically isolated from the sensor hardware; this is done by way of two voltage regulators providing separate isolate voltage supplies for each part. Figure 4.21 shows the schematic for the isolated voltage regulation using two Maxim Max 667 5V/Programmable Low Drop-Out Voltage Regulators (RS Components, UK).

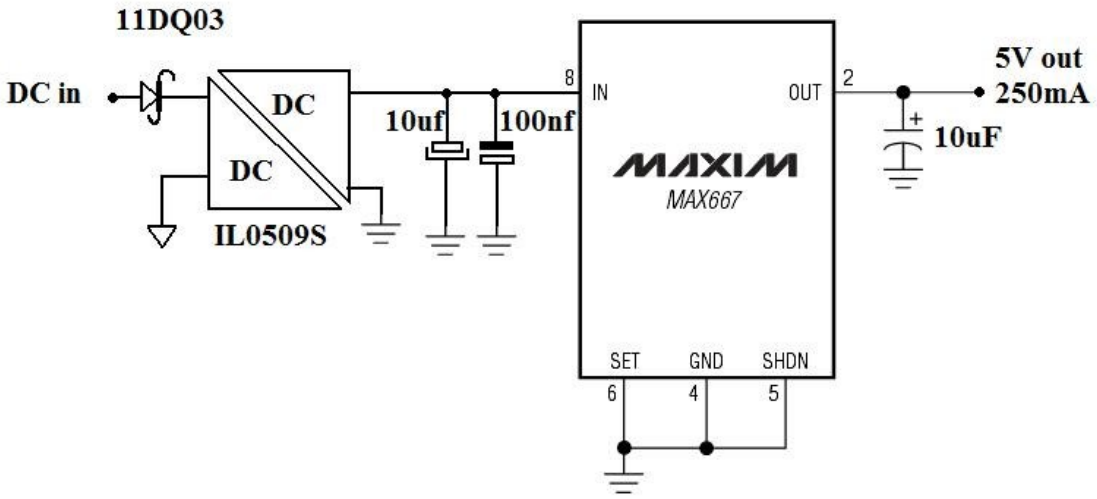

Figure 4.21 Isolated power supply for safe single fault operation.

4.2.30 Differential multiplexer

The initial testing for the AC sensor system was performed using a single sensor directly attached to a differential instrumentation amplifier, however as the axial movement needs to be measured, an array of sensors is required. In order to combine the output of several sensors a differential multiplexer is required, with sufficient differential inputs for the number of sensors in the array. For initial development there are 8 sensors, therefore an Analogue Devices ADG407 LC^{2}MOS Differential 8-Channel High Performance Analog Multiplexer (RS Components, UK) was

employed, as shown in Figure 4.22, to interface between the sensor outputs and the instrumentation amplifier on the analogue processing board.

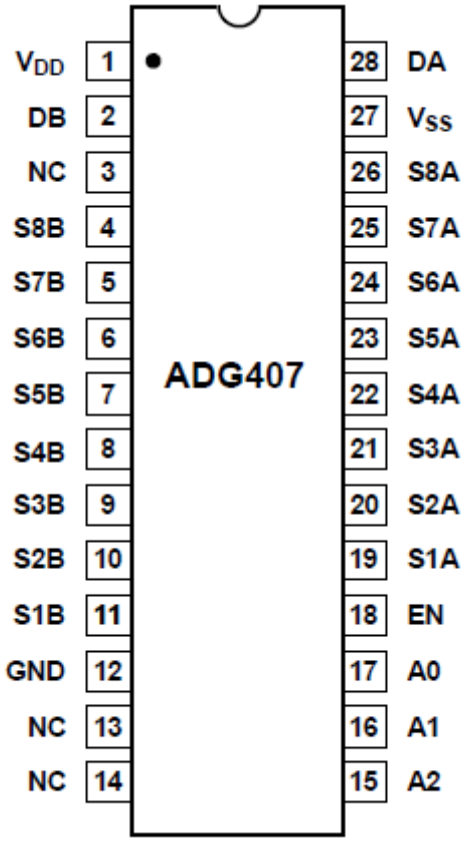

Figure 4.192 ADG407 Multiplexer, with differential outputs SxA & SxB, where A0, A1 and A2 are connected to a microprocessor for channel switching, and DA and DB are the differential output from the selected input pair. Acquired from datasheet.

4.2.31 RMS to DC converter

As an alternative and often simpler method of measuring the output of each sensor, and also for validating the output from the AC circuit, a Root Mean Squared (RMS) to DC converter IC was used; this measured the peak-to-peak alternating voltage, converting the RMS of the sine wave into a DC output. This required no set up other than the initial circuit manufacture and although it was more reliable than the

sensitive AC circuit, however was not as accurate. The set up for the test circuit is shown in figure 4.23.

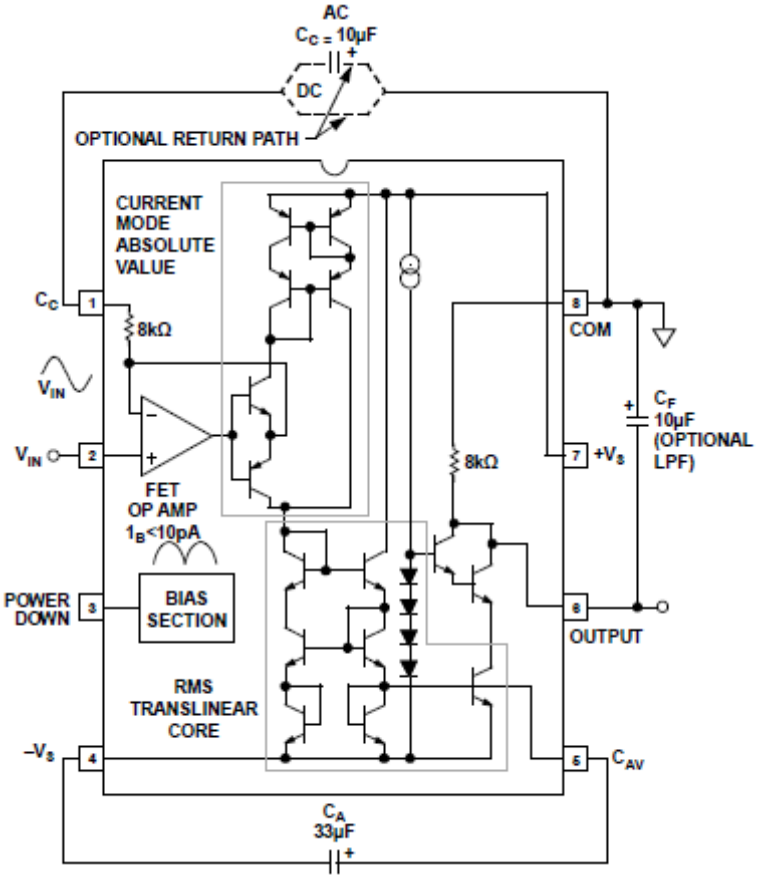

Figure 4.203 True RMS measurement circuit. Acquired from datasheet.

4.2.32 Microprocessor interface

In order to control the multiplexer and sample and process the analogue output from each sensor, a multiprocessor was required. For this task, an Arduino Uno R3 prototyping/development board (RS Components, UK) was employed; the Arduino Uno is a microcontroller board centred around the Atmega ATmega328. The board has 14 digital input/output pins, 6 analogue inputs, a 16 MHz ceramic resonator, a USB connection and power jack as shown in figure 4.24. The Arduino programs are written in C or C++, with the Arduino integrated development environment (IDE) a cross-platform application written in Java. The board is simple to interface and write software for, hence why it was chosen as the basis for the processing portion of the proof of concept prototype for this device. The USB output can be plugged into a

stand along laptop or desktop PC, with the former being safer, as it is not connected to the mains power; alternatively, the data recorded can be stored on a SD card with little addition to the hardware and software interface for portability. The multiplexer is controlled with this board, with the output of the PSD section of the AC circuit board sampled using the board's inbuilt analog-to-digital converter (ADC). The sampled data was used for calculation of the position of the magnet along the sensor array, with the position being interpolated between the two or three highest outputs.

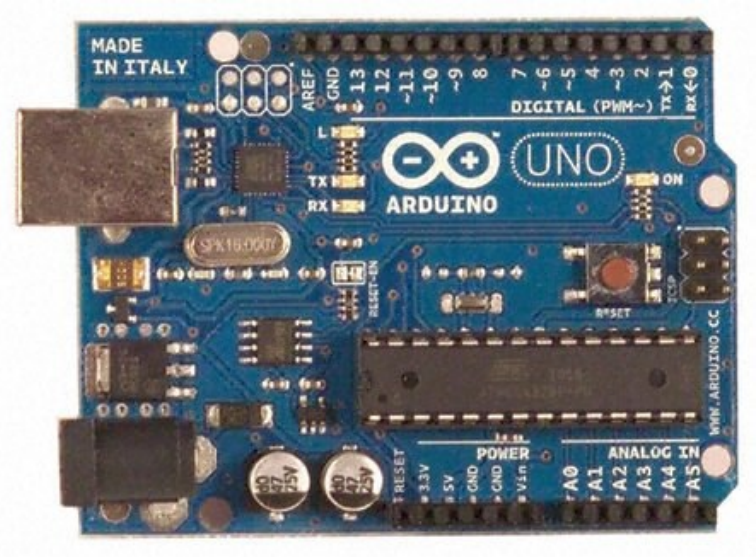

Figure 4.21 Arduino Uno microprocessor board. Acquired from Arduino (http://arduino.cc/en/Main/arduinoBoardUno).

4.2.33 LCD board

Real-time visualisation of the position and signal strength was employed in the catheter based SCJ locator probe and upon discussion with the medical doctors who used it, this feature greatly helped in testing and calibration, therefore it was decided to include an LCD display on this device. The Ardunio board has enough inputs and outputs to drive a LCD with inbuilt controller; a Displaytech 2 line, 16 character backlit monochrome alphanumeric LCD device was used which displayed calibration details when calibrating and signal strength with position measurement when

recording data, the latter two data streams were also outputted to a PC via the USB connection in the board for analysis and graphical display. The addition of an LCD with the possible inclusion of SD card recording capability means that the future generation of the prototype could be entirely portable with a battery pack; the application is subject to the users' intentions.

4.2.34 Microprocessor software

While in initial stages, the software output the values of multiplexed sensors one at a time in raw data format for post processing, a latter stage of the device compared the values from each of the sensors and outputted the value and sensor number onto an LCD screen and in serial data to a PC for validation. It is possible that after *In Vivo* validation, a combination algorithm could be written which is similar in nature to the original SCJ luminal locator, which enables calibration and data output which may be customised to the user's requirements. While no volunteer experiments were performed, a concept diagram can be seen in figure 4.25 which shows how the external apparatus could be set up with the internal magnet in a volunteer. The external orientation magnet is aligned and attached to the sensor array using a plastic C-arm which goes around the patient's abdomen (figure 4.26).

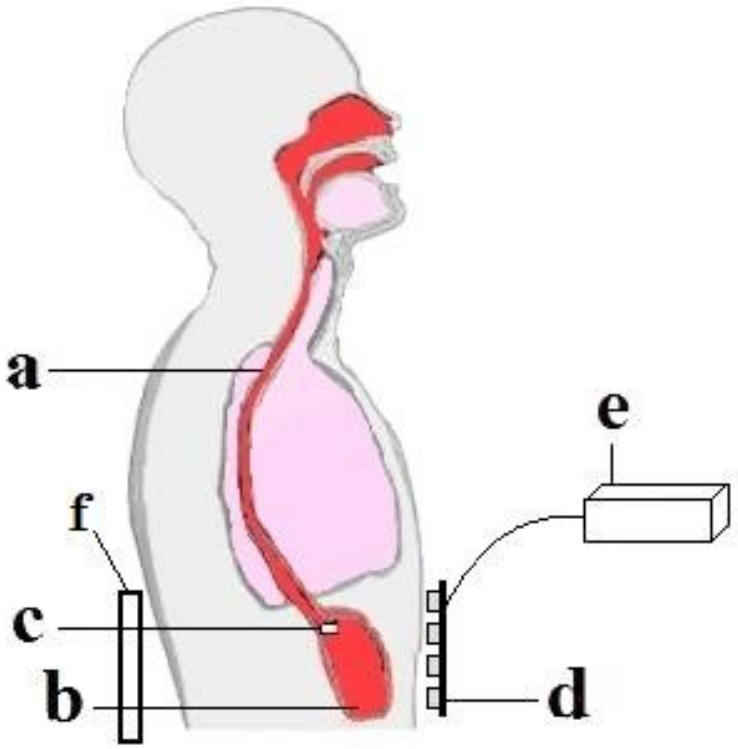

Figure 4.225 Concept diagram of sensor array (d) and supporting electronics (e) with the encapsulated magnet (c) attached to the oesophagus (a) at the SCJ above the stomach (b) and orientation magnet (f).

Figure 4.23 C-arm system with sensor electronics, orientation magnet and microprocessor box with LCD display.

4.3 Results

4.3.1 Hall effect sensor comparison

The implementation of a constant current supply produced much less noisy signals, which meant the values could be measured digitally rather than just visually, while the distance did not increase.

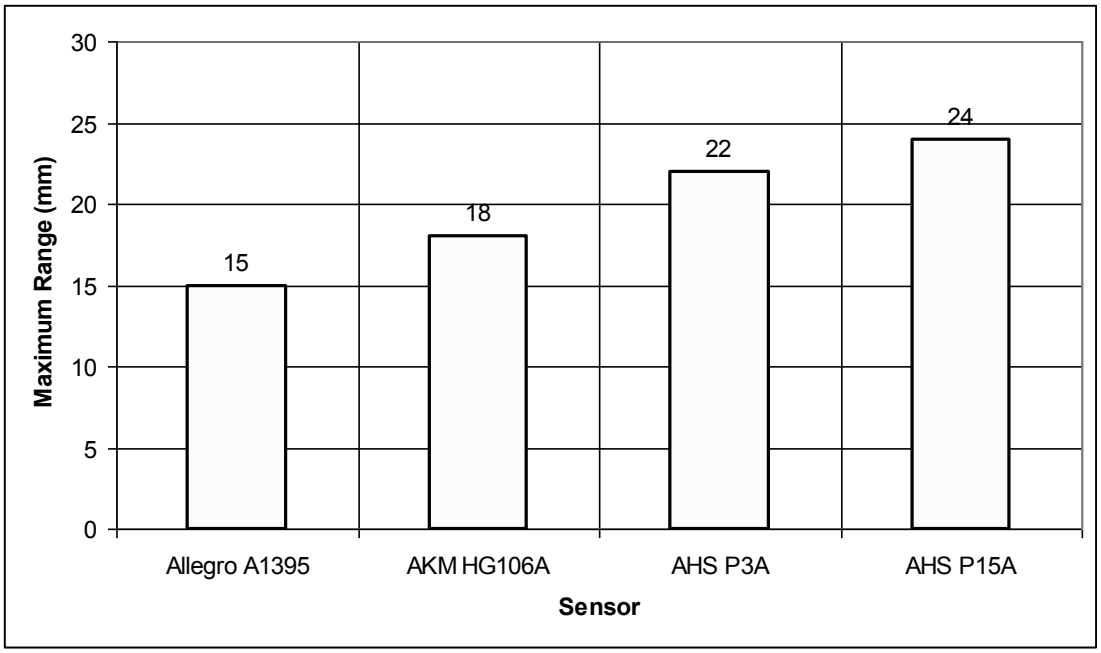

Figure 4.27 Basic Hall effect sensor comparison. 4 sensors were tested with a constant-current circuit as described in section 4.2.1 (figure 4.2), showing the maximum detectable range of a magnet and hence sensitivity for each sensor.

4.3.2 Alternating Current supply

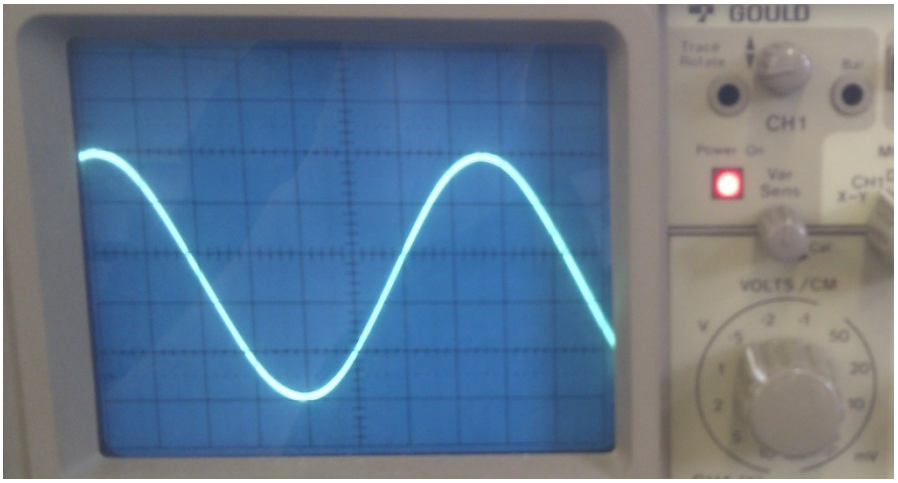

Figure 4.24 Voltage Oscillator. The AC supply described in section 4.2.3 can be seen with a frequency of 1600 hertz and amplitude of 3 volts.

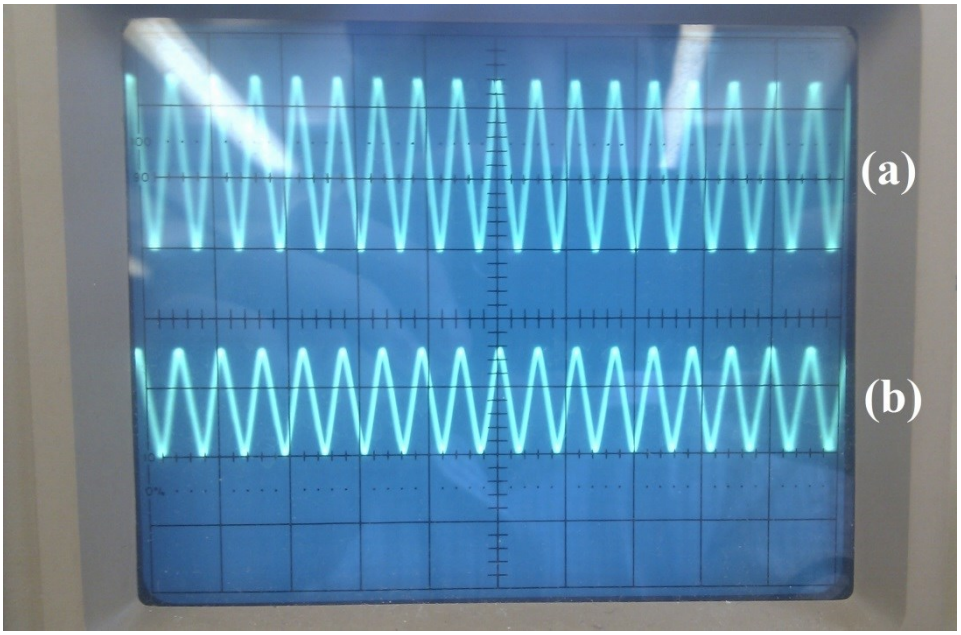

Figure 4.25 Instrument amplifier output with a theoretical gain of 11 using a variable resistor at 5k ohms Waveform (a) is the amplifier output showing amplitude of 4.9V, waveform (b) is the input of the amplifier showing amplitude 1.6V; the actual gain of this circuit was 9.9.

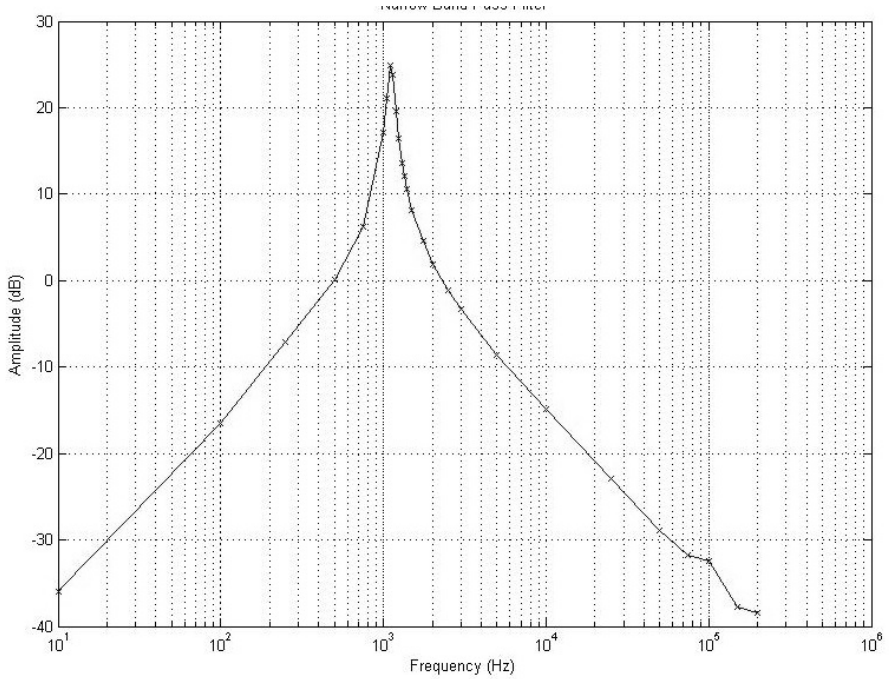

Figure 4.30 Narrow band pass filter with 25 dB amplification as described in section 4.2.11 with circuit diagram as shown in figure 4.10.

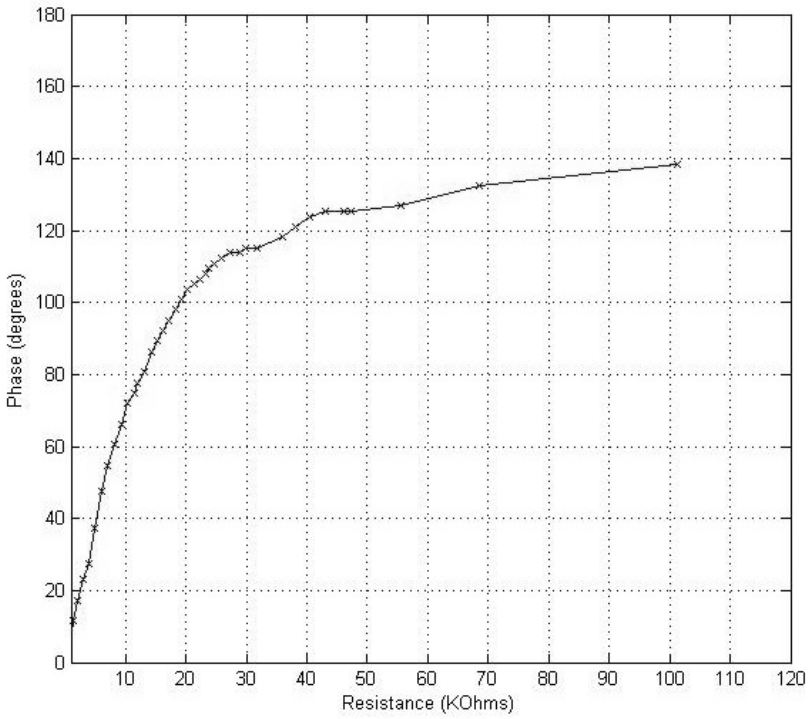

Figure 4.261 Phase shifter circuit showing the shift in phase with varying resistor as described in section 4.2.13, allowing the calibration of the subtractor and PSD.

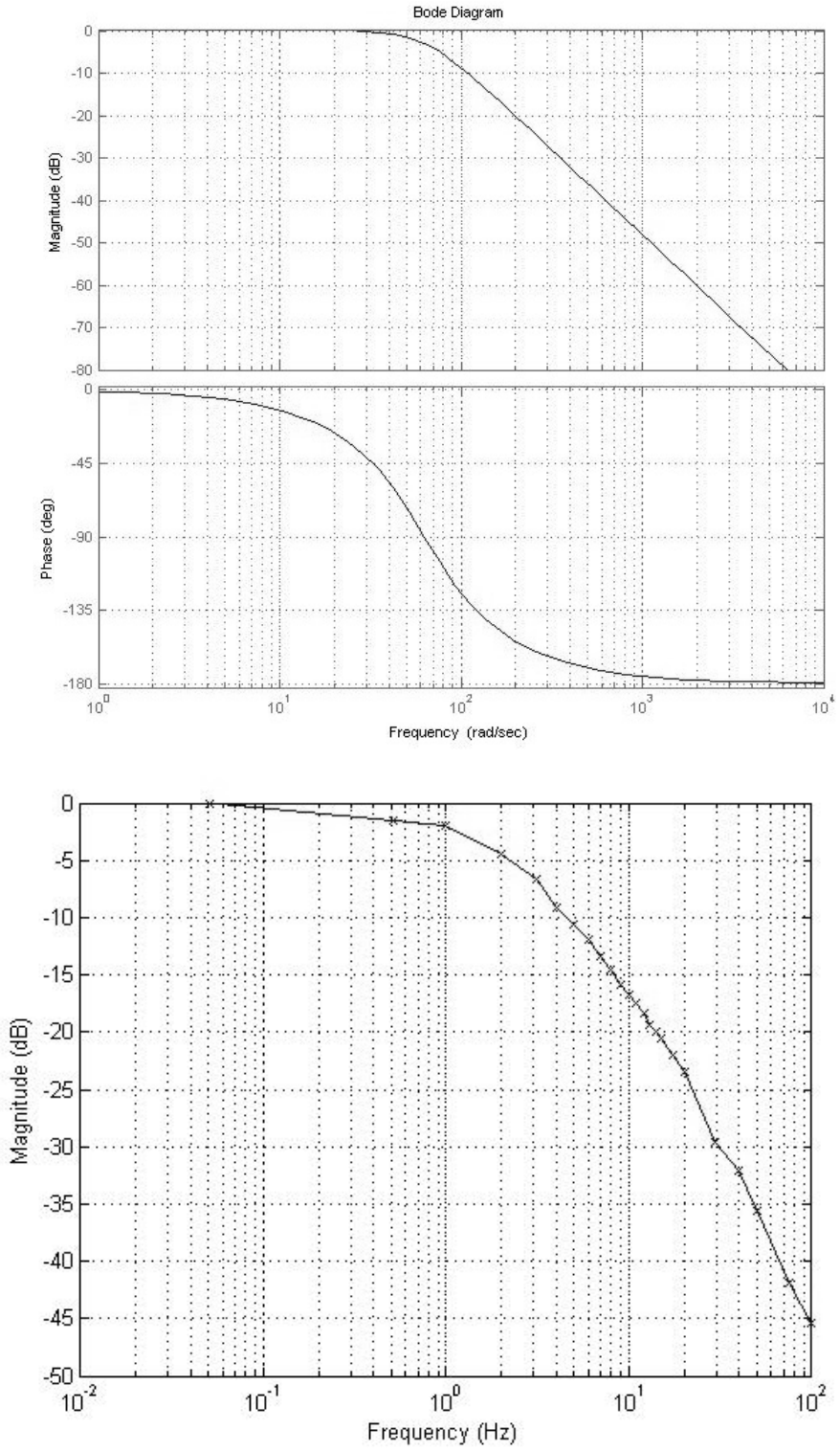

Figure 4.272 Sallen-Key topology Low Pass filter with cut off frequency at 10Hz as described in section 4.2.17. The theoretical bode diagram (top) is compared against the actual circuit performance (below) showing similar to theoretical performance of the low pass filter.

4.3.3 Flux Concentrators

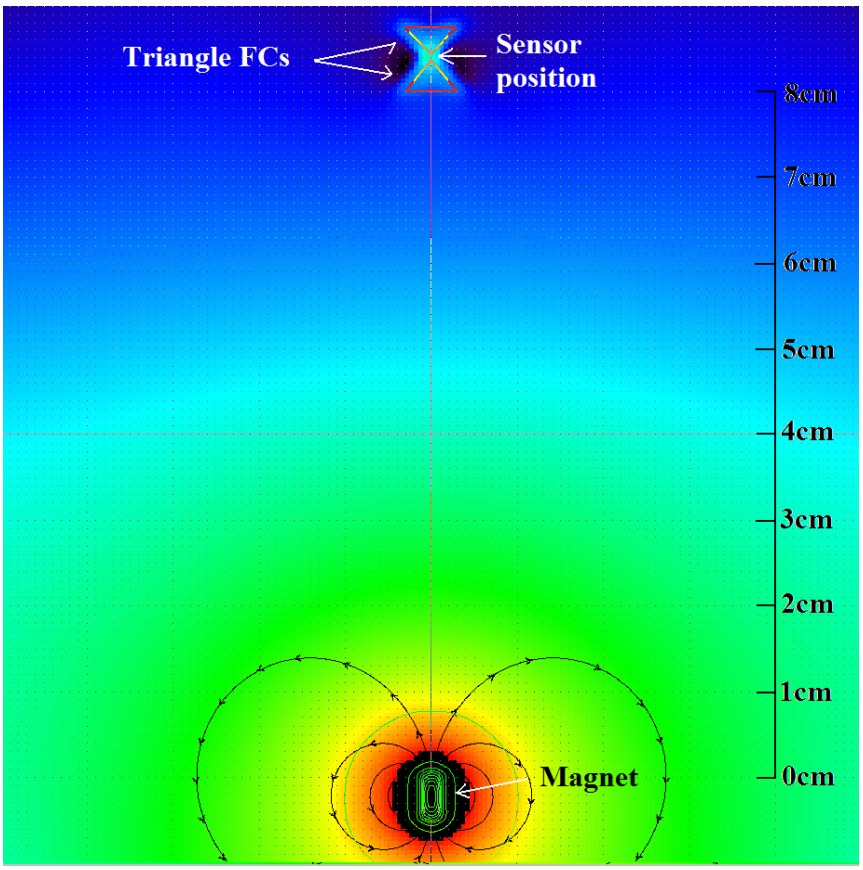

Figure 4.283 Example of Vizimag software output. This example shows the colour contour simulated magnetic field when amplified by a pair of triangle FCs from the magnet used in the experiment; the sensor is positioned in between the points of the FCs. The distance is shown between the edge of the magnet and edge of the closest of the FC.

Table 4.1 Simulated field strength at 8 centimetres using flux concentrators in Vizimag software.

Type of Concentrator	Gauss	Gain
1) No Concentrator	0.0804	1
2) Square backed Concentrator	0.143	1.78
3) Triangle Backed Concentrator	0.125	1.55
4) Triangle Fronted, Pointed Away	0.194	2.41
5) Triangle Fronted, Pointed Towards	0.359	4.47
6) Kite Shaped Concentrator	0.41	5.01
7) Paired Triangles	1.02	12.69

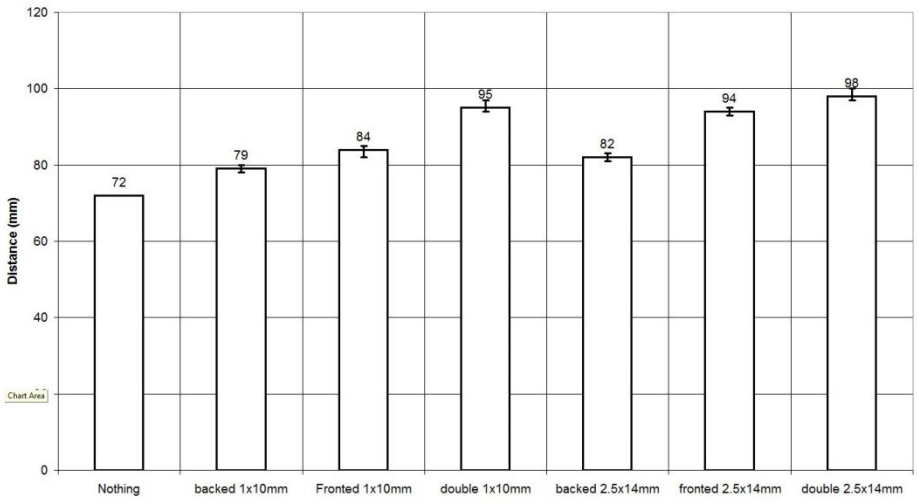

Figure 4.294 Amplification with physical FCs when used with DC system. The y-axis shows the increased distance at which the magnet can be detected when the FCs are employed.

There is noticeable decrease in experimental gain over simulated gain, suggesting that while simulated experiments used ideal equations and conditions, which exaggerate the actual gain which can be achieved. The difference could also be related to minute misalignment or difference in three dimensional geometry versus the two dimensional simulated geometry.

Table 4.2 Comparison of simulated against practical flux concentrators as described in section 4.2.20, 4.2.21 and 4.2.22.

Concentrator Type	**Simulation Gain**	**Experimental Gain**
No Concentrator	0.00	0.00
Square Behind	5.00	3.43
Triangle Behind	5.87	4.90
Triangle Fronted	13.00	10.78
Paired Triangles	22.07	14.70

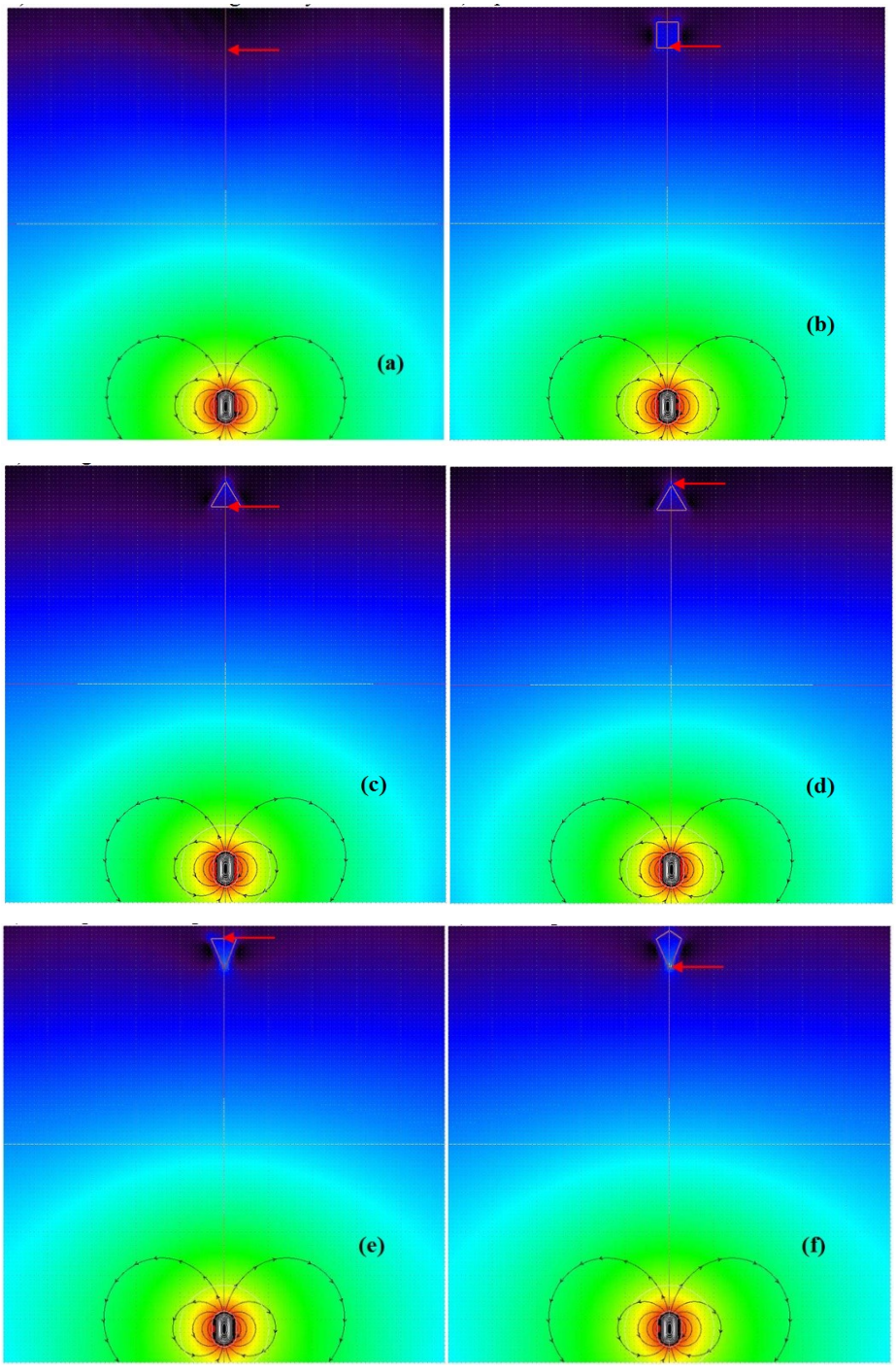
(a)
(b)
(c)
(d)
(e)
(f)

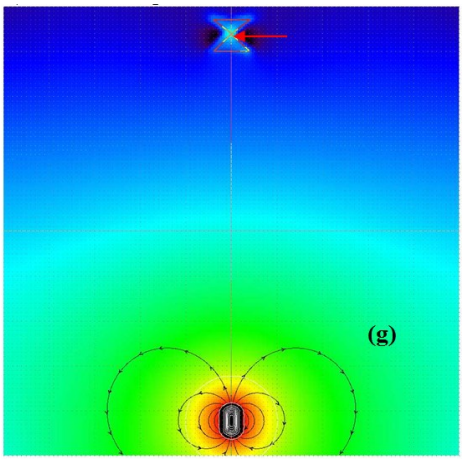

Figure 4.30 Simulations of flux concentrators in various orientations at 8 centimetres as described in section 4.2.21, with the sensor position indicated by the red arrow. (a) No magnet. (b) Square Backed. (c) Triangle backed. (d) Triangle fronted, pointed away. (e) Kite shaped backed. (f) Triangle pair. The colour contour plot indicated the field strength at that position; the actual field at the sensor's position can be measured by clicking on the point of interest for more accurate measurement. The magnet was a 6.4mm long 5mm wide bar magnet placed 8 cms from the FCs.

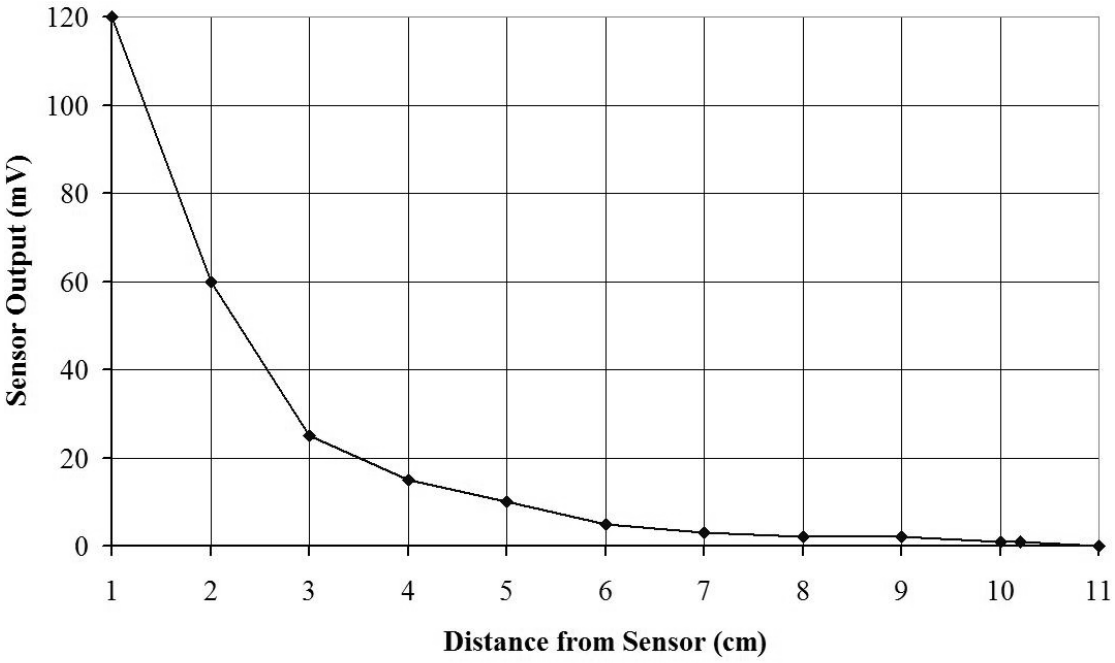

Figure 4.31 Output of system when the magnet is moved from the edge of sensor, demonstrating a maximum detection range of 10.2 centimetres.

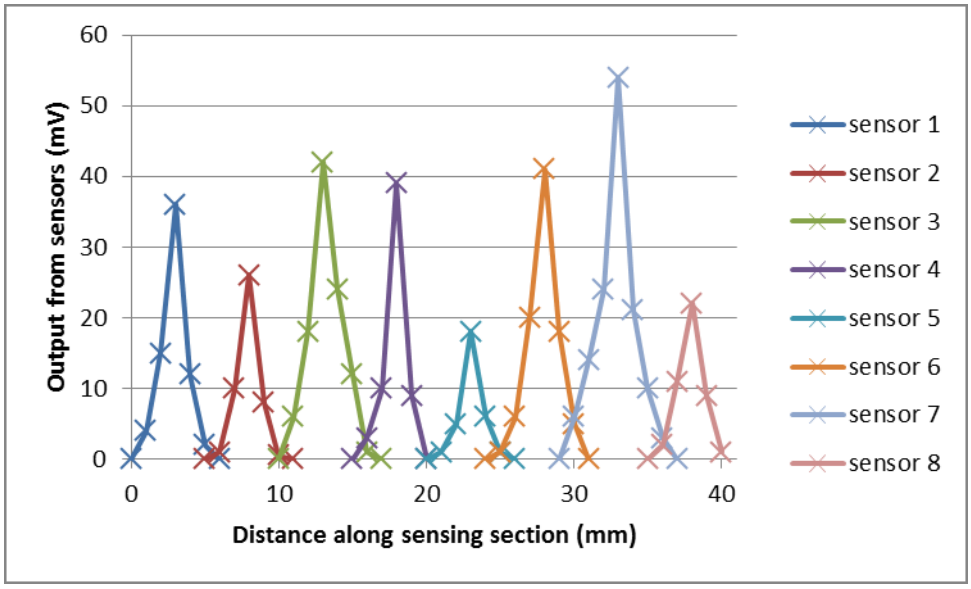

Figure 4.37 Output from C-arm system with a magnet moving along the length of the sensors, at 8 centimetres from the sensor face. Some descrepancy between maximum output from sensors is observed; likely due to difference in sensor resistance, this can be overcome with sensor calibration.

4.4 Discussion

4.4.1 External locator detection range

The ability to measure the SCJ from outside the body is very important; as Mittal et al have demonstrated, the presence of catheters in the pharynx increases the number of TLOSRs. This phenomenon is of utmost importance, as many catheters are inserted through the pharynx, for upper GI measurement or even for feeding tubes, the presence of one of these tubes could significantly increase the number of TLOSR episodes. TLOSRs are correlated with acid reflux as the relaxation and opening of the LOS, demonstrated with intraluminal manometry, allowing the passage of acid and other gastric contents into the oesophagus. Acid reflux causes damage to the sensitive squamous epithelium of the oesophagus which can lead to inflammation of the area known as oesophagitis, which itself is a precursor to GORD and adinocarcinoma. The stomach lining is well protected against acid due to its shielding secretions and high cell proliferation, whereas the oesophageal mucosa has neither of these abilities meaning it is highly susceptible to acid damage from reflux; increasing the frequency of acid reflux events by means of TLOSR induction may lead to an overestimation of an individual's acid reflux occurrence. This has significant impact on both the research used to investigate the antireflux barrier and the clinical diagnoses based on acid reflux incidence; manometry, pH catheters and multichannel intraluminal impedance probes are all intubated in such a way as they may stimulate the pharynx in a similar manner to that proven by Mittal et al to trigger TLOSR events. Work performed by Lee et al, using the catheter based SCJ locator probe has shown that SCJ proximal movement and restitution is the strongest and most reliable indicator of TLOSR occurrence, more so than manometric identification (Y Y Lee et al. 2012). While Mittal et al used an intrasphincteric pressure catheter inserted via gastrostomy, the probe did not appear to induce TLOSRs, and without testing this with a fully clear GI tract it is impossible to deduce whether or not catheters in the LOS can also induce TLOSRs. The design of a non-invasive method of continuously measuring SCJ movement hence TLOSR frequency

using the criteria suggested by Lee et al, would for the very first time, allow for real time continuous measurement of the number of TLOSRs without any pharyngeal, LOS or other GI tract stimulation, answering conclusively the question by Mittal et al; are TLOSRs merely artefact produced by the techniques used to measure them? It appears that the answer is unclear as yet, as the TLOSR itself a physiological action with belching initiating it, however how often this occurs without intubation is completely unknown. This device will allow for the first time, the continuous, non-invasive measurement of the SCJ.

Lee et al continued work using the catheter SCJ locator, reporting that the movement of the SCJ and GOJ during a TLOSR was similar to that of a hiatus hernia (YY Lee et al. 2012), with the difference being that while with a TLOSR, the SCJ returned to its original distal position as soon as it reached its peak movement, a hiatus hernia showed the proximal movement without immediate return to its resting position. The proceedings concluded that a hiatus hernia was the continuous stretching of the phrenoesophageal ligaments from many TLOSRs and that someone experiencing a high number of TLOSRs was more likely to develop a hiatus hernia. This conclusion is very important, the implications of increasing the number of TLOSRs with nasogastric feeding tubes or upper GI research tools could have significant health complications for the patients involved. It is vital therefore to develop the non-invasive method of SCJ position measurement.

While it was clear that the sensors used in the current catheter based SCJ locator were not sufficiently sensitive to detect a magnet at significant range, the prospect of higher sensitivity sensors suggested that externally measuring the position of the SCJ using a magnet was feasible. The papers mentioned in chapter 1 section 1.4.6, detailing the measurement of gastric motility using swallowed magnets showed the concept; while the technology was less accurate than the algorithm and sensor set up in the catheter SCJ locator, the detection of large, free roaming magnets inside the lower digestive tract was demonstrated. The major disadvantage of the technology detailed in the papers, is the processing requirements which were integral to the position calculation; the magnitude of calculation was such that the output was not real time, requiring significant post-processing in order to estimate the magnet's

position. The MRI and SQUID based systems were incredibly bulky and expensive; as well as limiting the patients' natural movement and posture, it did not allow any ambulatory studies, and with the MRI, was not compatible with any other upper GI tools, such as the Bravo pH capsule or manometry, which could be needed for further investigation. The magnometer based systems were much smaller but still required desktop computers or bulky laptops to perform the necessary processing to obtain a position. These systems also required large magnets to be used, due to the large distance involved in measuring the magnet anywhere in the GI tract; they also needed a great number of sensors in matrix layout due to the large area covered by the digestive system, this increased the bulk and complexity of the system, meaning it was not suitable for ambulatory studies. The nature of the magnet used with these magnetic measuring technologies is larger than that required for the measurement of the SCJ, also they don't have any method of attaching the magnet to the SCJ, nor do they have a method for aligning the magnet towards the sensors, instead they rely on trilateration of multiple three-axis sensors and significant mathematical processing to calculate the magnet's position.

4.4.2 AC improvement

Initially the detection range of the DC based circuit, with any sensor, was smaller than that required, however the development of the AC circuit allowed the magnet to be detected at a much greater range. The increased range was facilitated by the current flowing through the Hall effect element; while the DC circuit was limited with regards to current, as increasing current beyond the manufacturers limit would generally increase the internal heating, causing drift and subsequent errors. The alternating current circuit had the valuable feature of allowing no net current passing through the Hall effect device, while inputting a high peak current, greater than the DC limit; although the Hall effect sensor could still overheat given a large enough peak AC. The increased peak current means the Hall effect device is essentially more sensitive at the peak current, however this peak must be analysed carefully, extracting or identifying the wave's peak, otherwise the advantages will be lost. With the addition of band pass filters, the noise in the surrounding building, such as mains

interference at 60 hertz or background computer noise, can be removed since the sinusoidal frequency of the alternating current is chosen to be within a very low noise band. The subtraction of the sensor output from the original wave means the output of the sensor is zero with no magnet and effectively a very small sinusoidal signal with the presence of a small magnetic field; the addition of a Phase Sensitive Detector allows the detection of the of very small sinusoidal waves, even those apparently lost in large noisy environments, subject to being at the exact frequency and phase of a control square wave, taken from the voltage oscillator used to drive the sensor.

4.4.3 Flux concentrator

The addition of flux concentrators increased the range of the sensor by passively amplifying the magnetic field from the small internal magnet, however the magnitude of amplification was not as large as the simulations or other literature suggested; this is likely due to geometric or material discrepancies. There was a difficulty in obtaining and manufacturing flux concentrators, with very limited availability of material with a high magnetic permeability; those that were available were highly permeable at high frequencies in accordance with their use in RFID tags and other higher frequency applications. The materials were available from specialist suppliers in custom shapes but the cost and minimum quantity for the order, placed them well out of the budget associated with the doctorate. The ferrite rods which were acquired were for RFID coils and transformers, as they were the only reasonably priced materials with a high magnetic permeability in low quantity; these were highly permeable at high frequencies, however no information was provided as to the permeability at low or static frequencies such as with a permanent magnet. Due to the relatively low level of amplification when using these ferrite cylinders, it was assumed that the magnetic permeability of the material at static frequency was much lower than at the application frequency. There was some discrepancy between the high levels of amplification in simulations and papers, presumed to be the result of the high permeability used in simulations and stated in simulation based papers, as the relative permeabilities were quoted to be between 2000 and 30000; it is believed

that the difference was the result of the lower relative permeability in the material acquired and that the gap between two FCs was greater than that shown in simulations due to the sensor and circuit board thickness. The importance of correct alignment of the FCs was also highlighted in the experimental results, with small misalignments causing large decreases in amplification. The manufacture of cone-tipped FCs was somewhat difficult, with the ferrite rods being brittle and small, the rods would fracture or shatter when placed inside the chuck of a lathe, therefore the rods were manufactured using a circular abrasive disc held at an angle of approximately 45-50 degrees to the rod's length, and applying the sanding disc while slowly rotating the FC, a tapered cone was produced; because of this manual process there was slight variability in the angle and size of taper between each FC which may have accounted for a decreased amplification.

When combined, the whole apparatus provided an increase in range over the commercial sensors used of 580%; this improvement equates to a working detection range of 87 millimetres, a range which should be sufficient to detect the magnet within the body with ideal orientation. Ideal orientation is provided by the external magnet at the opposite side of the body, and will in increase the magnetic baseline but also increase the magnetic field from the small internal magnet proportionately. The low friction capsule will allow for free movement of the magnet inside so even though the movement of the clip and capsule itself may be limited by clipping angle or LOS pressure, the magnet will be free to move in alignment with the external magnet, maintaining ideal orientation. Ideally the detection range of the magnet would be well within the working range, however the technology, even with the increased strength magnet, is pushing the limit of what is detectable with this technology; the only alternative would be to use SQUID or MRI technology to detect a magnet inside the body with the degree of accuracy needed, however this would defeat the object of a simple method of measuring the SCJ non-invasively, and it would not be possible to use these technologies in ambulatory studies (Yeong Yeh Lee, Whiting, et al. 2012). Future *in vivo* experiments are required to test the reliability of the technology, with new ethical approval and patient recruitment; it is likely to work in smaller individuals, those who have a smaller chest measurement,

than those with a large chest measurement, as the distance from the oesophagus to the skin is important (Whiting et al. 2012).

Ethical approval is required to test this device with volunteers, at time of publication, this has not been applied for, however the use of this device with volunteers is mentioned below. The proposed volunteer apparatus is shown in figure 4.25 and 4.26, with a C-arm, with one end housing the sensors and FCs, and the other, the magnet; the external magnet is aligned with the sensors allowing the internal magnet to be aligned directly with the sensors and FCs. The sensors are then connected to the AC circuit and multiplexer, which in turn is attached to the Arduino microprocessor for position calculation; the multiplexer and Arduino board are mounted in a separate box which can be placed on a desk or with small modification could be worn by the subject for ambulatory studies. The position can then be recorded to a PC or with additional circuitry to a SD card in the case of future ambulatory applications. There is inevitable some accuracy loss when converting the output of the PSD for each sensor in turn, to digital; with any ADC there is a degree of error as the digital signal only has a limited bit resolution however with further amplifying and conditioning, this may be reduced. It was observed that each sensor, despite being connected to exactly the same AC supply, had different outputs with the same magnetic field, this is due to the difference in internal resistance of each sensor, exacerbated by the high level of amplification and processing. In order to overcome the difference between sensors, the system could be calibrated to detect the baseline and maximum output from each sensor; this would mean the position calculation was more accurate with more chance that if a magnet was exactly in between two sensors, the position was calculated as such because the two sensors has the same output.

The device should allow for the first time the measurement of the position of the SCJ without any catheters in the pharynx, upper oesophageal sphincter, oesophagus LOS or stomach as the experiments predict that it will be able to detect a magnetic field of 0.63 gauss at a distance of 80mm from the magnet when aligned. All previous studies measuring TLOSRs or the position of the SCJ have either used a catheter in the pharynx (Connor et al. 2009; Holloway 2000; Holloway 2006; Holloway & Sifrim 2008; Holloway et al. 1995; Pandolfino, Ghosh, et al. 2006; Pandolfino,

Zhang, et al. 2006)s; Pandolfino/Kharilas (Pandolfino, Zhang, et al. 2006) employed a multichannel perfusion catheter to detect the onset of a TLOSR before using fluoroscopy to measure the movement of the endoclipped SCJ while Mittal et al (Mittal et al., 1992) in a more specialised study, inserted a manometry catheter into the LOS via a hole in the stomach, allowing the detection of TLOSRs using the less reliable indicator of LOS pressure loss. The previously developed catheter based SCJ locator probe, although is the most accurate and simplest way of continuously measuring the SCJ position, it too required a catheter in the pharynx and oesophagus; if Nagler and Mittal are correct in hypothesising that the presence of a catheter in the upper GI tract artificially increases the number of TLOSRs, then the impact on all upper GI research is significant indeed; this device could once and for all answer this question, and progress to being a reliable method of measuring the SCJ position and with the Bravo Capsule, could reliably and minimally invasively measure acid reflux for extended periods of time.

Chapter 5

Summary of research outcomes.

5.1 Introduction

The upper Gastro-Intestinal (GI) tract is a complex anatomy, with many factors influencing organ position, internal pressures and stomach content position. For those who are unfortunate to suffer for acid reflux, anatomy is key in upper GI aetiology. The mechanisms of acid reflux are relatively ambiguous due to the difficulty of measuring the position, pressure and acidity of the oesophagus and stomach in real time without inducing measurement artefacts and anomalies. Acid reflux occurs when stomach contents which are acidic, retrograde into the oesophagus; it is one of the most common complaints to general practitioners worldwide, manifesting in heartburn, known medically as dyspepsia. While dyspepsia in itself is a mild pain, the prognosis is more severe; long term acid exposure in the oesophageal may lead to an increased likelihood of further Upper GI complications, such as oesophagitis, Barrett's oesophagus, metaplasia and adenocarcinoma.

There are many and varied commercially available technologies which measure acid reflux and anatomical pressures, including the intra-oesophageal pH Probe and the High Resolution Solid-State Manometer. Despite this, the underlying cause and the internal dynamics of acid reflux is still relatively unknown; it is established that a strong pressure gradient across the gastro-oesophageal junction in combination with decreased or absent lower oesophageal sphincter function increases the number of reflux incidents. Due to the dynamic conditions of the body however, the precise measurement of acid reflux is difficult; single pH sensors are placed several centimetres above the gastro-oesophageal junction in order to measure acid in the oesophagus rather than acid in the stomach. Due to pH sensor movement' however it

is this act which may grossly underestimate the number of acid reflux events. High resolution manometry can measure the pressure profiles along the upper GI tract with arguable accuracy, however as soon as sphincter pressure is lost, all knowledge of the gastro-oesophageal junction is lost, often during a vital time of acid reflux and Squamocolumnar Junction position.

Fluoroscopy is currently the unofficial gold standard of Squamocolumnar junction position measurement, with concurrent manometry and or pH-metry. This method is severely limited by radiation exposure and positional accuracy, the latter of which has to be measured and calculated by hand and often is subject to imprecision by ghosting effects on fluoroscopic images. Radiation exposure limits the duration of measurement to up to 5 periods of 30 seconds; capture of an acid reflux event is incomplete due to having to measure the event and initiate fluoroscopic recording after the event has been identified.

There is currently a gap in knowledge and technology of the long term movement and relative position of the squamocolumnar junction with respect to gastric acid. During catheter based measurement of the upper GI tract, the squamocolumnar junction moves vertically, due to contraction of longitudinal muscles in the oesophagus as well as pressures from the diaphragm and tension from phreno-oesophageal ligaments, other than during fluoroscopy, this important anatomical feature moves without being detected, yet it is the relative position of acid and the squamocolumnar junction which is vital.

The primary research aim of this thesis work was to develop and validate tools based on magnetic tracking and sensing which can monitor the position of the Squamocolumnar junction for an extended period of time, whilst removing the limitations of current methods such as fluoroscopy. The position measurement must be as accurate as possible to detect small movements of the important local anatomy as these may indicate significant findings with regards to acid reflux in the upper GI tract. These tools must be safe for use in patients and must also be compatible with the current set of Upper GI medical diagnostic and research devices such as high resolution manometry and pH-measurement.

The technology developed as part of this work could be used in conjunction with high resolution manometry, fluoroscopy, intraluminal impedance and pH-measurement devices in both clinical or research applications so must work adequately in their presence while not affecting their performance. The devices should ideally be largely reusable where some small parts may be single use, but the majority of technology should be reusable following sanitisation.

The high resolution manometer is a widely used clinical and research tool for upper GI investigation, however the solid state Manoscan HRM system has questionable accuracy, therefore another aspect of this thesis was to evaluate and where possible, compensate the inaccuracies of this device to allow more accurate profiling of upper GI pressures.

Chapter 3 documented the collaborative research with the group of Professor Kenneth McColl (Glasgow Western Infirmary), into the accuracy and reliability of measurements made with the Manoscan 360 oesophageal High resolution manometry system (Formerly Sierra Scientific Instruments, now Given Imaging, Israel) currently used in medical research laboratories and upper GI clinical diagnostics around the world (Conklin et al. 2009). Traditionally clinical use of oesophageal manometry would last approximately twenty to thirty minutes however prolonged use is not uncommon; it is generally used for gastro oesophageal investigation when a patient presents with dysphagia and other complications. It is possible to diagnose partial or full hiatus hernia with this device and is a clinically important diagnostic device in many specialist gastroenterology departments worldwide. The problem of accuracy was first highlighted by the medical clinicians working with Professor McColl of Glasgow University working in an upper GI medical research facility in Gartnavel General Hospital, Glasgow . At this facility the medical device is used for research investigation into disease aetiology and anatomy of the gastro-oesophageal junction, using the Manoscan system in conjunction with custom multi sensor pH catheters and occasional fluoroscopy in studies of up to two hours. After a two hour study it was noticed by Doctors Yeong Yeh Lee and Elaine Robertson, two researchers working under Professor McColl, that pressure readings upon withdrawal of the probe from the oesophagus were not at the baseline they should be, but rather at

irregular pressures of up to 60mmHg, pressures which exceed that often measured in the body. The major concern of this implication is that any pressure readings made during the studies or indeed clinically are invalid. This is very worrying when remembering that clinical diagnoses and treatments are given based on the output of this device which now appears to be subject to significant inaccuracies. This prompted a full collaborative investigation into the inaccuracy of this device and subsequent correction for the error.

The invasive nature of catheter devices in the throat, oesophagus and stomach can actually cause reflux episodes by inducing transient lower oesophageal sphincter relaxations (Noordzij et al. 2000; Mittal et al. 1992), allowed acid to reflux into the oesophagus due to the lack of physical barrier during the relaxation episode. Artificially causing these episodes while measuring acid reflux evidently can overestimate the number of natural reflux incidents, therefore it is a secondary research outcome to be able to measure the squamocolumnar junction position and acid exposure without the presence of catheter tubes in the throat, mouth or oesophagus.

Chapter 4 of this doctoral thesis details the development of a tool which is capable of measuring the position of the squamocolumnar junction without using a catheter. The system uses magnetic positioning, similar to that of the catheter based probe however uses much more sensitive equipment and larger magnets to be able to detect the squamocolumnar junction position form outside the body. The development of this device will allow the non-invasive measurement of the squamocolumnar junction for extended periods as it contains no catheter tubes leading to increased patient comfort and compliance. With the existence of the wireless oesophageal Bravo pH meter, acid reflux can be measured for a period of several days, limited only by the battery life and attachment of the Bravo capsule and magnet. Simultaneous use of these devices will allow monitoring of acid reflux without causing transient lower oesophageal sphincter relaxations.

The cumulative research output will facilitate health practitioners and medical researchers the opportunity and ability to investigate the upper GI tract for longer and in significantly more detail and accuracy than ever before; this may lead to a greater

understanding of acid reflux and other, more severe gastro-oesophageal complications.

This concluding chapter summarises the research output from this doctoral work and highlights significant empirical findings that have occurred as a direct result. The chapter also includes discussion of the implications these findings have on the field of medical device research and specifically to upper GI investigation. Also included is a section of suggested future work; research that can be undertaken to further advance the research outcomes and indeed the field of upper GI medical devices. Lastly this chapter will highlight and discuss the limitations of this research and its outcomes, followed by a small chapter conclusion.

5.2 Empirical findings and theoretical implications

5.2.1 Catheter based squamocolumnar junction locator

The primary research outcome was to develop a tool capable of measuring the position of the squamocolumnar junction; this objective has been met by the development of a catheterised intraluminal probe consisting of a flexible circuit board populated by small magnetic sensors placed at regular intervals along the probe, encased in medical grade silicone. The development of the catheter device is described in full in chapter 2. The attachment of a customised magnetic endoclip to the squamocolumnar junction, a procedure performed during endoscopy, allows the precise tracking of the squamocolumnar junction by the inferred magnetic endoclip. The output of the sensors which measure the position of the magnet along the axial length of the device, is handled and calculated by a multiplexer and microprocessor to which the catheter device is attached. It is safe for patient trials and offers visual output of magnet/squamocolumnar position as well as data output to a PC for interpretation and analysis. This system can be used to accurately measure the position of the squamocolumnar junction in real time with a median accuracy of 2.4 millimetres with respect to the nares (Yeong Yeh Lee, Seenan, et al. 2012).

When used in conjunction with simultaneous high resolution manometry and pH-measurement which also measure pressure and pH respectively, provides the user with a significantly more detailed view of the upper GI tract than the output from high resolution manometry and ph-metry alone. Evidence for this statement is provided by the current publications from this work in collaboration with the medical researchers of Glasgow University, who used the device to measure the position of the squamocolumnar junction during a full transient lower oesophageal sphincter relaxation (Y Y Lee et al. 2012) and separately during a swallow and during shallow and deep breathing (Yeong Yeh Lee, Seenan, et al. 2012). These studies found that the squamocolumnar junction showed a median proximal movement of 4.3 centimetres (IQR 2.0) over a median duration of 16.8 seconds (IQR 7.4) with the largest proximal movement measuring nearly 10 centimetres, a staggering distance of movement inside the body.

The measurement of this movement has only been once documented using the limited fluoroscopy technique when performed with concurrent high resolution manometry (Pandolfino, Zhang, et al. 2006); there are several limitations to this method. The aforementioned radiation exposure, limiting the recording time is a big drawback to this technique. It is only able to partially record the event due to the requirement of detection and subsequent fluoroscopic recording, so it misses the movement at onset. The data is also recorded and has to be manually translated into position measurements which was performed every 4 or 5 seconds in the initial trial, with questionable accuracy when taking into account ghosting effects and movement artefacts on the captured video. Lastly, fluoroscopic imaging machines are both costly and bulky, limiting the position of measurement and the commercial availability of such a device. It is for this reason that the catheter based squamocolumnar junction locator developed and tested as part of this thesis offers significant advancement in the field of upper GI medical devices. Validation studies performed with this device (Yeong Yeh Lee, Seenan, et al. 2012), documented in detail in this thesis, suggest that the device is at least as accurate as the unofficial gold standard of fluoroscopy if not vastly more accurate (Yeong Yeh Lee, Seenan, et al. 2012) as shown in figure 2.54.

A review by Lee et al, suggest that this device will form part of the arsenal of measurement tools available to the upper GI medical researcher and subsequently medical practitioner (Yeong Yeh Lee, Whiting, et al. 2012), increasing accuracy of measurement and furthering knowledge of the upper GI tract should the device be commercially produced; even without commercial production, continued research by Dr Yeong Yeh Lee and Professor Kenneth McColl using this device will undoubtedly add much to the field of gastroenterology and potentially lead us to understand and better treat upper GI disease.

5.2.2 Testing and improvement of the Manoscan High Resolution Manometer

The thorough investigation into the accuracy and performance of the Manoscan 360 Oesophageal High resolution Manometer highlighted some significant error in the system (figure 3.5) which will almost certainly have significant consequences for its intended use; this work is described in full in chapter 3. Quantification of the error was performed by measuring the change in time of the recorded pressure in a fixed pressure aqueous environment, with error increasing linearly over time for each sensor as demonstrated in figures 3.8, 3.8 and 3.13. The rate of this linear error increase or drift varied both between sensors and between probes (figure 3.16), suggesting that inter-sensor variability was high. Even following the manufacturer's suggested weekly pressure calibration which appeared to compensate only for sensor offset, the drift continued. Discussions with the manufacturer were then initiated, with the question of faulty probes arising followed by misuse or error on the part of the user during the study or calibration. Neither of these reasons answered the problem, as one probe was checked by the manufacturer and returned only to maintain drift. Initial publication and presentation of these results at the British Society of Gastroenterology Annual conference in 2011 (E. V. Robertson et al. 2011) and at Digestive Disease Week 2011 (E. Robertson et al. 2011), confirmed the concerns as Daniel Sifrim, Professor of Neurogastroenterology at Queen Mary University of London, acknowledged his research group has observed the same marked increase in pressure at the end of a prolonged study, only to be given the

same answers by the company. Whilst maintaining communications with the company, full investigation of the drift phenomenon continued, showing an offset in pressure recordings when the sensors were placed from room temperature to body temperature. Corrections for this drift were then calculated and implemented. In order to reduce and counteract the offset when using the probe at body temperature, calibration was performed in a water bath at body temperature; this all but removed the offset caused by the issue. The removal of drift over the study period was more difficult; luckily the drift was linear over the whole study, even though it varied between sensors. Drift for each sensor was predictable and occurred at a rate which could be calculated as proportional to the pressure at the end of the study and the duration of study. Upon withdrawal the probe was held in the air for a number of seconds before ceasing recording, this meant that a linear drift from the start of the study to the end of the study could be calculated for each sensor and thusly compensated. A software was written by Dr Andrew Kelman of Glasgow University which performed this procedure and compensated the drift every time point for each sensor in the probe for the duration of the study. This compensation software was validated in vivo and showed significant and marked reduction of error to less than 1 mmHg (figure 3.15), independent of study duration. Upon completion and during publication of this significant improvement (Robertson et al. 2012), the company contacted the research group, suggesting a similar compensation algorithm which was in addition to the standard calibration procedure. Despite this private admission of error, the company would still not publically include the compensation in the standard procedure or software, despite the clinical implications. It is hoped that publicity of this error will cause the company to either improve the accuracy of the system by removing the component responsible for drift or include in a public update the compensation algorithm which makes the system wholly more accurate and reliable for research and clinical gastroenterology investigation. A further comment to this point is one of wider concern, just how many devices are used in clinical and medical research areas that are not as accurate as they appear is unknown but it is suggested that this is not the only one.

5.2.3 External Squamocolumnar junction locator

Development of a custom analogue signal processing circuit is detailed in chapter 4; highly sensitive Hall effect elements were tested and the most sensitive was chosen to form the sensing portion of the device. While the elements are more sensitive with a higher direct current passing through them, they are subject to internal heating and resultant drift over time as the current passes through them; it also stresses the sensors producing a shorter working life. To counter this problem, an alternating current circuit was designed with a voltage oscillator and voltage-to-current converter powering the sensor (figure 4.3). The output of the sensor was a sinusoidal voltage proportional to the input current waveform and any magnetic field. The output was amplified and filtered to reduce noise as the alternating current oscillated at a frequency of 1.59kHz, other noise such and UK mains and computer interference was removed. The input voltage was amplified during calibration and phase shifted to be exactly in phase with the output of the sensor with no magnetic field; the two waveforms were then subtracted, leaving, if any, a sinusoidal waveform proportional to only a local magnetic field. This was then amplified and passed through a phase sensitive detector which transforms an in-phase waveform of 1.59kHz to a DC voltage proportional to its amplitude. The phase sensitive detector is capable of detecting very small sinusoidal voltages hidden in noise, so long as the phase and frequency is correct. The output is low pass filtered to produce a smooth DC output. Each sensor is multiplexed to allow sampling at a microprocessor in order to calculate each sensor's output and detect the sensor with highest amplitude and interpolate the magnet's position. An array of sensors allows axial movement of the squamocolumnar junction to be detected. The addition of magnetic field amplifying flux concentrators increase the field of the magnet outside the body; they are passive triangular cones of highly magnetic permeable material and allow for further detection distance. The small magnet used with the catheter device was too weak to be detected outside the body, so a larger magnet was used; the larger spherical magnet was 6.4mm diameter N38 neodymium magnet offering significantly more field strength for its size. The magnet was encased in biodegradable Polycaprolactone which is medically safe (FDA approved for internal use) and

allows attachment of an endoclip and facilitates magnet rotation inside. Hall effect sensors are very directional, which is a problem when using a mobile magnet, so to counter this, a large bar magnet is placed externally, on the opposite side of the body to the sensor array, in order to align and further increase the magnetic field strength. When using the modifications mentioned above, the magnet can be detected up to 10.2 centimetres. This is normally within the detection range for a human adult oesophagus.

5.3 Limitations

5.3.1 Catheter based squamocolumnar junction locator

The catheter based squamocolumnar junction locator is limited by its application; as with many other intraluminal and intra-pharyngeal probes, it has the potential to cause transient lower oesophageal sphincter relaxations. A limitation of the current manifestation of the device is its size, which when combined with the high resolution manometer and pH catheter, is certainly not easy for patients to tolerate nasally; the probe itself is 4 millimetres in diameter, the latest smallest high resolution manometer (Given Imaging, Israel) 2.75 millimetres in diameter and the customised pH probe approximately 1 millimetre, the apparatus is a substantial size when combined, requiring local xylocane spray to insert the combined probes.

The fragility of the device is also a limitation with flexion and tension from inserting and withdrawal, the solder joints and flexible circuit board itself would fracture after a number of uses. The probes started to develop faults due to broken solder connections or circuit board tracks after approximately 10-20 trials. It is difficult to detect faulty connections with the current software and microprocessor so each probe had to be manually tested before each use to ensure accurate positional recordings. The joint between rigid sensor and flexible circuit board was also a weak spot with sensors becoming detached; the attachment of the cable to the end of the flexible

circuit board was also another area where solder connections could break, though they could be re-soldered more easily than those on the sensors. The number of outputs from the sensors and the minimum manufactured circuit board track width and gap enforced a limit on the minimum width of the flexible circuit board, however with increasing manufacturing capabilities this could be overcome.

The cost of manufacture is high due to the manufacturing precision required for the flexible circuit board and the processing of board population with sensors and other components. The flexible board manufacturers stated that in one or two years time, the technology would be sufficient to offer lower cost and higher precision flexible board manufacture which would have the effect of reducing cost and minimum board width. Another problem encountered when the boards were manufactured was the length of the board, the manufacturers had to produce boards diagonally across the panel, leading to high wastage and increased cost. Also promised in the near future was the ability to embed small rigid panels in the board which could be placed under the sensors to stop solder fracture under joints; this was unsuccessfully attempted by the manufacturer. The Memsic MMC328XMS magnometer sensors are fairly expensive at approximately £2 per unit, however due to the minimum order quantity, the sensors were quite costly as they had to be purchased in bulk. The attachment of sensors onto the flexible circuit board was performed by automated pick and place population machines which provided greater accuracy than that done by hand but at greater cost.

The limitations off this developed device are noticeable however for small scale use in medical research they are acceptable; semi-reusable probes of a limited life still offer some insight into the workings of the upper GI tract, which has the benefit of expanding our knowledge of the related disease in the area. Recently Dr Lee and Professor McColl have published findings which update the definition of a normal gastro-oesophageal junction (Lee & McColl 2013) and detail the role obesity may play in increasing reflux incidents, hiatus hernia occurrence and other upper GI disease (Lee et al. 2013; YY Lee et al. 2012). For commercial application, there is work to be done which can increase reliability and reduce cost, covered in the following section on future work.

A significant and unavoidable limitation of the developed technology is the requirement of a magnet to be placed on the squamocolumnar junction; a procedure which is fairly invasive and takes several hours if sedation is used. A counter to that point however is that most people who are admitted to a gastroenterologist for investigation almost always undergo endoscopy for visualisation and biopsies, so the procedure of attaching a magnet can be added on to the end of the endoscopy. One vital part of the procedure is the attachment of the magnet to the squamocolumnar junction, a tricky procedure which is made more difficult by the mucosal folds and moving gastro-oesophageal junction when viewed from the endoscopic camera; it was observed however that the placement accuracy, like most endoscopic procedures, improved with practise. If the magnet is not placed accurately at the squamocolumnar junction then the related recordings are inaccurate and potentially invalid. Finally the issue of the internal magnet remains, while in everyday life it is unlikely to cause issues, its removal may be required if it persists on the gastro-oesophageal junction rather than falling off. An X-ray is required to check for the presence of the magnet which may require further endoscopy for removal however most clips has detached without intervention by 6 weeks. A magnet in the digestive tract while undergoing an MRI scan for example may have severe consequences, so removal is required; this would be more important when considering the large magnet used for the external squamocolumnar junction locator detailed in chapter 4.

A minimal limitation of the device as it stands is the lack of mobility when using the device; some pH studies are performed at the patient's home with a portable ambulatory device attached to a data logger, inclusion of a data logger in the current device is possible and would increase the number of uses and the possible duration of recording.

5.3.2 Testing and improvement of the Manoscan High Resolution Manometer

While the study into accuracy of the Manoscan high resolution manometry system was thorough, the potential implications are unknown and errors may still be made

despite publication in the public domain. While the Glasgow University research team now use equipment that is accurate following compensation, uptake of the calibration will be dependent on the manufacturer and their public notification of the error and inclusion of compensation in future software updates; something which is beyond the control of the researchers.

One limit of the study is the fact that it did not highlight the specific problem component of the device. It did however remove the problem by compensating the data, which means the effect of the problem component is removed. The understandable reluctance of the research team to disassemble the probe and processor system to test the device at a component level means the problem still occurs. The devices which are now accurate and not subject to thermal offset or drift act as though there is no erroneous component as this has been corrected so investigation into the hardware issues is unnecessary for investigation other than by the manufacturer.

A limitation which may be insignificant is that the error was only tested on three probes, as this number was limited by the itinerary of the research facility. It is unknown what effect age and storage conditions play on the magnitude of drift, perhaps the drift magnitude per unit time increases as the probe ages.

The problem with of the drift correction is it provides more work for the user, albeit a small amount; calibration must be performed using a water bath controlled at body temperature but it is believed that a research or clinical department would have regular access to or the ability to acquire such a water bath. Lastly the compensation required the selection of data that is post-withdrawal however this is relatively simple to do on the current software and could easily be incorporated or even automated by sophisticated software.

5.3.3 External Squamocolumnar junction locator

The implementation of the external squamocolumnar junction locator still required endoscopic magnet attachment however as mentioned previously, this is often routine in patients with upper GI complications so would not add an invasive procedure just for measurement. For validation or testing the hypothesis that TLOSRs are induced by catheterisation, endoscopy is required, for clip attachment, where it would not be in a clinical setting. There are slim risks of complications as the result of endoscopy, such as GI bleeding, infection, perforation of an organ or allergic reaction to anaesthetic, if used. The procedure itself is not a pleasant experience and is often not well tolerated by patients, so it is unlikely that volunteers would be very forthcoming. While the procedure of externally measuring the position of the SCJ for a prolonged time is non-invasive, it should be noted that endoscopy is an invasive process.

The magnet is larger than that previously used so it is not known how long it will remain attached; the larger size may mean it becomes detached quicker with the lower oesophageal sphincter pressure. Should the magnet stay on for longer however it may require removal; starch can be added to Polycaprolactone in order to increase its biodegradability and with experimentation may provide a more precise time until removal, removing the need for x-ray checks and endoscopic removal.

If used with the Bravo capsule pH meter, then interference tests must be performed as it is not known if either device would subject interference onto the other, which may cause compatibility issues. Should there be no issues of noise or interference then the device will facilitate long term and accurate ambulatory measurement of acid reflux.

Individuals with larger body mass will have a larger distance between the oesophagus and the skin, this potentially introduces a problem as if the distance is greater than the detection range, the sensors will not be able to detect the magnet. This is significant as an increased BMI or waist circumference is shown to indicate increased acid reflux, transient lower oesophageal sphincter relaxations and further upper GI complications.

Manufacturing limitations of the flux concentrators mean they do not amplify the magnetic field as much as they may be able to; the main limitation to custom flux concentrators is cost, with minimum order quanities and cost for custom shapes. Commercial development would allow custom flux concentrators, or collaboration with academics who develop flux concentrators may overcome this problem.

5.4 Future work

5.4.1 Catheter based squamocolumnar junction locator

The future potential for a catheter based squamocolumnar junction locator is promising, with work already published using the device which adds to the scientific and medical knowledge of upper GI anatomy and aetiology (Lee & McColl 2013; Lee et al. 2013; Y Y Lee et al. 2012; Yeong Yeh Lee, Whiting, et al. 2012; YY Lee et al. 2012). Future work may consist of both increasing physical reliability, obtaining more accurate results and producing a commercially viable device.

Reliability of the physical and mechanical properties of the device may be improved; owing to the limitations of manufacture, the device had semi-reusable properties but with increased development, could be significantly more reliable and robust. Development may be undertaken to reduce costs while increasing quality with more advanced manufacturing capabilities. Stevenage circuits, the company who made the flexible circuit boards aim to have improved machinery in the next year or two which will be capable of producing boards with smaller track width and gap sizes which could reduce the diameter of the device. Also Memsic have recently announced the release of a smaller 3-axis magnometer, the MMC328xMC, which is 2 millimetres by 2 millimetres by 1 millimetre, smaller than the previously used MMC328xMS which is 3 by 3 by 1.2 millimetres. Reducing the size of the device to 2 millimetres diameter plus producing custom silicone casing with a minimal wall thickness may see the device slimmed down to 2.5 millimetres diameter which would be significantly more tolerable than the current generation. Memsic also have

announced the intention to develop a more sensitive and ultra-small package 3-axis magnometer, the MMC3416xPJ, however the full details of this remain unknown at present, the dimensions of 1.6 x 1.6 x 1 millimetre have been announced which would further reduce size. The MMC3416xPJ has I2C capabilities however it is unknown how many addresses the device will be produced with, but if it is sufficient to enable a single SDA line, this would significantly reduce the flexible circuit board complexity which can also be reduced in size and cost. Obviously mass production should the device be commercialised would significantly reduce costs. Another area for improvement is the flexible circuit board to cable connection, which under flexion increases risk of solder joint fracture. The weight of the cable is determined by the number of cores it has, but if a single SDA line is used as mentioned above, then the number of cores need only be 4, which could produce a very light cable, minimising stress on circuit board to cable connection.

If the device is to be manufactured or developed it may be worth considering multiple probe combination; currently some manometer – pH devices and impedance – pH devices exist which combine two types of measurement technology into the same probe for maximum efficiency and minimal device diameter. Collaboration with a company or development of custom pH or manometry sensors integrated into a squamocolumnar junction locator would provide a very useful and accurate tool for measuring the upper GI tract with respect to acid reflux, hiatus hernia and other digestive diseases. Indeed the device, if it could be manufactured with minimal catheter diameter and data logger, could be used in ambulatory studies, removing the requirement of study at a research facility.

5.4.2 Testing and improvement of the Manoscan High Resolution Manometer

As briefly mentioned in the previous section, the future of the investigation into error in the high resolution manometer is limited however there are still potential areas of research in this topic. Identification of the components causing drift and offset could be performed however it would require destructive testing of components in the probe and processor system, which is undesirable in a system costing several

thousand pounds; also it could be argued that it is the responsibility of the manufacturer to find and correct the problem.

Testing of the medical device accuracy could be performed using more than three devices, in order to highlight the error in a larger sample, but would require the cooperation of a significant number of clinicians and research groups to acquire the probes.

While this error was highlighted and ultimately corrected in the Manoscan 360 Oesophageal high resolution manometry system, it is unknown if any other device produced by this manufacturer or even by rival companies is subject to the same drift. If they are, then the end-users need to be aware of this in order to make accurate recordings and conclusions based on the data. While the deformable capacitive plate technology used in this device appears to be inaccurate, there may be other medical devices which use totally different technology which have similar errors, but of which the end-users, the researchers and clinicians, are unaware; investigation into this probe, could form the basis of future work for the benefit of the medical device community and medical field.

5.4.3 External Squamocolumnar junction locator

The development of a novel minimally invasive external squamocolumnar junction locator offers much to the field of upper GI devices; the device will allow, for the first time, long term measurement of the position of the squamocolumnar junction without inducing artefactual transient lower oesophageal sphincter relaxations. It is unknown how many such relaxations occur naturally without invasive catheter monitoring; this device has the potential to answer that important question. If the answer is that very few occur naturally, then the field of catheter GI measurement will be forced to rethink methodology and device use with regards to research and clinical output. There is however much to be done on the device in order to produce a reliable, commercially applicable diagnostic and research tool. Mainly increasing the maximum range would allow the measurement of the squamocolumnar junction in

patients with a larger chest circumference and offer more reliable reading. The method of attachment of the magnet has only been suggested, as it is larger than previous designs, deployment and attachment is as yet untried, so development of the magnet and encapsulation may be required to facilitate accurate magnet placement during endoscopy. Encapsulation is performed manually by hand in order to minimise costs, but 3-d printing or injection moulding would lead to a more reliable encapsulation, potentially with the addition of attachment or deployment methods.

Each device currently requires calibration, which has to be performed manually; either automatic calibration would be desirable, or a one-time calibration would be acceptable. Software calibration would also correct individual sensor offset so all sensors would have the same linear response to the magnet. Currently the C-arm which holds the external magnet in alignment with the sensor array is fixed, however it would be useful to produce an adjustable C-arm for use on a variety of chest sizes. The addition of a battery and data storage would produce a more useful ambulatory device; currently the device outputs the data via a USB connection to a laptop with custom software, but storage of data would allow for long term monitoring of the squamocolumnar junction in the patients' homes, performing daily tasks. Currently no volunteer tests have been performed with this device and future work would likely involve acquiring ethics and performing a validation study on an advanced model.

The field of gastroenterology devices is almost constantly being improved by smaller diameter catheters; manufacturers are aware of the issues of compliance and tolerance in their larger catheters and find ways to reduce size for example with Given Imaging's reduction of size in manometer from the High Resolution Esophageal Catheter (diameter 4.2 millimetres) to the High-Resolution Esophageal Small Diameter Adult Catheter (diameter 2.75 millimetres). The manufacturers are often aware that research groups and diagnostic teams are using multiple catheter combinations in order to obtain both pH and manometery data simultaneously; recently manufacturers have been releasing devices with combined monitoring technology such as Given Imaging's High-Resolution Esophageal Catheter with Impedance, or Synmed's Zephr pH-Z Impedance/pH Monitoring System. It is possible that either development of combined devices could facilitate the next stage

of device, or that licensing the squamocolumnar junction device to one such manufacturer will allow the development of a single device with yet more accurate information regarding acid reflux and the prevailing disease areas.

5.5 Conclusion

The aim of the work presented in this thesis was to develop and validate a custom device for measuring the real-time position of the Squamocolumnar junction. This thesis documents such work, with the advancement and validation of the Hall effect based catheter squamocolumnar junction locator which has gone on to perform in several medical research trials with good results, advancing the field of gastroenterology understanding. The testing and improvement of the Manoscan high resolution manometer device has offered more accurate results when investigating research and clinical trials, hopefully leading to more reliable diagnosis and improving future medical device reliability by highlighting the manufacturer's flaws and suggesting improvements.

Design and development of the external squamocolumnar locator device has the potential to advance the field of acid reflux monitoring by offering a long term minimally invasive method of accurately measuring the position of the squamocolumnar junction; this could be used with other devices such as the wireless Bravo pH capsule which is attached to the oesophagus above the SCJ (Kwiatek & Pandolfino 2008) or other catheter based systems. When used with wireless systems, transient lower oesophageal sphincter relaxations will not be artificially induced leading to more representative recordings. It is believed that the field of medical research and subsequently medical diagnostics will be improved by the development of these devices; papers have already been published which document novel research performed using the catheter squamocolumnar junction locator and improved Manoscan manometer, highlighting the importance of accurate medical monitoring and devices.

References

Abele, J.E., 1989. Overview of Impedance Sensors. In *Catheter-Based Sensing and Imaging Technology*.

Al-Motabagani, M.A.H., 2002. An Anatomical Study Of The Phrenoesophageal Ligament. *J Anat. Soc. India*, 51(1), pp.18–22.

Ando, T. et al., 2006. Interleukin 1B proinflammatory genotypes protect against gastro-oesophageal reflux disease through induction of corpus atrophy. *Gut*, 55(2), pp.158–64. Available at: http://www.pubmedcentral.nih.gov/articlerender.fcgi?artid=1856489&tool=pmcentrez&rendertype=abstract [Accessed March 25, 2014].

Andrä, W. et al., 2000. A novel method for real-time magnetic marker monitoring in the gastrointestinal tract A novel method for real-time magnetic marker monitoring in. , 3081.

Anggiansah, A., Sumboonnanonda, K. & Wang, K., 1993. Significantly reduced acid detection at 10 centimeters compared to 5 centimeters above lower esophageal sphincter in patients with acid reflux. *American Journal of Gastroenterology*, 88, pp.842–846.

Arndorfer, R.C. et al., 1977. Improved infusion system for intraluminal esophageal manometry. *Gastroenterology*, 73(1), pp.23–7. Available at: http://www.ncbi.nlm.nih.gov/pubmed/324861 [Accessed November 1, 2012].

Ayazi, S. et al., 2009. The Value of High-Resolution Manometry in the Assessment of the Resting Characteristics of the Lower Esophageal Sphincter. *Journal of Gastrointestinal Surgery*, 13(12), pp.2113–2120.

Babaei, A. et al., 2008. A unique longitudinal muscle contraction pattern associated with transient lower esophageal sphincter relaxation. *Gastroenterology*, 134(5), pp.1322–31. Available at: http://www.ncbi.nlm.nih.gov/pubmed/18384786 [Accessed November 26, 2012].

Baxter, L.K., 1996. Capacitive Sensors. , pp.1–17. Available at: http://ieeexplore.ieee.org/xpl/bkabstractplus.jsp?bkn=5264832.

Blanchard, H., 1999. *Hall sensors with integrated magnetic flux concentrators*.

Bonavina, L. et al., 1986. Length of the distal esophageal sphincter and competency of the cardia. *American journal of surgery*, 151(1), pp.25–34. Available at: http://www.ncbi.nlm.nih.gov/pubmed/3946748 [Accessed October 9, 2012].

Bonnelycke, B.E., 1972. Analysis of operational-amplifier drift. *Anal. Chem.*, 44(3), pp.610–613.

Boyle, J.T., 2006. Gastroesophageal reflux disease in 2006. *pediatric radiology*, 36, pp.192–195.

Bredenoord, A., 2007. High-resolution manometry – bliss upon bliss for esophagology? *European Surgery*, 39(3), pp.167–173. Available at: http://www.springerlink.com/index/10.1007/s10353-007-0329-1 [Accessed October 9, 2012].

Bredenoord, A., 2008. Impedance-pH monitoring: new standard for measuring gastro-oesophageal reflux. *Neurogastroenterology and motility : the official journal of the European Gastrointestinal Motility Society*, 20(5), pp.434–9. Available at: http://www.ncbi.nlm.nih.gov/pubmed/18416700 [Accessed October 4, 2012].

Bredenoord, A. et al., 2005. Sleeve sensor versus high-resolution manometry for the detection of transient lower esophageal sphincter relaxations. *American journal of physiology. Gastrointestinal and liver physiology*, 288(6), pp.G1190–4. Available at: http://www.ncbi.nlm.nih.gov/pubmed/15650131 [Accessed October 9, 2012].

Bredenoord, A.J. et al., 2005. Reproducibility of multichannel intraluminal electrical impedance monitoring of gastroesophageal reflux. *American Journal of Gastroenterology*, 100(2), pp.265–269.

Bredenoord, A.J. et al., 2007. Technology review: Esophageal impedance monitoring. *The American journal of gastroenterology*, 102(1), pp.187–94. Available at: http://www.ncbi.nlm.nih.gov/pubmed/17100961 [Accessed October 9, 2012].

Bredenoord, A.J. et al., 2003. The gastro-oesophageal pressure inversion point revisited. *Scandinavian journal of gastroenterology*, 38(8), pp.812–8. Available at: http://www.ncbi.nlm.nih.gov/pubmed/12940432 [Accessed October 9, 2012].

Bruley des Varannes, S. et al., 2005. Simultaneous recordings of oesophageal acid exposure with conventional pH monitoring and a wireless system (Bravo). *Gut*, 54(12), pp.1682–6. Available at: http://www.pubmedcentral.nih.gov/articlerender.fcgi?artid=1774783&tool=pmcentrez&rendertype=abstract [Accessed November 12, 2012].

Cameron, A.J. et al., 2002. Gastroesophageal reflux disease in monozygotic and dizygotic twins. *Gastroenterology*, 122(1), pp.55–9. Available at: http://www.ncbi.nlm.nih.gov/pubmed/11781280 [Accessed March 25, 2014].

Castell, D.O. et al., 1992. Alginic acid decreases postprandial upright gastroesophageal reflux. Comparison with equal-strength antacid. *Digestive diseases and sciences*, 37(4), pp.589–93. Available at: http://www.ncbi.nlm.nih.gov/pubmed/1551350.

Chandrasoma, P.T. & DeMeester, T.R., 2006. *GERD: Reflux to Esophageal Adenocarcinoma*, London: Elsevier.

Chourasia, D. & Ghoshal, U.C., 2008. Pathogenesis of gastro-oesophageal reflux disease: what role do Helicobacter pylori and host genetic factors play? *Tropical gastroenterology : official journal of the Digestive Diseases Foundation*, 29(1), pp.13–9. Available at: http://www.ncbi.nlm.nih.gov/pubmed/18564661 [Accessed March 25, 2014].

Clark, G.W.B., 2003. Effect of Helicobacter pylori infection in Barrett's esophagus and the genesis of esophageal adenocarcinoma. *World journal of surgery*, 27(9), pp.994–8. Available at: http://www.ncbi.nlm.nih.gov/pubmed/14560364 [Accessed May 21, 2014].

Clarke, a T. et al., 2009. Paradox of gastric cardia: it becomes more acidic following meals while the rest of stomach becomes less acidic. *Gut*, 58(7), pp.904–9. Available at: http://www.ncbi.nlm.nih.gov/pubmed/19060017 [Accessed October 4, 2012].

Clarke, a T. et al., 2008. Severe reflux disease is associated with an enlarged unbuffered proximal gastric acid pocket. *Gut*, 57(3), pp.292–7. Available at: http://www.ncbi.nlm.nih.gov/pubmed/17272648 [Accessed October 4, 2012].

Colas-Atger, E. et al., 2002. Relationship between acid reflux episodes and gastroesophageal reflux symptoms is very inconstant. *Digestive diseases and sciences*, 47(3), pp.645–51. Available at: http://www.ncbi.nlm.nih.gov/pubmed/11911354.

Conklin, J., Pimentel, M. & Soffer, E., 2009. *Color Atlas of High Resolution Manometry* 2009, ed., New York: Springer US.

Connor, F.L. et al., 2009. Interobserver variability in antroduodenal manometry. *Neurogastroenterology and motility : the official journal of the European Gastrointestinal Motility Society*, 21(5), pp.500–7, e3. Available at: http://www.ncbi.nlm.nih.gov/pubmed/18665977 [Accessed October 4, 2012].

DeMeester, T.R. et al., 1980. Technique, indications, and clinical use of 24 hour esophageal ph monitoring. *Journal of Thoracic and Cardiovascular Surgery*, 79(5), pp.656–667.

Demierre, M. et al., 2004. Contactless 360° absolute angular CMOS microsystem based on vertical Hall sensors. *Sensors and Actuators A: Physical*, 116(1), pp.39–44. Available at:

http://linkinghub.elsevier.com/retrieve/pii/S0924424704001888 [Accessed October 4, 2012].

Dent, J., 1976. A new technique for continuous sphincter pressure measurement. *Gastroenterology*, 71(2), pp.263–7. Available at: http://www.ncbi.nlm.nih.gov/pubmed/939387 [Accessed November 5, 2012].

Dodds, W.J. et al., 1975. A rapid pull-through technique for measuring lower esophageal sphincter pressure. *Gastroenterology*, 68(3), pp.437–43. Available at: http://www.ncbi.nlm.nih.gov/pubmed/1089576 [Accessed November 5, 2012].

Dodds, W.J., Dent, J. & Hogan, W., 1982. Mechanisms of gastro-oesophageal reflux in patiends with reflux oesophagitis. *New England Journal of Medicine*, 307, pp.1547–52.

Drljaca, P.M. et al., 2002. Design of planar magnetic concentrators for high sensitivity Hall devices. *Sensors and Actuators A: Physical*, 97-98, pp.10–14.

Edelstein, A.S. & Fischer, G. a., 2002. Minimizing 1/f noise in magnetic sensors using a microelectromechanical system flux concentrator. *Journal of Applied Physics*, 91(10), p.7795. Available at: http://link.aip.org/link/JAPIAU/v91/i10/p7795/s1&Agg=doi [Accessed October 4, 2012].

Feldman, M., Smith, H.J. & Simon, T.R., 1984. Gastric emptying of solid radiopaque markers: studies in healthy subjects and diabetic patients. *Gastroenterology*, 87(4), pp.895–902. Available at: http://www.ncbi.nlm.nih.gov/pubmed/6468877 [Accessed November 22, 2012].

Feng, D. & Jin, G., 2005. *Introduction to condensed matter physics, Volume 1.*, Hackensack, NJ: World Scientific Publishing.

Fletcher, J. et al., 2004. Studies of acid exposure immediately above the gastro-oesophageal squamocolumnar junction: evidence of short segment reflux. *Gut*, 53(2), pp.168–73. Available at: http://www.pubmedcentral.nih.gov/articlerender.fcgi?artid=1774939&tool=pmcentrez&rendertype=abstract.

Fujiwara, Y. & Arakawa, T., 2009. Epidemiology and clinical characteristics of GERD in the Japanese population. *Journal of gastroenterology*, 44(6), pp.518–34. Available at: http://www.ncbi.nlm.nih.gov/pubmed/19365600 [Accessed March 25, 2014].

Ghoshal, U.C. & Chourasia, D., 2010. Gastroesophageal Reflux Disease and Helicobacter pylori: What May Be the Relationship? *Journal of neurogastroenterology and motility*, 16(3), pp.243–50. Available at:

http://www.pubmedcentral.nih.gov/articlerender.fcgi?artid=2912116&tool=pmcentrez&rendertype=abstract [Accessed October 31, 2012].

Goodman, K. et al., 2010. Assessing gastrointestinal motility and disintegration profiles of magnetic tablets by a novel magnetic imaging device and gamma scintigraphy. *European journal of pharmaceutics and biopharmaceutics : official journal of Arbeitsgemeinschaft für Pharmazeutische Verfahrenstechnik e.V*, 74(1), pp.84–92. Available at: http://www.ncbi.nlm.nih.gov/pubmed/19602377 [Accessed October 4, 2012].

Gordon, C. et al., 2004. The role of the hiatus hernia in gastro-oesophageal reflux disease. *Alimentary pharmacology & therapeutics*, 20(7), pp.719–32. Available at: http://www.ncbi.nlm.nih.gov/pubmed/15379832 [Accessed October 9, 2012].

Griffith, G., Owen, G. & Shields, R., 1966. Measurement of gastric emptying time using a meal labelled with Chromium-51. *British Journal of Surgery*, 53(2), p.150. Available at: http://apps.webofknowledge.com/full_record.do?product=UA&search_mode=GeneralSearch&qid=12&SID=T192KMJgF67jNcdbNC2&page=1&doc=2 [Accessed November 22, 2012].

Griffith, W.C. et al., 2009. Miniature atomic magnetometer integrated with flux concentrators. *Applied Physics Letters*, 94(2), p.023502. Available at: http://link.aip.org/link/APPLAB/v94/i2/p023502/s1&Agg=doi [Accessed October 4, 2012].

Guo, X., Yan, G. & He, W., 2008. A position telemetric method for implantable microcapsules in the gastrointestinal tract. *Measurement Science and Technology*, 19(4), p.045201. Available at: http://stacks.iop.org/0957-0233/19/i=4/a=045201?key=crossref.f833aca2f39cff809d8cd1be47afed7a [Accessed October 4, 2012].

Heerens, W.-C., 1986. Application of capacitance techniques in sensor design. *Journal of Physics E: Scientific Instruments*, 19(11), pp.897–906. Available at: http://stacks.iop.org/0022-3735/19/i=11/a=002?key=crossref.7bdb5f3969a523151776a2ff8ef0ef01.

Hill, L.D. et al., 1996. The gastroesophageal flap valve: in vitro and in vivo observations. *Gastrointestinal Endoscopy*, 44(5), pp.541–547. Available at: http://dx.doi.org/10.1016/S0016-5107(96)70006-8 [Accessed October 26, 2012].

Hinton, J.M., Lennard-Jones, J.E. & Young, a C., 1969. A ne method for studying gut transit times using radioopaque markers. *Gut*, 10(10), pp.842–7. Available at: http://www.pubmedcentral.nih.gov/articlerender.fcgi?artid=1552992&tool=pmcentrez&rendertype=abstract.

Hirano, I., 2006. Review article: modern technology in the diagnosis of gastro-oesophageal reflux disease--Bilitec, intraluminal impedance and Bravo capsule pH monitoring. *Alimentary pharmacology & therapeutics*, 23 Suppl 1(December 2005), pp.12–24. Available at: http://www.ncbi.nlm.nih.gov/pubmed/16483266.

Ho, K.Y. & Kang, J.Y., 2000. Esophageal mucosal acid sensitivity can coexist with normal pH. *Journal of Gastroenterology*, 35, pp.261–264.

Holloway, R.H., 2005. Capsule pH monitoring: is wireless more? *Gut*, 54(12), pp.1672–3. Available at: http://www.pubmedcentral.nih.gov/articlerender.fcgi?artid=1774798&tool=pmcentrez&rendertype=abstract [Accessed November 6, 2012].

Holloway, R.H. et al., 1997. Effect of intraduodenal fat on lower oesophageal sphincter function and gastro-oesophageal reflux. *Gut*, 40(4), pp.449–53. Available at: http://www.pubmedcentral.nih.gov/articlerender.fcgi?artid=1027116&tool=pmcentrez&rendertype=abstract [Accessed March 25, 2014].

Holloway, R.H., 2006. Esophageal manometry. *GI Motility online*. Available at: http://www.nature.com/gimo/contents/pt1/full/gimo30.html#B5 [Accessed November 1, 2012].

Holloway, R.H. et al., 1985. Gastric distention: a mechanism for postprandial gastroesophageal reflux. *Gastroenterology*, 89(4), pp.779–84. Available at: http://www.ncbi.nlm.nih.gov/pubmed/4029557 [Accessed March 25, 2014].

Holloway, R.H., 2000. The anti-reflux barrier and mechanisms of gastro-oesophageal reflux. *Baillière's best practice & research. Clinical gastroenterology*, 14(5), pp.681–99. Available at: http://www.ncbi.nlm.nih.gov/pubmed/11003803 [Accessed October 9, 2012].

Holloway, R.H., Kocyan, P. & Dent, J., 1991. Provocation of transient lower esophageal sphincter relaxations by meals in patients with symptomatic gastroesophageal reflux. *Digestive diseases and sciences*, 36(8), pp.1034–9. Available at: http://www.ncbi.nlm.nih.gov/pubmed/1864194 [Accessed March 25, 2014].

Holloway, R.H., Penagini, R. & Ireland, a C., 1995. Criteria for objective definition of transient lower esophageal sphincter relaxation. *The American journal of physiology*, 268(1 Pt 1), pp.G128–33. Available at: http://www.ncbi.nlm.nih.gov/pubmed/7840195.

Holloway, R.H. & Sifrim, D.A., 2008. The acid pocket and its relevance to reflux disease. *Gut*, 57(3), pp.285–6. Available at: http://www.ncbi.nlm.nih.gov/pubmed/18268050 [Accessed October 9, 2012].

Holloway, R.H. & Zhang, Q., 2000. The GABA-B receptor agonist Ba- clofen inhibits transient lower oesophageal sphincter relaxations and gastro-oesophageal reflux in patients with reflux disease. *Gut*, 47 (SIII), p.A24.

Hopkins, J.A. & Wehrli, F.W., 1997. Magnetic susceptibility measurement of insoluble solids by NMR: magnetic susceptibility of bone. *Magnetic resonance in medicine : official journal of the Society of Magnetic Resonance in Medicine / Society of Magnetic Resonance in Medicine*, 37(4), pp.494–500. Available at: http://www.ncbi.nlm.nih.gov/pubmed/9094070 [Accessed January 29, 2014].

Hu, Z. et al., 2000. Application of a biomagnetic measurement system (BMS) to the evaluation of gastrointestinal transit of intestinal pressure-controlled colon delivery capsules (PCDCs) in human subjects. *Pharmaceutical research*, 17(2), pp.160–7. Available at: http://www.ncbi.nlm.nih.gov/pubmed/10751030.

Ishiki, K. et al., 2004. Helicobacter pylori eradication improves pre-existing reflux esophagitis in patients with duodenal ulcer disease. *Clinical gastroenterology and hepatology : the official clinical practice journal of the American Gastroenterological Association*, 2(6), pp.474–9. Available at: http://www.ncbi.nlm.nih.gov/pubmed/15181615 [Accessed March 25, 2014].

Janiak, P. et al., 2001. Changes in upper esophageal motor function in reflux esophagitis defined by high resolution manometry (HRM). *Gastroenterology*, 120(5), pp.A219–A219. Available at: http://apps.webofknowledge.com/full_record.do?product=WOS&search_mode=GeneralSearch&qid=6&SID=V2@8EoHnM5naJBe3JEC&page=4&doc=35&cacheurlFromRightClick=no [Accessed November 2, 2012].

Janiak, P. et al., 2000. Does high resolution manometry detect esophageal motility disorders more reliable than conventional manometry? *Gastroenterology*, 118(4), pp.A132–A132. Available at: http://apps.webofknowledge.com/full_record.do?product=WOS&search_mode=GeneralSearch&qid=6&SID=V2@8EoHnM5naJBe3JEC&page=3&doc=22&cacheurlFromRightClick=no [Accessed November 2, 2012].

Kahrilas, P.J. et al., 2000. Increased frequency of transient lower esophageal sphincter relaxation induced by gastric distention in reflux patients with hiatal hernia. *Gastroenterology*, 118(4), pp.688–95. Available at: http://www.ncbi.nlm.nih.gov/pubmed/10734020 [Accessed March 25, 2014].

Kahrilas, P.J. et al., 1999. The effect of hiatus hernia on gastro-oesophageal junction pressure. *Gut*, 44(4), pp.476–82. Available at: http://www.pubmedcentral.nih.gov/articlerender.fcgi?artid=2891431&tool=pmcentrez&rendertype=abstract.

Kahrilas, P.J. et al., 1986. Upper esophageal sphincter function during belching. *Gastroenterology*, 91(1), pp.133–40. Available at: http://www.ncbi.nlm.nih.gov/pubmed/3710062 [Accessed March 25, 2014].

Kaye, M.D. & Showalter, J.P., 1971. Manometric configuration of the lower esophageal sphincter in normal human subjects. *Gastroenterology*, 61(2), pp.213–23. Available at: http://www.ncbi.nlm.nih.gov/pubmed/5563404 [Accessed November 5, 2012].

Koike, T. et al., 2001. Helicobacter pylori infection prevents erosive reflux oesophagitis by decreasing gastric acid secretion. *Gut*, 49(3), pp.330–4. Available at: http://www.pubmedcentral.nih.gov/articlerender.fcgi?artid=1728422&tool=pmcentrez&rendertype=abstract [Accessed March 22, 2014].

Kuo, P., Holloway, R.H. & Nguyen, N.Q., 2012. Current and future techniques in the evaluation of dysphagia. *Journal of gastroenterology and hepatology*, 27(5), pp.873–81. Available at: http://www.ncbi.nlm.nih.gov/pubmed/22369033 [Accessed November 24, 2012].

Kusters, J.G., van Vliet, A.H.M. & Kuipers, E.J., 2006. Pathogenesis of Helicobacter pylori infection. *Clinical microbiology reviews*, 19(3), pp.449–90. Available at: http://www.pubmedcentral.nih.gov/articlerender.fcgi?artid=1539101&tool=pmcentrez&rendertype=abstract [Accessed March 21, 2014].

Kwiatek, M. a & Pandolfino, J.E., 2008. The Bravo pH capsule system. *Digestive and liver disease : official journal of the Italian Society of Gastroenterology and the Italian Association for the Study of the Liver*, 40(3), pp.156–60. Available at: http://www.ncbi.nlm.nih.gov/pubmed/18096447 [Accessed November 6, 2012].

Lawrie, J.H. & Forrest, A.P.M., 1965. The measurement of gastric acid. *Postgrad. Med. J.*, 41, pp.408–417.

Lee, Y. et al., 2012. Transient hiatus hernia during transient lower oesophageal sphincter realxations. In *British Society of Gastroenterology Annual Meating*. pp. Sup 2, A39–A39.

Lee, Y.Y., Seenan, J.P., et al., 2012. Development and validation of a probe allowing accurate and continuous monitoring of location of squamo-columnar junction. *Medical engineering & physics*, 34(3), pp.279–89. Available at: http://www.ncbi.nlm.nih.gov/pubmed/21852175 [Accessed October 4, 2012].

Lee, Y.Y. et al., 2012. Kinetics of transient hiatus hernia during transient lower esophageal sphincter relaxations and swallows in healthy subjects. *Neurogastroenterology and motility : the official journal of the European Gastrointestinal Motility Society*, 24(11), pp.990–e539. Available at: http://www.ncbi.nlm.nih.gov/pubmed/22680279 [Accessed November 13, 2012].

Lee, Y.Y., Whiting, J.G.H., et al., 2012. Measuring movement and location of the gastroesophageal junction: research and clinical implications. *Scandinavian*

journal of gastroenterology, (October), pp.1–11. Available at: http://www.ncbi.nlm.nih.gov/pubmed/23205940 [Accessed January 16, 2013].

Lee, Y.Y. et al., 2013. Partial Hiatus Herniation Occurs in Asymptomatic Individuals With Central Obesity or With Abdominal Belt Compression. *Gastroenterology*, 144(5), p.S–787–S–788. Available at: http://www.sciencedirect.com/science/article/pii/S0016508513629121.

Lee, Y.Y. et al., 2011. Squamo-columnar junction locator probe: an in vivo validation study. In *Annual Meeting of British-Society of Gastroenterology*. pp. A181–182.

Lee, Y.Y. et al., 2011. The development of squamo-columnar junction locator probe and its performance on bench studies. In *Annual Meeting of British-Society-of-Gastroenterology*. pp. A181–A182.

Lee, Y.Y. & McColl, K.E.L., 2013. Pathophysiology of gastroesophageal reflux disease. *Best practice & research. Clinical gastroenterology*, 27(3), pp.339–51. Available at: http://www.ncbi.nlm.nih.gov/pubmed/23998973 [Accessed March 20, 2014].

Leroy, P. et al., 2006. High magnetic field amplification for improving the sensitivity of Hall sensors. *IEEE Sensors Journal*, 6(3), pp.707–713. Available at: http://ieeexplore.ieee.org/lpdocs/epic03/wrapper.htm?arnumber=1634424.

Levine, R.L. et al., 1994. Equivalence of litmus paper and intragastric pH probes for intragastric pH monitoring in the intensive care unit. *Critical Care Medicine*, 22(6), pp.945–948. Available at: http://europepmc.org/abstract/MED/7911416 [Accessed November 6, 2012].

Lidums, I. et al., 2000. Control of transient lower esophageal sphincter relaxations and reflux by the GABA(B) agonist baclofen in normal subjects. *Gastroenterology*, 118(1), pp.7–13. Available at: http://www.ncbi.nlm.nih.gov/pubmed/10611148 [Accessed March 25, 2014].

Lieberman, D. a, 1988. 24-hour esophageal pH monitoring before and after medical therapy for reflux esophagitis. *Digestive diseases and sciences*, 33(2), pp.166–71. Available at: http://www.ncbi.nlm.nih.gov/pubmed/3338365.

Lodhia, N. et al., 2007. High-resolution manometry in determining bolus transit through the esophagogastric junction: A validation study using flouroscopy. *Gastroenterology*, 132(4), pp.A597–A597. Available at: http://apps.webofknowledge.com/full_record.do?product=UA&search_mode=GeneralSearch&qid=23&SID=T192KMJgF67jNcdbNC2&page=1&doc=1 [Accessed November 22, 2012].

Logan, R.P.H. et al., 2002. *ABC of the Upper Gastrointestinal Tract* First Edit., London: BMJ Books.

Lutsi, B. & Hirano, I., 2006. Ambulatory pH Monitoring: New Advances and Indications. *Hepatology*, 2(11), pp.835–842.

Luzio, S. et al., 1989. A biomagnetic method for studying gastro-intestinal activity. *Il Nuovo Cimento D*, 11(12), pp.1853–1859. Available at: http://link.springer.com/article/10.1007/BF02459126 [Accessed November 26, 2012].

Maerten, P. et al., 2007. Wireless capsule pH monitoring: does it fulfil all expectations? *Digestion*, 76(3-4), pp.235–40. Available at: http://www.ncbi.nlm.nih.gov/pubmed/18174686 [Accessed November 6, 2012].

Martini, F.H. & Nath, J.I., 2009. *Fundamentals of Anatomy and Physiology* Eighth. L. Berriman, ed., Pearson Benjamon Cummings.

Mattox, H.E. et al., 1992. Gastroesophageal pH step-up inaccurately locates proximal border of lower esophageal sphincter. *Digestive diseases and sciences*, 37(8), pp.1185–91. Available at: http://www.ncbi.nlm.nih.gov/pubmed/1499441 [Accessed March 25, 2014].

Mattox, H.E. & Richter, J.E., 1990. Prolonged ambulatory esophageal pH monitoring in the evaluation of gastroesophageal reflux disease. *The American journal of medicine*, 89(3), pp.345–56. Available at: http://www.ncbi.nlm.nih.gov/pubmed/2203264 [Accessed March 25, 2014].

McClelland, G.R. & Sutton, J. a, 1985. Epigastric impedance: a non-invasive method for the assessment of gastric emptying and motility. *Gut*, 26(6), pp.607–14. Available at: http://www.pubmedcentral.nih.gov/articlerender.fcgi?artid=1432755&tool=pmcentrez&rendertype=abstract.

McColl, K.E.L., 2010. Clinical practice. Helicobacter pylori infection. *The New England journal of medicine*, 362(17), pp.1597–604. Available at: http://www.ncbi.nlm.nih.gov/pubmed/20427808 [Accessed March 21, 2014].

Menon, S. et al., 2013. Do differences in female sex hormone levels contribute to gastro-oesophageal reflux disease? *European journal of gastroenterology & hepatology*, 25(7), pp.772–7. Available at: http://www.ncbi.nlm.nih.gov/pubmed/23470358 [Accessed March 25, 2014].

Miller, L., Liu, J.B., et al., 1992. High frequency endoluminal sonography of the esophagus using a 20MHz ultrasound transducer compared to endoscopic grading of the size of esophageal varices. *Gastroenterology*, 102(4 PART 2), p.A853. Available at: http://apps.webofknowledge.com/full_record.do?product=UA&search_mode=GeneralSearch&qid=5&SID=V1NkhmMPDHepdaNDjMm&page=3&doc=27&cacheurlFromRightClick=no [Accessed November 26, 2012].

Miller, L., Liu, J.-B., et al., 1992. High frequency endoluminal sonography of the esophagus using a 20MHz ultrasound transducer correlation with cross-sectional histology in human autopsy specimens. *Gastroenterology*, 102(4(2)), p.A486. Available at: http://apps.webofknowledge.com/full_record.do?product=UA&search_mode=GeneralSearch&qid=5&SID=V1NkhmMPDHepdaNDjMm&page=3&doc=26&cacheurlFromRightClick=no [Accessed November 26, 2012].

Mittal, R.K. et al., 2005. Sensory and motor function of the esophagus: Lessons from ultrasound imaging. *Gastroenterology*, 128(2), pp.487–497. Available at: http://dx.doi.org/10.1053/j.gastro.2004.08.004 [Accessed November 26, 2012].

Mittal, R.K., Stewart, W.R. & Schirmer, B.D., 1992. Effect of a catheter in the pharynx on the frequency of transient lower esophageal sphincter relaxations. *Gastroenterology*, 103(4), pp.1236–40. Available at: http://www.ncbi.nlm.nih.gov/pubmed/1397880 [Accessed October 9, 2012].

Mohammed, I. et al., 2003. Genetic influences in gastro-oesophageal reflux disease: a twin study. *Gut*, 52(8), pp.1085–9. Available at: http://www.pubmedcentral.nih.gov/articlerender.fcgi?artid=1773757&tool=pmcentrez&rendertype=abstract [Accessed March 25, 2014].

Murphy, D.W., Yuan, Y. & Castell, D.O., 1989. Does the intraesophageal pH probe accurately detect acid reflux? Simultaneous recording with two pH probes in humans. *Digestive diseases and sciences*, 34(5), pp.649–56. Available at: http://www.ncbi.nlm.nih.gov/pubmed/2714140.

Nagler, R. et al., 1960. Effect of gastric intubation on the normal mechanisms preventing gastroesophageal reflux. *New England Journal of Medicine*, 262, pp.1325–6. Available at: http://www.ncbi.nlm.nih.gov/pubmed/14425796.

Nagler, R. & Spiro, H., 1963. Persistent gastroesophageal reflux induced during prolonged gastric intubation. *New England Journal of Medicine*, 269, pp.495–500. Available at: http://www.ncbi.nlm.nih.gov/pubmed/14043246.

Nebel, O.T., Fornes, M.F. & Castell, D.O., 1976. Symptomatic gastroesophageal reflux: incidence and precipitating factors. *The American journal of digestive diseases*, 21(11), pp.953–6. Available at: http://www.ncbi.nlm.nih.gov/pubmed/984016.

Neill, K.M., Rice, K.T. & Ahern, H.L., 1993. Comparison of two methods of measuring gastric pH. *Heart & lung : the journal of critical care*, 22(4), pp.349–55. Available at: http://www.ncbi.nlm.nih.gov/pubmed/8360068 [Accessed November 6, 2012].

Nguyen, H.N. et al., 1997. Dynamics of esophageal bolus transport in healthy subjects studied using multiple intraluminal impedancometry Dynamics of

esophageal bolus transport in healthy subjects studied using multiple intraluminal impedancometry. *Am J Physiol*, 273(4), pp.G958–64.

Nicosia, M. a et al., 2001. Local longitudinal muscle shortening of the human esophagus from high-frequency ultrasonography. *American journal of physiology. Gastrointestinal and liver physiology*, 281(4), pp.G1022–33. Available at: http://www.ncbi.nlm.nih.gov/pubmed/11557523.

Noar, J.H. et al., 2003. An in vitro study into the corrosion of intra-oral magnets in the presence of dental amalgam. *European journal of orthodontics*, 25(6), pp.615–9. Available at: http://www.ncbi.nlm.nih.gov/pubmed/14700268 [Accessed March 25, 2014].

Noar, J.H. & Evans, R.D., 1999. Rare earth magnets in orthodontics: an overview. *British journal of orthodontics*, 26(1), pp.29–37. Available at: http://www.ncbi.nlm.nih.gov/pubmed/10333885.

Noordzij, J.P. et al., 2000. The effect of mechanoreceptor stimulation of the laryngopharynx on the oesophago-gastric junction. *Neurogastroenterology and motility : the official journal of the European Gastrointestinal Motility Society*, 12(4), pp.353–9. Available at: http://www.ncbi.nlm.nih.gov/pubmed/10886677.

Odze, R.D., 2009. Barrett esophagus: histology and pathology for the clinician. *Nature reviews. Gastroenterology & hepatology*, 6(8), pp.478–90. Available at: http://dx.doi.org/10.1038/nrgastro.2009.103 [Accessed May 22, 2014].

Paixão, F.C. et al., 2007. A novel biomagnetic instrumentation with four magnetoresistive sensors to evaluate gastric motility. *Conference proceedings : ... Annual International Conference of the IEEE Engineering in Medicine and Biology Society. IEEE Engineering in Medicine and Biology Society. Conference*, 2007, pp.2215–8. Available at: http://www.ncbi.nlm.nih.gov/pubmed/18002430.

Pandolfino, J.E., Zhang, Q., et al., 2005. Acid reflux event detection using the Bravo wireless versus the Slimline catheter pH systems: why are the numbers so different? *Gut*, 54(12), pp.1687–92. Available at: http://www.pubmedcentral.nih.gov/articlerender.fcgi?artid=1774796&tool=pmcentrez&rendertype=abstract [Accessed November 12, 2012].

Pandolfino, J.E. et al., 2007. Acidity surrounding the squamocolumnar junction in GERD patients: “acid pocket” versus “acid film”. *The American journal of gastroenterology*, 102(12), pp.2633–41. Available at: http://www.ncbi.nlm.nih.gov/pubmed/17714553 [Accessed October 9, 2012].

Pandolfino, J.E. et al., 2003. Ambulatory esophageal pH monitoring using a wireless system. *The American Journal of Gastroenterology*, 98(4), pp.740–749. Available at: http://apps.webofknowledge.com/full_record.do?product=WOS&search_mode=

GeneralSearch&qid=1&SID=T2lfKBjA6LN7eHe67h6&page=1&doc=1 [Accessed November 8, 2012].

Pandolfino, J.E., Shi, G., et al., 2005. Measuring EGJ opening patterns using high resolution intraluminal impedance. *Neurogastroenterology and motility : the official journal of the European Gastrointestinal Motility Society*, 17(2), pp.200–6. Available at: http://www.ncbi.nlm.nih.gov/pubmed/15787940 [Accessed November 13, 2012].

Pandolfino, J.E., 2005. Prolonged pH monitoring: Bravo capsule. *Gastrointestial Endoscopy Clinics of North America*, 15(2), pp.307–318. Available at: http://europepmc.org/abstract/MED/15722243/reload=0;jsessionid=zhbZ4RD8xIwohccSIxk9.4 [Accessed November 6, 2012].

Pandolfino, J.E., Ghosh, S.K., et al., 2006. Quantifying EGJ morphology and relaxation with high-resolution manometry: a study of 75 asymptomatic volunteers. *American journal of physiology. Gastrointestinal and liver physiology*, 290(5), pp.G1033–40. Available at: http://www.ncbi.nlm.nih.gov/pubmed/16455788 [Accessed October 9, 2012].

Pandolfino, J.E., Zhang, Q.G., et al., 2006. Transient lower esophageal sphincter relaxations and reflux: mechanistic analysis using concurrent fluoroscopy and high-resolution manometry. *Gastroenterology*, 131(6), pp.1725–33. Available at: http://www.ncbi.nlm.nih.gov/pubmed/17087957 [Accessed October 4, 2012].

Parks, T. & Son, J., 2005. High Resolution Solid State Pressure Sensor. , p.19.

Peek, R.M., 2004. Helicobacter Pylori and Gastroesophageal Reflux Disease. *Current Treatment Options in Gastroenterology*, 7(4), pp.59–70.

Penagini, R. et al., 1996. Motor events underlying gastro-oesophageal reflux in ambulant patients with reflux oesophagitis. *Neurogastroenterology and motility : the official journal of the European Gastrointestinal Motility Society*, 8(2), pp.131–41. Available at: http://www.ncbi.nlm.nih.gov/pubmed/8784797 [Accessed March 25, 2014].

Penagini, R., Mangano, M. & Bianchi, P.A., 1998. Effect of increasing the fat content but not the energy load of a meal on gastro-oesophageal reflux and lower oesophageal sphincter motor function. *Gut*, 42(3), pp.330–333. Available at: http://gut.bmj.com/content/42/3/330.full [Accessed March 25, 2014].

Pitt, G. et al., 1983. Method of making a hall effect device. , p.7.

Pitt, G. & Extance, P., 1986. Hall effect device with overlapping flux concentrators.

Pohl, D. & Tutuian, R., 2009. Reflux monitoring: pH-metry, Bilitec and oesophageal impedance measurements. *Best practice & research. Clinical gastroenterology*,

23(3), pp.299–311. Available at: http://www.ncbi.nlm.nih.gov/pubmed/19505660 [Accessed October 9, 2012].

Popovic, R.., Randjelovic, Z. & Manic, D., 2001. Integrated Hall-effect magnetic sensors. *Sensors and Actuators A: Physical*, 91(1-2), pp.46–50. Available at: http://linkinghub.elsevier.com/retrieve/pii/S0924424701004782.

Popovic, R.S., 1989. Hall-effect devices. *Sensors and Actuators*, 17, pp.39–53.

Puers, R., 1993. Capacitive sensors: When and how to use them. *Sensors and Actuators A: Physical*, 37-38, pp.93–105. Available at: http://linkinghub.elsevier.com/retrieve/pii/092442479380019D.

Queiroz, D.M.M. et al., 2004. IL1B and IL1RN polymorphic genes and Helicobacter pylori cagA strains decrease the risk of reflux esophagitis. *Gastroenterology*, 127(1), pp.73–9. Available at: http://www.ncbi.nlm.nih.gov/pubmed/15236174 [Accessed March 25, 2014].

Ramsden, E., 2006. *Hall Effect Sensors: Theory and Applications*, London: Elsevier.

Rastegarpanah, M. & Mojtahedzadeh, M., 2007. Medical Hypotheses & Ideas Original article Suppress or not to suppress gastric acid ? Intra-gastric pH monitoring vs . Litmus paper in critically ill patients. *Medical Hypotheses*, pp.8–12.

Reig, C., Cubells-Beltran, M.-D. & Muñoz, D.R., 2009. Magnetic Field Sensors Based on Giant Magnetoresistance (GMR) Technology: Applications in Electrical Current Sensing. *Sensors (Basel, Switzerland)*, 9(10), pp.7919–42. Available at: http://www.pubmedcentral.nih.gov/articlerender.fcgi?artid=3292089&tool=pmcentrez&rendertype=abstract [Accessed March 25, 2014].

Robertson, E. et al., 2011. High Resolution Oesophageal Manometry: Addressing Thermal Drift. In *Conference on Digestive Disease Week*. W B SAUNDERS CO-ELSEVIER INC, pp. S164–S164. Available at: http://apps.webofknowledge.com/full_record.do?product=UA&search_mode=GeneralSearch&qid=1&SID=Q1MEGCgbmn@km4ahJM8&page=2&doc=12&cacheurlFromRightClick=no [Accessed March 21, 2013].

Robertson, E. V et al., 2012. High-resolution esophageal manometry: addressing thermal drift of the manoscan system. *Neurogastroenterology and motility*, 24(1), pp.61–4, e11. Available at: http://www.ncbi.nlm.nih.gov/pubmed/22188326 [Accessed March 21, 2013].

Robertson, E. V. et al., 2011. High resolution oesophageal manometry: addressing thermal drift. *Gut*, 60(Suppl 1), pp.A22–A23. Available at: http://apps.webofknowledge.com/full_record.do?product=UA&search_mode=G

eneralSearch&qid=1&SID=Q1MEGCgbmn@km4ahJM8&page=2&doc=14&cacheurlFromRightClick=no [Accessed March 21, 2013].

Roman, S., Pandolfino, J. & Mion, F., 2009. High-resolution manometry: a new gold standard to diagnose esophageal dysmotility? *Gastroentérologie clinique et biologique*, 33(12), pp.1061–7. Available at: http://www.ncbi.nlm.nih.gov/pubmed/19896310 [Accessed November 1, 2012].

Roy, S. et al., 2012. The gastro-esophageal reflux barrier: biophysical analysis on 3D models of anatomy from magnetic resonance imaging. *Neurogastroenterology and motility : the official journal of the European Gastrointestinal Motility Society*, 24(7), pp.616–25, e269. Available at: http://www.ncbi.nlm.nih.gov/pubmed/22417158 [Accessed October 26, 2012].

Rubenstein, J.H. et al., 2014. Association between Helicobacter pylori and Barrett's esophagus, erosive esophagitis, and gastroesophageal reflux symptoms. *Clinical gastroenterology and hepatology : the official clinical practice journal of the American Gastroenterological Association*, 12(2), pp.239–45. Available at: http://www.ncbi.nlm.nih.gov/pubmed/23988686 [Accessed May 21, 2014].

Scheffer, R.C.H. et al., 2010. Effect of proximal gastric volume on hiatal hernia. *Neurogastroenterology and motility : the official journal of the European Gastrointestinal Motility Society*, 22(5), pp.552–6, e120. Available at: http://www.ncbi.nlm.nih.gov/pubmed/20105278 [Accessed October 9, 2012].

Schlageter, V. et al., 2001. Tracking system with 5 degrees of freedom using a 2D-array of Hall sensors and a permanent magnet. , 92, pp.37–42.

Schoeman, M.N. et al., 1995. Mechanisms of gastroesophageal reflux in ambulant healthy human subjects. *Gastroenterology*, 108(1), pp.83–91. Available at: http://www.ncbi.nlm.nih.gov/pubmed/7806066 [Accessed March 25, 2014].

Seefeld, U. et al., 1977. Esophageal histology in gastroesophageal reflux. Morphometric findings in suction biopsies. *The American journal of digestive diseases*, 22(11), pp.956–64. Available at: http://www.ncbi.nlm.nih.gov/pubmed/920705.

Shay, S.S., Bomeli, S. & Richter, J., 2002. Multichannel intraluminal impedance accurately detects fasting, recumbent reflux events and their clearing. *American journal of physiology. Gastrointestinal and liver physiology*, 283(2), pp.G376–83. Available at: http://www.ncbi.nlm.nih.gov/pubmed/12121885 [Accessed October 4, 2012].

Sierra Scientific, *ManoScan 360 Users Guide*,

Sifrim, D., 2004. Gastro-oesophageal reflux monitoring: review and consensus report on detection and definitions of acid, non-acid, and gas reflux. *Gut*, 53(7), pp.1024–1031. Available at:

http://gut.bmj.com/cgi/doi/10.1136/gut.2003.033290 [Accessed October 9, 2012].

Sifrim, D. & Holloway, R., 2001. Transient lower esophageal sphincter relaxations: how many or how harmful? *The American journal of gastroenterology*, 96(9), pp.2529–32. Available at: http://www.ncbi.nlm.nih.gov/pubmed/11569671.

Silny, J., 1991. Intraluminal Multiple Electric Impedance Procedure for Measurement of Gastrointestinal Motility Jiri S h y. *Journal of Gastrointestinal Motility*, 3(3), pp.151–162.

Silny, J. et al., 1993. Verification of the intraluminal multiple electrical impedance measurement for the recording of gastrointestinal motility. *Journal of Gastrointestinal Motility*, 5(January), pp.107–122.

Sinatra, F., 2010. Understanding the Interaction Between Blood Flow and an Applied Magnetic Field. *Theses and Dissertations, University of South Florida*.

Sofi, A. et al., 2011. Comparison of esophageal placement of Bravo capsule system under direct endoscopic guidance with conventional placement method. *Journal of Gastroenterology*, 2011(3), pp.243–248.

Srinivasan, R. et al., 2001. Esophageal function testing using multichannel intraluminal impedance. *American journal of physiology. Gastrointestinal and liver physiology*, 280(3), pp.G457–62. Available at: http://www.ncbi.nlm.nih.gov/pubmed/11171628.

Stathopoulos, E. et al., 2005. Magnetic pill tracking: a novel non-invasive tool for investigation of human digestive motility. *Neurogastroenterology and motility : the official journal of the European Gastrointestinal Motility Society*, 17(1), pp.148–54. Available at: http://www.ncbi.nlm.nih.gov/pubmed/15670274 [Accessed October 4, 2012].

Thorpe, J. a, 1981. Oesophageal manometry. Experience with the Arndorfer hydraulic-capillary infusion system. *Annals of the Royal College of Surgeons of England*, 63(3), pp.192–4. Available at: http://www.pubmedcentral.nih.gov/articlerender.fcgi?artid=2493913&tool=pmcentrez&rendertype=abstract.

Trudgill, N.J. & Riley, S.A., 2001. Transient lower esophageal sphincter relaxations are no more frequent in patients with gastroesophageal reflux disease than in asymptomatic volunteers. *The American journal of gastroenterology*, 96(9), pp.2569–74. Available at: http://www.ncbi.nlm.nih.gov/pubmed/11569677 [Accessed March 25, 2014].

Tsai, H.-F. & Hsu, P.-N., 2010. Interplay between Helicobacter pylori and immune cells in immune pathogenesis of gastric inflammation and mucosal pathology. *Cellular & molecular immunology*, 7(4), pp.255–9. Available at:

http://www.nature.com/cmi/journal/v7/n4/full/cmi20102a.html#References [Accessed March 25, 2014].

Tutuian, R. & Castell, D.O., 2006. Gastroesophageal reflux monitoring: pH and impedance. *GI Motility online*. Available at: http://www.nature.com/gimo/contents/pt1/full/gimo31.html [Accessed March 25, 2014].

Vela, M.F., 2008. Can nonacid reflux cause heartburn? *Current GERD Reports*, 1(3), pp.144–148. Available at: http://www.springerlink.com/index/10.1007/s12171-007-0011-3.

De Vries, A.C., Kuipers, E.J. & Rauws, E.A.J., 2009. Helicobacter pylori eradication and gastric cancer: when is the horse out of the barn? *The American journal of gastroenterology*, 104(6), pp.1342–5. Available at: http://www.ncbi.nlm.nih.gov/pubmed/19491846 [Accessed March 25, 2014].

Wallace, J.L. & Granger, D.N., 1996. The cellular and molecular basis of gastric mucosal defence. *FASEB J.*, 10(7), pp.731–40.

Wang, X., Meng, M.Q.-H. & Hu, C., 2006. A localization method using 3-axis magnetoresistive sensors for tracking of capsule endoscope. *Conference proceedings : ... Annual International Conference of the IEEE Engineering in Medicine and Biology Society. IEEE Engineering in Medicine and Biology Society. Conference*, 1(3), pp.2522–5. Available at: http://www.ncbi.nlm.nih.gov/pubmed/17946518.

Weisskoff, R.M. & Kiihne, S., 1992. MRI susceptometry: image-based measurement of absolute susceptibility of MR contrast agents and human blood. *Magnetic resonance in medicine : official journal of the Society of Magnetic Resonance in Medicine / Society of Magnetic Resonance in Medicine*, 24(2), pp.375–83. Available at: http://www.ncbi.nlm.nih.gov/pubmed/1569876 [Accessed January 29, 2014].

Weitschies, W. et al., 1997. High-resolution monitoring of the gastrointestinal transit of a magnetically marked capsule. *Journal of pharmaceutical sciences*, 86(11), pp.1218–22. Available at: http://www.ncbi.nlm.nih.gov/pubmed/9383729.

Weitschies, W. et al., 2005. Magnetic Marker Monitoring: An application of biomagnetic measurement instrumentation and principles for the determination of the gastrointestinal behavior of magnetically marked solid dosage forms. *Advanced drug delivery reviews*, 57(8), pp.1210–22. Available at: http://www.ncbi.nlm.nih.gov/pubmed/15935870 [Accessed October 4, 2012].

Weitschies, W. et al., 1994. Magnetic markers as a noninvasive tool to monitor gastrointestinal transit. *IEEE transactions on bio-medical engineering*, 41(2), pp.192–5. Available at: http://www.ncbi.nlm.nih.gov/pubmed/8026852.

Weitschies, W., Blume, H. & Mönnikes, H., 2010. Magnetic marker monitoring: high resolution real-time tracking of oral solid dosage forms in the gastrointestinal tract. *European journal of pharmaceutics and biopharmaceutics : official journal of Arbeitsgemeinschaft für Pharmazeutische Verfahrenstechnik e.V*, 74(1), pp.93–101. Available at: http://www.ncbi.nlm.nih.gov/pubmed/19619649 [Accessed October 4, 2012].

Wernly, J.A. et al., 1980. Intra-abdominal pressure and manometric data of the distal esophageal sphincter. Their relationship to gastroesophageal reflux. *Archives of surgery (Chicago, Ill. : 1960)*, 115(4), pp.534–9. Available at: http://www.ncbi.nlm.nih.gov/pubmed/7189112 [Accessed October 9, 2012].

Whiting, J.G.H. et al., 2012. Towards minimally invasive monitoring for gastroenterology - An external Squamocolumnar Junction Locator. *Conference proceedings : ... Annual International Conference of the IEEE Engineering in Medicine and Biology Society. IEEE Engineering in Medicine and Biology Society. Conference*, 2012(d), pp.1574–7. Available at: http://www.ncbi.nlm.nih.gov/pubmed/23366205.

Worsøe, J. et al., 2011. Gastric transit and small intestinal transit time and motility assessed by a magnet tracking system. *BMC gastroenterology*, 11(1), p.145. Available at: http://www.pubmedcentral.nih.gov/articlerender.fcgi?artid=3295650&tool=pmcentrez&rendertype=abstract [Accessed October 4, 2012].

Wu, X. et al., 2005. A new method of medical robotic device locating and tracking techniques. *Conference proceedings : ... Annual International Conference of the IEEE Engineering in Medicine and Biology Society. IEEE Engineering in Medicine and Biology Society. Conference*, 5, pp.4674–7. Available at: http://www.ncbi.nlm.nih.gov/pubmed/17281283.

Yaghoobi, M., Bijarchi, R. & Narod, S.A., 2010. Family history and the risk of gastric cancer. *British journal of cancer*, 102(2), pp.237–42. Available at: http://dx.doi.org/10.1038/sj.bjc.6605380 [Accessed March 25, 2014].

Appendix 1

Table 2.1 Effects of magnet rotation in horizontal plane anterior to Hall sensors on position and signal strength

Table showing Mean difference, Average difference, Standard Deviation and Mean Signal Strength for 1mm steps experiment (total distance of 120mm at 1mm steps along FRONT of Hall sensor arrays) with Neodymium (N42) magnet rotation (HORIZONTAL plane) 0, 20, 40, 60 and 90 degrees at increasing magnet distance away from Hall sensor arrays at 0, 5, 10 and 15mm calculated using Locator box LCD panel readings of position (mm) and signal strength (mV).

Degrees	Magnet Distance															
	0mm				5mm				10mm				15mm			
	Mean Diff	AvgDiff	SD	Mean SignalStrength	Mean Diff	AvgDiff	SD	Mean Signal Strength	Mean Diff	AvgDiff	SD	Mean Signal Strength	Mean Diff	Avg Diff	SD	Mean Signal Strength
0	-0.44	0.70	0.64	695	0.64	1.08	0.86	30.4	-	-	-	-	-	-	-	-
20	-0.29	0.95	0.84	674	0.36	1.84	1.20	40.8	-	-	-	-	-	-	-	-
40	-0.16	1.02	0.81	845	0.55	0.96	0.81	34.4	-0.67	0.90	0.79	13.1	-	-	-	-
60	-0.06	0.88	0.74	823	0.23	0.88	0.82	39.2	0.23	0.51	0.67	15.9	-0.98	1.17	1.01	11.5
90	-0.26	0.29	0.90	856	0.04	0.29	0.46	225	0.36	0.54	0.62	35.9	0.75	1.07	0.89	13.4

Deg=degree of magnet rotation on the horizontal plane of Hall sensor array or X-axis. Mean Diff=Mean difference was derived from average of differences between actual position readings on the Hall sensor arrays (mounted on a standard ruler of 1mm scale) and position readings from the locator box LCD panel (including both negative and positive readings). A negative result indicated that position from LCD was lower than actual position and vice-versa for a positive result. Avg Diff=Average difference derived from average of differences between actual position readings and locator LCD position readings similar to the mean difference but the negative readings were regarded as positive readings. SD=standard deviation of differences between actual position readings and locator LCD readings. Mean signal

strgth=mean signal strength derived from average of signal strength readings (in mV or millivolt) from the locator LCD. There were no readings for 0 degree at 10mm and 15mm, 20 degrees at 10mm and 15mm and 40 degrees at 1mm due to poor or unreliable signal strengths.

Table 2.2 Effects of magnet rotation in horizontal plane anterior to Hall sensors on position and signal strength

Table showing mean difference, average difference, standard deviation and mean signal strength for 1mm steps experiment (total distance of 120mm at 1mm steps along front of Hall sensor arrays) with neodymium (n42) magnet rotation (horizontal plane) 0, 20, 40, 60 and 90 degrees at increasing magnet distance away from Hall sensor arrays at 0, 5, 10 and 15mm calculated using Polygraf (medtronic®) readings of position (mm) and signal strength (mv).

Degrees	Magnet Distance															
	0mm				5mm				10mm				15mm			
	Mean Diff	Avg Diff	SD	Mean Signal Strgth	Mean Diff	Avg Diff	SD	Mean Signal Strength	Mean Diff	Avg Diff	SD	Mean Signal Strgth	Mean Diff	Avg Diff	SD	Mean Signal Strength
en0	-1.07	1.40	1.29	499	-0.82	2.39	3.05	72.1	-	-	-	-	-	-	-	-
20	-0.63	1.19	1.31	498	0.63	3.49	4.07	138	-3.36	3.93	3.39	1.18	-	-	-	-
40	-0.18	0.96	1.16	499	-0.34	1.11	1.37	240	-0.17	1.10	1.36	56.6	-0.40	1.10	1.36	4.89
60	-0.32	1.01	1.31	495	-0.20	0.93	1.20	472	-0.06	0.95	1.20	83.0	0.32	2.89	3.67	7.77
90	-0.36	1.00	1.23	498	-0.80	1.14	1.15	499	-1.53	1.60	0.86	139	0.39	1.48	2.19	23.5

Deg=degree of magnet rotation on the horizontal plane of Hall sensor array or X-axis. Mean Diff=Mean difference was derived from average of differences between actual position readings on the Hall sensor arrays (mounted on a standard ruler of 1mm scale) and position readings from the Polygraf using the PolygramNET™ software (including both negative and positive readings). Avg Diff=Average difference derived from average of differences between actual position readings and Polygraf position readings similar to the mean difference but the negative readings were regarded as positive readings. SD=standard deviation of differences between actual position readings and Polygraf readings. Mean signal strgth=mean signal strength derived from average of signal strength readings (in mV or millivolt) from the Polygraf. The signal strength reading from the Polygraf was capped at 500mV due to default setup of PolygramNET™ software. There were no readings for 0 degree at 10mm, 15mm and 20 degrees at 15mm due to poor or unreliable signal strengths.

Table 2.3 Effects of magnet rotation in vertical plane anterior to Hall sensors on position and signal strength

Table showing mean difference, average difference, standard deviation and mean signal strength for 1mm steps experiment (total distance of 20mm along front of Hall sensor arrays) with neodymium (n42) magnet rotation (vertical plane) 20, 40, 60 and 90 degrees at increasing magnet distance away from Hall sensor arrays at 0, 5, 10 and 15mm calculated using Polygraf (medtronic®) readings of position (mm) and signal strength (mv).

Degrees	Magnet Distance															
	0mm				5mm				10mm				15mm			
	Mean Diff	Avg Diff	SD	Mean Signal Strgth	Mean Diff	Avg Diff	SD	Mean Signal Strgth	Mean Diff	Avg Diff	SD	Mean Signal Strgth	Mean Diff	Avg Diff	SD	Mean Signal Strgth
0	-1.07	1.40	1.29	499.7	-0.82	2.39	3.05	72.17	-	-	-	-	-	-	-	-
20	-1.40	1.47	1.00	499.5	-3.51	4.74	4.68	469.2	-2.89	4.79	5.75	133.4	-3.37	11.77	12.04	-0.09
40	-1.03	1.05	0.84	499.9	-3.70	4.79	4.73	499.7	-3.41	4.53	4.21	167.2	-4.58	5.21	3.91	28.85
60	-0.96	1.07	1.05	499.1	-2.29	4.45	4.87	496.3	-2.66	3.90	3.90	263.3	-4.31	4.56	3.46	11.40
90	-0.36	1.00	1.23	498.5	-0.80	1.14	1.15	499.1	-1.53	1.60	0.86	139.2	0.39	1.48	2.19	23.57

Deg=degree of magnet rotation on the vertical plane of Hall sensor array or Y-axis. Mean Diff=Mean difference was derived from average of differences between actual position readings on the Hall sensor arrays (mounted on a standard ruler of 1mm scale) and position readings from the Polygraf using the PolygramNET™ software (including both negative and positive readings). Avg Diff=Average difference derived from average of differences between actual position readings and Polygraf position readings similar to the mean difference but the negative readings were regarded as positive readings. SD=standard deviation of differences between actual position readings and Polygraf readings. Mean signal strgth=mean signal strength derived from average of signal strength readings (in mV or millivolt) from the Polygraf. The signal strength reading from the Polygraf was capped at 500mV due to default setup of PolygramNET™ software. Experiment for 0 degree magnet orientation was not possible due to alignment or arrangement of Hall sensors along vertical plane of printed circuit board.

Table 2.4 Effects of magnet rotation in horizontal plane posterior to Hall sensors on position and signal strength

Table showing Mean difference, Average difference, Standard Deviation and Mean Signal Strength for 1mm steps experiment (total distance of 20mm along BACK of Hall sensor arrays) with Neodymium (N42) magnet rotation (HORIZONTAL plane) 20, 40, 60 and 90 degrees at increasing magnet distance away from Hall sensor arrays at 0, 5, 10 and 15mm calculated using Polygraf (Medtronic®) readings of position (mm) and signal strength (mv).

Degrees	Magnet Distance															
	0mm				5mm				10mm				15mm			
	Mean Diff	Avg Diff	SD	Mean Signal Strgth	Mean Diff	Avg Diff	SD	Mean Signal Strgth	Mean Diff	Avg Diff	SD	Mean Signal Strgth	Mean Diff	Avg Diff	SD	Mean Signal Strgth
0	-1.07	1.40	1.29	499.7	-0.82	2.39	3.05	72.17	-	-	-	-	-	-	-	-
20	1.40	4.90	5.03	499.9	4.38	5.44	4.25	270.9	0.23	3.68	4.50	26.70	0.11	4.96	5.79	1.59
40	1.08	4.68	4.97	499.4	3.27	4.91	4.40	400.2	1.90	3.44	3.79	66.12	-0.36	4.25	5.08	10.70
60	0.60	4.48	4.81	491.4	2.65	4.57	4.68	431.9	0.66	3.09	3.78	110.2	-0.38	4.77	5.49	22.60
90	0.24	4.34	4.91	499.1	-3.18	4.75	4.74	498.1	-2.37	3.59	3.92	125.6	-1.08	2.74	3.20	19.08

Deg=degree of magnet rotation on the horizontal plane of Hall sensor array or X-axis. Mean Diff=Mean difference was derived from average of differences between actual position readings on the Hall sensor arrays (mounted on a standard ruler of 1mm scale) and position readings from the Polygraf using the PolygramNET™ software (including both negative and positive readings). Avg Diff=Average difference derived from average of differences between actual position readings and Polygraf position readings similar to mean difference but the negative readings were regarded as positive readings. SD=standard deviation of differences between actual position readings and Polygraf readings. Mean signal strgth=mean signal strength derived from average of signal strength readings (in mV or millivolt) from the Polygraf. The signal strength reading from the Polygraf was capped at 500mV due to default setup of PolygramNET™ software.

Table 2.5 Effects of magnet rotation in vertical plane posterior to Hall sensors on position and signal strength

Table showing mean difference, average difference, standard deviation and mean signal strength for 1mm steps experiment (total distance of 20mm along back of Hall sensor arrays) with neodymium (n42) magnet rotation (vertical plane) 20, 40, 60 and 90 degrees at increasing magnet distance away from Hall sensor arrays at 0, 5, 10 and 15mm calculated using Polygraf (medtronic®) readings of position (mm) and signal strength (mv).

Degrees	Magnet Distance															
	0mm				5mm				10mm				15mm			
	Mean Diff	Avg Diff	SD	Mean Signal Strgth	Mean Diff	Avg Diff	SD	Mean Signal Strgth	Mean Diff	Avg Diff	SD	Mean Signal Strgth	Mean Diff	Avg Diff	SD	Mean Signal Strgth
0	-1.07	1.40	1.29	499.73	-0.82	2.39	3.05	72.17	-	-	-	-	-	-	-	-
20	-1.57	4.06	4.53	499.51	-4.03	5.22	4.97	465.08	-6.40	11.0	10.0	27.71	-	-	-	-
40	-2.72	4.50	4.61	499.62	-3.99	4.83	4.45	469.88	-3.77	7.76	7.62	79.66	-	-	-	-
60	-1.45	4.36	4.71	499.58	-2.22	4.36	4.66	499.55	-4.81	7.03	6.31	143.79	-8.01	9.59	6.91	19.68
90	0.24	4.34	4.91	499.13	-3.18	4.75	4.74	498.09	-2.37	3.59	3.92	125.56	-1.08	2.74	3.20	19.08

Deg=degree of magnet rotation on the vertical plane of Hall sensor array or Y-axis. Mean Diff=Mean difference was derived from average of differences between actual position readings on the Hall sensor arrays (mounted on a standard ruler of 1mm scale) and position readings from the Polygraf using the PolygramNET™ software (including both negative and positive readings). Avg Diff=Average difference derived from average of differences between actual position readings and Polygraf position readings similar to mean difference but the negative readings were regarded as positive readings. SD=standard deviation of differences between actual position readings and Polygraf readings. Mean signal strgth=mean signal strength derived from average of signal strength readings (in mV or millivolt) from the Polygraf. The signal strength reading from the Polygraf was capped at 500mV due to default setup of PolygramNET™ software. Experiment for 0 degree magnet orientation was not possible due to alignment or arrangement of Hall sensors along vertical plane of printed circuit board. There were no readings for 20 degrees at 15mm and 40 degrees at 15mm due to poor or unreliable signal strength.

Table 2.6 Effects of magnet rotation in horizontal plane anterior to Hall sensors on position and signal strength

Table showing mean difference, average difference, standard deviation and mean signal strength for 1mm steps experiment (total distance of 20mm from 50 to 70mm along front of Hall sensor arrays) with samarium cobalt (smco26) magnet rotation (horizontal plane) 0, 20, 40, 60 and 90 degrees at increasing magnet distance away from Hall sensor arrays at 0, 5, 10 and 15mm calculated using Polygraf (medtronic®) readings of position (mm) and signal strength (mv).

Degrees	Magnet Distance															
	0mm				5mm				10mm				15mm			
	Mean Diff	Avg Diff	SD	Mean Signal Strgth	Mean Diff	Avg Diff	SD	Mean Signal Strgth	Mean Diff	Avg Diff	SD	Mean Signal Strgth	Mean Diff	Avg Diff	SD	Mean Signal Strgth
0	-1.30	1.42	1.02	1025	-1.05	2.89	3.27	33.01	-	-	-	-	-	-	-	-
20	-0.96	1.10	1.00	785.9	-1.08	2.43	2.71	51.96	0.26	1.47	1.85	3.70	-	-	-	-
40	-1.00	1.40	1.37	907.2	-1.13	1.39	1.34	142.0	-1.23	1.30	0.86	29.34	0.44	1.18	1.45	3.22
60	-1.32	1.51	1.22	642.8	-3.40	3.40	1.32	350.0	-1.52	1.52	0.76	15.5	-2.15	2.25	1.35	3.11
90	-0.03	0.93	1.13	946.4	-1.32	1.36	0.93	95.22	0.07	0.76	0.88	19.35	2.66	2.70	2.12	1.06

Deg=degree of magnet rotation on the horizontal plane of Hall sensor array or X-axis. Mean Diff=Mean difference was derived from average of differences between actual position readings on the Hall sensor arrays (mounted on a standard ruler of 1mm scale) and position readings from the Polygraf using the PolygramNET™ software (including both negative and positive readings). Avg Diff=Average difference derived from average of differences between actual position readings and Polygraf position readings similar to the mean difference but the negative readings were regarded as positive readings. SD=standard deviation of differences between actual position readings and Polygraf readings. Mean signal strgth=mean signal strength derived from average of signal strength readings (in mV or millivolt) from the Polygraf. There were no readings for 0 degree at 10mm, 15mm and 20 degrees at 15mm due to poor or unreliable signal strengths.

Table 2.7 Effects of magnet rotation in horizontal plane posterior to Hall sensors on position and signal strength

Table showing mean difference, average difference, standard deviation and mean signal strength for 1mm steps experiment (total distance of 20mm from 50 to 70mm along back of Hall sensor arrays) with samarium cobalt (smco26) magnet rotation (horizontal plane) 0, 20, 40, 60 and 90 degrees at increasing magnet distance away from Hall sensor arrays at 0, 5, 10 and 15mm calculated using Polygraf (medtronic®) readings of position (mm) and signal strength (mv).

Degrees	Magnet Distance															
	0mm				5mm				10mm				15mm			
	Mean Diff	Avg Diff	SD	Mean Signal Strgth	Mean Diff	Avg Diff	SD	Mean Signal Strgth	Mean Diff	Avg Diff	SD	Mean Signal Strgth	Mean Diff	Avg Diff	SD	Mean Signal Strgth
0	-1.30	1.42	1.02	1025.24	-1.05	2.89	3.27	33.01	-	-	-	-	-	-	-	-
20	-1.32	1.54	1.35	711.25	-1.63	1.75	1.19	103.87	-1.37	1.38	0.84	7.81	-	-	-	-
40	-2.89	2.96	1.56	799.99	-2.66	2.67	1.35	166.91	-2.55	2.55	0.81	7.17	3.40	5.30	5.98	-0.10
60	-2.37	2.39	1.20	760.88	-2.61	2.62	1.11	158.65	-2.53	2.53	0.79	18.61	-0.54	3.61	4.54	2.49
90	-2.46	2.50	1.71	674.39	-3.14	3.14	1.41	156.36	-2.02	2.04	1.51	24.42	-2.02	3.06	3.72	3.55

Deg=degree of magnet rotation on the horizontal plane of Hall sensor array or X-axis. Mean Diff=Mean difference was derived from average of differences between actual position readings on the Hall sensor arrays (mounted on a standard ruler of 1mm scale) and position readings from the Polygraf using the PolygramNET™ software (including both negative and positive readings). Avg Diff=Average difference derived from average of differences between actual position readings and Polygraf position readings similar to the mean difference but the negative readings were regarded as positive readings. SD=standard deviation of differences between actual position readings and Polygraf readings. Mean signal strgth=mean signal strength derived from average of signal strength readings (in mV or millivolt) from the Polygraf. There were no readings for 0 degree at 10mm, 15mm and 20 degrees at 15mm due to poor or unreliable signal strengths.

Table 2.8 Effects of magnet rotation in anterior-vertical plane to Hall sensors (middle) on position and signal strength

Table showing mean difference, average difference, standard deviation and mean signal strength for 1mm steps experiment (total distance of 20mm from 50 to 70mm along front of Hall sensor arrays) with samarium cobalt (smco26) magnet rotation (vertical plane) 0, 20, 40, 60, 90, 120, 140, 160 and 180 degrees at increasing magnet distance away from Hall sensor arrays at 0, 5, 10 and 15mm calculated using Polygraf (medtronic®) readings of position (mm) and signal strength (mv).

Degrees	Magnet Distance															
	0mm				5mm				10mm				15mm			
	Mean Diff	Avg Diff	SD	Mean Signal Strgth	Mean Diff	Avg Diff	SD	Mean Signal Strgth	Mean Diff	Avg Diff	SD	Mean Signal Strgth	Mean Diff	Avg Diff	SD	Mean Signal Strgth
0	-0.18	0.87	1.15	1060.14	1.71	2.31	2.26	204.47	7.15	7.15	1.22	19.31	7.93	7.93	1.59	3.51
20	-2.36	2.39	1.40	621.77	-4.44	4.44	1.58	207.75	-7.58	7.58	1.00	30.66	-2.58	2.58	0.85	2.40
40	-1.97	2.05	1.44	783.41	-4.88	4.88	1.27	202.67	-6.56	6.56	0.84	35.23	0.32	6.33	7.72	0.49
60	-1.87	1.89	1.20	666.98	-4.15	4.15	0.98	264.65	-5.67	5.67	0.66	41.60	-6.79	6.79	1.21	4.71
90	-0.03	0.93	1.13	946.40	-1.32	1.36	0.93	95.22	0.07	0.76	0.88	19.35	2.66	2.70	2.12	1.06
120	1.97	1.97	1.14	971.82	-2.43	2.43	1.04	266.38	-1.95	2.03	1.03	20.67	-	12.45	3.89	-7.01
140	-0.69	0.91	0.81	972.71	-2.37	2.42	1.27	175.81	-1.22	1.30	1.02	31.18	-	10.88	2.71	-8.14
160	0.94	1.03	0.74	1106.48	-2.84	2.89	1.43	249.51	-0.62	1.17	1.29	22.05	-10.14	10.14	5.92	-9.26
180	0.37	0.67	0.78	1023.72	-1.10	2.22	2.70	132.82	-7.65	7.65	1.02	11.19	-15.86	15.86	6.05	3.75

Deg=degree of magnet rotation on the vertical plane of Hall sensor array or Y-axis. Mean Diff=Mean difference was derived from average of differences between actual position readings on the Hall sensor arrays (mounted on a standard ruler of 1mm scale) and position readings from the Polygraf using the PolygramNET™ software (including both negative and positive readings). Avg Diff=Average difference derived from average of differences between actual position readings and Polygraf position readings similar to the mean difference but the negative readings were regarded as positive readings. SD=standard deviation of differences between actual position readings and Polygraf readings. Mean signal strgth=mean signal strength derived from average of signal strength readings (in mV or millivolt) from the Polygraf. Experiment for 0 degree magnet orientation was not possible due to alignment or arrangement of Hall sensors along vertical plane of printed circuit board. There were no results for 20 degrees, 40 degrees and 90 degrees at 15mm magnet distance due to unreliable signal strengths.

Table 2.9 Effects of magnet rotation in anterior-vertical plane to Hall sensors (distal end) on position and signal strength

Table showing mean difference, average difference, standard deviation and mean signal strength for 1mm steps experiment (total distance of 20mm from 100 to 120mm along front of Hall sensor arrays) with samarium cobalt (smco26) magnet rotation (vertical plane) 0, 20, 40, 60, 90, 120, 140, 160 and 180 degrees at increasing magnet distance away from Hall sensor arrays at 0, 5, 10 and 15mm calculated using Polygraf (medtronic®) readings of position (mm) and signal strength (mv).

Degrees	Magnet Distance															
	0mm				5mm				10mm				15mm			
	Mean Diff	Avg Diff	SD	Mean Signal Strgth	Mean Diff	Avg Diff	SD	Mean Signal Strgth	Mean Diff	Avg Diff	SD	Mean Signal Strgth	Mean Diff	Avg Diff	SD	Mean Signal Strgth
0	-2.82	2.89	1.64	1176.20	-3.94	4.59	3.66	165.60	5.43	6.62	4.71	17.94	7.46	7.46	3.11	5.87
20	-2.51	2.56	1.66	768.50	-3.43	3.43	1.41	68.51	-2.75	2.75	3.41	16.72	-9.01	9.01	2.82	-9.99
40	-0.95	1.89	2.12	874.71	-2.30	2.30	0.99	232.07	-3.12	3.12	1.02	31.13	-6.79	8.33	5.48	-
60	-1.48	2.12	2.06	829.06	-1.29	1.33	0.97	628.00	-2.90	2.90	0.91	36.72	-6.72	6.72	1.65	-
90	1.48	1.54	1.09	967.57	0.23	0.79	0.89	106.91	0.26	0.93	1.14	23.51	2.51	3.30	3.53	4.16
120	-2.63	2.87	2.16	921.21	-0.46	0.87	0.97	245.65	-0.22	0.57	0.78	24.39	-2.00	2.30	1.78	-9.36
140	-3.66	3.74	1.93	1072.30	0.10	1.00	1.22	238.98	0.91	1.20	1.16	29.68	-0.79	2.08	2.29	-7.71
160	-2.57	2.74	1.86	1167.44	-0.92	1.82	1.95	252.06	-	10.23	3.51	8.86	-1.32	3.36	3.81	-
180	-2.13	2.32	2.19	693.10	-2.02	3.17	2.94	69.93	-11.19	11.19	2.09	-3.60	-19.28	19.28	3.25	-12.18

Deg=degree of magnet rotation on the vertical plane of Hall sensor array or Y-axis. Mean Diff=Mean difference was derived from average of differences between actual position readings on the Hall sensor arrays (mounted on a standard ruler of 1mm scale) and position readings from the Polygraf using the PolygramNET™ software (including both negative and positive readings). Avg Diff=Average difference derived from average of differences between actual position readings and Polygraf position readings similar to the mean difference but the negative readings were regarded as positive readings. SD=standard deviation of differences between actual position readings and Polygraf readings. Mean signal strgth=mean signal strength derived from average of signal strength readings (in mV or millivolt) from the Polygraf. Experiment for 0 degree magnet orientation was not possible due to alignment or arrangement of Hall sensors along vertical plane of printed circuit board. There was no result for 0 degrees at 15mm magnet distance due to unreliable signal strengths.

Table 2.10 Effects of magnet rotation in posterior-vertical plane to Hall sensors (middle) on position and signal strength

Table showing mean difference, average difference, standard deviation and mean signal strength for 1mm steps experiment (total distance of 20mm from 50 to 70mm along back of Hall sensor arrays) with samarium cobalt (smco26) magnet rotation (vertical plane) 0, 20, 40, 60, 90, 120, 140, 160 and 180 degrees at increasing magnet distance away from Hall sensor arrays at 0, 5, 10 and 15mm calculated using Polygraf (medtronic®) readings of position (mm) and signal strength (mv).

Deg	Magnet Distance															
	0mm				5mm				10mm				15mm			
	Mean Diff	Avg Diff	SD	Mean Signal Strgth	Mean Diff	Avg Diff	SD	Mean Signal Strgth	Mean Diff	Avg Diff	SD	Mean Signal Strgth	Mean Diff	Avg Diff	SD	Mean Signal Strgth
0	0.30	0.48	0.53	1120.5	-3.35	3.70	2.12	58.67	-5.28	5.28	1.24	13.09	-	-	-	-
20	0.68	0.83	0.69	1061.97	-3.70	3.70	1.77	136.56	-7.68	7.68	0.97	10.75	-	-	-	-
40	1.31	1.35	0.66	1005.08	-3.61	3.61	0.93	165.46	-4.44	4.44	0.91	37.66	-	-	-	-
60	0.26	0.94	1.15	954.78	-4.23	4.23	0.80	85.64	-4.62	4.62	1.12	15.11	-	-	-	-
90	-2.46	2.50	1.71	674.39	-3.14	3.14	1.41	156.36	-2.02	2.04	1.51	24.42	-2.02	3.06	3.72	3.55
120	-0.86	0.98	0.86	965.37	-2.42	2.44	1.19	511.9	0.08	0.53	0.64	26.58	-	-	-	-
140	-1.44	1.57	1.21	901.04	-0.18	0.95	1.13	145.47	0.43	0.73	0.80	30.80	-	-	-	-
160	-0.15	0.59	0.69	1083.72	1.56	1.75	1.38	55.90	2.48	2.48	0.92	15.92	-	-	-	-
180	1.05	1.11	0.81	964.72	-1.07	3.42	3.78	66.34	-1.73	5.29	5.32	10.68	-	-	-	-

Deg=degree of magnet rotation on the vertical plane of Hall sensor array or Y-axis. Mean Diff=Mean difference was derived from average of differences between actual position readings on the Hall sensor arrays (mounted on a standard ruler of 1mm scale) and position readings from the Polygraf using the PolygramNET™ software (including both negative and positive readings). Avg Diff=Average difference derived from average of differences between actual position readings and Polygraf position readings similar to the mean difference but the negative readings were regarded as positive readings. SD=standard deviation of differences between actual position readings and Polygraf readings. Mean signal strgth=mean signal strength derived from average of signal strength readings (in mV or millivolt) from the Polygraf. Experiment for 0 degree magnet orientation was not possible due to alignment or arrangement of Hall sensors along vertical plane of printed circuit board. There were no results for 0, 20, 40, 60, 120, 140, 160 and 180 degrees at 15mm magnet distance due to unreliable position readings or signal strengths.

Table 2.11 Effects of magnet rotation in posterior-vertical plane to Hall sensors (distal end) on position and signal strength

Table showing mean difference, average difference, standard deviation and mean signal strength for 1mm steps experiment (total distance of 20mm from 100 to 120mm along back of Hall sensor arrays) with samarium cobalt (smco26) magnet rotation (vertical plane) 0, 20, 40, 60, 90, 120, 140, 160 and 180 degrees at increasing magnet distance away from Hall sensor arrays at 0, 5, 10 and 15mm calculated using Polygraf (medtronic®) readings of position (mm) and signal strength (mv).

Deg	Magnet Distance															
	0mm				5mm				10mm				15mm			
	Mean Diff	Avg Diff	SD	Mean Signal Strgth	Mean Diff	Avg Diff	SD	Mean Signal Strgth	Mean Diff	Avg Diff	SD	Mean Signal Strgth	Mean Diff	Avg Diff	SD	Mean Signal Strgth
0	0.59	0.91	0.92	1068.75	-4.22	4.22	1.68	41.83	-6.80	6.80	1.17	9.02	-	-	-	-
20	0.37	0.77	0.88	972.86	-0.87	1.35	1.43	142.19	-4.69	4.69	1.22	13.43	-	-	-	-
40	0.64	1.14	1.26	991.58	-0.95	1.07	0.85	159.51	-2.48	2.48	0.84	23.84	-	-	-	-
60	-0.72	1.14	1.26	1006.88	-2.28	2.28	0.82	78.31	-2.74	2.74	0.65	30.23	-	-	-	-
90	0.63	1.17	1.26	978.04	1.31	1.45	1.26	116.02	1.52	2.06	1.72	16.82	-	14.48	15.95	3.62
120	-1.33	1.34	0.80	980.11	0.37	0.71	0.81	181.40	-0.27	0.73	0.84	17.26	-	-	-	-
140	-2.15	2.15	1.28	936.37	1.24	1.32	0.92	171.50	1.34	1.81	1.39	19.46	-	-	-	-
160	-0.60	0.80	0.80	1032.52	1.76	2.21	1.94	141.96	3.56	3.65	1.75	19.71	-	-	-	-
180	0.67	0.97	0.98	562.64	-1.33	3.45	3.59	46.5	1.79	6.32	6.52	1.16	-	-	-	-

Deg=degree of magnet rotation on the vertical plane of Hall sensor array or Y-axis. Mean Diff=Mean difference was derived from average of differences between actual position readings on the Hall sensor arrays (mounted on a standard ruler of 1mm scale) and position readings from the Polygraf using the PolygramNET™ software (including both negative and positive readings). Avg Diff=Average difference derived from average of differences between actual position readings and Polygraf position readings similar to the mean difference but the negative readings were regarded as positive readings. SD=standard deviation of differences between actual position readings and Polygraf readings. Mean signal strgth=mean signal strength derived from average of signal strength readings (in mV or millivolt) from the Polygraf. Experiment for 0 degree magnet orientation was not possible due to alignment or arrangement of Hall sensors along vertical plane of printed circuit board. There was no result for 0,20,40,60,120,140,160 and 180 degrees at 15mm magnet distance due to unreliable position readings or signal strengths.

Table 2.12 Effects of magnet rotation in anterior - horizontal plane to Hall sensors on position and signal strength

Table showing mean difference, average difference, standard deviation and mean signal strength comparing 2 different methods of 1mm steps (between 50-70mm of array) experiment for magnet rotation (horizontal plane) at 0, 20, 40, 60 and 90 degrees with increasing magnet distance away from front of Hall sensor arrays at 5 and 10mm calculated using Polygraf (medtronic) readings of position (mm) and signal strength (mv).

Deg(M1)	Magnet Distance							Deg (M2)		Magnet Distance						
	5mm				10mm					5mm				10mm		
	Mean Diff	Avg Diff	SD	Mean Signal Strgth	Mean Diff	Avg Diff	SD	Mean Signal Strgth		Mean Diff	Avg Diff	SD	Mean Signal Strgth	Mean Diff	Avg Diff	SD	Mean Signal Strgth
0	-1.05	2.89	3.27	33.01	-	-	-	-	0	0.39	1.41	1.65	3.33	-	-	-	-
20	-1.08	2.43	2.71	51.96	0.26	1.47	1.85	3.70	20	0.22	0.61	0.83	58.08	0.12	1.11	1.42	12.61
40	-1.13	1.39	1.34	142.06	-1.23	1.30	0.86	29.34	40	0.89	1.01	0.82	361.87	1.21	1.45	1.08	29.46
60	-3.40	3.40	1.32	350.08	-1.52	1.52	0.76	15.5	60	0.61	0.90	0.96	309.62	1.00	1.04	0.62	31.09
90	-2.26	2.26	0.75	382.19	-2.88	2.88	0.62	34.32	90	-2.26	2.26	0.75	382.19	-2.88	2.88	0.62	34.32

Deg=degree of magnet rotation on the vertical plane of Hall sensor array or Y-axis. M1=Method 1 and M2=Method 2 (as illustrated). Mean Diff=Mean difference was derived from average of differences between actual position readings on the Hall sensor arrays (mounted on a standad ruler of 1mm scale) and position readings from the Polygraf using the PolygramNET™ software (including both negative and positive readings). Avg Diff=Average difference derived from average of differences between actual position readings and Polygraf position readings similar to the mean difference but the negative readings were regarded as positive readings. SD=standard deviation of differences between actual position readings and Polygraf readings. Mean signal strgth=mean signal strength derived from average of signal strength readings (in mV or millivolt) from the Polygraf. No results for 0 degree at 10mm distance due to unreliable readings. Results for 90 degrees were similar since both methods were not different at this particular magnet position.

Table 2.13 Comparing effects of magnet rotation (from 0 to 90 degrees) in anterior - horizontal plane versus anterior – vertical plane to Hall sensors on position and signal strength.
Table showing Mean difference, Average difference, Standard Deviation and Mean Signal Strength Comparing 2 different planes (HORIZONTAL VERSUS VERTICAL) of 1mm steps (between 50-70mm of array) experiment for magnet rotation at 0, 20, 40, 60 and 90 degrees with increasing magnet distance away from FRONT of Hall sensor arrays at 5 and 10mm calculated using Polygraf (Medtronic®) readings of position (mm) and signal strength (mv).

Degrees	Magnet Distance (HORIZONTAL)									Magnet Distance (VERTICAL)							
	5mm				10mm					5mm				10mm			
	Mean Diff	Avg Diff	SD	Mean Signal Strgth	Mean Diff	Avg Diff	SD	Mean Signal Strgth		Mean Diff	Avg Diff	SD	Mean Signal	Mean Diff	Avg Diff	SD	Mean Signal Strgth
0	0.39	1.41	1.65	3.33	-	-	-	-		1.71	2.31	2.26	204.47	7.15	7.15	1.22	19.31
20	0.22	0.61	0.83	58.08	0.12	1.11	1.42	12.61		-4.44	4.44	1.58	207.75	-7.58	7.58	1.00	30.66
40	0.89	1.01	0.82	361.87	1.21	1.45	1.08	29.46		-4.88	4.88	1.27	202.67	-6.56	6.56	0.84	35.23
60	0.61	0.90	0.96	309.62	1.00	1.04	0.62	31.09		-4.15	4.15	0.98	264.65	-5.67	5.67	0.66	41.60
90	-2.26	2.26	0.75	382.19	-2.88	2.88	0.62	34.32		-2.26	2.26	0.75	382.19	-2.88	2.88	0.62	34.32

Deg=degree of magnet rotation on the vertical plane of Hall sensor array or Y-axis. M1=Method 1 and M2=Method 2 (as illustrated below). Mean Diff=Mean difference was derived from average of differences between actual position readings on the Hall

sensor arrays (mounted on a standard ruler of 1mm scale) and position readings from the Polygraf using the PolygramNET™ software (including both negative and positive readings). Avg Diff=Average difference derived from average of differences between actual position readings and Polygraf position readings similar to the mean difference but the negative readings were regarded as positive readings. SD=standard deviation of differences between actual position readings and Polygraf readings. Mean signal strgth=mean signal strength derived from average of signal strength readings (in mV or millivolt) from the Polygraf. No results for 0 degree at 10mm distance due to unreliable readings. Results for 90 degrees were similar since both methods were not different at this particular magnet position.

Table 2.14 Comparing effects of magnet rotation in anterior - horizontal plane (0 to 90 degrees) versus anterior – vertical plane (90 to 180 degrees) to Hall sensors on position and signal strength

Table showing mean difference, average difference, standard deviation and mean signal strength comparing 2 different planes (horizontal versus vertical) of 1mm steps (between 50-70mm of array) experiment for magnet rotation at 0, 20, 40, 60 and 90 degrees with increasing magnet distance away from front of Hall sensor arrays at 5 and 10mm calculated using Polygraf (medtronic®) readings of position (mm) and signal strength (mV).

Deg	Magnet Distance (HORIZONTAL)									Magnet Distance (VERTICAL)							
	5mm				10mm					5mm				10mm			
	Mean Diff	Avg Diff	SD	Mean Signal Strgth	Mean Diff	Avg Diff	SD	Mean Signal Strgth		Mean Diff	Avg Diff	SD	Mean Signal Strgth	Mean Diff	Avg Diff	SD	Mean Signal Strgth
0	0.39	1.41	1.65	3.33	-	-	-	-		-1.10	2.22	2.70	132.82	-7.65	7.65	1.02	11.19
20	0.22	0.61	0.83	58.08	0.12	1.11	1.42	12.61		-2.84	2.89	1.43	249.51	-0.62	1.17	1.29	22.05
40	0.89	1.01	0.82	361.87	1.21	1.45	1.08	29.46		-2.37	2.42	1.27	175.81	-1.22	1.30	1.02	31.18
60	0.61	0.90	0.96	309.62	1.00	1.04	0.62	31.09		-2.43	2.43	1.04	266.38	-1.95	2.03	1.03	20.67
90	-2.26	2.26	0.75	382.19	-2.88	2.88	0.62	34.32		-2.26	2.26	0.75	382.19	-2.88	2.88	0.62	34.32

Deg=degree of magnet rotation on the vertical plane of Hall sensor array or Y-axis. M1=Method 1 and M2=Method 2 (as illustrated below). Mean Diff=Mean difference was derived from average of differences between actual position readings on the Hall sensor arrays (mounted on a standard ruler of 1mm scale) and position readings from the Polygraf using the PolygramNET™ software (including both negative and positive readings). Avg Diff=Average difference derived from average of differences between actual position readings and Polygraf position readings similar to the mean difference but the negative readings were regarded as positive readings. SD=standard

deviation of differences between actual position readings and Polygraf readings. Mean signal strgth=mean signal strength derived from average of signal strength readings (in mV or millivolt) from the Polygraf. No results for 0 degree at 10mm distance due to unreliable readings.

Appendix 2

Calculation of component values in a Band pass filter.

Choose Band-Pass frequency, f and Capacitor, C1

$$C1 = C2,\ R1 = R4 = \frac{1}{2.\pi.C1.f},\ R3 = 19 \times R1,\ R2 = \frac{R1}{19}$$

Using practical Resistor values and a centre frequency (to reduce harmonics):

f = 1663Hz, C1 = C2 = 0.12uF, R1 = R4 = 750R, R2 = 39.47K » 39K, R3 = 14.3K

If the transfer function is derived, the band pass filter acts with:

$$H_o = -\frac{(R3 + R4)}{2 \cdot R1}$$

With centre frequency and bandwidth:

$$\omega_o = \frac{1}{C1 \cdot \sqrt{\left(\frac{R1 \cdot R2}{R1 + R2}\right)(R3 + R4)}} \text{ radians where } f_o = \frac{\omega_o}{2 \cdot \pi} \text{ degrees}$$

$$\beta = \frac{2}{C1 \cdot (R3 + R4)} \text{ radians}$$

Where $B = \frac{\beta}{2 \cdot \pi}$ hertz